

# Lawrence Berkeley National Laboratory

## Recent Work

### Title

RELAXATION TIME MEASUREMENTS IN ELECTRON PARAMAGNETIC RESONANCE

### Permalink

<https://escholarship.org/uc/item/482821dj>

### Author

Chang, James J.

### Publication Date

1971-02-01

RECEIVED  
LAWRENCE  
RADIATION LABORATORY

UCRL-19691

c.2

DOCUMENTS SECTION

RELAXATION TIME MEASUREMENTS IN ELECTRON  
PARAMAGNETIC RESONANCE

James J. Chang  
(Ph. D. Thesis)

February 1971

AEC Contract No. W-7405-eng-48

**TWO-WEEK LOAN COPY**

*This is a Library Circulating Copy  
which may be borrowed for two weeks.  
For a personal retention copy, call  
Tech. Info. Division, Ext. 5545*

LAWRENCE RADIATION LABORATORY  
UNIVERSITY of CALIFORNIA BERKELEY

34

UCRL-19691

c.2

## **DISCLAIMER**

This document was prepared as an account of work sponsored by the United States Government. While this document is believed to contain correct information, neither the United States Government nor any agency thereof, nor the Regents of the University of California, nor any of their employees, makes any warranty, express or implied, or assumes any legal responsibility for the accuracy, completeness, or usefulness of any information, apparatus, product, or process disclosed, or represents that its use would not infringe privately owned rights. Reference herein to any specific commercial product, process, or service by its trade name, trademark, manufacturer, or otherwise, does not necessarily constitute or imply its endorsement, recommendation, or favoring by the United States Government or any agency thereof, or the Regents of the University of California. The views and opinions of authors expressed herein do not necessarily state or reflect those of the United States Government or any agency thereof or the Regents of the University of California.

## RELAXATION TIME MEASUREMENTS IN ELECTRON PARAMAGNETIC RESONANCE

James J. Chang

Inorganic Materials Research Division, Lawrence Radiation Laboratory  
Department of Chemistry, University of California  
Berkeley, California 94720

## ABSTRACT

We have measured the electron paramagnetic resonance (EPR) spectra of  $\text{VO}(\text{H}_2\text{O})_5^{2+}$ , obtained from vanadyl perchlorate in solutions of both ordinary water and in heavy water, as a function of temperature. The linewidths in the vanadyl system are fit quite well by a combination of the relaxation theory for the tumbling of an anisotropic complex and the theory of spin-rotation interaction. The linewidths for the vanadyl ion in ordinary water solution are well fit with the glass spectrum values of  $g_{\parallel} = 1.9311$ ,  $g_{\perp} = 1.9785$ ,  $A_{\parallel} = -203.3$  gauss,  $A_{\perp} = -75.8$  gauss, and the average solution values of  $g = 1.9652$ ,  $A = -115.9$  gauss. The correlation time is consistent with a hydrodynamic radius of 3.67 Å. In the deuterated system the radius is changed to 3.48 Å, with the other parameters remaining the same. The small residual linewidths which have been observed for the vanadyl ion in ordinary water are also observed in the deuterated system. These residual linewidths cannot be due to hyperfine interaction with ligand protons, and must be due to terms neglected in the relaxation theory.

We have also measured the EPR spectra of  $\text{Cu}(\text{H}_2\text{O})_6^{2+}$  obtained from copper perchlorate in aqueous solution as a function of temperature. Isotopically pure (99.62%) copper-63 was used in order to remove uncertainties which could occur in the normal isotropic mixture. The EPR

spectrum of the hexaquocopper (II) ion consists of a broad, unresolved line. The spectra obtained as a function of temperature were digitized with a data acquisition system. A least squares fit of Lorentz line-shapes to the digitized spectra was used to obtain the spectral parameters and linewidths. The linewidths are found to depend upon hyperfine component and to increase with increasing temperature. We have attempted to fit the linewidths to a combination of the spin-rotation interaction theory and the theory of a tumbling anisotropic species. It is not possible to fit the linewidths with both of these theories consistently. Hence, we propose that a third relaxation mechanism contributes to the linewidths in the copper system.

We have developed a system for the measurement of spin-lattice relaxation times consisting of a pulse-saturation spectrometer and a computer based data acquisition and analysis system. We have applied this system to the measurement of relaxation times for  $\text{Ni}^{2+}$  ions diluted in a host crystal of lanthanum magnesium nitrate. Relaxation times for the two strongest lines of the three line spectrum have been obtained. The data are well fit by  $T_1^{-1} = .087 T^2$  ( $\text{msec}^{-1}$ ). This relationship is consistent with a phonon bottleneck process. Measurements of a more dilute crystal support this theory since the relaxation times are slightly shorter.

TABLE OF CONTENTS

ABSTRACT

I. INTRODUCTION----- 1

II. THEORIES OF ELECTRON SPIN RELAXATION IN SOLUTION----- 5

    A. Anisotropic  $g$  and  $A$  Tensors----- 7

    B. Spin-Rotation Interactions----- 10

    C. Al'tshuler and Valiev Mechanism----- 12

    D. Inversion Mechanism----- 15

    E. Electric Field Fluctuation Mechanisms----- 16

III. VANADYL LINEWIDTHS----- 20

    A. Introduction----- 20

    B. Experimental Methods----- 23

    C. Discussion and Results----- 27

IV. COPPER LINEWIDTHS----- 52

    A. Introduction----- 52

    B. Experimental Methods----- 55

    C. Discussion and Results----- 56

V. SPIN-LATTICE RELAXATION TIME MEASUREMENTS WITH AN ON-LINE  
COMPUTER----- 90

    A. Introduction----- 90

    B. Experimental Methods----- 93

    C. Rate Equations----- 98

    D. Discussion and Results-----102

APPENDIX I. Lorentz Lineshapes and Least Squares Theory-----	113
APPENDIX II. Digital Programs-----	119
A. Data Acquisition System Programs-----	119
1. SUMTAP3-----	119
2. FITESR-----	134
3. GAUSS-----	148
B. Simulation Programs-----	152
1. IMITATE-----	152
2. VAESR-----	160
C. $T_1$ Analysis Program LOGLINE-----	167
REFERENCES-----	196
ACKNOWLEDGEMENTS-----	204

## I. INTRODUCTION

Although magnetic resonance phenomena have been studied since 1946, magnetic relaxation phenomena have been studied for a much longer time. The early non-resonant experiments (Gorter, 1947) in magnetic phenomena served to establish many of the important ideas of magnetic relaxation. These experiments were usually interpreted in thermodynamic terms since many of the early experiments involved temperature measurements of magnetic systems. However, magnetic relaxation is usually more easily understood in terms of the resonance phenomenon.

According to the Bloch (1946) formalism a magnetic system may be characterized by two relaxation times which describe the return of a perturbed spin system to equilibrium. The spin-lattice relaxation time,  $T_1$ , is the characteristic time for spin populations in the available energy levels to return to a Boltzmann equilibrium. In terms of the phenomenological Bloch equations this is known as the longitudinal relaxation time, or the time constant for the z component of the magnetization to return to its equilibrium value. The spin-spin relaxation time,  $T_2$ , is a measure of the time for the spins to come to equilibrium among themselves or to dephase.  $T_2$  is also known as the transverse relaxation time since it is the time constant for the x and y components of the magnetization to decay to zero.

The spin-spin relaxation time,  $T_2$ , is experimentally the easiest to determine and it is obtained from the widths of the measured magnetic resonance lines. For a Lorentz line,  $T_2$  is related to the linewidth by

$$T_2^{-1} = \pi \sqrt{3} \Delta\nu \quad (1.1)$$



where  $\Delta\nu$  is the peak-to-peak separation in Hz of the first derivative of the absorption line. The independent variable in magnetic resonance experiments is usually magnetic field rather than frequency, and  $T_2$  is given by

$$T_2 = \frac{h}{g\beta} \frac{1}{\pi\sqrt{3}} \frac{1}{\Delta H} \quad (1.2)$$

where  $\Delta H$  is the first derivative separation in gauss,  $h$  is Planck's constant,  $\beta$ , the Bohr magneton, and  $g$ , the "g" value or spectroscopic splitting constant for the absorption.

The spin lattice relaxation time,  $T_1$ , is usually determined by other methods such as c.w. saturation or pulse methods. However, the factors which influence  $T_1$  also influence  $T_2$ . In many cases, especially in solution,  $T_1 = T_2$ . In many cases when the value of  $T_1$  is required, but is unknown, the equality is assumed. In any case,  $T_2$  sets a lower limit for the value of  $T_1$ .

The relaxation effects characterized by  $T_1$  and  $T_2$  can be related to time dependent magnetic or electric fields which influence the spins. There has been much interest in magnetic relaxation because of the information which may be derived about the environment of the spins. The early theories of relaxation dealt mostly with the solid state. However, the liquid state has been of increasing interest since the original observation of magnetic resonance.

The original work on relaxation in solution was due to Bloembergen, Purcell and Pound (1948), hereinafter referred to as BPP. These workers computed relaxation times using time dependent perturbation theory and correlation functions. They utilized the methods of the theory of Brownian

motion and related the relaxation times to the bulk viscosity of the solution. This has attracted much interest in the possibility of studying the structure of liquids by means of magnetic resonance linewidths in solution. Analysis of the linewidths could yield a correlation time which is characteristic of the solvent and of the complex being studied.

Indeed, nuclear magnetic resonance (NMR) linewidths have been extensively used to provide information about ion-solvent and ion-ion interactions (Burgess and Symons, 1968). The temperature dependence of  $^{17}\text{O}$  NMR linewidths has been extensively used to study waters of hydration and their rates of exchange (Swift and Connick, 1962). However, in systems containing paramagnetic ions the nuclear magnetic moments are influenced by the magnetic moment of the paramagnetic species. The NMR linewidths may then have some dependence on the electron relaxation. An understanding of electron relaxation mechanisms is then useful in interpreting the data.

An understanding of electron paramagnetic resonance (EPR) linewidths is important both in understanding EPR itself, and in interpreting complicated EPR spectra. The EPR linewidths may also be used to study ligand exchange reactions, and to study exchange narrowing effects in concentrated solutions. The EPR linewidths of so-called spin-labels are proving to be important for the study of macromolecules.

The present study was undertaken to extend our knowledge of two important spin 1/2 systems: hexaquocopper (II),  $\text{Cu}(\text{H}_2\text{O})_6^{2+}$ , and pentaquooxovanadium (IV),  $\text{VO}(\text{H}_2\text{O})_5^{2+}$ . Past studies of these ions have provided some qualitative understanding of the relaxation effects. However, a complete quantitative interpretation was not possible with the available data. Only dilute solutions are studied so that exchange effects are unimportant.

Both ions are also rather stable in aqueous solution, and their perchlorate salts will give these ions in solution without further complications.

The measurement of the linewidths in these systems was greatly facilitated by the development and use of a digital data acquisition system. Indeed, the measurements of the hexaquocopper (II) complex would not have been feasible without this system. The data acquisition system operated in an "off-line" mode with the digitized spectra stored on the magnetic tape for later analysis by a digital computer. The successful operation of this system was conducive to the development of an "on line" digital computer system. An "on-line" digital computer system has been developed to measure spin-lattice relaxation times from pulse saturation experiments. This laboratory has been interested in  $\text{Ni}^{+2}$  ions in various lattices for some time (Batchelder, 1970; and Jindo, 1971) and preliminary measurements of  $T_1$  for  $\text{Ni}^{2+}$  in lanthanum magnesium nitrate single crystals have been performed.

## II. THEORIES OF ELECTRON SPIN RELAXATION IN SOLUTION

In this section the results of the various relaxation theories for electron paramagnetic resonance (EPR) of spin  $1/2$  systems in dilute solution are presented. The theories which are specific to systems with spin greater than  $1/2$  or which apply to concentrated solutions are not presented. The results will not be derived in detail. The reader is referred to the original papers for detail or to the general discussions which are available. Two excellent reviews of relaxation in solution have appeared recently: Hudson and Luckhurst (1969) and Lewis and Morgan (1968). In addition a number of discussions of the general techniques have appeared: Fraenkel (1967); McClachlan (1964); Carrington and Luckhurst (1964).

The first treatment of magnetic resonance relaxation in liquids was due to Bloembergen, Purcell and Pound (1948). Although the original derivation was for nuclear magnetism, the method may also be used in electron paramagnetism. BPP considered the relaxation of protons in solution. The perturbation causing the relaxation was a magnetic dipole interaction which fluctuated in time due to random thermal motions in solution. BPP used time dependent perturbation theory to compute transition probabilities which could be directly related to the relaxation times. However, they were forced to use the correlation function methods of the theory of Brownian motions since the perturbation was random rather than periodic. The correlation functions were related to spectral densities which were then related to relaxation times. Yariv and Louisell (1962) have also applied perturbation theory to linewidths.

More elegant methods for computing relaxation times have since been developed. The best known methods are the linear response theory of Kubo and Tomita (1954), and the relaxation matrix theory of Redfield and of Wangsness and Bloch (Redfield, 1957, 1965; Wangsness and Bloch, 1953; Bloch, 1956, 1957). Both of these methods apply the technique of density matrices to the computation of relaxation times.

Although both methods involve the same assumptions and generally arrive at the same answers, the Kubo and Tomita method has not come into widespread use (Deutch and Oppenheim, 1968). The theory has mainly been applied by Kivelson (1957, 1960).

The relaxation matrix method has been widely used in relaxation theories. In this method the relaxation matrix is computed from the correlation functions derived from the perturbation Hamiltonian. The relaxation times are obtained from the components of the relaxation matrix. The method is discussed in detail in Abragam (1961) and in Slichter (1963). The method has been extended and applied by Freed and Fraenkel (1963).

The additional theories which have appeared, and which are extensions of the relaxation matrix theory, have not yet become popular: Fulton (1964); Argyres and Kelley (1964); Freed (1968); Sillescu and Kivelson (1968).

The procedure for the computation of a linewidth or a relaxation time begins with the assumption of a mechanism or time dependent interaction which could cause relaxation. The next step in the development of the theory is the formulation of a time dependent term (consistent with the mechanism) in the Hamiltonian for the system. The derivation of a mathematically tractable form is perhaps the most difficult part of the theory. The final, though by no means trivial, step is the application of one of

general time dependent perturbation methods to compute the relaxation times.

A. Anisotropic g and A Tensors

The relaxation theory of anisotropic systems is probably the most important theory for transition metal complexes with spin 1/2. The essential ideas behind the anisotropic theory were first proposed by McConnell (1956). The basic idea was that the transition metal complex existed as a stable microcrystallite in solution. The complex therefore possessed the same anisotropic spin Hamiltonian which it would possess in the solid state. The microcrystalline complex could tumble in solution due to Brownian motion. The Zeeman interaction, which is orientation dependent for anisotropic systems, is modulated by the rotation of the complex as it undergoes random thermal motions.

This situation is very similar to the dipolar case treated by BPP. McConnell applied the BPP methods to a complex with axial symmetry and arrived at the following result:

$$\frac{1}{T_1} \approx (\Delta g_{\beta} H_0 + b m_I)^2 h^{-2} \frac{\tau_c}{1 + 4\pi^2 \nu^2 \tau_c^2} \quad (2.1)$$

where

$$\Delta g = g_{\parallel} - g_{\perp} \quad (2.2)$$

$$b = A_{\parallel} - A_{\perp}$$

and  $g_{\parallel}$ ,  $g_{\perp}$ ,  $A_{\parallel}$ , and  $A_{\perp}$  are the principal values of the g and A tensors, respectively,  $H_0$ , the resonance field corresponding to the microwave frequency,  $\nu_0$ ;  $m_I$ , the nuclear spin quantum number; and  $\tau_c$ , the correlation time characteristic of tumbling in solution. The correlation time,  $\tau_c$ ,

can be related to the hydrodynamic radius,  $r$ , of the complex and the viscosity,  $\eta$ , of the solution by the Stokes-Einstein equation

$$\tau_c = 4\pi \eta \frac{r^3}{3kT} \quad (2.3)$$

where  $k$  is Boltzmann's constant, and  $T$ , the absolute temperature.

Equation 2.1 gives a linewidth with the following characteristics. The linewidths vary with  $m_I$ , the nuclear hyperfine quantum number. Secondly, the linewidths vary with the magnetic field. This is reasonable since the Zeeman interaction is proportional to magnetic field. Finally, the linewidths vary directly with the correlation time, or inversely with the temperature. This is opposite to the behavior usually observed in solid state where the temperature must be decreased to narrow the line.

Examination of Eq. 2.1 shows three kinds of terms: a term independent of  $m_I$ , a term linear in  $m_I$ , and a term quadratic in  $m_I$ . The  $m_I$  independent term is characteristic of the anisotropy on the  $g$  tensor; the quadratic term is related to the anisotropy of the  $A$  tensor; and the linear term is a cross term related to both anisotropies. Qualitatively a sample has a strong anisotropy in the  $A$  tensor if the spectrum shows a symmetric dependence on  $m_I$ , and a strong  $g$  tensor anisotropy if the spectrum is not symmetric in  $m_I$ .

Later, Kivelson (1960,1964) applied the Kubo and Tomita (1954) method and derived essentially the same result. However, he also showed that the linewidth could be expressed as a sum of secular and nonsecular parts. The secular parts do not contribute to  $T_1$  processes, and  $T_1$  may be estimated by using only the nonsecular parts of the theory.

Wilson and Kivelson (1966a) performed more extensive computations, retaining cross terms which had been neglected in the previous theory. They concluded that the linewidth must be expressed as a cubic polynomial in  $m_I$  rather than a quadratic:

$$\frac{1}{T_2} = \alpha' + \alpha'' + \beta m_I + \gamma m_I^2 + \delta m_I^3 \quad (2.4)$$

where  $\alpha''$ , the residual width, accounts for contributions from effects not included in the tumbling theory. The coefficients of  $m_I$  are given by Eq. 2.5 - 2.8.

$$\begin{aligned} \frac{\alpha'}{T_R} = & \frac{4}{15} (\Delta\gamma B_0)^2 + \frac{3}{40} b^2 I(I+1) - \frac{1}{30} b \frac{a}{\omega_0} \Delta\gamma B_0 I(I+1) \\ & + u \left\{ \frac{1}{15} (\Delta\gamma B_0)^2 + \frac{7}{40} b^2 I(I+1) - \frac{1}{30} b \frac{a}{\omega_0} \Delta\gamma B_0 I(I+1) \right. \\ & \left. - \frac{5}{40} b^2 \frac{a}{\omega_0} I(I+1) f \right\} \end{aligned} \quad (2.5)$$

$$+ \frac{4}{15} (\delta\gamma B_0)^2 + \frac{2}{5} I(I+1) c^2 + u \left[ \frac{1}{5} (\delta\gamma B_0)^2 + \frac{14}{15} I(I+1) c^2 \right]$$

$$\begin{aligned} \frac{\beta}{T_R} = & \frac{4}{15} b \Delta\gamma B_0 - \frac{8}{45} (\Delta\gamma B_0)^2 \frac{a}{\omega_0} - b^2 \frac{a}{\omega_0} \left[ -\frac{1}{20} I(I+1) + \frac{3}{40} \right] \\ & + u \left\{ \frac{1}{5} [b\Delta\gamma B_0 - \frac{2}{3} (\Delta\gamma B_0)^2 \frac{a}{\omega_0} (1+f)] - \frac{1}{20} b^2 \frac{a}{\omega_0} \right. \end{aligned} \quad (2.6)$$

$$\left. \times [I(I+1) + 1 + 7I(I+1) f] \right\} + \frac{16}{15} c \delta\gamma B_0 + \frac{4}{5} c \delta\gamma B_0 u$$

$$\frac{\gamma}{T_R} = \frac{1}{8} b^2 - \frac{7}{30} b \frac{a}{\omega_0} \Delta\gamma B_0 \quad (2.7)$$

$$- u \left\{ \frac{1}{14} b^2 + \frac{1}{6} b \frac{a}{\omega_0} \Delta\gamma B_0 + \left( \frac{2}{5} b \frac{a}{\omega_0} \Delta\gamma B_0 - \frac{5}{40} b^2 \frac{a}{\omega_0} \right) f \right\}$$

$$+ \frac{2}{3} c^2 - \frac{2}{15} c^2 u$$



$$\frac{\delta}{\tau_R} = \frac{1}{20} b^2 \frac{a}{\omega_0} + \frac{1}{20} b^2 \frac{a}{\omega_0} u (1+f) \quad (2.8)$$

where

$$\begin{aligned} b &= \frac{2}{3} [A_z - \frac{1}{2} (A_x + A_y)] & \Delta\gamma &= \beta\Delta g/\hbar \\ \Delta g &= g_z - \frac{1}{2}(g_x + g_y) & \delta g &= \frac{1}{2}(g_x - g_y) \\ c &= \frac{1}{4} (A_x - A_y) & B_0 &= \hbar\omega_0/g\beta \\ u &= 1/(1+\omega_0^2 \tau_R^2) & \delta\gamma &= \beta\delta g/\hbar \\ f &= \omega_0^2 \tau_R^2 u \end{aligned}$$

In the axial case all of the terms containing  $c$ , or  $\delta\gamma$  vanish. Furthermore, we have

$$\begin{aligned} \Delta g &= g_{\parallel} - g_{\perp} \\ b &= A_{\parallel} - A_{\perp} \end{aligned} \quad (2.9)$$

Qualitatively, the linewidth has the same characteristics as the McConnell linewidth. However, the detailed behavior is much more complicated. The coefficients no longer have a simple interpretation in terms of a given anisotropy but include cross terms (however, the major contribution from a given anisotropy to a given coefficient is as discussed above). The temperature dependence of the linewidth is also slightly changed.

These results have also been derived by other workers using the relaxation matrix theory: Hudson and Luckhurst (1969); McClachlan (1964). Sames (1967) has also derived similar results.

### B. Spin-Rotation Interactions

As a molecule tumbles in solution, the rotating electron cloud of the molecule produces a magnetic dipole moment. This moment can interact

with the nuclear and the electronic spins in the molecule. This interaction can be considered as an interaction of the spin angular momenta with the rotational angular momentum of the molecule. The problem was treated for nuclear relaxation by a number of workers, notably Hubbard (1963).

Hubbard considered molecules with cylindrical symmetry and obtained

$$T_1^{-1} = T_2^{-1} = (20kT \tau_\omega / 3h^2) (2C_{\perp}^2 + C_{\parallel}^2) \quad (2.10)$$

where  $C_{\parallel}$  and  $C_{\perp}$  are the principal values of the spin-rotation interaction tensor;  $\tau_\omega$ , the correlation time characteristic of the spin-rotation interaction, and  $\mathcal{I}$ , the molecular moment of inertia. The correlation time  $\tau_\omega$ , is not the same as the correlation time for the tumbling process and is given by

$$\tau_\omega = \mathcal{I} / (8\pi r^3 \eta) \quad (2.11)$$

where  $r$  is the hydrodynamic radius and  $\eta$  the viscosity. The spin-rotation linewidth is then independent of magnetic field and proportional to  $T/\eta$ . In contrast the anisotropic contribution of Eq. 2.1 is usually proportional to  $\eta/T$ .

The theory is difficult to apply in this form and was extended by Atkins and Kivelson (1966) for the problem in EPR. They related the electron spin-rotation tensor,  $C$ , to the  $g$  tensor and derived a linewidth

$$T_2^{-1} = (12 \pi r^3)^{-1} (\Delta g_{\parallel}^2 + 2\Delta g_{\perp}^2) kT/\eta \quad (2.12)$$

where

$$\begin{aligned} \Delta g_{\parallel} &= g_{\parallel} - 2.0023 \\ \Delta g_{\perp} &= g_{\perp} - 2.0023 \end{aligned} \quad (2.13)$$

The linewidth is now independent of the moment of inertia of the molecule. The spin-rotation mechanism should be distinguished from the rotational-spin-orbit mechanism which will be discussed later.

Wilson and Kivelson (1966c) and McClung and Kivelson (1968) have shown that in many cases the hydrodynamic radius,  $r$ , must be replaced by

$$r = \kappa r_0 \quad (2.14)$$

where  $\kappa$  is a constant which depends upon the solvent and its interaction with the solute, and  $r_0$  is a radius determined by other measurements or by calculation of the molecular dimensions. The radius,  $r_0$ , is a constant characteristic of the molecule and may be determined from translational diffusion measurements. The parameter,  $\kappa$ , is related to the anisotropy of the intermolecular potential energy between the solvent and the solute, and is expected to be small for an isotropic interaction. It is expected to be large, i.e.,  $\kappa \gg 1$ , for  $H_2O$  and hydrogen bonded solutes. The usual Stokes-Einstein equation should be adequate in aqueous solution with solutes (complexes) which are hydrogen bonded.

### C. Al'tshuler and Valiev Mechanism

Al'tshuler and Valiev (1958) have proposed a relaxation mechanism for solutions which should be applicable to isotropic systems as well as to anisotropic systems. In contrast to the McConnell tumbling mechanism which is produced through rotational modulation of the spin Hamiltonian, the Al'tshuler and Valiev mechanism is produced by vibrational modulation.

In accord with the Van Vleck (1939) development for solid state, the complex is no longer regarded as a rigid molecule which can only rotate; the ligands around the central ion are permitted to vibrate. As a result

the crystalline potential field of the complex, which is determined by the configuration of the ligands, is modulated. Spin relaxation may be produced through spin-orbit interaction.

The vibrational modulation is introduced into the spin Hamiltonian through the potential energy which is expressed as an expansion in the normal coordinates of an octahedral complex (Van Vleck, 1939)

$$\mathcal{H}' = \sum_{i=2}^6 V^i Q_i \quad (2.15)$$

where  $Q_i$  is the  $i$ th symmetry coordinate of the octahedron, and  $V^i = \partial V / \partial Q_i$ .

The perturbation is then independent of the anisotropy of the complex.

The vibrations of the complex are stochastic since the ligands are influenced by the Brownian motions of the surrounding particles. Al'tshuler and Valiev assume an exponential form for the correlation function and derive a transition probability  $A_{lk}$  between energy levels  $l$  and  $k$

$$A_{lk} = \frac{\overline{Q^2}}{\hbar^2} \sum_i |V_{lk}^i|^2 \frac{2 \tau_c}{1 + \omega_{lk}^2 \tau_c^2} \quad (2.16)$$

$\overline{Q^2}$  is a kind of average measure for the amplitude of the normal vibrations. Al'tshuler and Valiev assume that the mean square amplitude of the oscillator is given by

$$\langle Q^2 \rangle = (\hbar/2m \omega_0) \coth (\hbar\omega_0/2kT) \quad (2.17)$$

where  $\omega_0$  is an average frequency for the vibration and  $m$  is a mass close to the mass of the complex. To find the temperature dependence of  $A_{lk}$  they further assume that the correlation time,  $\tau_c$ , is inversely proportional to the square root of the absolute temperature. Hence, they show the temperature dependence of the transition probability to be

$$A_{1k} \sim T^{-1/2} \coth(\hbar\omega_0/2kT) \quad (2.18)$$

for

$$\tau_c^2 \omega_{1k}^2 \ll 1$$

and

$$A_{1k} \sim T^{1/2} \coth(\hbar\omega_0/2kT) \quad (2.19)$$

for

$$\tau_c^2 \omega_{1k}^2 \gg 1.$$

Hayes (1961) reconsidered the Al'tshuler and Valiev theory and indicates that two of the assumptions of the theory are incorrect. First, the spectral density for the random variable is not normalized, but should be since the total power in the system should not change with the correlation time. Furthermore, the mean square value of  $Q^2$  is correct only at frequencies far removed from the resonant frequency.

In light of these criticisms Hayes rederived the result for the result for the transition probability with this mechanism. He concluded that the transition probability should be directly proportional to temperature. However, he comments that the proportionality constant would be very difficult to determine.

In a later work Valiev and Zaripov (1962) reconsidered the original theory. They indicate that a second term, quadratic in the normal coordinates, should be added to the perturbation. Furthermore, the quadratic term should be more effective than the linear term in producing relaxation. The original theory produced reasonable results because of the form assumed for the correlation functions. Valiev and Zaripov revise the correlation functions in accord with Hayes. Their result for the transition probability cannot be presented in a simple form. However, the temperature dependence can be shown to be

$$T_1^{-1} \approx \coth^2 \left( \frac{\hbar\omega_0}{2kT} \right) \frac{\tau_c}{1 + \omega_{lk}^2 \tau_c^2} \quad (2.20)$$

The temperature dependence is similar to the McConnell temperature dependence until  $T \approx \hbar\omega_0/2k$ . For  $T \gg \hbar\omega_0/2k$ ,  $T_1^{-1}$  may in some cases increase with increasing temperature.

#### D. Inversion Mechanism

Spencer (1965) has considered a process which is applicable to complexes which have a number of equivalent ground state configurations, such as Jahn-Teller systems. In particular, an octahedral complex such as  $\text{Cu}(\text{H}_2\text{O})_6^{2+}$  may distort tetragonally along either of the equivalent x, y, and z axes. The result of passage from distortion along one axis to distortion along another axis is equivalent to a  $90^\circ$  rotation of the complex. However, unlike the tumbling mechanism, the complex does not pass continually through all possible orientations. The complex "inverts" or "jumps" from one orientation to another.

Spencer describes this process in the spin Hamiltonian by defining special delta functions. The delta functions are one or zero depending upon the orientation. Performing a McConnell type of derivation, Spencer shows that the linewidth contribution,  $1/T_2'$ , from this mechanism is

$$\frac{1}{T_2'} = \frac{32\pi}{9h^2} (\Delta g \beta H_0 + b m_I)^2 \tau_i$$

where  $\tau_i$  is the correlation time for inversion, and the other terms have their usual meanings. The contribution from this mechanism should be larger than the tumbling mechanism, but both mechanisms should have the same kind of dependence on field and  $m_I$ . However, this mechanism

should have very little contribution to  $T_1$  processes, unlike the tumbling process which has a strong contribution. Spencer does not discuss a temperature dependence for this mechanism. However, we expect  $1/T_2'$  to be proportional to  $\eta/T$ .

#### E. Electric Field Fluctuation Mechanisms

Kivelson (1966) has considered a number of relaxation mechanisms which he calls electric field fluctuation (eff) mechanisms. In these mechanisms the crystal field of the complex is modulated by vibrations of collisions with surrounding molecules. Spin relaxation occurs through spin-orbit coupling. Among the eff mechanisms are the vibrational spin-orbit, the rotational spin-orbit, the Van Vleck Direct, the Van Vleck Raman, and the Orbach processes.

Kivelson and Collins (1962) originally considered the vibrational spin-orbit and the rotational spin-orbit processes. The rotational spin-orbit process which is an Orbach type of process is to be distinguished from the spin rotational interaction described above. Relaxation by the rotational spin-orbit process occurs through an excited electronic state in contrast to the spin rotation interaction which does not involve excited states. Kivelson and Collins show that the contribution to the linewidth from this mechanism is given by

$$T_2^{-1}(\text{RBO}) = \frac{4}{3} \sum_n \sum_\alpha |\langle 0 | L_\alpha | n \rangle|^2 (\lambda/\Delta_{on})^2 \tau_r^{-1} \quad (2.22)$$

where  $\lambda$  is the spin-orbit coupling constant,  $\Delta_{on}$  the frequency of an electronic transition from the ground to the  $n^{\text{th}}$  state,  $\tau_r$  the rotational correlation time, and  $\langle 0 | L_\alpha | n \rangle$  the matrix elements for the orbital angular

momentum operator  $L_\alpha$ . They compare this to the contribution from the tumbling mechanism and conclude that this is much smaller than the tumbling mechanism contribution. This mechanism can then be neglected.

The Van Vleck Direct, the Van Vleck Raman, and the Orbach processes are analogous to the solid state processes for which they were named. The direct process is a one phonon process and the Raman process is a two phonon process involving a virtual excited state. The Orbach process is a two phonon process involving an actual excited state.

The Orbach process, discussed by Kivelson (1966), was called the vibrational spin-orbit process by Kivelson and Collins (1962). The perturbation in the process is not due to the molecular normal coordinates, but rather to the lattice or liquid modes, that is, the fluctuations of the intermolecular coordinates in liquids. Kivelson considers the molecular normal coordinates only in a direct vibrational process. His results indicate that the contribution from the vibrational process is negligible. Atkins and Kivelson (1966) also consider the effect of molecular normal coordinates in direct, Orbach, and Raman types of processes. They indicate that the linewidth contribution is negligible.

Kivelson has computed the contribution of the Orbach process in the limit  $\delta_{on} \tau_c \gg 1$  to be

$$T_1^{-1} = T_2^{-1} = 16 (\lambda/\Delta)^2 \left( \frac{\phi' g_o}{\Delta r_o} \right)^2 \left( \frac{\Delta}{\delta_{on}} \right)^2 \frac{\tau_c^{-1}}{[\exp(\hbar \delta_{on}/kT) - 1]} \quad (2.23)$$

where  $\Delta$  is the energy from the ground orbital state to the lowest excited orbital state (connected by spin-orbit coupling),  $\tau_c$  the correlation time characteristic of the eff process,  $\delta_{on}$  the energy of the lowest



excited electronic state above the ground state. The term,  $\phi' q_0 / r_0$ , is the measure of the time dependent electric field potential (Lewis and Morgan, 1968) with  $q_0$  a typical amplitude for a lattice (liquid) modes,  $r_0$  a characteristic intermolecular distance, and  $\phi'$  a measure of the change in electric field with respect to the lattice mode. The Orbach linewidth contribution which depends on the phonon spectrum at a frequency not directly related to the EPR transition is independent of the applied field. Kivelson also indicates that the very similar process suggested by Al'tshuler and Valiev (1958) does not appear to give spin relaxation.

The contribution of the Van Vleck direct process to the linewidth is given by

$$T_1^{-1} = T_2^{-1} = 64 (\lambda/\Delta)^2 \left( \frac{\phi' q_0}{\Delta r_0} \right)^2 \frac{(\omega_0 \tau_c)^2 \tau_c^{-1}}{1 + \omega_0^2 \tau_c^2} \quad (2.24)$$

where  $\omega_0$  is the frequency of the spin transition. If  $\omega_0^2 \tau_c^2 \ll 1$  the linewidth contribution is proportional to the applied field squared whereas if  $\omega_0^2 \tau_c^2 \gg 1$ , it is independent of the applied field.

Kivelson considered the linewidth contribution from both a first order Raman process and a second order Raman process. The first order process is less important than the second order process. The contribution from the second order process under the condition  $\omega_0^2 \tau_c^2 \ll 1$  is given by

$$T_1^{-1} = T_2^{-1} = 32 (\lambda/\Delta)^2 \left( \frac{\phi' q_0}{\Delta r_0} \right)^4 \tau_c^{-1} \quad (2.25)$$

This process is independent of the applied field.

However, in the case of a symmetric or nearly symmetric molecule the contribution from the Orbach process could be quite significant. The contributions from the direct and the Raman processes seem to be quite small.

### III. VANADYL LINEWIDTHS

#### A. Introduction

The EPR spectrum of the oxovanadium (IV) ion (vanadyl ion)\* in aqueous solution has been known for many years. It was first reported by Garif'yanov and Kozyrev (1954) in Russia and by Pake and Sands (1955) in this country. The spectrum exhibited eight hyperfine lines arising from an interaction with the nuclear spin  $I=7/2$  of the vanadium-51 nucleus. The interesting feature of the spectrum was that the linewidths varied with the nuclear quantum number,  $m_I$ . The lines also narrowed as the temperature was increased.

The Kivelson (1957, 1960) extension of the McConnell (1956) theory was applied to explain the linewidths. The theory has been found to be quite successful in explaining the linewidths in spin  $1/2$  complexes and many complexes with vanadyl are well characterized by the Kivelson theory. However, although the vanadyl system is now used as a prime example of the success of the McConnell mechanism, the pentaquo-coordinated vanadyl ion itself has been very little studied (Lewis and Morgan, 1968).

The first confirmation of the Kivelson theory for the vanadyl system was reported by Rogers and Pake (1960). These workers measured the EPR spectra for aqueous solutions of the vanadyl ion at 9.25 GHz (X-band) and at 24.3 GHz (K-band). Using the X-band spectrum they determined the coefficients of the Kivelson linewidth polynomial which they wrote as

$$\frac{1}{T_2} = \pi \sqrt{3} (\alpha_1 + \alpha_2 m_I + \alpha_3 m_I^2) \quad (3.1)$$

\* Strictly, vanadyl (IV) ion (Selbin, 1965). In this work the term vanadyl will be used to represent vanadyl (IV),  $VO^{2+}$ .

where the coefficients are given by

$$\begin{aligned}\alpha_1 &= \tau_c \{7/45 (\Delta\gamma B_0)^2 + 63 b^2/16\} + K \\ \alpha_2 &= -\tau_c \{7/15 b \Delta\gamma B_0\} \\ \alpha_3 &= \tau_c \{b^2/10\}\end{aligned}\tag{3.2}$$

In these expressions K is a constant accounting for linewidth not explained by the theory. The other variables are as defined previously. From their X-band measurements Rogers and Pake predicted the K-band linewidths. The predicted widths were in relatively good agreement with the measured widths.

However, this work was unable to provide a quantitative check of the Kivelson theory. The authors lacked the anisotropic spin Hamiltonian parameters necessary to compute the Kivelson parameters. They also did not have a value for the correlation time, and neglected higher order terms in the Kivelson theory.

In a later work, McCain (1966, 1967) extended the study of the vanadyl system. He determined the anisotropic spin Hamiltonian parameters for the vanadyl ion from a glass spectrum. He also measured the solution EPR spectra at 3.12 GHz (S-band) as well as at 9.07 GHz. From the spectra he determined experimental values for the Kivelson coefficients in a polynomial which he wrote as\*

$$\frac{1}{T_{2e}} = \alpha'_2 + \alpha_2 + \beta_2 m + \gamma_2 m^2 + \delta_2 m^3\tag{3.3}$$

He also computed theoretical values for these coefficients. However, he was forced to assume a correlation time for his computations. His comparisons indicated reasonable agreement between the theoretical and experimental terms for all the parameters except the alpha term. His

---

\*The subscript e emphasizes that this is an electronic as opposed to the nuclear linewidth.

results indicated a 30% discrepancy at X-band and an even larger discrepancy at S-band. Some of this error could be attributed to the uncertainty in the correlation time and some to terms which were neglected in the theory. Another mechanism, the spin-rotation mechanism, could also account for part of the discrepancy.

Lewis and Morgan (1968) later reconsidered these results. They assumed a correlation time and computed both the tumbling and spin-rotation contributions to  $\alpha$ . Their estimate of 9.4 gauss is 3.3 gauss less than the value of  $\alpha$  which McCain observed. They suggested that the residual width was due to superhyperfine interaction with the protons of the water ligands. They predict a hyperfine coupling constant of about 2.2 G.

However, in another study Garif'yanov, et al. (Garif'yanov, Kozyrev, Timerov and Usacheva, 1962b) studied the EPR of dilute vanadyl chloride solutions at different temperatures and viscosities. They concluded from their data that, although the McConnell mechanism contributed to the line-width of vanadyl solutions, it was not the dominant relaxation mechanism. Instead, they suggested that the Al'tshuler and Valiev (1958) mechanism was the most probable line broadening mechanism.

The present study was begun to clarify the situation in the vanadyl system. Moreover, McCain (1967) had also determined relative  $T_{1e}$  values for the S-band spectrum using an ingenious saturation method. Using the nonsecular parts of the Kivelson theory he also computed theoretical values for the relative  $T_{1e}$ 's. His comparisons indicated that the theory was not perfect. However, he did not have a good value for the correlation time. These results are reconsidered in this work.

B. Experimental Methods

1. Samples

All aqueous solution experiments were performed using samples of vanadyl perchlorate which were made in one of the following methods. In the first method, due to Selbin and Holmes (1962), a solution of vanadyl sulfate was treated with an equivalent amount of a solution of sodium hydroxide. The precipitate of vanadyl hydroxide was filtered and then dissolved in the necessary amount of perchloric acid. The solution of vanadyl perchlorate was then adjusted to the proper concentration.

In the second method vanadyl perchlorate was prepared by ion exchange using the following procedure (Lee et. al., 1968). An exchange column was loaded with a slurry of a cation exchange resin (AG50W-X2, 200-400 mesh, hydrogen form) in 2 M HCl. The column was then rinsed with distilled water to remove acid. A solution of vanadyl sulfate was then added to the column and the column was rinsed to remove sulfuric acid. A solution of barium perchlorate was used to elute the vanadyl perchlorate from the column. The separation is quite clean and may easily be followed by observing the blue color characteristic of the vanadyl ion move down the column.

In all cases the solutions were adjusted to a concentration between .01 and .02 F.\* The solutions were made slightly acidic with perchloric acid to inhibit the decomposition of the vanadyl perchlorate. Both methods of preparation were found to be satisfactory for this work.

---

\* Formula weights per liter.

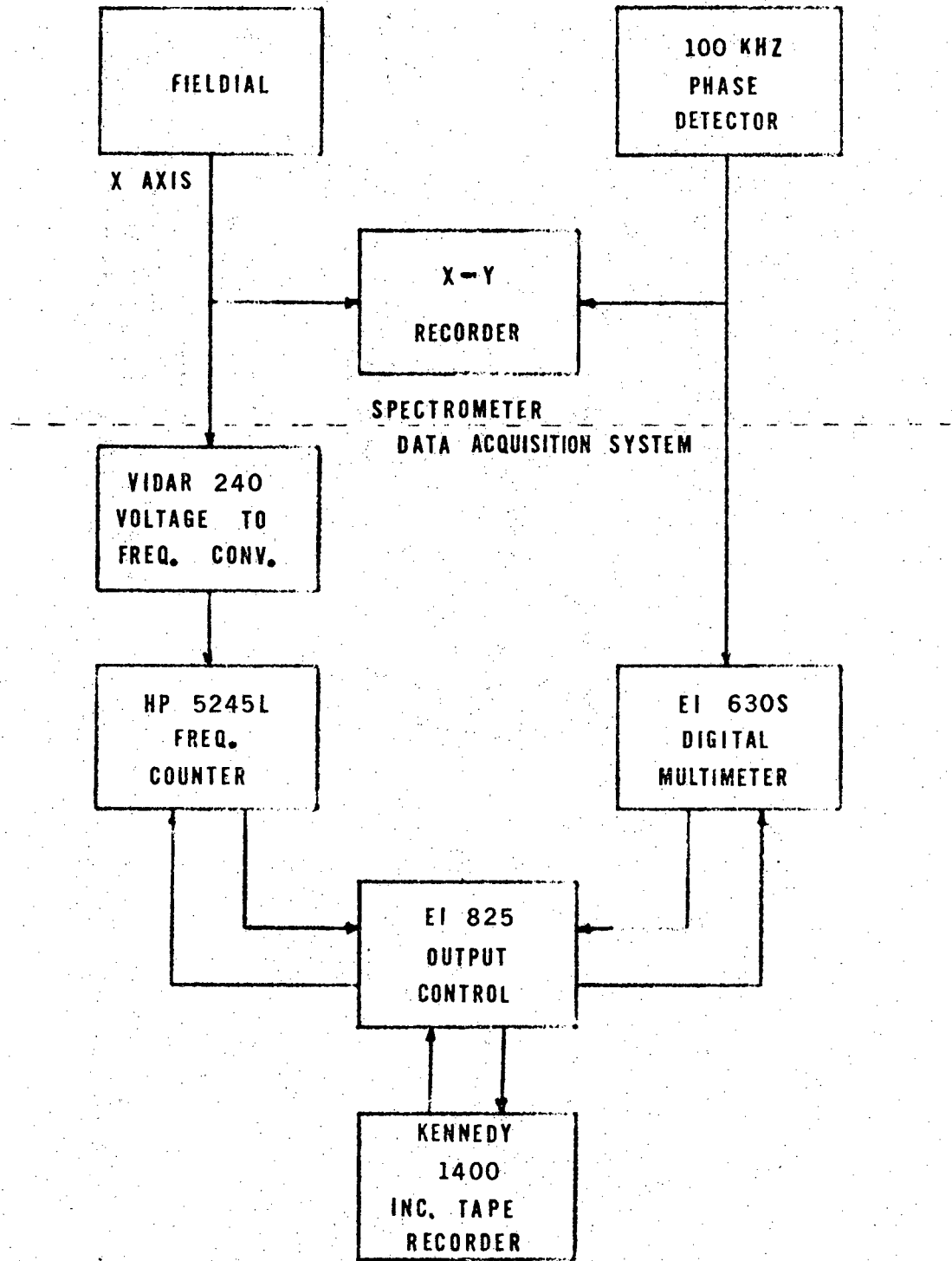
Solutions of vanadyl ion in  $D_2O$  were made by evaporating a stock solution of aqueous vanadyl ion almost to dryness and then dissolving the residue in heavy water. This process was repeated several times to insure a completely deuterated solution. The solutions were never evaporated completely to dryness in order to prevent decomposition from occurring. Deuterated perchloric acid, used in some of the experiments, was obtained in a similar manner.

## 2. Apparatus

EPR spectra were recorded using a standard Varian V-4502 homodyne EPR spectrometer operating at 9.2 GHz. Samples for linewidth studies were held in a V-4548 aqueous solution sample cell. This cell is specially designed to confine the sample to a thin plane, thus eliminating line distortion problems which could arise due to solution conductivity. The sample temperature was controlled with a V-4557 Variable Temperature Accessory which controlled the temperature of a stream of nitrogen gas. Temperature was measured with a copper-constantan thermocouple which was placed in the gas stream before or after each experiment in the same position as the sample.

The spectra were digitized using a Honeywell-EI Model S6114 Automatic Data Logging System (see Fig. 1). This system consists of a Hewlett-Packard Model 5245L electronic counter, a Honeywell-EI Model 630S multimeter, a Honeywell-EI Model 825 Output Control Unit, and a Kennedy Model 1400 incremental magnetic tape recorder.

The multimeter (digital voltmeter) measures the EPR signal from the 100 KHz phase detector. The electronic counter measures the magnetic field. In the Varian spectrometer a voltage proportional to the magnetic



XBL 7012-7165

Fig. 1. Schematic of data acquisition system.



field is obtained from the x-axis retransmitting potentiometer of the Fieldial. This voltage, which originally varied from 0 to 15 volts in order to drive an x-y recorder, was changed to vary from 0 to 10 volts to drive a Vidar Model 240 voltage-to-frequency converter. The electronic counter measures the output from the Vidar and obtains a frequency measurement which can be related to the magnetic field.

The data logging system operates independently of the spectrometer and records the spectrum as a normal scan is in progress. The process of measurement involves simultaneously measuring the EPR signal and the magnetic field coordinates and then encoding and recording the measurement on magnetic tape. The system is capable of making measurements at the rate of 6 to 8 points per second. A digitized spectrum of 2400 points for a normal five minute scan can be routinely acquired with this system.

A measured point consists of seven digits from the frequency counter and five digits plus a sign from the digital voltmeter. The output control unit adds a "word mark" to form a 14 character word for the measurement. The output unit records the data in 80 word blocks separated by record gaps on the tape. This is, unfortunately, not compatible with the FORTRAN system on most computation centers. The data tape is preprocessed with a special program, SUMTAP (see appendix), before the actual analysis is performed. The SUMTAP program puts the data into a form compatible with the FORTRAN system, smooths the data to reduce noise, and reduces the number of data points in the spectrum for convenience in handling by the analysis programs. SUMTAP can also average several spectra to improve signal to noise.

The magnetic field is calibrated by measuring both the magnetic field and the Vidar frequency at several points in the sweep. The

magnetic field was measured with a marginal oscillator (Harvey-Wells 0-502) equipped with a proton probe. The magnetic field may be computed at any point from the Vidar frequency by using a quadratic interpolation equation which is fit to the calibration points. The microwave frequency was measured with an HP 5245L frequency counter equipped with a HP 5255A 3-12.4 GHz frequency converter.

### C. Discussion and Results

#### 1. Spectra

Before a proper treatment of linewidths can be made, the anisotropic spin Hamiltonian parameters, which are utilized in the relaxation theories, must be known. Unfortunately, it is not possible to determine anisotropic parameters from solution (isotropic) spectra, and these parameters must be determined from solid state measurements. There is, however, no guarantee that the complex which exists in a crystal lattice is the same complex in solution. Distortions often occur in a crystal lattice which do not occur in solution. Hence, it is not clear that the anisotropic parameters determined from a crystal lattice bear a close relationship to those for a complex in solution, but these are the best parameters which are available.

Although solid state parameters are best determined from single crystal measurements, single crystals are not readily available for many transition metal complexes. Furthermore, it is usually necessary to obtain a crystal with the paramagnetic species diluted in a diamagnetic host lattice in order to avoid dipole-dipole broadening effects. In some cases, the parameters may be determined from polycrystalline or glass spectra. This method was originally used by Sands (1955).

The methods for analyzing polycrystalline spectra have been well developed (Blinder, 1960; Gersmann and Swalen, 1962; Ibers and Swalen, 1962; Johnston and Hecht, 1965; Kneubuhl, 1960; Neiman and Kivelson, 1961; Vanngard and Aasa, 1963). The spectrum of a polycrystalline sample consists of an envelope of absorption lines rather than distinct single lines. The anisotropic parameters, for example,  $g_{\parallel}$  and  $g_{\perp}$  in an axial case, are determined from the extrema of the absorption envelope.

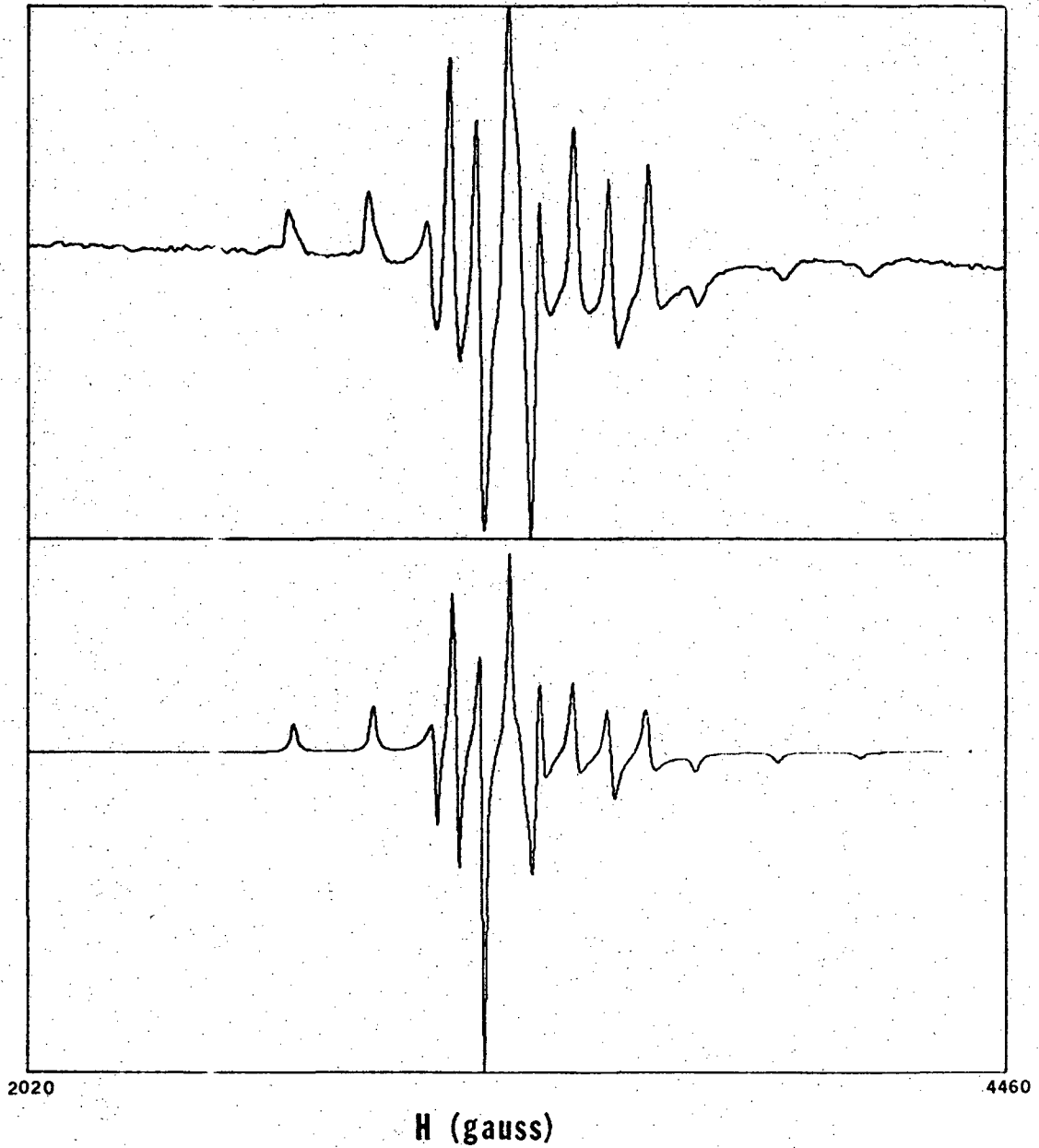
If hyperfine structure is present, the spectrum can be quite difficult to assign. This is especially true if the parameters are such that the spectral features are severely overlapped. In these cases a detailed study of the lineshape is useful. A digital computer can be used to simulate the theoretical absorption spectrum. The spectral parameters may be adjusted until satisfactory agreement between the theoretical and experimental spectrum is obtained. The parameters for quite complex spectra can be determined by this technique.

The major problem with polycrystalline spectra seems to be the production of a usable glass. Frozen aqueous solutions are not suitable due to aggregation of the solute and dipolar broadening (Ross, 1965). It is usually necessary to use solvent mixtures in order to obtain a useful glass medium and many such mixtures have been developed (Smith, et al., 1962). These media have an additional problem in that the solvent may complex with the solute. Spencer (1965) has developed a technique of using 5.26 F perchloric acid as a glass medium. A solution of the transition metal complex in perchloric acid can be quick frozen to near liquid nitrogen temperature to obtain an excellent glass. The advantage of the perchloric acid medium is that the perchlorate anion does not appear to form complexes with transition metals.

TABLE I Anisotropic Magnetic Parameters for Vanadyl

Solute/Solvent	$g_{\parallel}$	$g_{\perp}$	$A_{\parallel}^*$	$A_{\perp}^*$	Reference
$\text{VOCl}_2/\text{Methanol}$	1.92	1.98	190	82	Garif'yanov and Usacheva (1964)
$\text{VOSO}_4/5.26\text{F HClO}_4$	1.9312	1.9778	205.4	76.5	McCair (1967)
$\text{VO}(\text{ClO}_4)_2/5.26\text{F HClO}_4$	1.9311	1.9785	203.3	75.8	This work

\* Coupling constants in gauss



2020

4460

H (gauss)

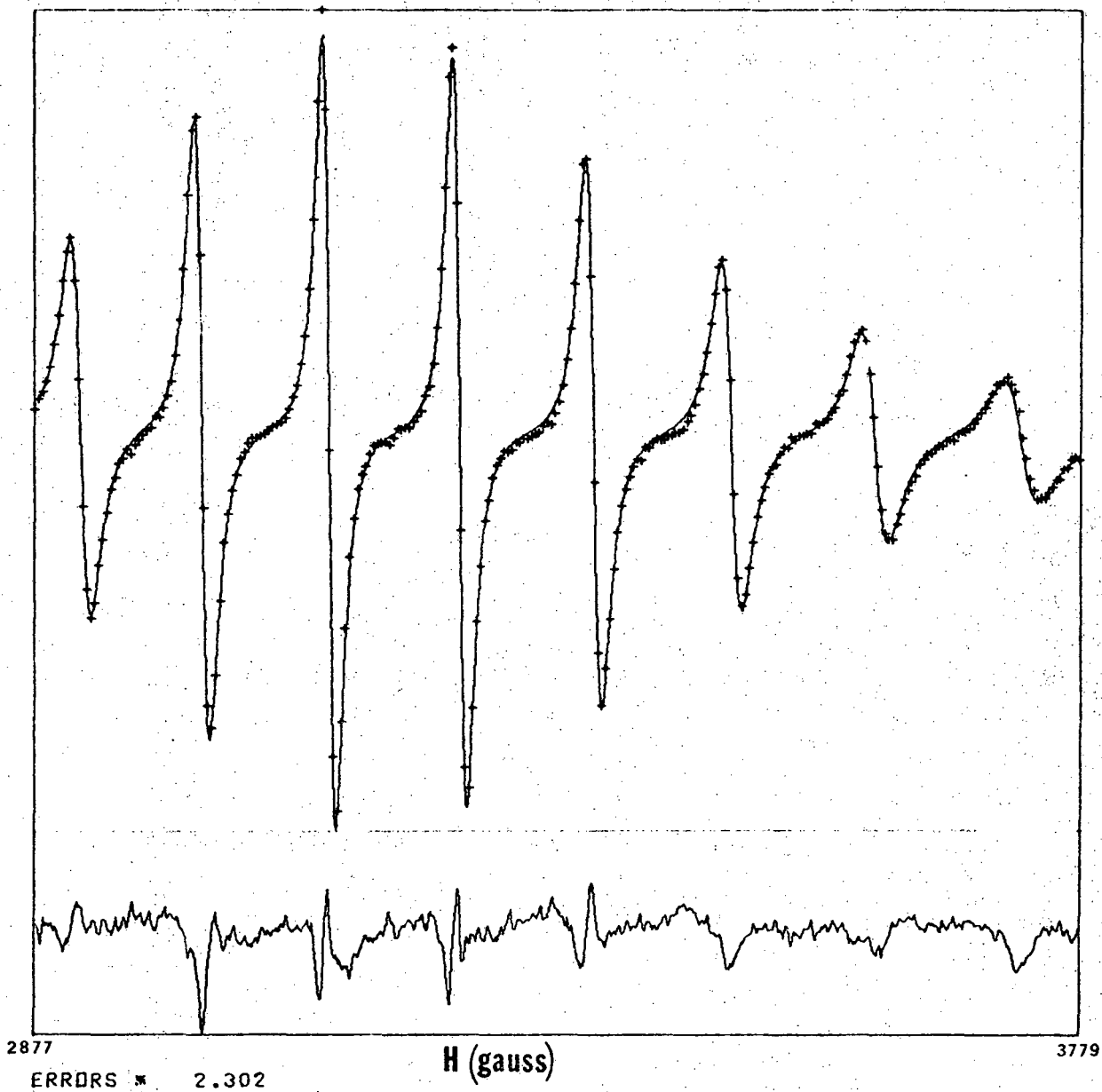
XBL 7012-7167

Fig. 2.  $\text{VO}(\text{F}_2\text{O})_5^{2+}$  glass spectrum. Upper spectrum is experimental; lower spectrum is simulation.

The anisotropic parameters for  $\text{VO}(\text{H}_2\text{O})_5^{2+}$  have been determined from spectra of perchloric acid glasses. The glass spectra were analyzed by spectrum simulation with the method of Vanngard and Aasa (1963) (see Fig. 2). The vanadyl parameters are presented in Table I with those determined by other workers for comparison.

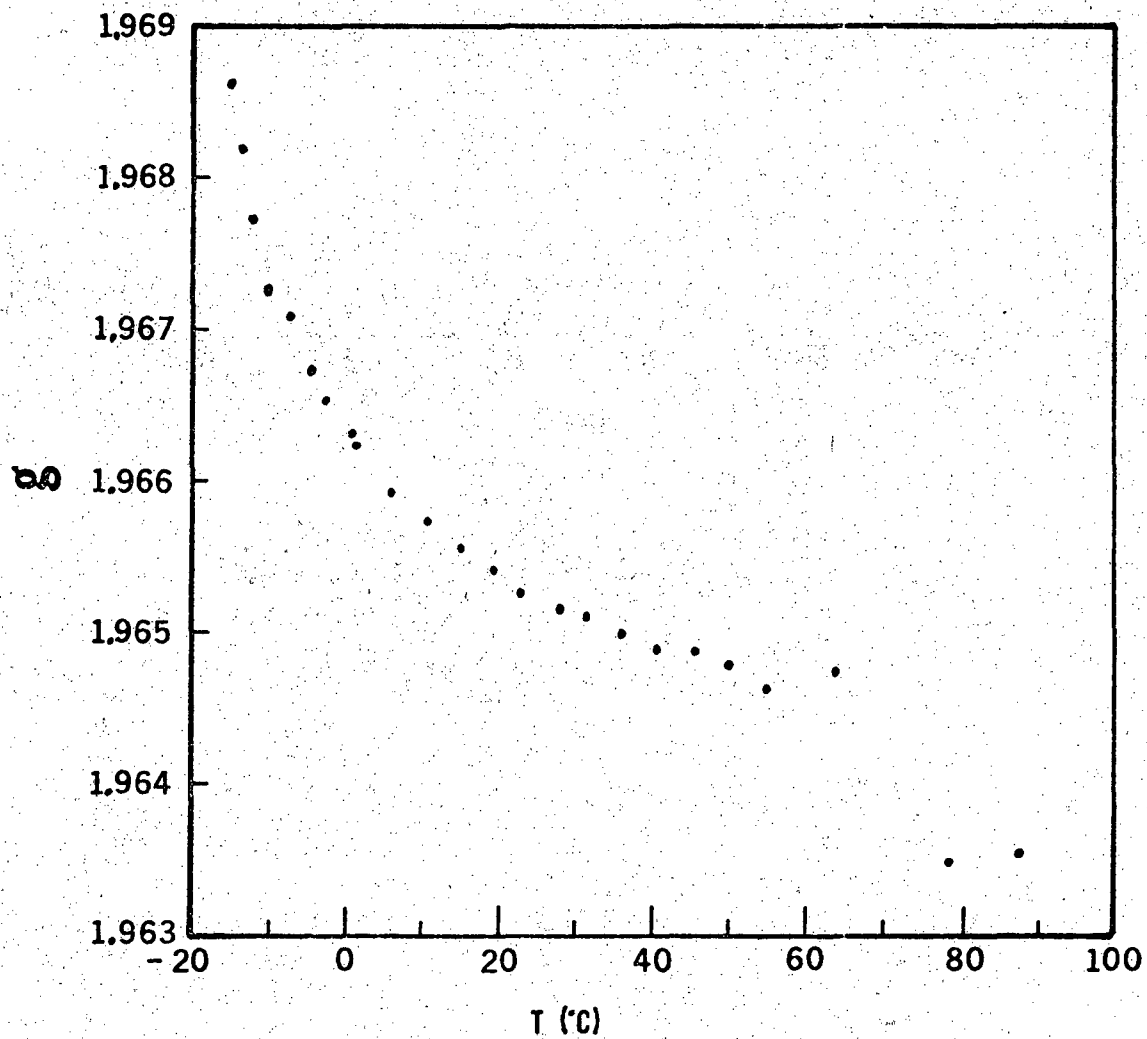
The EPR spectra for vanadyl ions in solution were measured at X band at temperatures between  $-15$  and  $100^\circ\text{C}$  in order to determine the linewidths and the isotropic spin Hamiltonian parameters. The digitized spectra were analyzed by a least squares fitting procedure with the program FITESR which is described in the appendix (Bauder and Myers, 1968). The eight line vanadyl spectrum may be completely described with eleven parameters consisting of the spectrum center, the intensity, the coupling constant, and eight linewidths. Very good values for these parameters are obtained from the least squares fitting procedure. Two parameters to account for baseline offset and baseline drift are also used. An example of the fit to a vanadyl spectrum is shown in Fig. 3. The experimental data are plotted as the crosses and the fitted curve as a continuous line. The bottom curve (error curve) is the difference between the theoretical and experimental curves, and is useful for judging whether the fit has properly converged.

The vanadyl  $g$  and  $A$  value vary as a function of temperature as shown in Figs. 4 and 5. This variation, which is similar to that observed for vanadyl acetylacetonate, is thought to be due to changes in solvation and bonding (Wilson and Kivelson, 1966a). Indeed, the magnitudes of these parameters change in opposite directions as would be expected from bonding theories. Additional mechanisms are mentioned later in the discussion of



XBL 7012-7166

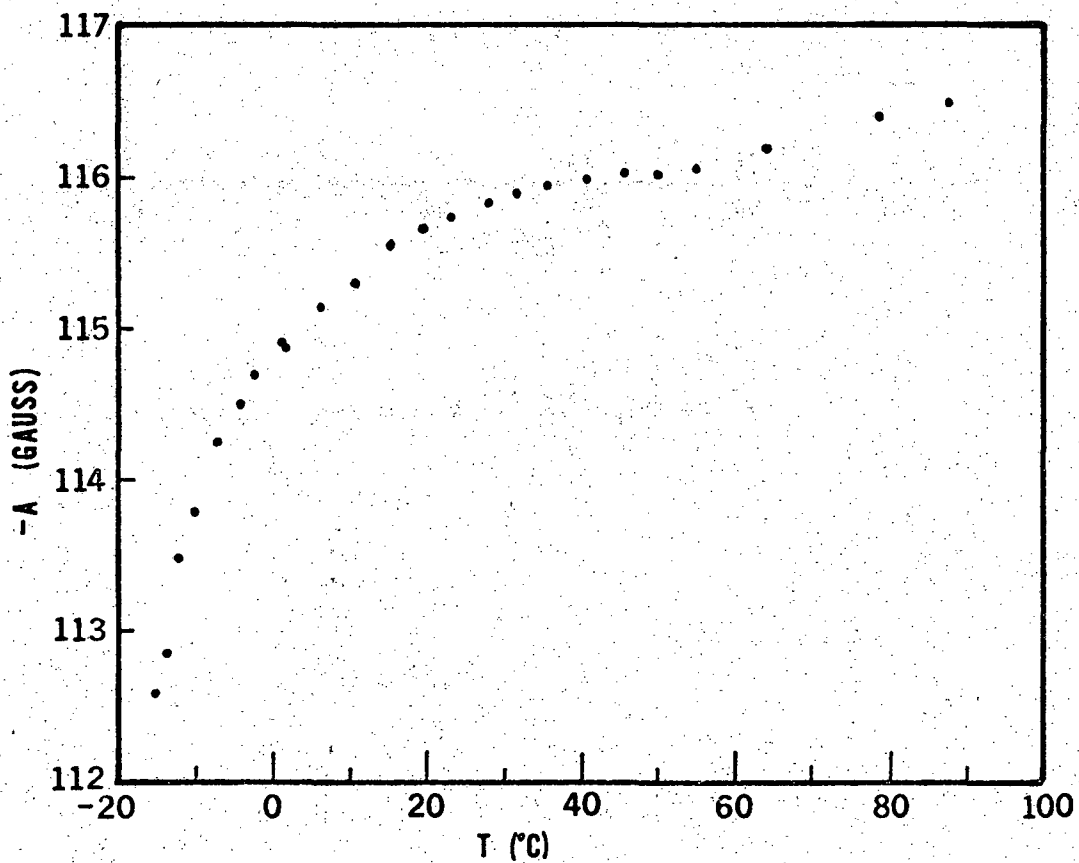
Fig. 3. Example of fit to solution spectrum of  $\text{VO}(\text{H}_2\text{O})_5^{2+}$ . The crosses are the experimental points. The continuous line is the theoretical fit to the data. The lower curve is the difference between the theoretical and experimental curves and has a scale expansion of 2.3.



XBL 7012-7349

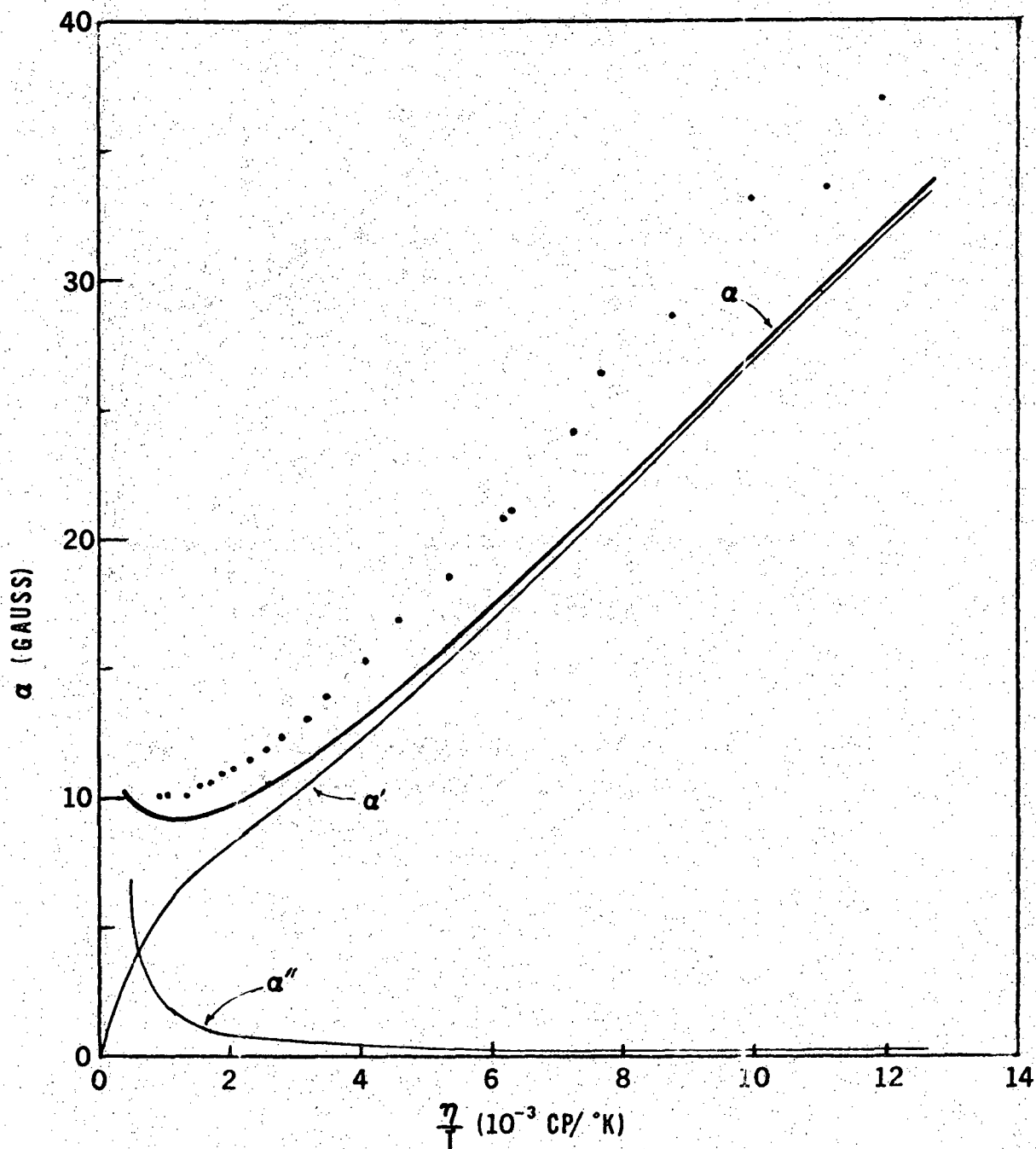
Fig. 4  $g$  vs.  $T$  for  $\text{VO}(\text{H}_2\text{O})_5^{2+}$ .





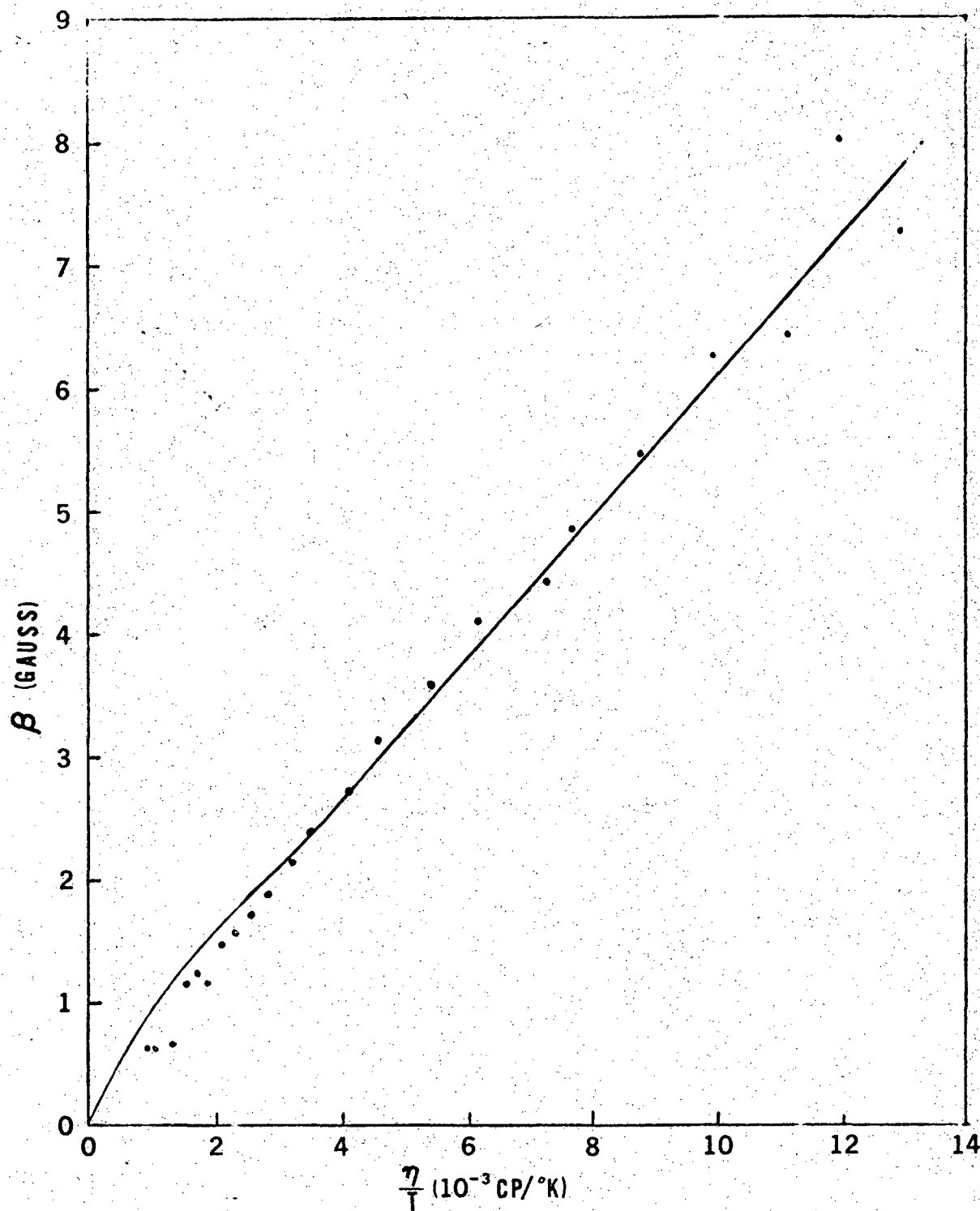
XBL 7012-7348

Fig. 5.  $-A$  vs.  $T$  for  $\text{VO}(\text{H}_2\text{O})_5^{2+}$ .



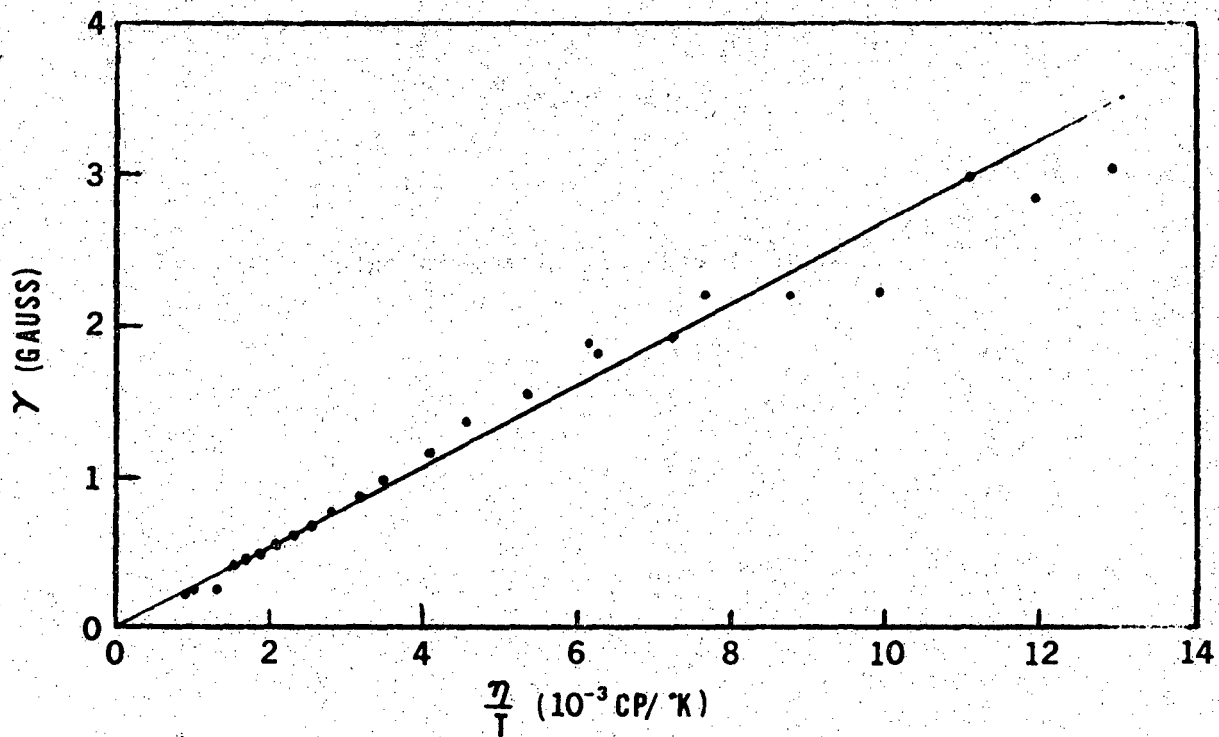
XBL 7012-7342

Fig. 6. Alpha parameter vs  $\eta/T$  for  $\text{VO}(\text{H}_2\text{O})_5^{2+}$ . Points are experimental data continuous; line is theoretical.



XBL 7012-7341

Fig. 7. Beta parameter vs.  $\eta/T$  for  $\text{VO}(\text{H}_2\text{O})_5^{2+}$ .



XBL 7012-7343

Fig. 8. Gamma parameter vs.  $\eta/T$  for  $\text{VO}(\text{H}_2\text{O})_5^{2+}$ .

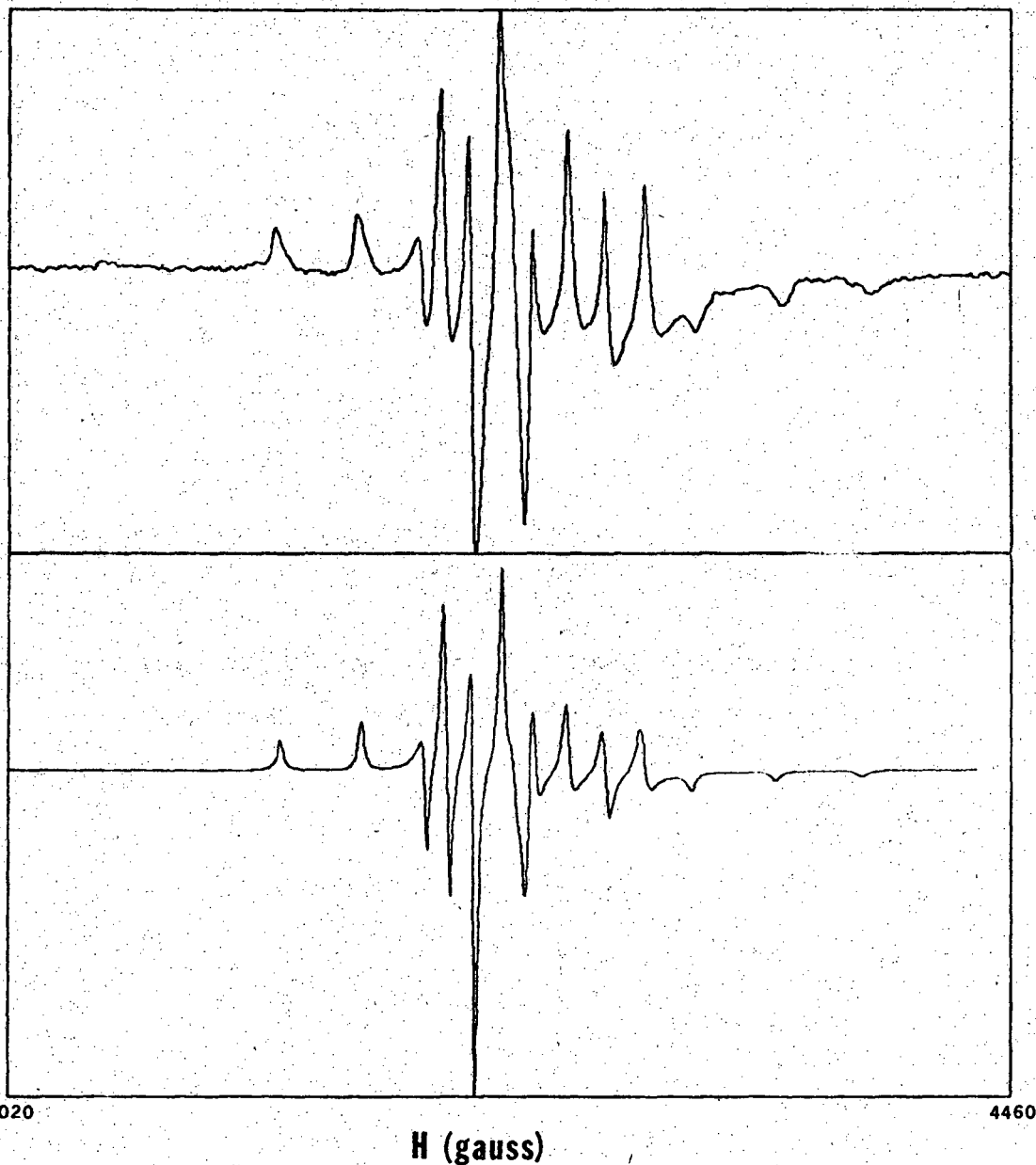
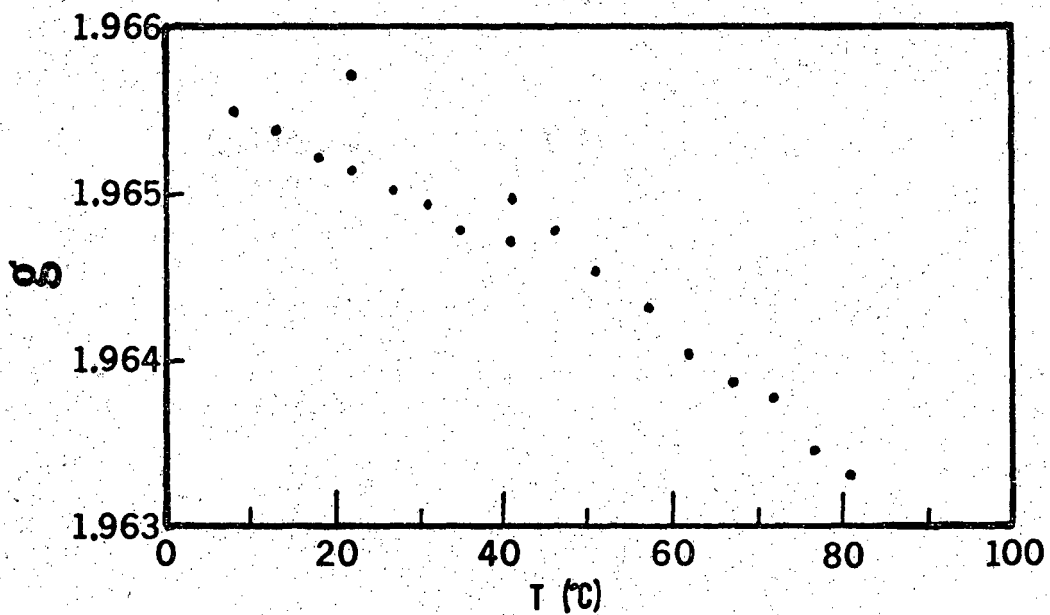


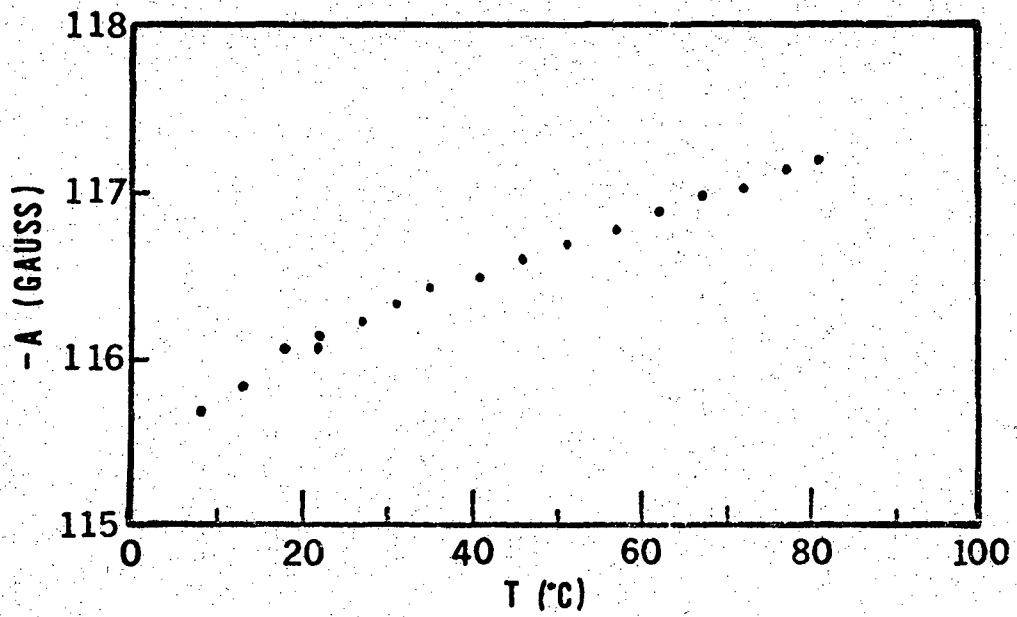
Fig. 9.  $\text{VO}(\text{D}_2\text{O})_5^{2+}$  glass spectrum. Upper spectrum is experimental; lower spectrum is simulation.

XBL 7012-7176



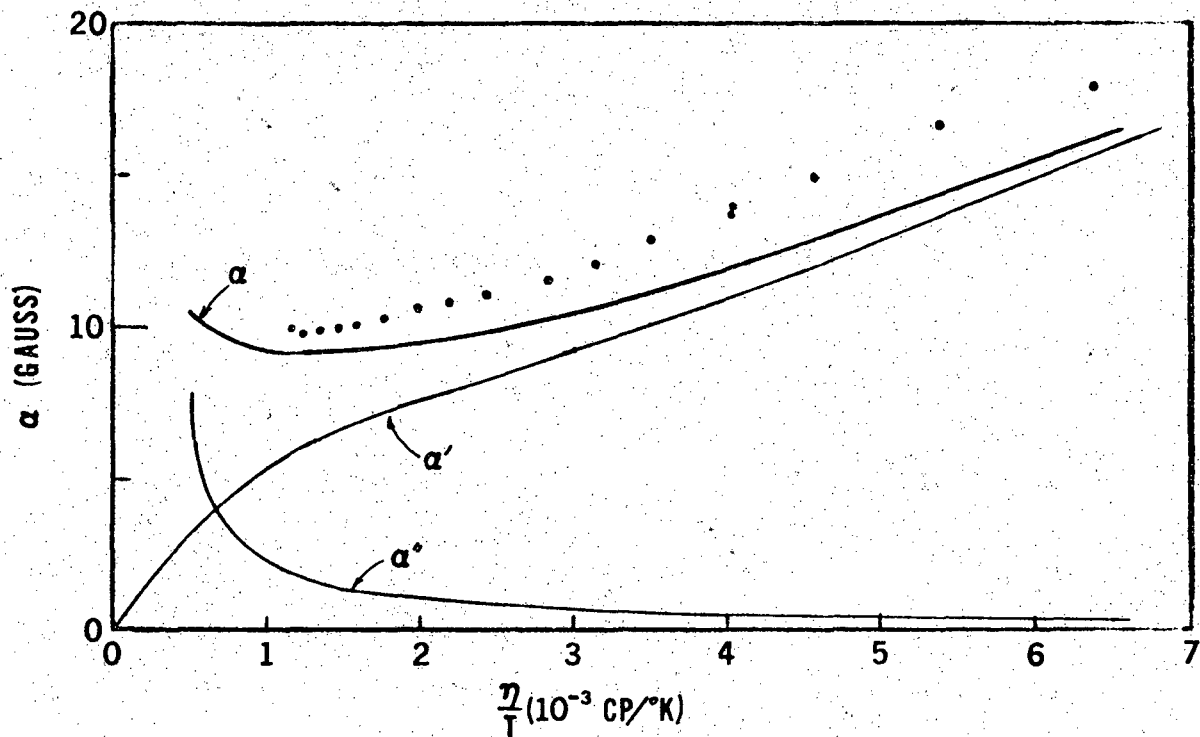
XBL 7012-7347

Fig. 10.  $g$  vs.  $T$  for  $\text{VO}(\text{D}_2\text{O})_5^{2+}$ .



XBL 7012-7346

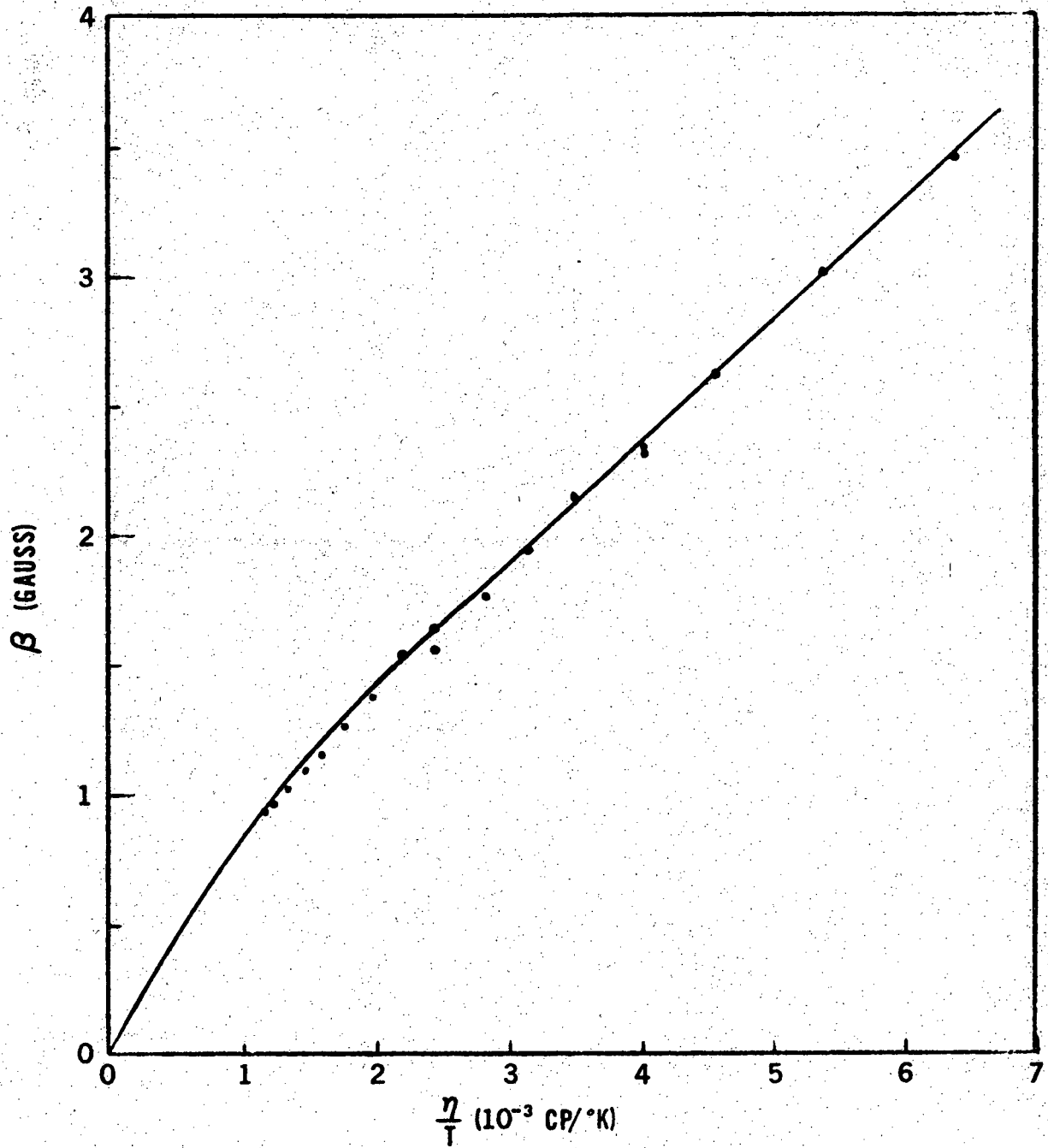
Fig. 11. -A vs. T for  $\text{VO}(\text{D}_2\text{O})_5^{2+}$ .



XBL 7012-7344

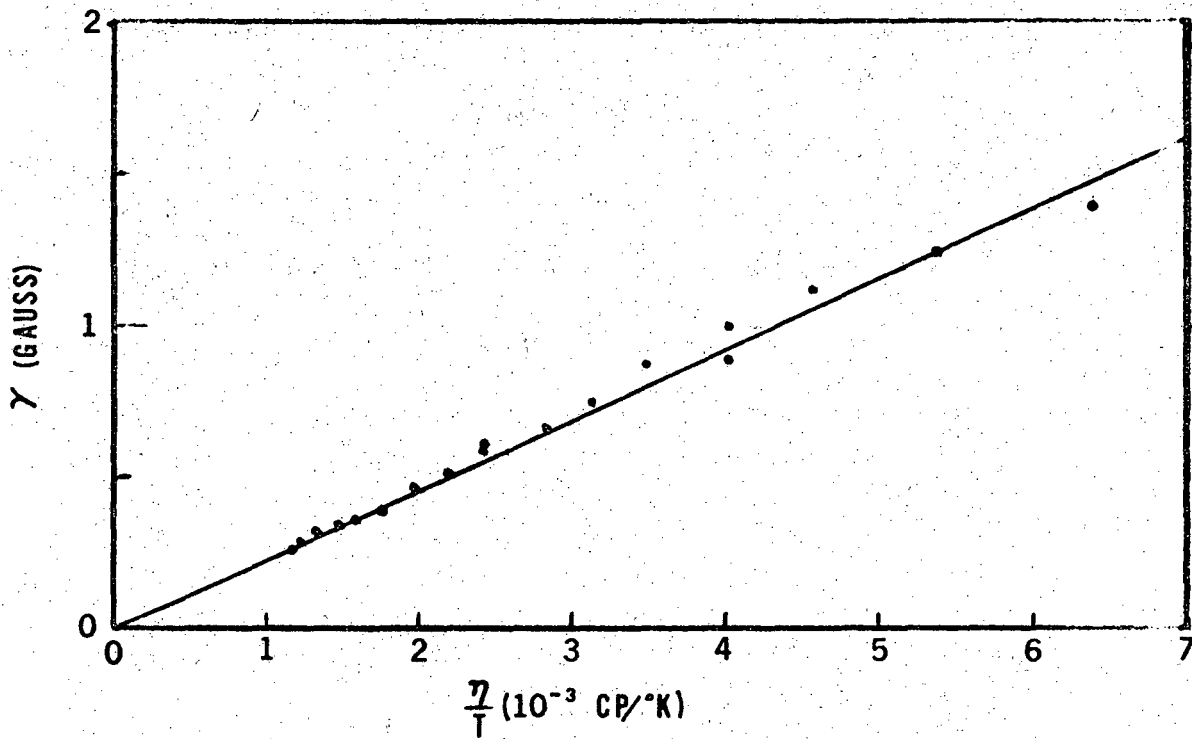
Fig. 12. Alpha parameter vs.  $\eta/T$  for  $\text{VO}(\text{D}_2\text{O})_5^{2+}$ .





XBL 7012-7345

Fig. 13. Beta parameter vs.  $\eta/T$  for  $\text{VO}(\text{D}_2\text{O})_5^{2+}$ .



XBL 7012-7350

Fig. 14. Gamma parameter vs.  $\eta/T$  for  $\text{VO}(\text{D}_2\text{O})_5^{2+}$ .

TABLE II. Viscosities of H<sub>2</sub>O and D<sub>2</sub>O

T (°C)	H <sub>2</sub> O		D <sub>2</sub> O	
	$\eta$	$\eta/T$	$\eta$	$\eta/T$
-10	2.66	10.11		
0	1.7921	6.56		
10	1.3077	4.62	1.685	5.95
20	1.0050	3.43	1.2514	4.27
25	.8937	3.00	1.103	3.70
30	.8007	2.64	.972	3.21
40	.6560	2.09	.7872	2.51
50	.5494	1.70	.671	2.08
60	.4688	1.41	.5513	1.65
70	.4061	1.18	.488	1.42
80	.3565	1.01	.4141	1.17
90	.3165	.871	.3658	1.01
100	.2838	.760	.3265	.875

Note: Viscosities are in centipoises. Viscosities divided by temperature are in  $10^{-3}$  cP/°K.

Viscosities for H<sub>2</sub>O are from the Handbook of Chemistry and Physics, 43rd edition, CHEMICAL RUBBER PUBLISHING CO.

Viscosities for D<sub>2</sub>O are from R. C. Hardy and R. L. Cottingham, J. Chem. Phys. 17, 509 (1949), and from the Landolt-Bornstein Tables, Vol. 5, Transport phenomena, Springer-Verlag (1969).

copper linewidths. The variation of these parameters with temperature forms a limitation on the interpretation of the linewidths. However, the variation is relatively small and does not seriously affect the theory. The values assumed for the linewidth treatment are  $g=1.9652$  and  $A=-115.9G$ . The values used by McCain (1967) were  $g=1.9623$  and  $A=-119.5G$ . The values predicted from the anisotropic parameters ( $g=1.9627$  and  $A=-117.62G$ ) are slightly different, but the above values are thought to be better.

## 2. Relaxation

The vanadyl linewidths were least squares fit to a polynomial cubic in  $m_I$  in order to determine experimental values for the coefficients in Eq. 2.4. These values are plotted vs. viscosity divided by temperature as the points in Figs. 6-8. Selected values of the viscosity of water are presented in Table II to aid in the interpretation of the scales. The beta parameter was used to determine a value for the hydrodynamic radius of the complex from Eqs. 2.6 and 2.3. The radius,  $r=3.67 \text{ \AA}$ , determined in this manner was used with Eqs. 2.5 and 2.7 to compute theoretical values for  $\alpha'$  and  $\gamma$ . The value for  $\alpha''$  was computed using Eq. 2.12. The theoretical values are shown as the smooth curves in Figs. 6-8.

The theoretical and experimental values of the gamma parameter agree very well. This provides strong support for the Kivelson relaxation mechanism. Furthermore, the hydrodynamic radius determined from the theory is reasonable compared with the radius one would obtain from only structural considerations. The delta parameter is in relatively poor agreement with experiment, but terms of order  $(a/\omega_0)^2$  have been neglected in the theory which contribute appreciably to the delta term

(Wilson and Kivelson, 1966a).

However, although the theoretical alpha parameter ( $\alpha = \alpha' + \alpha''$ ) is in good qualitative agreement with the experimental values, the magnitudes are not in good agreement. Lewis and Morgan (1968) proposed that this discrepancy could be due to superhyperfine interaction with the protons of the complexed water molecules. To check this proposal we have made measurements of vanadyl ions dissolved in heavy water.

The anisotropic parameters for this system were determined from a deuterated perchloric acid glass. As expected (since the vanadium crystal field is determined mainly by the strongly bonded vanadyl oxygen), the parameters were the same as those for the aqueous system (in this section only, the term "aqueous" refers to ordinary water solutions as opposed to heavy water). The polycrystalline spectrum is shown in Fig. 9. The theoretical curve in Fig. 9 is the same as that in Fig. 2. The isotropic g and A values for the deuterated vanadyl system are shown in Figs. 10 and 11. The magnetic parameters used in the linewidth treatment were the same as those in the aqueous system.

The linewidth parameters are shown in Figs. 12-14. As in the aqueous system, the beta parameter was used to determine a hydrodynamic radius from the theory. It is interesting that the radius,  $r = 3.48 \text{ \AA}$ , for the deuterated system is  $0.19 \text{ \AA}$  smaller than the radius in the aqueous system. This may indicate an actual change in the effective size of the complex, or more likely, a change in the value of  $\kappa$  (see Eq. 2.14) for the deuterium oxide solvent from the hydrogen oxide solvent.

The agreement between the theoretical and experimental values for the gamma term is excellent. However, the alpha term shows a discrepancy

similar to that in the aqueous system. If the residual linewidth is due to a superhyperfine interaction, it would decrease by close to a factor of three since the magnetic moment of the deuteron is that much smaller than that of the proton. A comparison of the two residual widths indicates that the deuterated complex does not have a smaller discrepancy.

Recently, however, the proton magnetic resonance work was reported for the vanadyl system (Reuben and Fiat, 1969a, b). These workers give a proton superhyperfine coupling constant of 3.2 MHz, or 1.2 G for  $g=1.97$ . Although this is sufficiently large to provide the residual linewidth in the aqueous vanadyl system, it does not explain the behavior of the deuterated complex.

It must be noted that the samples were not degassed so that the residual linewidth could be due to oxygen broadening. However, McCain (1967) indicates that the vanadyl widths did not narrow upon degassing. A preliminary investigation by the author also produced this result. The effect of dissolved oxygen is, therefore, expected to be quite small.

We are then led to somewhat of a dilemma for the vanadyl system. Since the residual width did not change upon deuteration, this width cannot be due to superhyperfine structure. However, if the residual width is ascribed to other causes, we must show why no hyperfine effect is shown. We must therefore reexamine the premises of the experiment.

A resonance line may be homogeneously or inhomogeneously broadened. A homogeneously broadened line is a single line which may be characterized by a "true" linewidth. An inhomogeneous line is a superposition of several homogeneous lines which have a "true" linewidth. The inhomogeneous line has an apparent width which is, in general, not the "true" width.

However, as the "true" width becomes larger and larger the apparent width of an inhomogeneously broadened line should be closer to the natural width. If the "true" width is very large compared to the separation of the components, the apparent width will become equal to the "true" width.

A proton hyperfine coupling constant of 1.2 G would surely produce a superhyperfine pattern in the vanadyl lines since proton exchange is slow. This should cause the vanadyl lines to be inhomogeneously broadened so that a least squares fit to determine the linewidth should produce an error in the linewidth. However, as the true linewidth becomes larger, the error in the linewidth is expected to become smaller. Since the linewidths in the vanadyl spectrum at low temperatures are quite large compared to the hyperfine splitting, the residual linewidth due to hyperfine structure should go to zero. We see from Figs. 6 and 12 that the residual width is either constant with temperature or increases as temperature is decreased. Hence, we must conclude that, because the residual width neither decreased with deuteration nor decreased with decreasing temperature, the main contribution to the residual width is not a superhyperfine interaction.

We would expect some contribution to the width from superhyperfine interaction. The residual width should have changed some upon changing to the heavy water solvent. The effect, however, is reduced because of the variation of linewidth with hyperfine component. The error of residual width in each hyperfine component due to superhyperfine interaction changes from component to component. The error in the alpha parameter would be a kind of average over the errors for all the components. For some of the lines the widths are large enough that the error is close

to zero. Hence, the average contribution to the residual width is much smaller than the maximum possible contribution. Furthermore, the linewidth variation is not symmetric with respect to the center of the spectrum. The narrowest line in the spectrum is to the low field side of the spectrum center. The result of this is that the beta and gamma parameters must also be affected by the superhyperfine interaction. The contribution of superhyperfine structure to the alpha parameter is much smaller than the possible contribution to a given line. The change in the residual width upon going to a deuterated solvent is smaller than the residual width due to superhyperfine interaction. It is not observed because it is so small.

We, therefore, have an unexplained residual width in the vanadyl system. The residual width cannot be due to the Al'tshuler and Valiev (1958) mechanism since this mechanism is temperature dependent. Furthermore, this mechanism would predict a linewidth increasing as temperature increases. The residual width on the other hand is constant or decreases with increasing temperature.

The linewidth in the vanadyl system is, nevertheless, almost completely explained by a combination of the spin-rotation and anisotropic  $g$  and  $A$  tensor mechanisms. We may test the field dependence of the mechanism by comparing theoretical predictions with the parameters measured by McCain (1967) and by Rogers and Pake (1960). These parameters are presented in Table III.

A comparison of the S band experimental and theoretical values shows a considerable disagreement. The alpha term is off by 5 gauss; the beta and gamma terms also disagree. McCain indicated that this disagreement



TABLE III. Comparison of Theoretical and Experimental Linewidth Parameters for  $\text{VO}(\text{H}_2\text{O})_5^{2+}$

S band (3.12 GHz) (McCain, 1967)		K band (24.3 GHz) (Rogers and Pake, 1960)	
Exp.	Th.	Exp.	Th.
21.9	17.	13.6	13.
1.333	2.15	2.8	4.5
.4977	.65	.47	.82
-.0544	-.05	***	-.004

was probably due to terms of order  $(a/\omega_0)^2$  which were neglected in the theory. We feel that this is the most probable reason. Furthermore, this is probably also the reason for the residual width in the X band data. The neglected terms have relatively little effect on the beta and gamma parameters, but seriously affect the alpha parameter. This discrepancy is expected to be smaller at K band where the neglected terms would be quite small. A comparison of the K band experimental and theoretical data is somewhat disappointing. Although, the alpha term agrees well with theory, the beta and gamma terms are extremely wrong. We suspect that this is due to an error in the data rather than in the theory. Rogers and Pake indicate that the lines have some non-Lorentz character which we believe is an experimental problem which produced an error in the results. K bands experiments are quite difficult because the sample must be small to avoid distortion problems. The Kivelson theory is then expected to completely explain the linewidths. It would be interesting to obtain some additional K band data.

The theory may be used to compute theoretical estimates of the relative  $T_{1e}$  values for comparison with McCain's (1967) experimental values. However, the theory is only approximately correct for the S band data. McCain used a correlation time of  $\tau=3 \times 10^{-11}$  sec in his work where the value determined in this work is  $\tau=3.8 \times 10^{-11}$  sec. However, this change does not change the results enough. The agreement between theory and experiment is quite poor, but this is expected since the linewidth predictions are also poor.

#### IV. COPPER LINEWIDTHS

##### A. Introduction

The EPR spectrum of the hexaquocopper (II) complex in solution was certainly one of the first to be studied though it is difficult to say when it was first observed. Among the earliest studies of the system were those of Kozyrev (1955) and McGarvey (1956, 1957). These workers reported a spectrum consisting of a single line at ordinary temperatures with a  $g$  value of about 2.2 and a peak-to-peak linewidth of about 150 gauss. Although the copper nucleus has a nuclear spin  $I=3/2$ , no hyperfine structure was observed in the spectrum.

The intriguing characteristic of the spectrum was that the linewidth was observed to increase with increasing temperature (Kozyrev, 1957; Avvakumov, et al., 1960). At first glance the linewidth of this spin  $1/2$  complex would have been expected to decrease with increasing temperature on the basis of the McConnell theory (1956).

A number of explanations were proposed for the anomalous behavior of the copper system. Indeed, Kozyrev (1955) early proposed that the broadening and subsequent lack of hyperfine structure in the copper spectrum was due to the formation of copper dimers. This suggestion was based on an incomplete understanding of some of the early data, and is not tenable since the linewidth behavior persists in dilute solutions where copper dimers are quite unlikely. McGarvey (1957) proposed that the linewidth was due to a combination of tumbling and an interaction with a low lying excited state which was expected in the hexaquocopper (II) system as a result of the Jahn-Teller effect. Al'tshuler (Al'tshuler and Valiev, 1958; Al'tshuler and Kozyrev, 1964) proposed a theory involving vibrational

modulation of the crystal field. He showed that this theory would fit their data quite well.

However, all the early theories suffered from incomplete information as to the true linewidth in the system. The linewidth was taken as the derivative peak-to-peak distance of the broad single line observed in the spectrum. But the EPR spectrum of hexaquocopper (II) must certainly consist of hyperfine structure. Hayes (1961) detected hyperfine structure in the spectrum by cooling to near 0°C. The coupling constant between 31 to 38 gauss, indicated that the linewidth was in a large part due to hyperfine structure.

Among other workers who have used the overall linewidth are Valiev and Zaripov (1966) and Fujiwara and Hayashi (1965). Valiev and Zaripov proposed a relaxation mechanism specific to the hexaquocopper (II) system. This mechanism, a modification of the Al'tshuler and Valiev (1958) mechanism, involved a vibrationally induced transition to the lowest orbital excited state with subsequent relaxation to the ground state. This is a kind of Orbach mechanism involving ligand vibrations rather than lattice modes. Valiev and Zaripov's work shows reasonable agreement with the overall linewidth if the hyperfine contributions are ignored.

Fujiwara and Hayashi studied the linewidth as a function of temperature, as a function of concentration, and as a function of the anion associated with the copper cation. These workers report no anion dependence in dilute solutions and also no concentration dependence for solutions less than .1 F. These results are qualitatively correct since although the true linewidth was not measured, a concentration effect would be observed in the overall line. Although these workers report measurements

near 0°C, they report no hyperfine structure in the spectrum.

Spencer (1965) measured the EPR spectra of hexaquocopper (II) over a wide range of temperatures for both aqueous solutions and for perchloric acid solutions. He also measured the spectra of the hexamminecopper (II) system which was expected to be quite similar in behavior. Using the hyperfine coupling constant of  $.0053 \text{ cm}^{-1}$  he was able to perform crude corrections to the linewidths. At low temperatures he observed the linewidth to decrease as the temperature increased. Spencer discusses two mechanisms to explain the linewidth: the anisotropic tumbling mechanism and an inversion mechanism. Although a definite conclusion was not reached, Spencer proposed that the linewidth could be explained by a combination of these mechanisms. Another explanation was that the linewidth was controlled by the rate of chemical exchange of the water molecules in the hydration sphere. Additional support for this proposal was obtained from the  $^{17}\text{O}$  NMR data (Meredith, 1965). The  $^{17}\text{O}$  linewidth was observed to vary with the same temperature dependence as the EPR linewidth.

Lewis, Alei, and Morgan (1966) also studied the copper system as a function of temperature. They study the copper system by means of a lineshape analysis using a simulation technique. At high temperatures (above room temperature) they assume that all the linewidths are equal. From their analysis they conclude that the linewidth should be due to a combination of the spin-rotational process and a second process which they describe as a Raman process. They propose the Raman process on the basis of extrapolation from reported solid state measurements. However, Kivelson (1966) indicates that Raman processes are not expected to be large in solution. Lewis, Alei and Morgan propose the following

function for the linewidth

$$T_2^{-1} = 2.04 \times 10^4 [(T/\eta) + 0.23 T^2] \quad (4.1)$$

The main difficulty with the hexaquocopper (II) system, other than the actual interpretation of the linewidth behavior, is the measurement of the true linewidths for the hyperfine lines. The large linewidths leading to extreme overlap and lack of resolution in the spectrum produces an extremely frustrating problem. Simulation methods of analysis for lines as unresolved as the copper lines are very difficult. The present study was begun because it was felt that the use of a data acquisition system in connection with a least squares treatment would facilitate the treatment of the data and improve the results.

#### B. Experimental Methods

The apparatus and measurement procedures were the same as those described for the vanadyl experiments (see Sec. III-B). The initial experiments were performed with copper perchlorate obtained from the G. Frederick Smith Company. The final experiments were performed with isotopically enriched  $^{63}\text{Cu}$ (99.62%) which was obtained from Oak Ridge National Laboratories in the form of the oxide. The oxide was dissolved in an equivalent amount of perchloric acid with gentle heating. The concentration of the resulting copper perchlorate solution was adjusted to .01-.02 F. Solutions in 5.26 F perchloric acid for glass spectra were obtained by evaporating the necessary amount of the copper perchlorate aqueous solutions and then redissolving the residue in perchloric acid.

### C. Discussion and Results

#### 1. Spectra

The anisotropic magnetic parameters for the hexaquocopper (II) system have proven to be quite elusive. A number of workers have determined these parameters in different glass systems, but have obtained varying results. These results are presented in Table III. In addition, we have repeated the measurements in the perchloric acid glass system.

Spencer (1965) originally measured the parameters for the perchloric acid glass system by measuring the line positions. The spectrum is quite simple and consists of a parallel band containing four resolved hyperfine components and a perpendicular band containing a doublet. The interpretation of this doublet is difficult without a simulation method to analyze the spectrum. We have redetermined the anisotropic magnetic parameters by using a simulation technique to analyze the spectrum.

Spencer suggests that the doublet could arise from either hyperfine structure or from two  $g$  values due to the complex having less than tetragonal symmetry in the glass, or from so-called "extra" absorptions. Hyperfine structure would produce four components and hence was expected to give four lines rather than two. However, the theoretical simulation in Fig. 15 shows that the spectrum can be fit quite well with an axial spin Hamiltonian. Only a doublet is observed because of a second order hyperfine effect which shifts two lines of the quartet further than the others. A variable linewidth further accentuates a doublet appearance over a quartet. The parameters determined from the analysis are presented in Table IV.

Table IV shows a large spread in the results of the various workers. Of the three systems utilized, the methanol results are probably the least correct for the hexaquo complex. These measurements were performed with



Fig. 15. Spectrum of  $\text{Cu}(\text{H}_2\text{O})_6^{2+}$  in perchloric acid glass. Upper spectrum is experimental; lower spectrum is simulation.

XBL 7012-7175



TABLE IV. Anisotropic Magnetic Parameters for  $\text{Cu}(\text{H}_2\text{O})_6^{2+}$

Solute/Solvent	$g_{\parallel}$	$g_{\perp}$	$A_{\parallel}^a$	$A_{\perp}^a$	$g^b$	$A^{a,b}$	Reference
$\text{Cu}(\text{NO}_3)_2/\text{methanol}$	2.39	2.07	106	70	2.1767	83.2	Garif'yanov and Usacheva (1964)
$\text{Cu}(\text{ClO}_4)_2/5.3 \text{ HClO}_4$	2.379	2.066	139.6	7	2.1703	46.5	Spencer (1965)
$\text{Cu}(\text{NO}_3)_2/\text{glycerol}$	2.400	2.099	114.05	12.86	2.1993	33.3	Lewis, et al. (1966)
$^{63}\text{Cu}(\text{ClO}_4)_2/5.3 \text{ HClO}_4$	2.387	2.072	137	5	2.177	46.9	This work

a. Coupling constants are in gauss

b. Average values computed from anisotropic values

the hydrated salt in almost pure methanol. The results are probably incorrect due to the formation of copper-methanol complexes.

The results obtained for the 5.26 F perchloric acid and the 60% glycerol glasses are somewhat harder to reconcile. Initially, the perchloric acid system is expected to provide a better glass medium for the hexaquo complex since it is generally accepted that the perchlorate anion does not form complexes with transition metals although the same is not true for glycerol. Furthermore, there are more water molecules (40 F) available in 5.26 F perchloric acid than in 7.5 F glycerol (25 F in water).

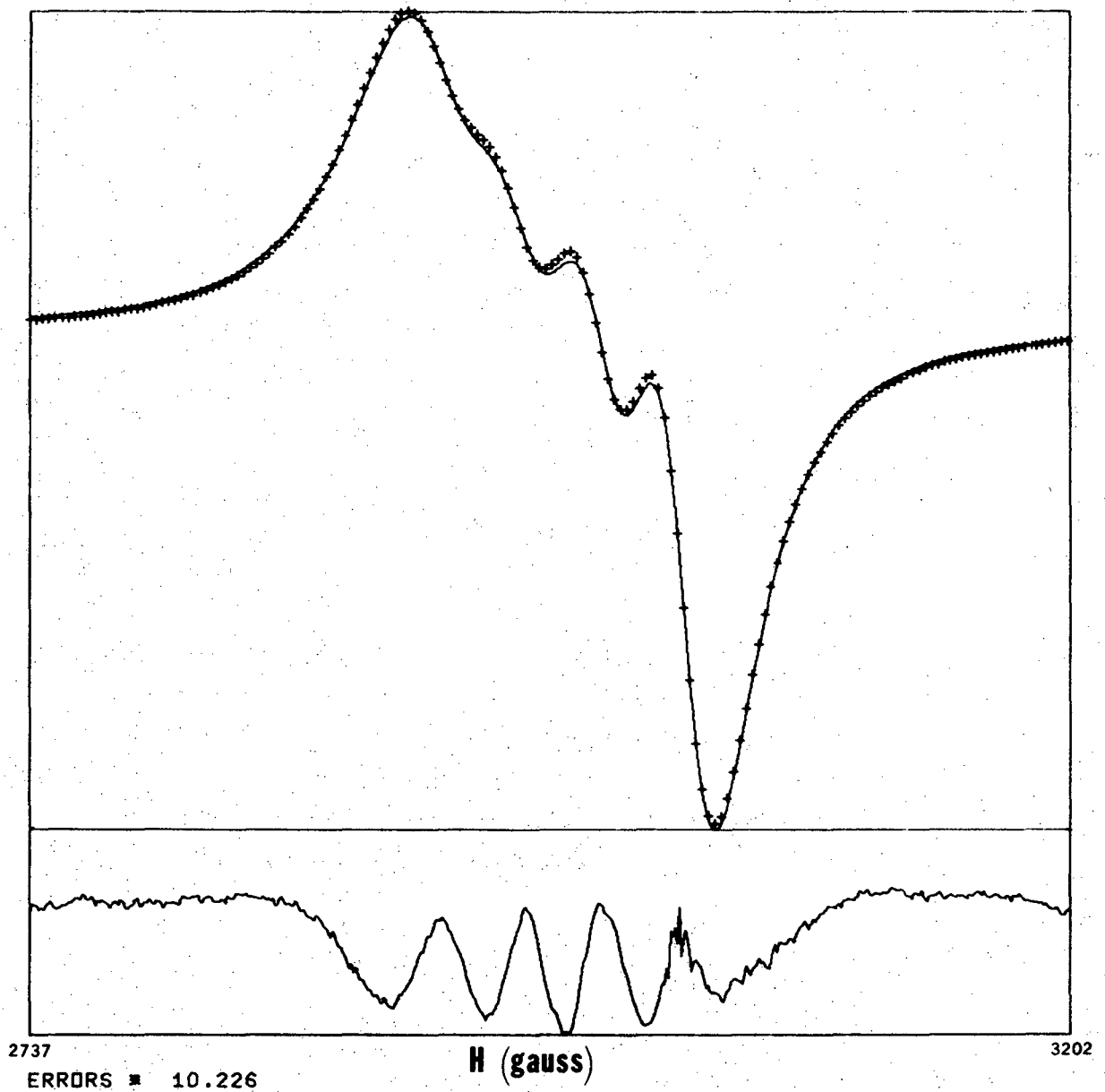
However, the anisotropic parameters may be used to compute average  $g$  and  $A$  values which are expected to be close to the isotropic  $g$  and  $A$  values. The computed average values are also presented in Table IV. A comparison of these values with the experimental isotropic values which are presented later shows that the glycerol parameters agree quite well. But the perchloric acid parameters are very different from the experimental values. As mentioned in the vanadyl discussion, glass spectra need not necessarily produce correct values for the complex in solution. However, the measured difference is striking.

We may note that the  $g$  and  $A$  values are expected to be correlated due to bonding effects (Kivelson and Neiman, 1961). As the  $g$  value decreases, the  $A$  value should increase. This correlation seems to hold for the parallel parameters between the glycerol and the perchloric acid glass. However, the correlation breaks down in the perpendicular parameters. This might be a possible indication that different complexes are being observed. If both spectra were due to copper ions with octahedrally coordinated water

molecules, the correlation would be expected to hold. The choice of which set of parameters to use is somewhat arbitrary. Fortunately, the parameters desired for a linewidth theory are the anisotropies, i.e., the differences between the parallel and perpendicular values, rather than the actual parameters. The anisotropies are in somewhat better agreement than the actual parameters. In fact, both sets of parameters were used for the linewidth study.

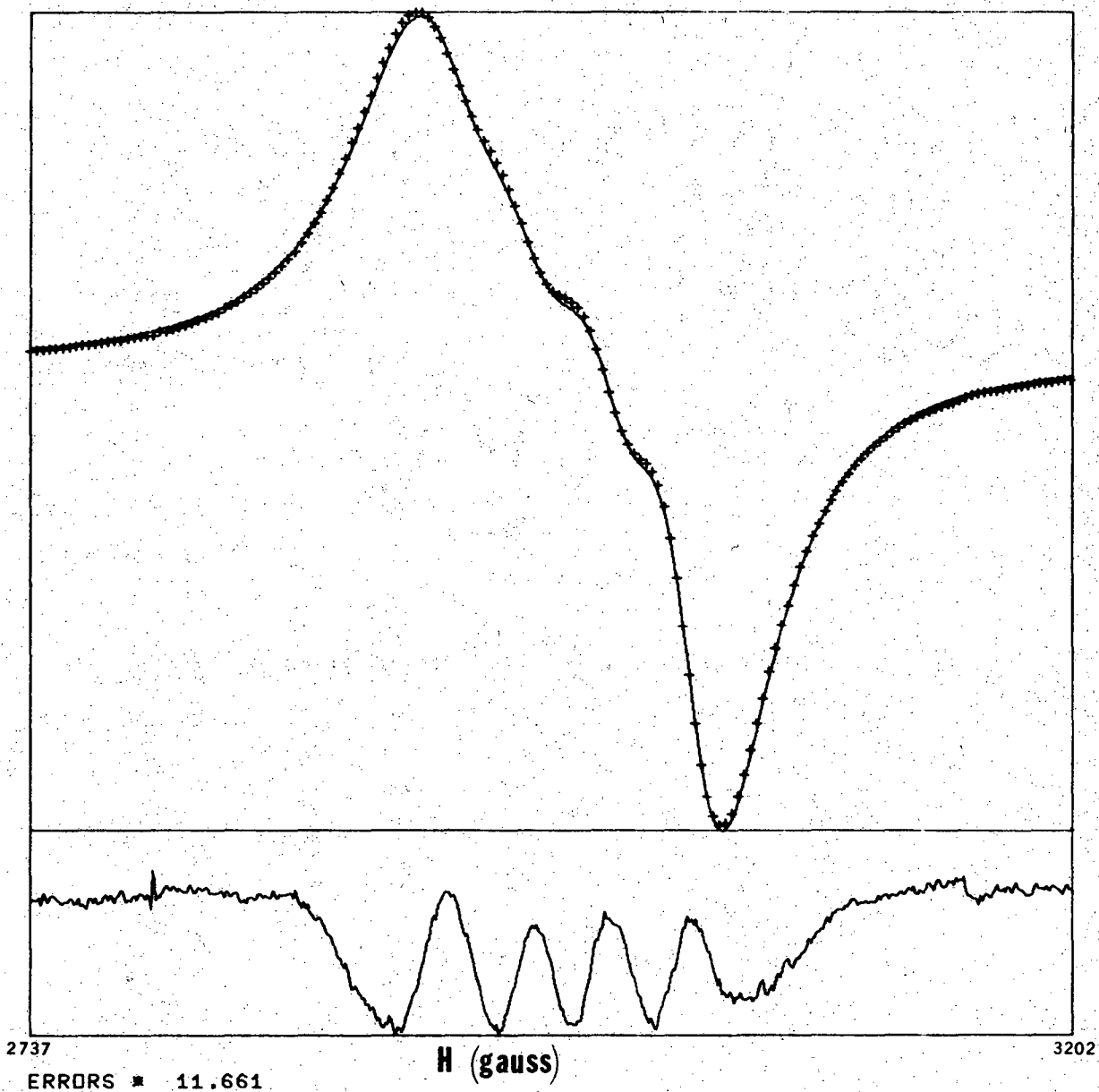
The EPR spectra for hexaquocopper (II) ions in solution have been measured between -15 and 100°C. The spectral parameters were obtained from the digitized spectra using the least squares fitting procedure described previously. The spectra could be fit very well using one intensity, one g value, one coupling constant, and four linewidths. Examples of the fits to the spectra at various temperatures are shown in Figs. 16-19. The crosses are the experimental points; the continuous lines are the theoretical fit. The lower curves in the figures are plots of the difference between the theoretical and experimental curves. We can see from the error curves that the fits are very good. The low temperature spectra (Figs. 16 and 17) exhibit the presence of four hyperfine lines quite clearly. However, the spectra at higher temperatures (Fig. 19) do not exhibit structure.

At room temperature and above the spectra consist of a single, broad, symmetric line. Much of the early work has considered the peak-to-peak width of the unresolved line to be the true width of the line. This would be true if the hyperfine coupling constant were small compared to the linewidth. The observed line would then be very nearly a Lorentz lineshape whose peak-to-peak width would be an excellent



XBL 7012-7169

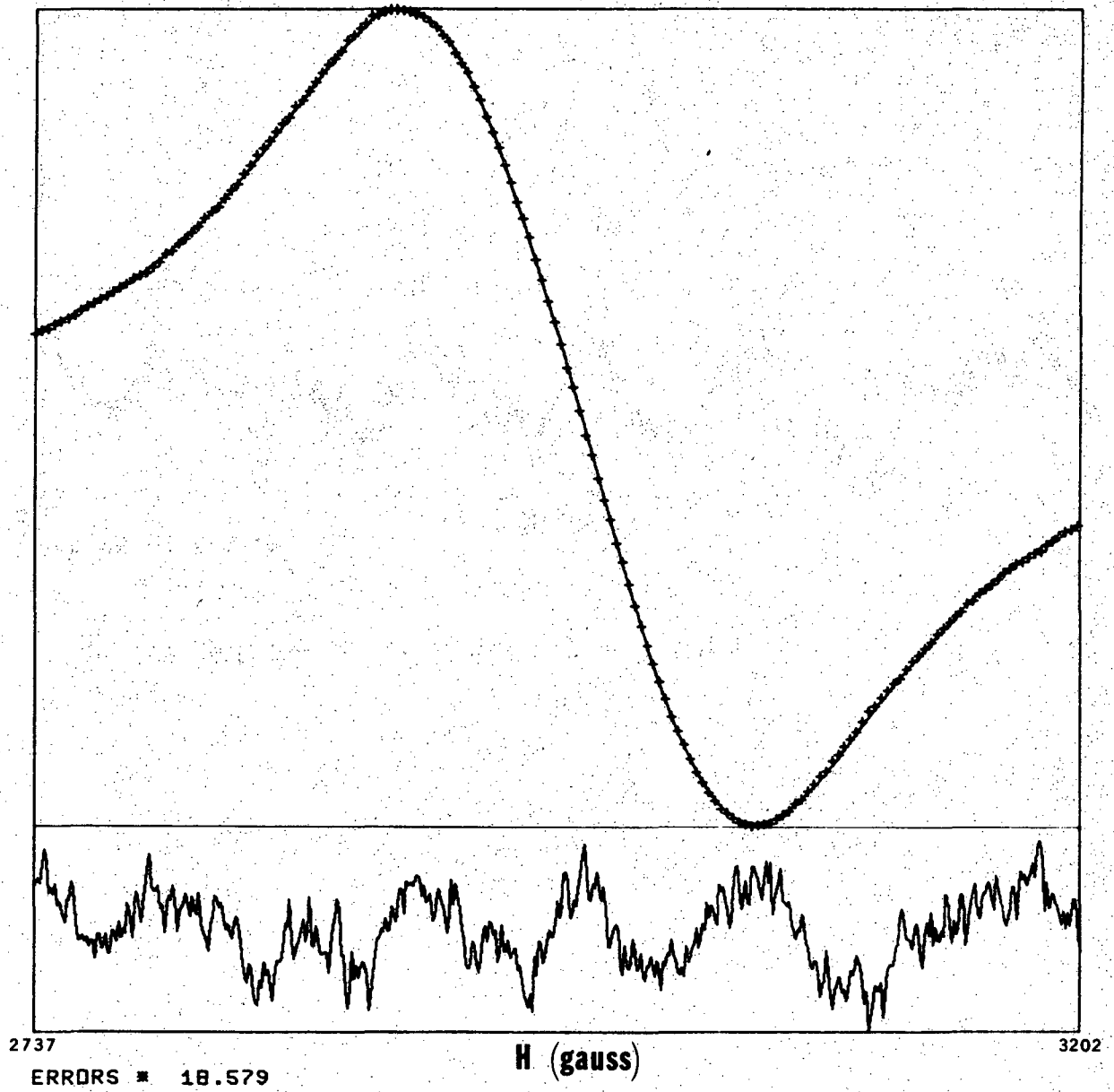
Fig. 16. Example of fit to solution spectrum of  $\text{Cu}(\text{H}_2\text{O})_6^{2+}$  at  $-10^\circ\text{C}$ . In this spectrum and in the following spectra the crosses are the experimental points; the continuous line is the theoretical fit to the data; and the lower curve is the difference between the theoretical and experimental spectra with a scale expansion given by the ERROR\* number.



XBL 7012-7170

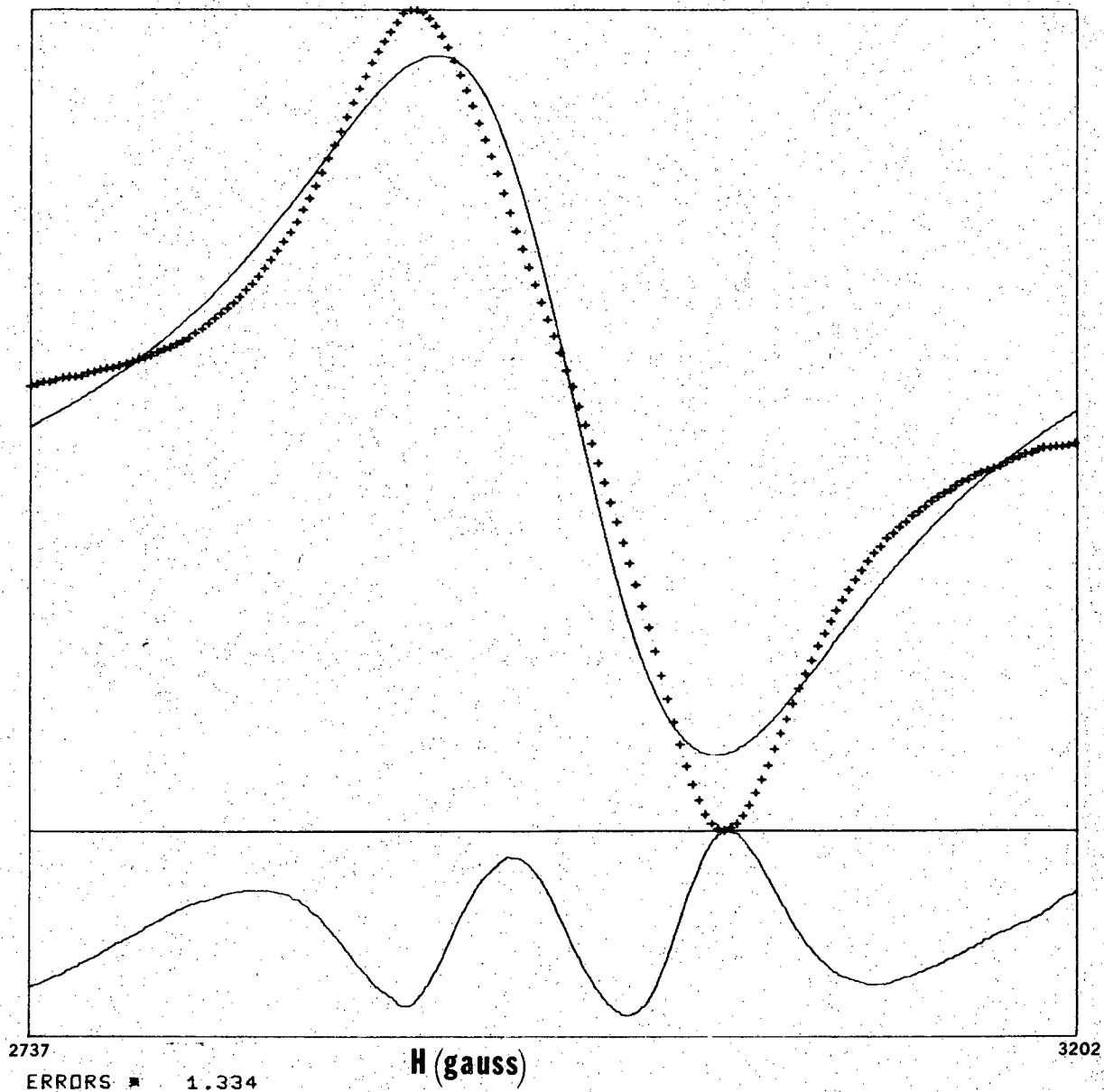
Fig. 17. Example of fit to solution spectrum of  $\text{Cu}(\text{H}_2\text{O})_6^{2+}$  at  $1^\circ\text{C}$ .





XBL 7012-7173

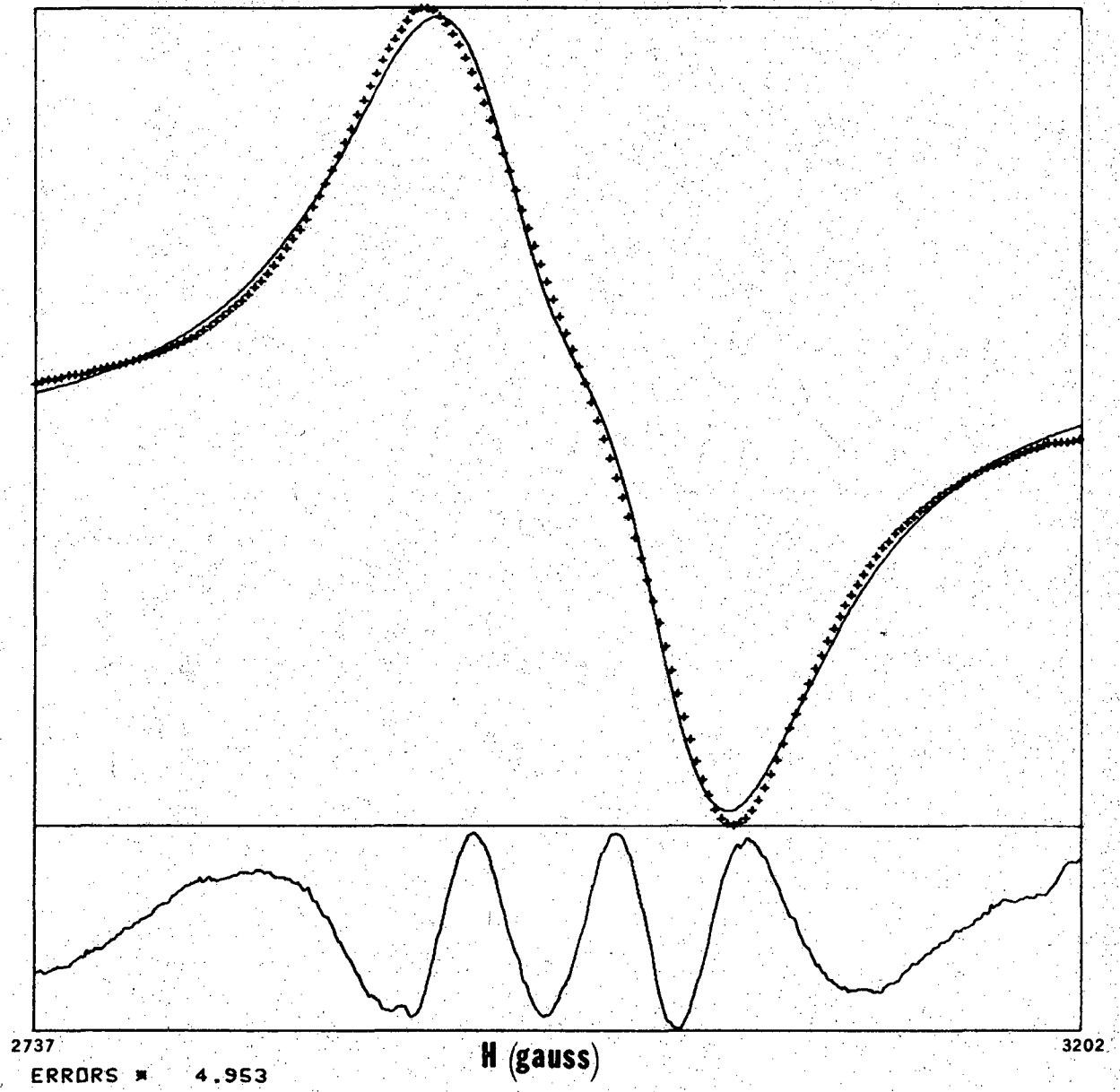
Fig. 19. Example of fit to solution spectrum of  $\text{Cu}(\text{H}_2\text{O})_6^{2+}$  at  $60^\circ\text{C}$ .



XBL 7012-7174

Fig. 20. Attempt to fit spectrum of Fig. 18 with 1 Lorentz line.





XBL 7012-7168

Fig. 21. Attempt to fit spectrum of Fig. 18 with 2 Lorentz lines.

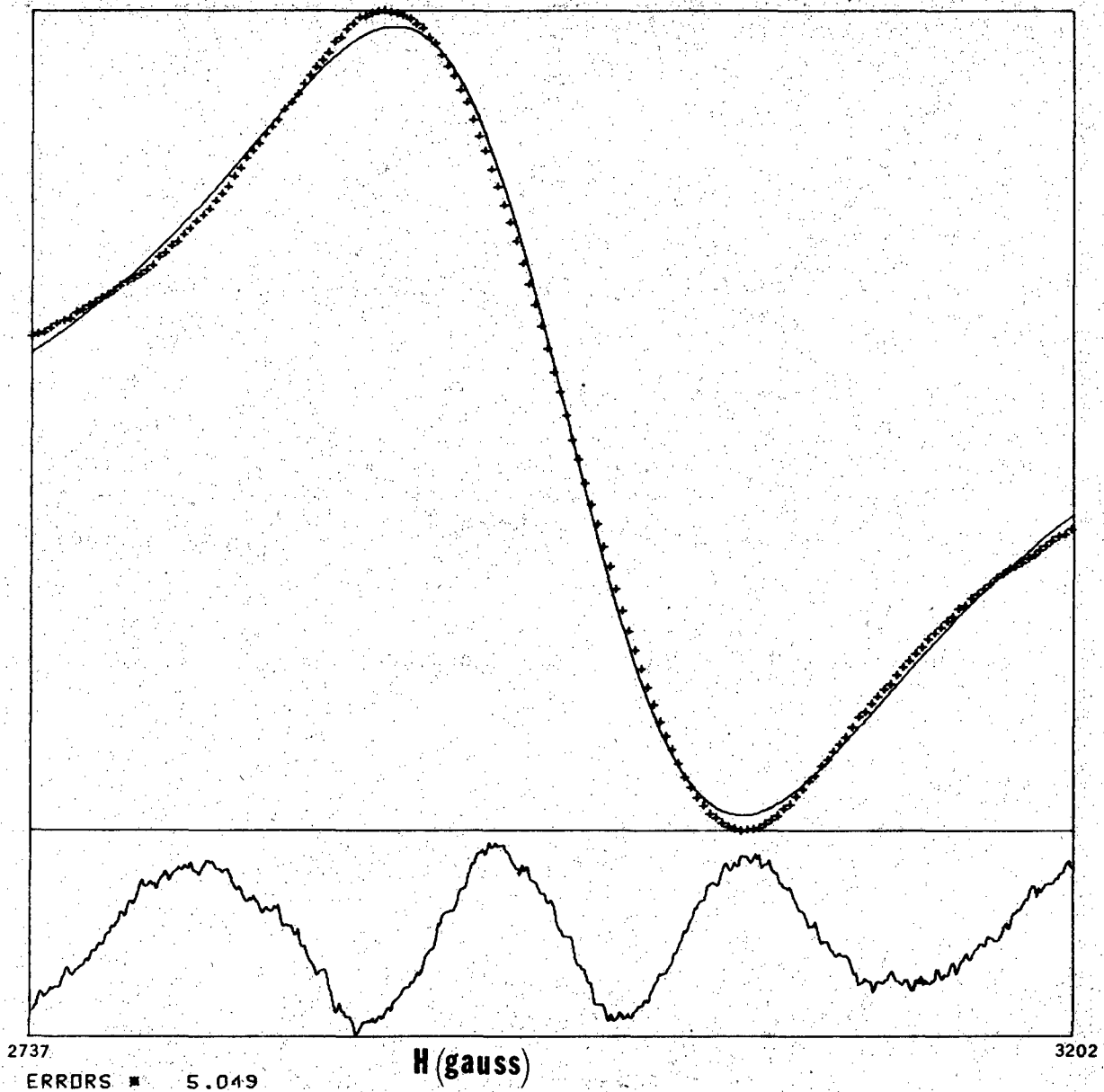
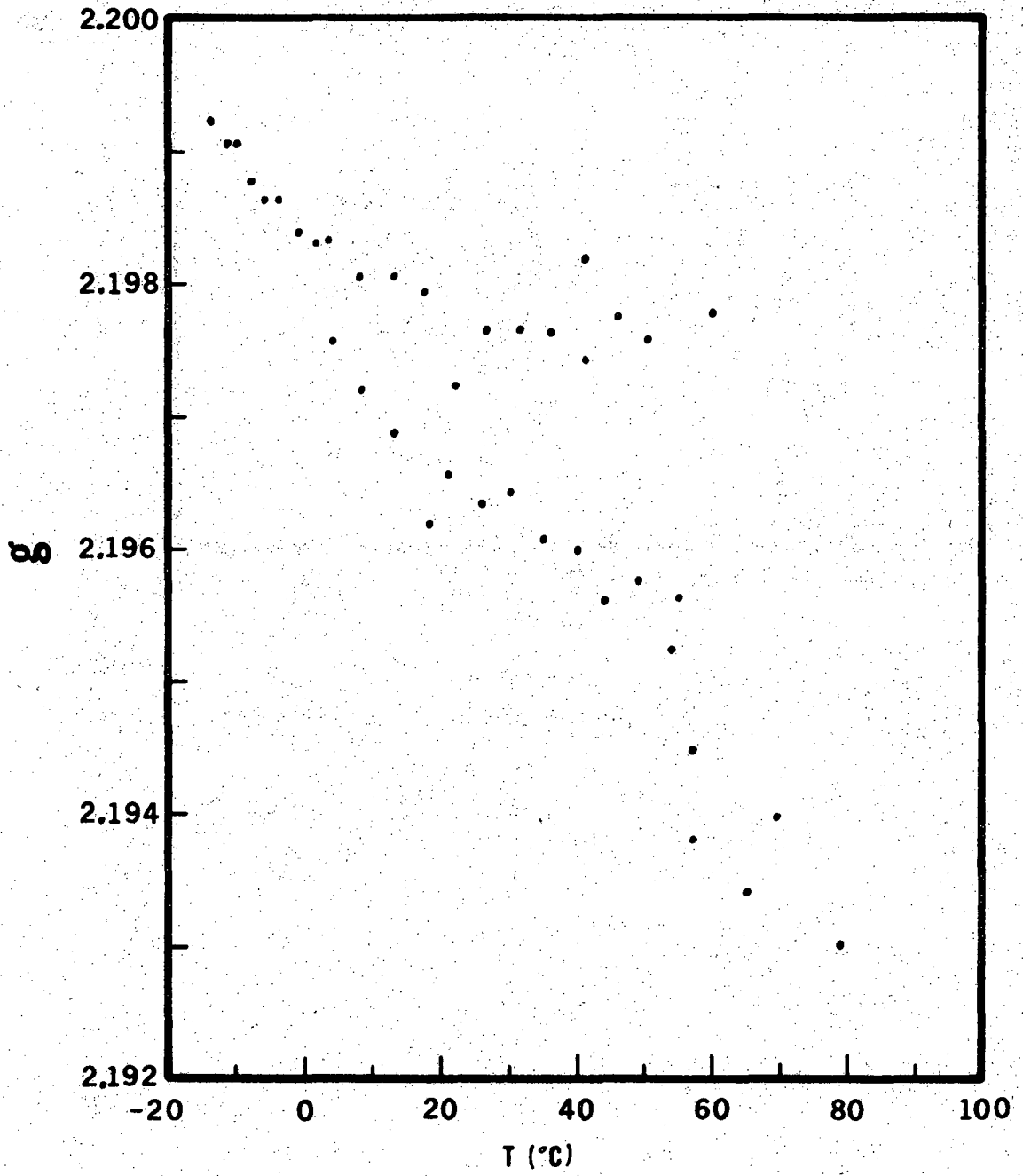
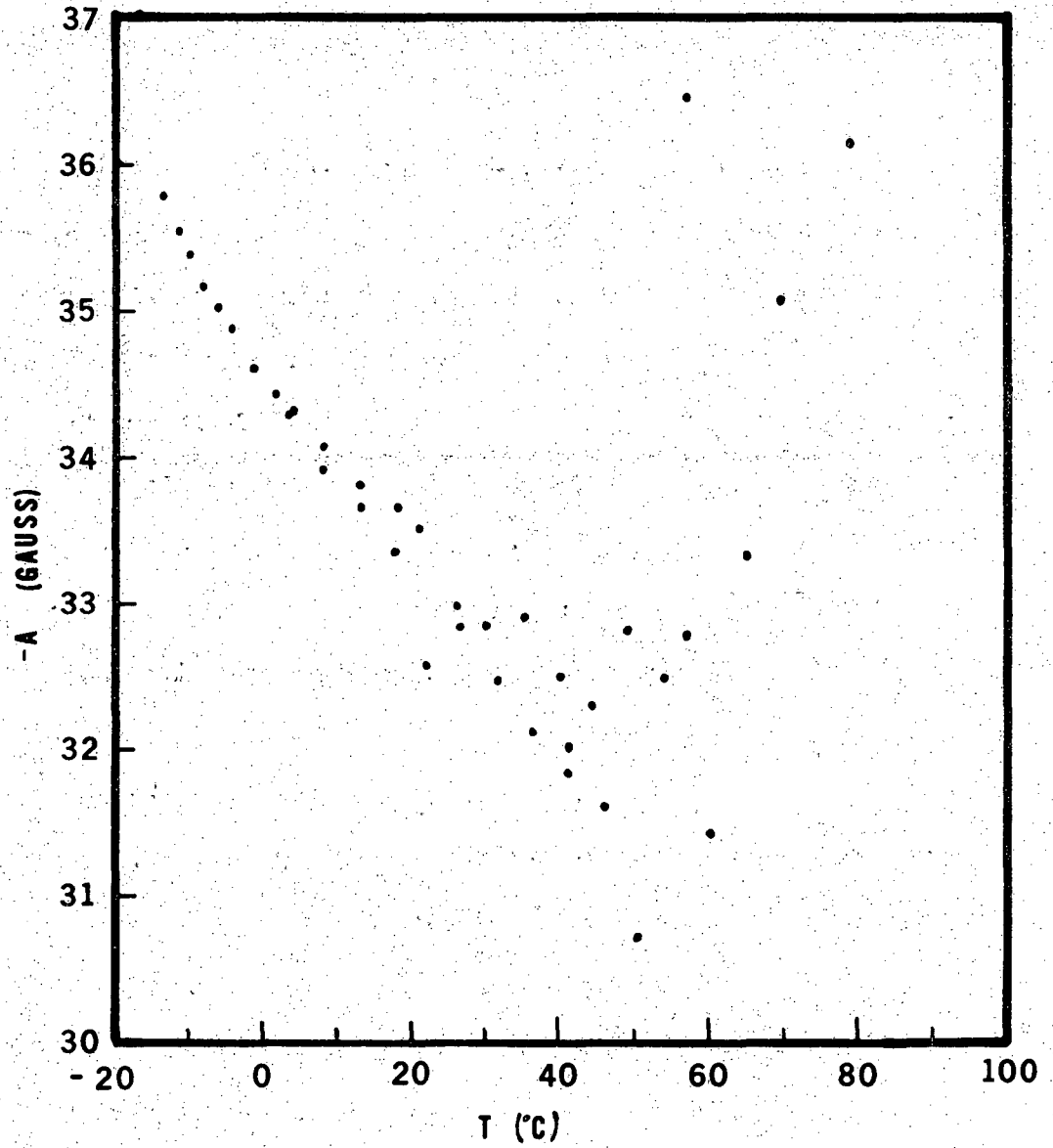


Fig. 22. Attempt to fit spectrum of Fig. 19 with 1 Lorentz line.



XBL 711-18

Fig. 23.  $g$  vs.  $T$  for  $\text{Cu}(\text{H}_2\text{O})_6^{2+}$  ?



XBL 711-19

Fig. 24. -A vs. T for Cu(H<sub>2</sub>O)<sub>6</sub><sup>2+</sup>.

measure of the true width. Without knowledge of the low temperature spectra we would also be tempted to use the overall width as the true width. However, we can convince ourselves that this is incorrect by examining the spectra closely.

The results of an attempt to fit the room temperature spectrum with a single Lorentz line is shown in Fig. 20. This is the same spectrum that was presented in Fig. 18. The spectrum quite clearly does not possess a Lorentz lineshape. In fact close examination of the spectrum reveals several inflections near the center of the spectrum. This is shown more clearly in Fig. 21 which shows the result of fitting two Lorentz lines to the same spectrum. We may confidently infer from this that the observed spectrum consists of more than two lines. It is, therefore, quite reasonable to fit the spectrum with four hyperfine components.

Figure 22 shows the result of fitting the spectrum of Fig. 19 with one Lorentz line. Even at 60°C the spectrum is not Lorentz in shape. Hence, a lineshape analysis indicates that the EPR spectra for hexaquo-copper (II) must be analyzed in terms of four hyperfine components.

The variation with temperature of the isotropic and A values for hexaquo-copper (II) is shown in Figs. 23 and 24. A variation of these parameters with temperature is not unexpected since such variations were observed for the aqueous vanadyl system and for vanadyl acetylacetonate (Wilson and Kivelson, 1966a). However, the usual observation is that the magnitudes of the g and A value change in opposite directions as the temperature is changed, that is, the g value decreases as the A value increases. In the present case the g and A values change in the same direction.

One might at first consider this effect to be an artifact because of the method of analysis. The line positions are determined by a second order spin Hamiltonian. The effect of the second order term is to shift all of the lines downfield. If the second order term is neglected, an apparent  $g$  value is obtained which is higher than the true  $g$  value. Furthermore, if the least squares fit erroneously causes the  $A$  value to decrease, then, the shift due to the second order term would decrease and the apparent  $g$  value would decrease. However, the shifts due to the second order term are on the order of a gauss and the changes in the second order term are somewhat less. Since the changes in the  $g$  value correspond to shifts of several gauss, the effect must be real.

The usual interpretation of the temperature variation is that changes in solvation and bonding are occurring (Wilson and Kivelson, 1966a). However, this theory would require that the  $g$  and  $A$  values change in opposite directions since changes in bonding affect these parameters in opposite ways. Therefore, the variation in the hexaquocopper (II) system cannot be explained by this mechanism.

A number of mechanisms may be responsible for variations of the  $g$  value or of the  $A$  value with temperature. Van Gerven, Talpe, and van Itterbeck (1967) have suggested a shift due to demagnetizing effects. They show that the shift in the  $g$  value,  $\Delta g$  is approximately given by

$$\Delta g \sim (2N_s - N_1) \chi_s \quad (4.2)$$

where  $N_s$  and  $N_1$  are so-called demagnetizing factors, which are computed from the geometry of the sample, and  $\chi_s$  is the static volume susceptibility of the sample. The  $g$  value variation is expected to follow a Curie

law. However, the magnitude of this effect is quite small and would not account for the large  $g$  value changes which are observed. Furthermore, this mechanism is not expected to cause a variation in the hyperfine coupling constant.

A second source of shifts are dynamic effects due to relaxation effects in solution. Such effects have been discussed by Fraenkel (1967) and by Kivelson (1960). These effects are found in most treatments of relaxation theories but are generally ignored by assuming that the static Hamiltonian can be redefined to include these terms (Slichter, 1963). The spin Hamiltonian is rarely redefined in practice. Kivelson derives a nonsecular shift to be

$$\Delta = \tau_c \omega_o T_1^{-1} \quad (4.3)$$

where here  $T_1^{-1}$  is the nonsecular contribution from the linewidth theory and is dependent upon  $m_I$ . The shift is then dependent upon the hyperfine component and follows a temperature dependence involving the correlation time and linewidth. Since the shifts are different for each hyperfine component, the hyperfine coupling constant may change as well as the  $g$  value although the effect of the shifts on the least squares determination is not clear. The effect of Eq. 4.3 can be estimated if the full linewidth is assumed to be due to  $T_1^{-1}$ . In fact the magnitude of the changes with temperature could account for the magnitude of the  $g$  value changes. However, the computed shift is a downfield shift which increases with temperature. This should cause an increase of the  $g$  value with temperature whereas the  $g$  value decreases with increasing temperature. Hence, nonsecular shifts cannot be the reasons for the  $g$  value variation.

Another possible dynamic effect is the thermal vibrations of the ligands. Benedek, Englman, and Armstrong (1963) have studied the temperature dependence of NMR chemical shifts due to thermal vibrations. The effective crystal field splitting changes because the amplitudes of vibration change as a function of temperature. Unfortunately this effect would predict that the  $g$  and  $A$  values should change in opposite directions.

Walsh, Jeener, and Bloembergen (1965) and Soos (1968) have studied the variation of the  $g$  tensor as a function of temperature in the solid state. Soos explains his variations for organic radicals in terms of delocalization of the electrons over radicals with slightly different  $g$  tensors. As the temperature changes, the delocalization changes and the observed  $g$  tensor changes. Walsh, et al., explain their behavior in terms of changes in the crystal field due to thermal expansion effects. In these experiments, the  $g$  value decrease with increasing temperature was well explained by crystal field changes due to lattice expansion.

However, Walsh observed that the hyperfine interaction (for  $Mn^{2+}$ ) decreased as the temperature increased, whereas the explanation for the  $g$  value change would predict an increase in the  $A$  value. Orbach (Simanek and Orbach, 1966; Calvo and Orbach, 1967) has studied this behavior and proposed that excited state configurations were mixed into the ground state by a "dynamic phonon-induced" field. This explanation was proposed for  $S$  state ions but might be applicable to other states.

Admittedly, these solid state explanations are not directly applicable to solution, but temperature dependent mixing of excited state configurations with the ground state is a possible explanation for the  $g$  and  $A$  value variation. Indeed, the hexaquoocopper (II) complex is



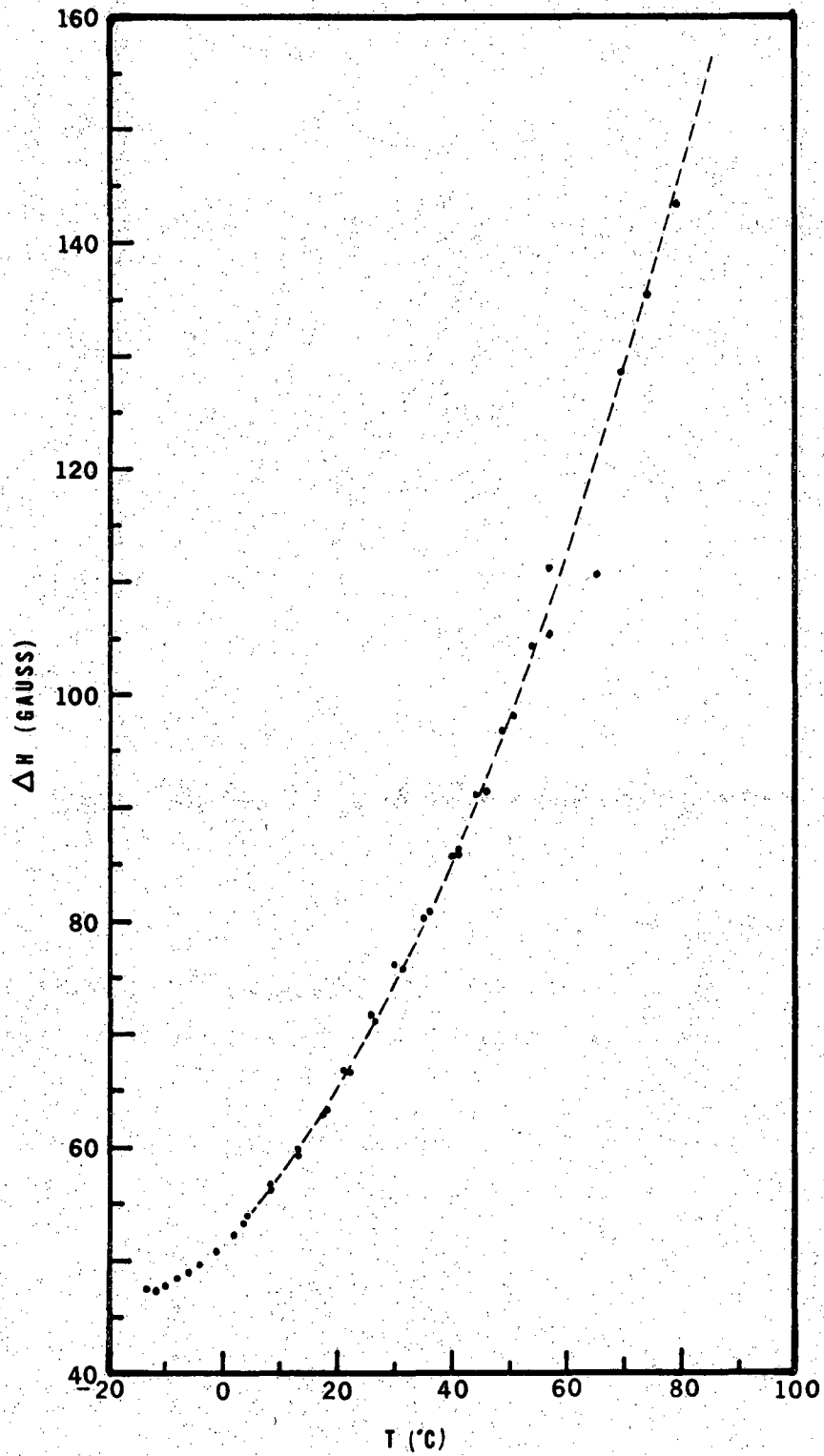
expected to have a low lying excited state due to the Jahn-Teller effect. This state could have an appreciable effect on the  $g$  and  $A$  tensors.

The source of the variation of the  $g$  and  $A$  tensors is not well understood. Fortunately, the variation in the parameters is relatively small so that the variation is neglected for the linewidth theories. The values of the isotropic parameters used for the linewidth analysis are  $g=2.1983$  and  $A = -34.4$  gauss.

## 2. Relaxation

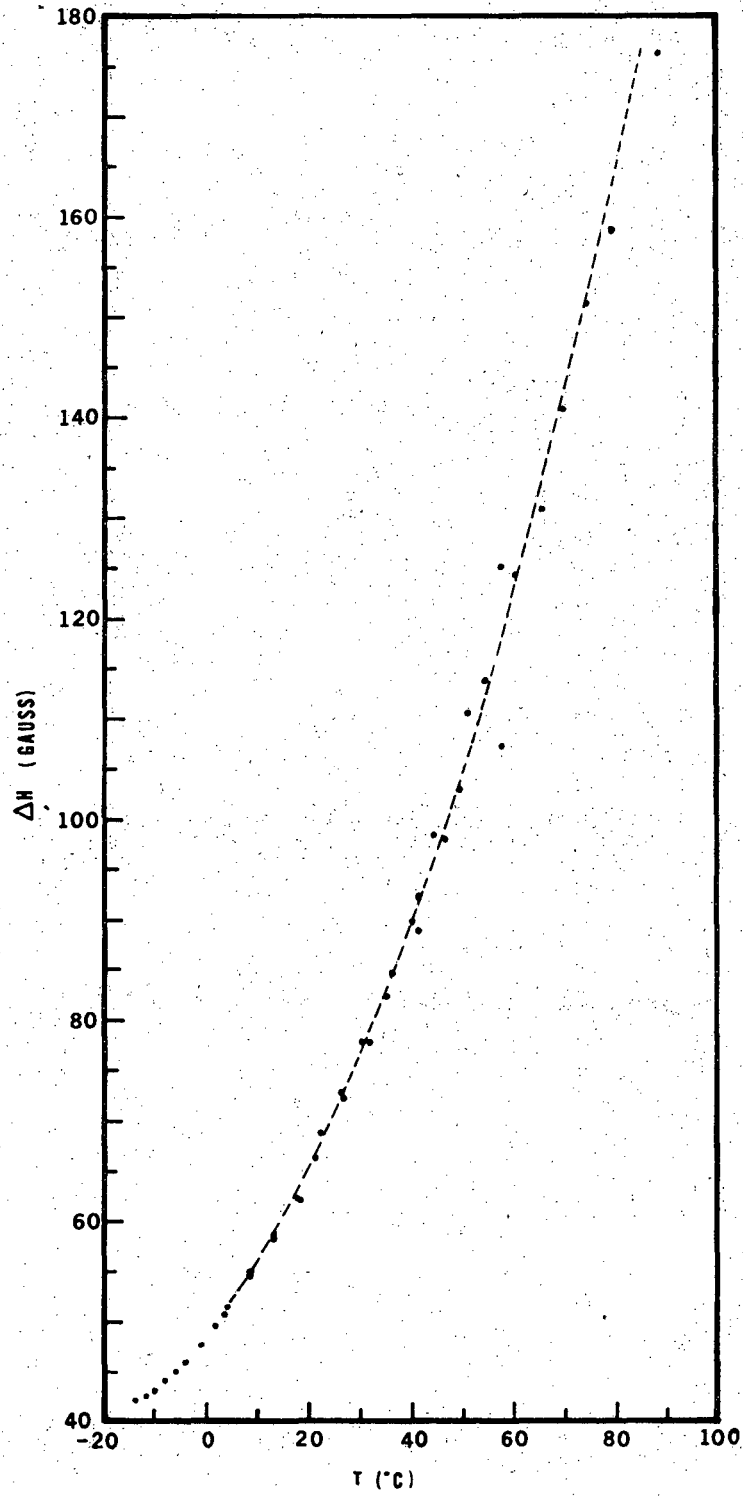
The linewidths for hexaquocopper (II), which were also determined from the least squares fits, are presented in Figs. 25-28. The components are identified by  $m_I$ , the nuclear magnetic quantum number, and since the hyperfine coupling constant is assumed to be negative, the  $m_I = -3/2$  line is the lowest field line and the  $m_I = +3/2$  line is the highest field line. The linewidths for the components show a smooth functional dependence on the temperature, increasing monotonically with the temperature. Below  $40^\circ\text{C}$  the deviations in the data are small. Above this temperature, there is increasing scatter in the data. At the lowest temperatures where hyperfine components are distinctly visible, the linewidths are known to about .5%. Near room temperature where the line is unresolved, but definitely not Lorentzian, the error is expected to be about 1%. There is much less confidence in the data at higher temperatures where the line is near Lorentzian, and the error is expected to be several per cent. The dashed curves in the figures are arbitrary interpolation curves.

The linewidths for the hyperfine components are compared in Fig. 29. Examination of the low temperature region reveals a distinct dependence on hyperfine component, with the narrowest line being the  $m_I = +3/2$  or



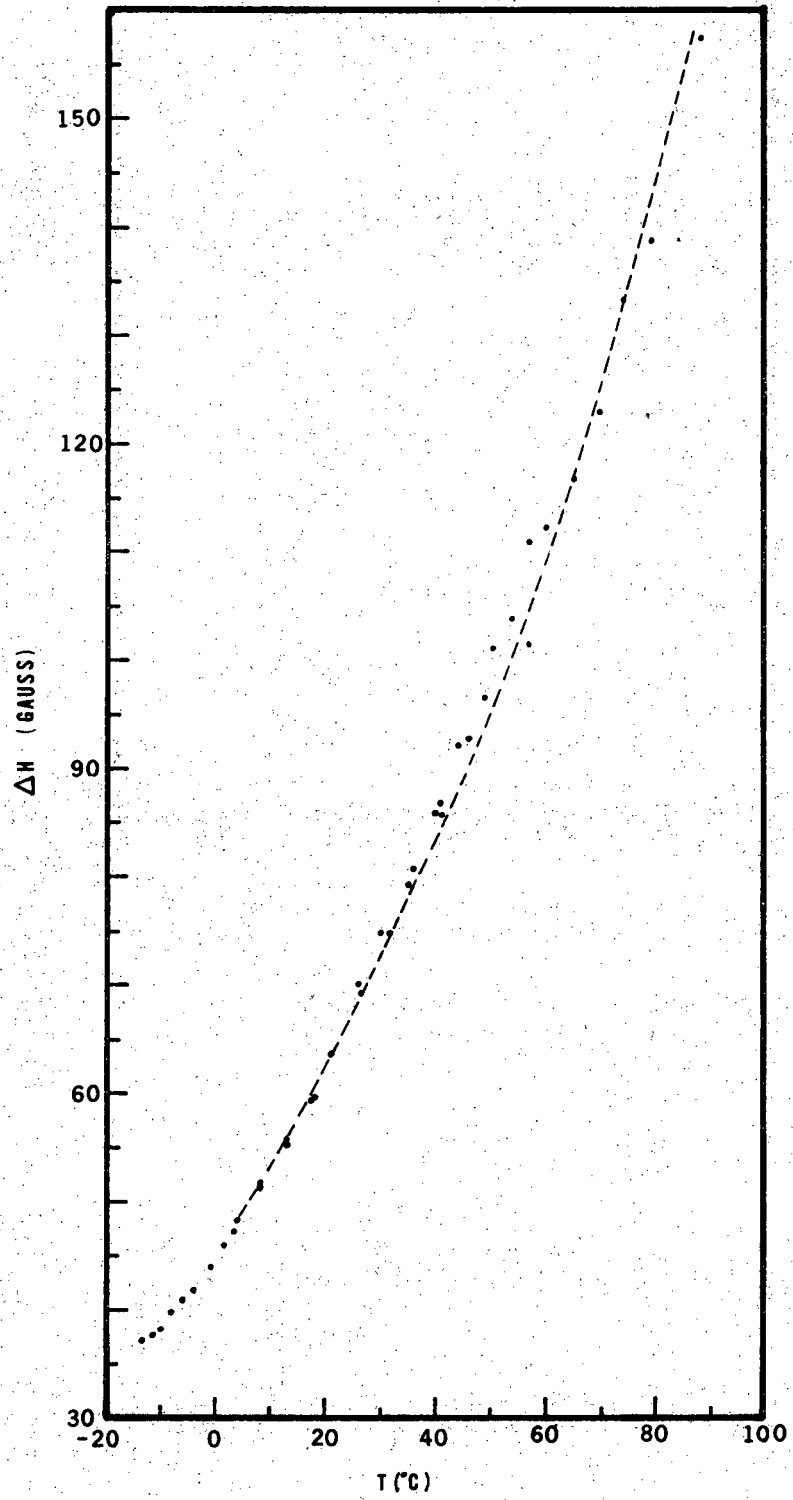
XBL 7012-7490

Fig. 25. Peak-to-peak linewidth of  $-3/2$  component vs.  $T$ . Dashed curve is interpolation graphical.



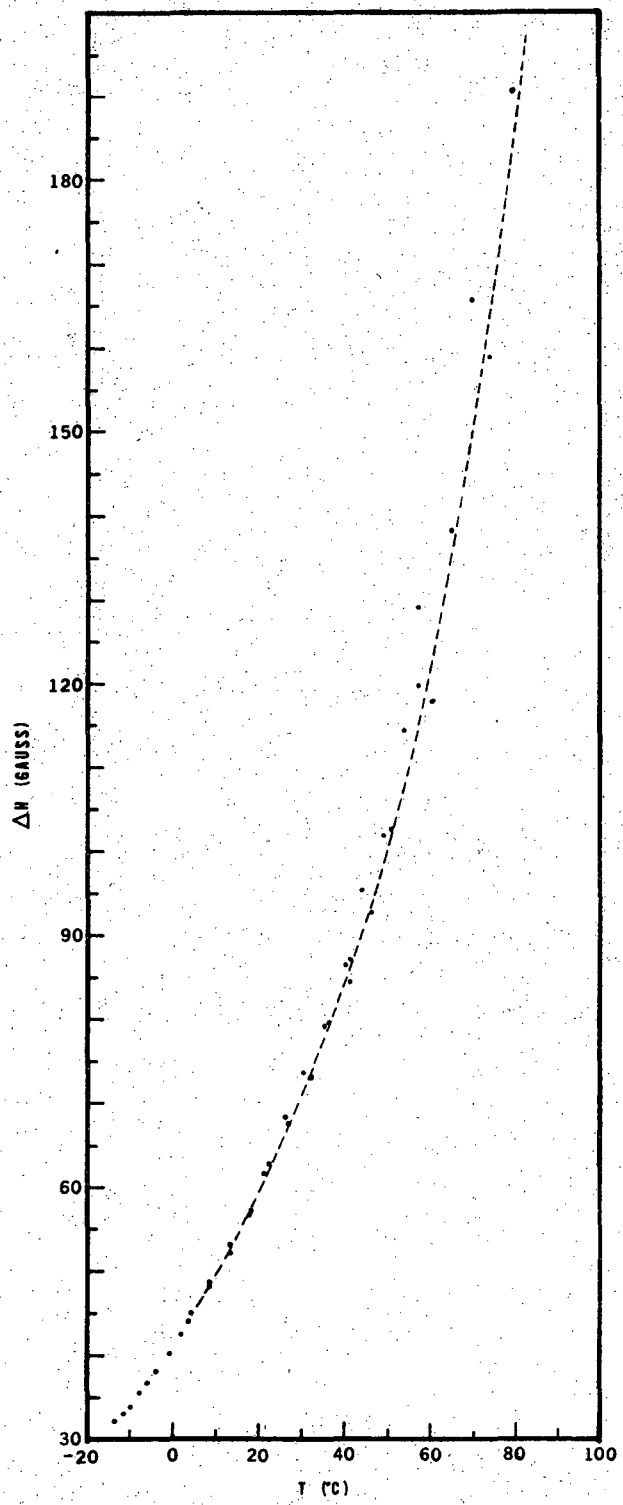
XBL 7012-7493

Fig. 26. Peak-to-peak linewidth of  $-1/2$  component vs.  $T$ .



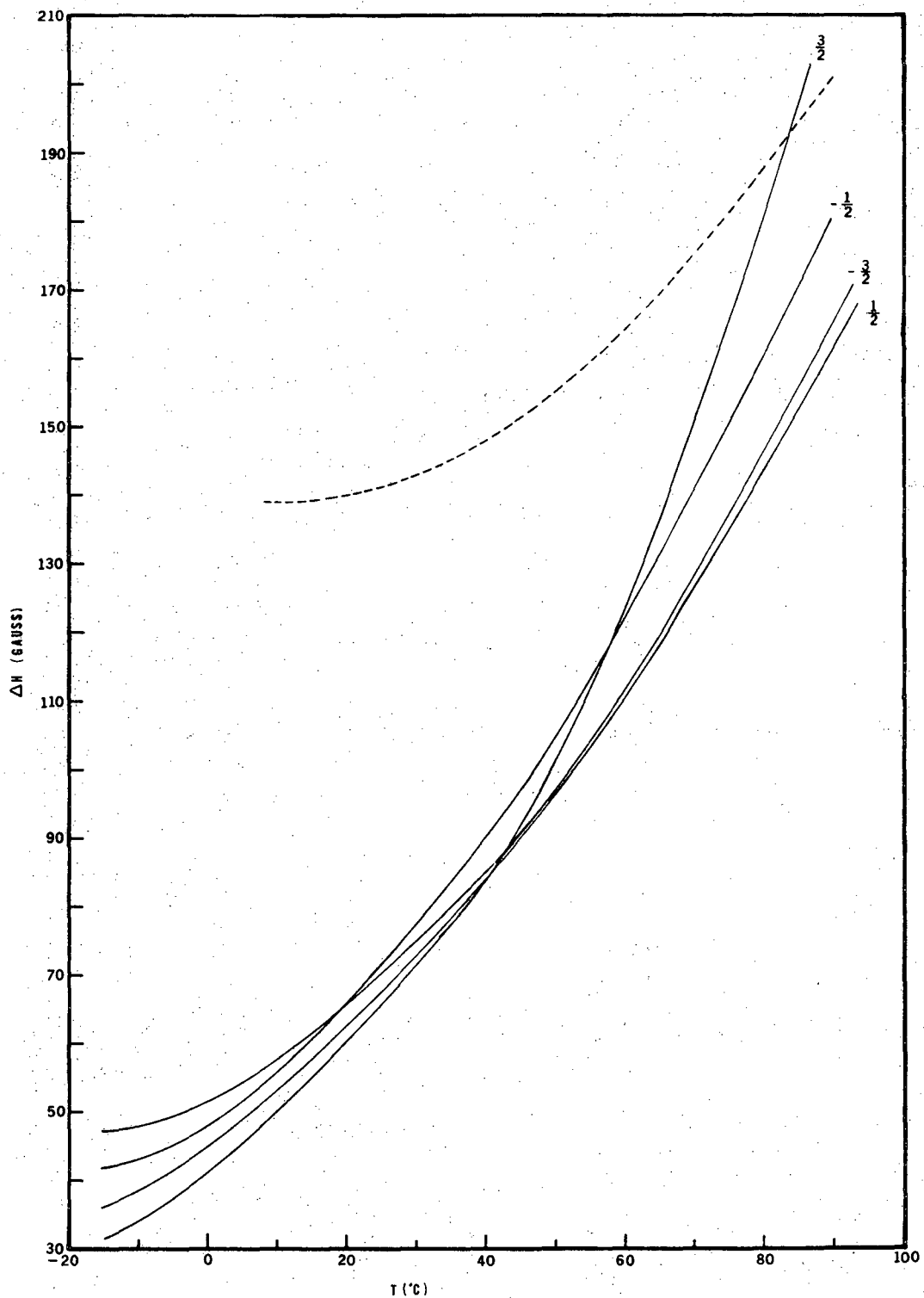
XBL 7012-7489

Fig. 27. Peak-to-peak linewidth of +1/2 component vs. T.



XBL 7012-7491

Fig. 28. Peak-to-peak linewidth of +3/2 component vs. T.



XBL 7012-7492

Fig. 29. Comparison of linewidths for hyperfine components of  $\text{Cu}(\text{H}_2\text{O})_6^{2+}$ .

highest field line. The lines are progressively broader as  $m_I$  is decreased, with  $m_I = -3/2$  as the broadest line. As the temperature is increased, the relative widths change until the  $m_I = -1/2$  line becomes the broadest line. At still higher temperatures, the  $m_I = +3/2$  line appears to become the broadest line. We are not certain that this behavior is real. At the high temperatures least squares procedures are quite difficult. Noise and drifts in the spectrum could cause large changes in the least squares fits. However, the linewidths definitely depend on the hyperfine component at low temperatures and appear to depend on the hyperfine component at higher temperatures.

The dashed line in Fig. 29 is the linewidth determined from the overall peak-to-peak distance of the unresolved line. The fallacy of using the overall width as the true width is clearly seen. The temperature dependence and the magnitudes of the width are incorrect. Valiev and Zaripov (1966) indicate that their mechanism is consistent with this data, so that the mechanism is probably incorrect for the copper system.

The dependence of the linewidths on hyperfine component leads one to suspect a Kivelson tumbling mechanism (Wilson and Kivelson, 1966a) to be contributing to the linewidth. In accord with this idea, the linewidths were fit to a cubic polynomial. The polynomial is exactly determined by four linewidths, so that the polynomial coefficients may be strongly influenced by small errors in the linewidths. The parameters which were determined are presented as the points in Figs. 30-32. The alpha parameter appears to vary quite smoothly with temperature. The beta and gamma parameters exhibit much scatter which is extreme at high temperatures. The delta parameter is even worse (not presented). (The correlation of temperature with viscosity divided by temperature is presented in Table II.)

As was done with the vanadyl data, the beta parameter was used to determine a hydrodynamic radius for the complex using Eqs. 2.6 and 2.3. The theoretical values for  $\alpha'$  and  $\gamma$  were then computed from Eqs. 2.5 and 2.7 and are presented as the smooth curves in Figs. 30-32. These curves were computed using the anisotropic magnetic parameters which were determined in this work (see Sec. IV.C.1). The curves computed with the Lewis, Alei, and Morgan parameters are quite similar, and, therefore, are not plotted. We can see immediately that the theoretical and experimental parameters are in marked disagreement. The beta fit is relatively good at low temperatures. However, the experimental values for the gamma parameter are negative until the lowest temperatures are reached. The theory predicts that the gamma parameter should be positive over the entire temperature range. The theoretical prediction of the alpha parameter is also far from agreement with experiment.

Furthermore, the values of the correlation time and the hydrodynamic radius which are determined from the fit to the beta parameter are anomalously low. The radius,  $r=1.71$  A, which was determined using the anisotropic parameters from this work, is of the order of the ionic radius for copper. If the Lewis, Alei, and Morgan (1966) magnetic parameters are used, the radius is  $r=1.83$  A, which, although better, is still too small. By analogy to the vanadyl system, the radius is expected to be on the order of 3 A. Cox and Morgan (1959) and Morgan and Nolle (1959) have measured the proton NMR for copper solutions. The proton relaxation is due to a dipolar interaction modulation by molecular tumbling, so that the correlation time is related to the hydrodynamic radius by Eq. 2.3. These workers obtain a radius  $r=2.8$  A. Frankel (1968) in a more recent study obtained  $r=2.3$ A.



The validity of the Kivelson tumbling model for the hexaquocopper (II) system is doubtful. Further evidence is obtained from the dependence of the theory on magnetic field. The EPR spectrum for hexaquocopper (II) was measured at S band (3.12 GHz) at room temperature (about 22°C). The spectrum is presented in Fig. 33. The linewidths obtained from a least squares fit to the S band spectrum are 67.8, 66.9, 65.7 and 65.9 gauss, respectively, for the  $-3/2$  to  $+3/2$  component. The corresponding linewidths for the X band spectrum are 66.6, 67.7, 64.1, and 62.0 gauss (from Fig. 29). Although there is a definite dependence upon hyperfine component, there is relatively little difference between the S band and X band linewidths. The Kivelson theory would predict a strong dependence of the linewidths with magnetic field. In addition, if we ignore these problems and continue to use the Kivelson mechanism, we may compute a linewidth contribution from the spin-rotation mechanism. If this is done, we compute linewidth contributions which are five times the experimental linewidths. Therefore, this procedure cannot be used to explain the linewidths, although it was very successful for the vanadyl case.

We must, therefore, proceed in another manner to explain the linewidths. The increase of the linewidths with temperature strongly indicates a spin-rotation mechanism. Ignoring the  $m_I$  dependent terms for the present, we plot the  $m_I$  independent linewidth, the alpha term, vs.  $T/\eta$  in Fig. 34. The alpha term is quite linear with temperature divided by viscosity. (The alpha term has not been corrected for a contribution from the tumbling mechanism because of the uncertainty with the theory). This is consistent with the prediction of a spin-rotation mechanism except that the extrapolation of alpha to zero temperature does not pass through zero. Nevertheless, we may use the slope of a straight line fit to the

data with Eq. 2.12 to determine a hydrodynamic radius of  $r=3.08$  A. This is a reasonable value.

If we assume the spin-rotation mechanism to be dominant, we may compute a contribution from the tumbling mechanism using the new hydrodynamic radius. If this is done, the predicted linewidth parameters are found to be much larger than the experimental parameters. Since we expect the tumbling mechanism and the spin-rotation mechanism to be consistent with each other, we must conclude that these mechanisms cannot both be fully operative in the hexaquoocopper (II) system.

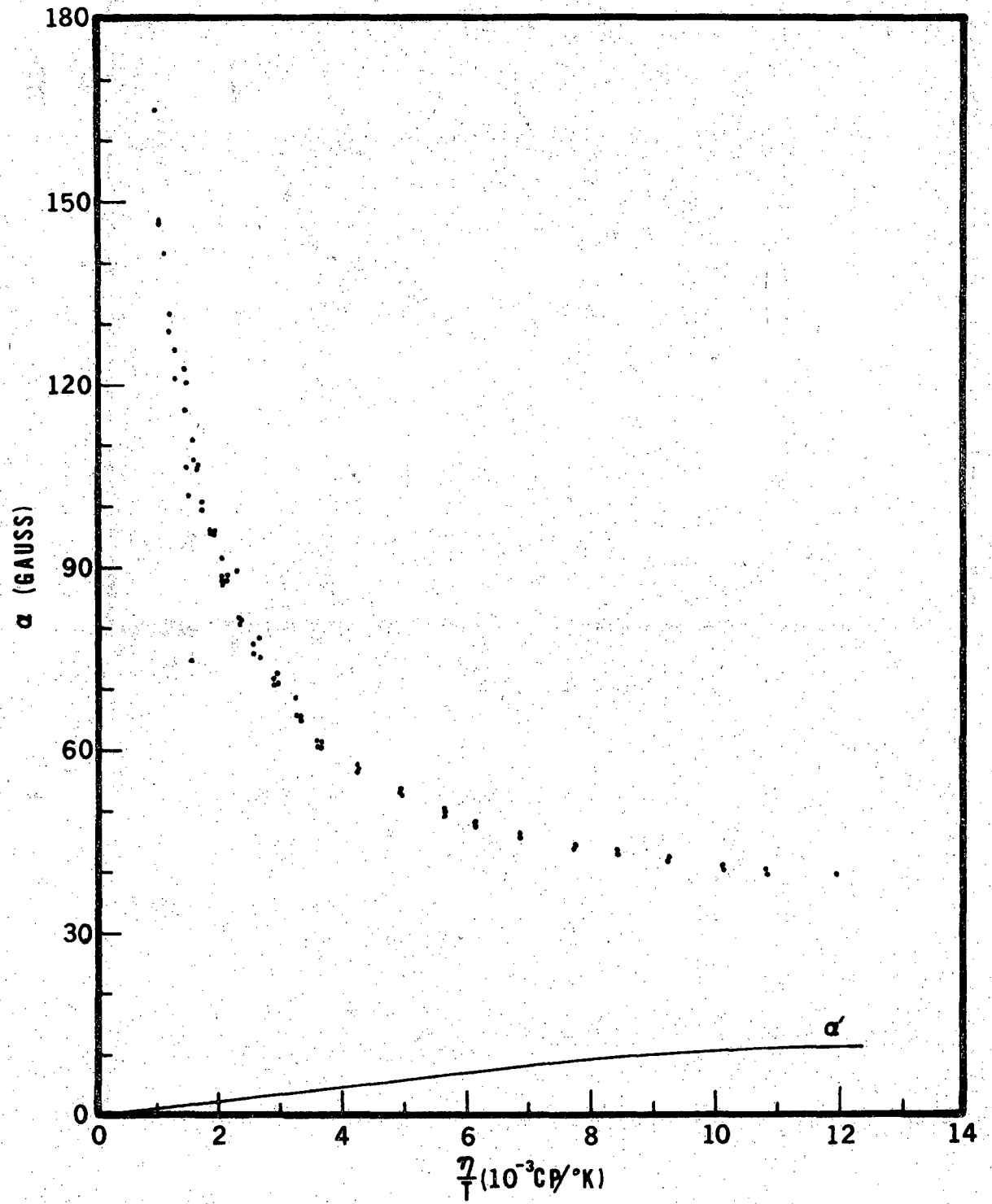
Lewis, Alei, and Morgan (1966) propose that the anisotropy of the copper complex is less in the aqueous solution than in the glass. They reduce the anisotropies,  $\Delta g$  and  $b$ , and compute a contribution of the tumbling mechanism to the linewidth. After correcting the  $m_I$  independent term for the tumbling contribution, they fit the remainder to a spin-rotation mechanism. They also include a term quadratic in temperature which they describe as a Raman process (see Eq. 4.1). This term is necessary to account for the curvature which appears in the alpha term after the tumbling correction is made.

The Raman mechanism was proposed on the basis of an extrapolation from the solid state work of Gill (Gill, 1965; Stoneham, 1965) on copper ions in Tutton salts. However, the more recent calculations of Kivelson (1966) have shown that the contributions of the Raman process in liquids is small. Therefore, although Lewis, Alei, and Morgan fit the  $m_I$  independent term well with a spin-rotation interaction and a  $T^2$  term, the Raman process is not indicated.

Furthermore, Lewis, et al., are slightly inconsistent in their adjustment of the anisotropies. Although they adjust the anisotropies

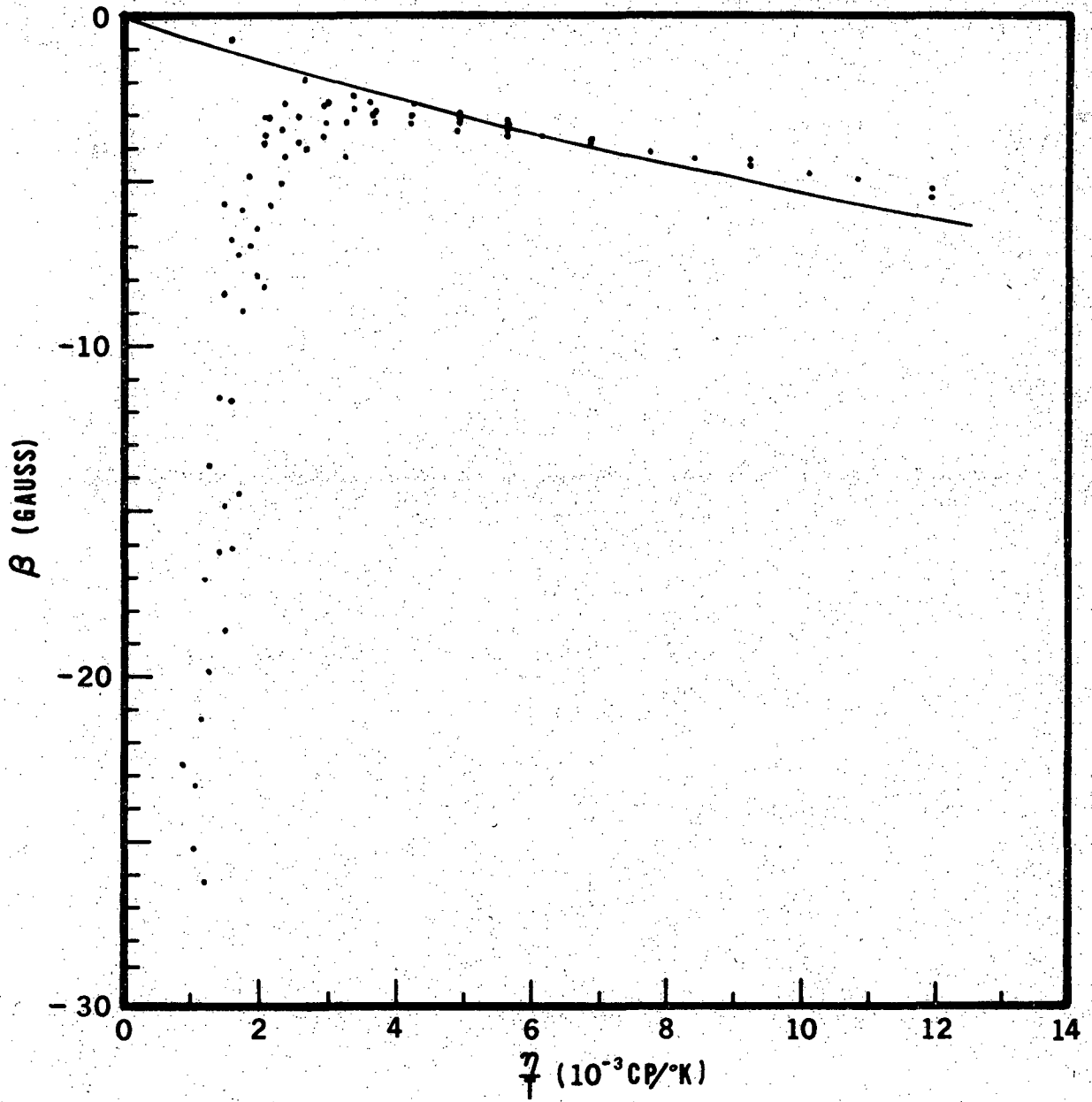
to compute the tumbling width, they do not adjust the  $g$  values in computing the spin-rotation width. Furthermore, they show that the magnitude of the  $^{17}\text{O}$  coupling constant, which they measure from temperature dependent shifts of the  $^{17}\text{O}$  NMR line, is consistent with the anisotropic parameters determined in a glass. In addition, they argue from Stoneham's work (Stoneham, 1965) that the first orbitally excited state for the hexaquocopper (II) complex is expected to be  $7700\text{ cm}^{-1}$  above the ground state. This is consistent with a large tetragonal distortion and, hence large anisotropy.

The linewidths in hexaquocopper (II) are then somewhat of a mystery. The solution Raman process is unlikely. The solution Orbach process is unlikely if the lowest excited state is  $7700\text{ cm}^{-1}$  above the ground state. The increase of the linewidth with increasing temperature is most likely explained by a spin-rotation interaction. However, the contribution from a tumbling mechanism consistent with the spin-rotation interaction and with the large anisotropy is too large. The tumbling mechanism cannot contribute its full effect and must be interrupted by some other relaxation process which is also  $m_I$  dependent. This would be something similar to the inversion mechanism discussed by Spencer (1965). Spencer treated both mechanisms separately. A more proper treatment is probably to treat both the tumbling process and the inversion process together. The linewidths in hexaquocopper (II) are then due to a spin-rotation interaction, a tumbling mechanism, and a third process, similar to inversion, which interrupts the tumbling mechanism, and which is essentially independent of magnetic field.



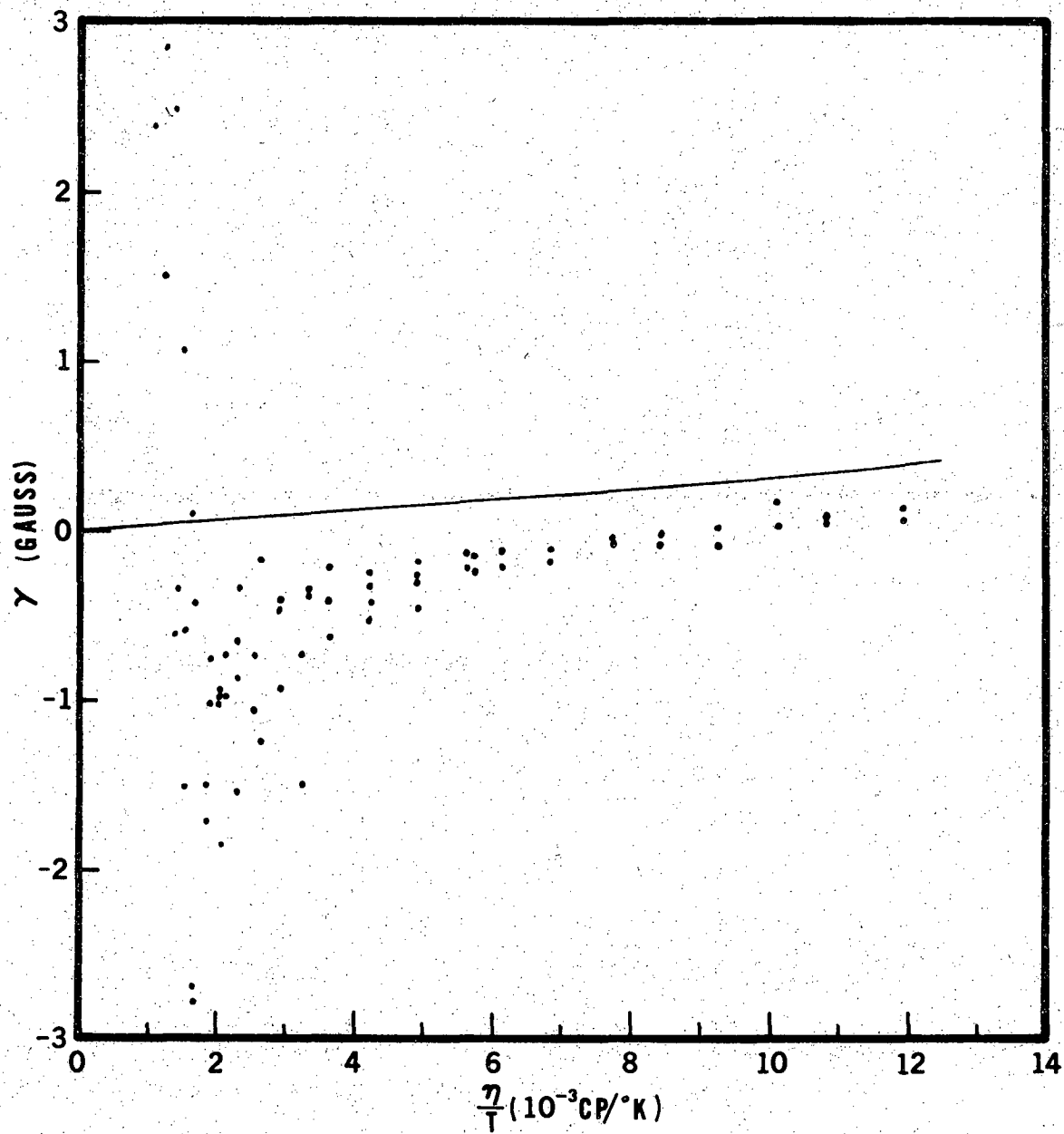
XBL 711-15

Fig. 30. Alpha parameter vs.  $\eta/T$  for  $\text{Cu}(\text{H}_2\text{O})_6^{2+}$ .



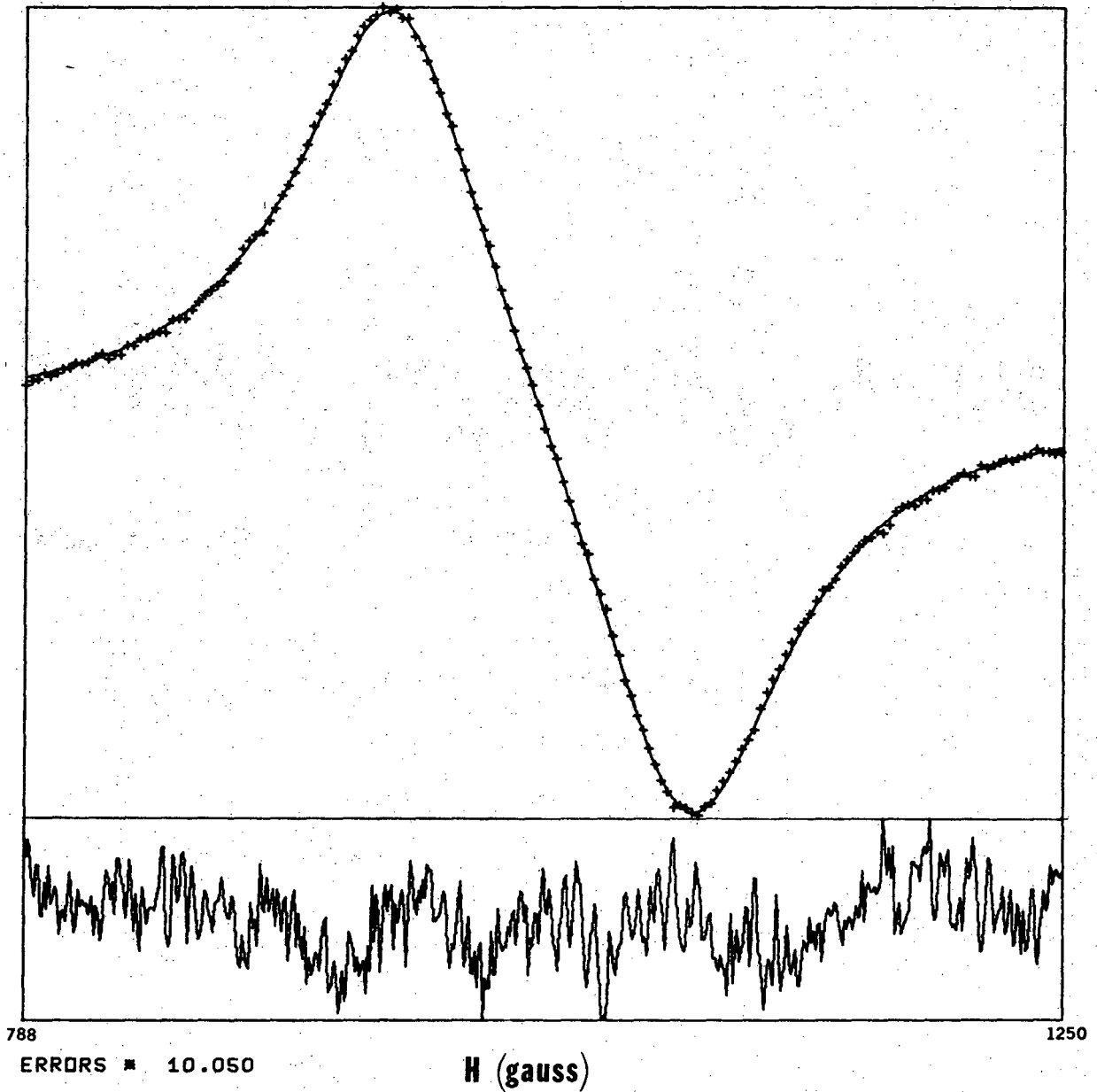
XBL 711-16

Fig. 31. Beta parameter vs.  $\eta/T$  for  $\text{Cu}(\text{H}_2\text{O})_6^{2+}$ .



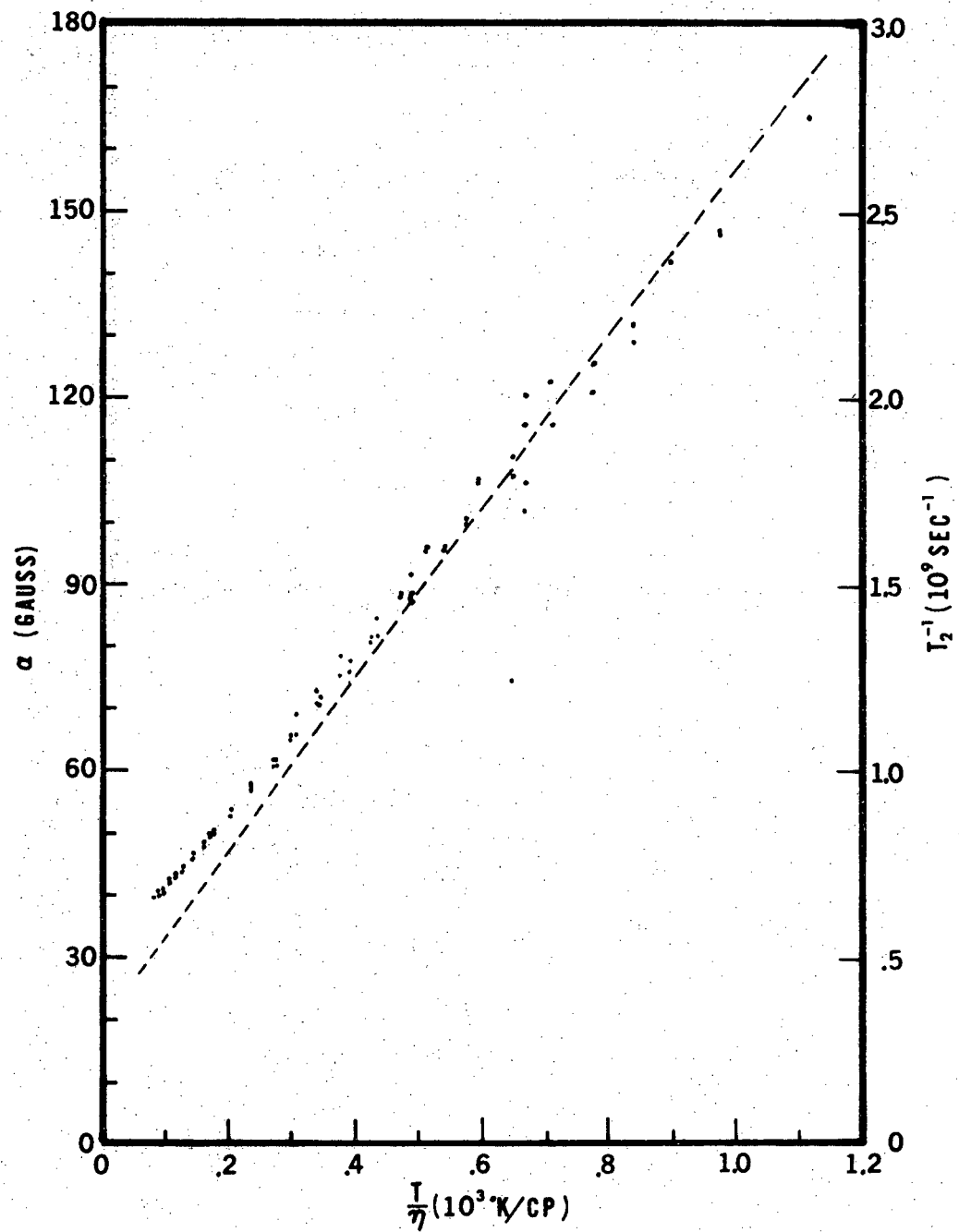
XBL 711-17

Fig. 32. Gamma parameter vs.  $\eta/T$  for  $\text{Cu}(\text{H}_2\text{O}_2)_6$ .



XBL 7012-7320

Fig. 33. Example to fit to solution spectrum of  $\text{Cu}(\text{H}_2\text{O})_6^{2+}$  at room temperature with a microwave frequency of 3.12 GHz.



XBL 711-95

Fig. 34. Alpha parameter vs.  $T/\eta$  for  $\text{Cu}(\text{H}_2\text{O})_6^{2+}$ . The dashed curve is plotted with Eq. 4.1 (see text).



## V. SPIN-LATTICE RELAXATION TIME MEASUREMENTS WITH AN ON-LINE COMPUTER

### A. Introduction

The longitudinal or spin-lattice relaxation time is extremely important in magnetic resonance, for magnetic resonance phenomena would not be observable if satisfactory relaxation mechanisms did not exist. The spin-lattice relaxation times of transition metal ions diluted in various host lattices is of considerable interest. A knowledge of these times aids in the theoretical understanding of electron paramagnetic resonance and in the interpretation of the interactions which may occur in solids. Furthermore, the relaxation times which are related to transition probabilities are important in understanding the operation of masers (Bloembergen, 1956). Stevens (1967) and Standley and Vaughan (1969) have recently reviewed the theoretical and experimental aspects of the spin relaxation measurements.

A number of techniques have been developed for the measurement of relaxation times. One of the most popular is the pulse saturation-recovery method (Davis et al., 1958). In this method the spin system to be studied is saturated with a relatively high power pulse, and the recovery of the absorption signal as a function of time is monitored, usually on an oscilloscope. The relaxation time is determined either by measuring the slope of a plot of the logarithm of the recovery curve or by comparing the recovery curve with standard exponentials whose time constants are known. The logarithmic method requires a knowledge of the baseline to which the recovery curve is returning. This is done experimentally by providing a second scan at low power to show the recovered signal on the

oscilloscope. This could involve experimental complications. The comparison method suffers if the recovery curve is not a single exponential. Furthermore, in many cases, the recovery curve contains a large amount of noise which makes the measurements from the oscilloscope traces difficult and inaccurate. Much experimental effort is usually expended to reduce this noise. Indeed, the improvement of the signal-to-noise ratio is one of the most serious problems in experimental science.

A technique for improving signal-to-noise is that of signal averaging. The usual method is to use a highly specialized computer of averaged transients (CAT) to acquire the data. Successive recovery curves are accumulated with the CAT until the signal-to-noise is acceptable. The data are then usually printed for analysis by the techniques described above, or punched for analysis with a digital computer.

However, we had been interested for some time in the application of small computers to laboratory problems. The advantages of using a computer are now well known. Interest in the technique has grown to such an extent that the January, 1969, issue of the IBM J. of Research and Development is devoted to laboratory automation. The problem of spin-lattice relaxation time measurements appears to be tailor made for a small computer. Not only can the data be acquired with the computer, for which time is a natural independent variable, but the data analysis can also be performed. In the case of simple exponential recoveries the analysis is straightforward and easily automated. Baseline problems are easily handled simply by acquiring data out to times where the baseline is well defined. More complicated recovery curves may be analyzed by an

interactive technique using relatively simple conversational programs and a display oscilloscope. An additional advantage of a computer is that an analysis of the data can be performed quickly so that results are known instantly.

The  $\text{Ni}^{2+}$  ion was chosen for study since this was a transition metal ion of current interest in the laboratory (Jindo, 1971 ; Batchelder, 1969). Of interest is the D value which is negative for most nickel compounds. However, in nickel sulfate the D value is positive. This behavior is discussed by Jindo, 1971. Studies of nickel ions in other lattices were undertaken to obtain information to aid in a theoretical interpretation of this behavior. The EPR spectrum of nickel ion in a lanthanum magnesium nitrate host (Ni/LMN) has been studied in this laboratory (Jindo, 1971) and was selected as a suitable system in which to study relaxation times. Furthermore, relatively few measurements of relaxation times in nickel ions have been reported.

Bowers and Mims (1959) and Valishev (1965) have reported measurements of nickel ions diluted in zinc fluosilicate. The results did not agree with the predictions of the usual theories of spin-lattice relaxation. Indeed, Valishev's results seem to be somewhat anomalous in that the relaxation time was observed to decrease with decreasing concentrations of nickel ions. However, this may possibly be explained by a phonon bottleneck. Lewis and Stoneham (1967) and Jones and Lewis (1967) report measurements for nickel in magnesium oxide. The relaxation times were explained in terms of a direct process at low temperatures and a Raman process at higher temperatures. However, the measured relaxation times were shorter than would be predicted from the relaxation theories.

## B. Experimental Methods

### 1. Samples

The crystals of lanthanum magnesium nitrate hydrate ( $\text{La}_2\text{Mg}_3(\text{NO}_3)_{12} \cdot 24 \text{H}_2\text{O}$ ) doped with  $\text{Ni}^{2+}$  were supplied by Mr. Akira Jindo. These crystals were grown by slow evaporation from a solution containing the correct proportions of  $\text{La}(\text{NO}_3)_3$  and  $\text{Mg}(\text{NO}_3)_2$  and a small amount of  $\text{Ni}(\text{NO}_3)_2$ . The crystals which are of rhombohedral symmetry, grow in the form of hexagonal plates with the crystal c axis located perpendicular to the plane of the plate. The nickel ions are substitutional impurities for the magnesium ions. There are two kinds of magnesium sites which are called site 1 and site 2 (Zalkin, et al., 1963). The spectra studied were due to nickel ions of trigonal symmetry in site 1.

Relaxation measurements were performed on two crystals one of which was more dilute in nickel ions than the other. The exact concentration of the nickel ions in the crystals is not known, but is not expected to exceed a maximum of 4%. The concentration of the more concentrated sample is expected to be 1-2%. The other crystal, which is known to be more dilute from a comparison of the relative spectrum intensities, is expected to have a concentration less than 1%.

### 2. Apparatus

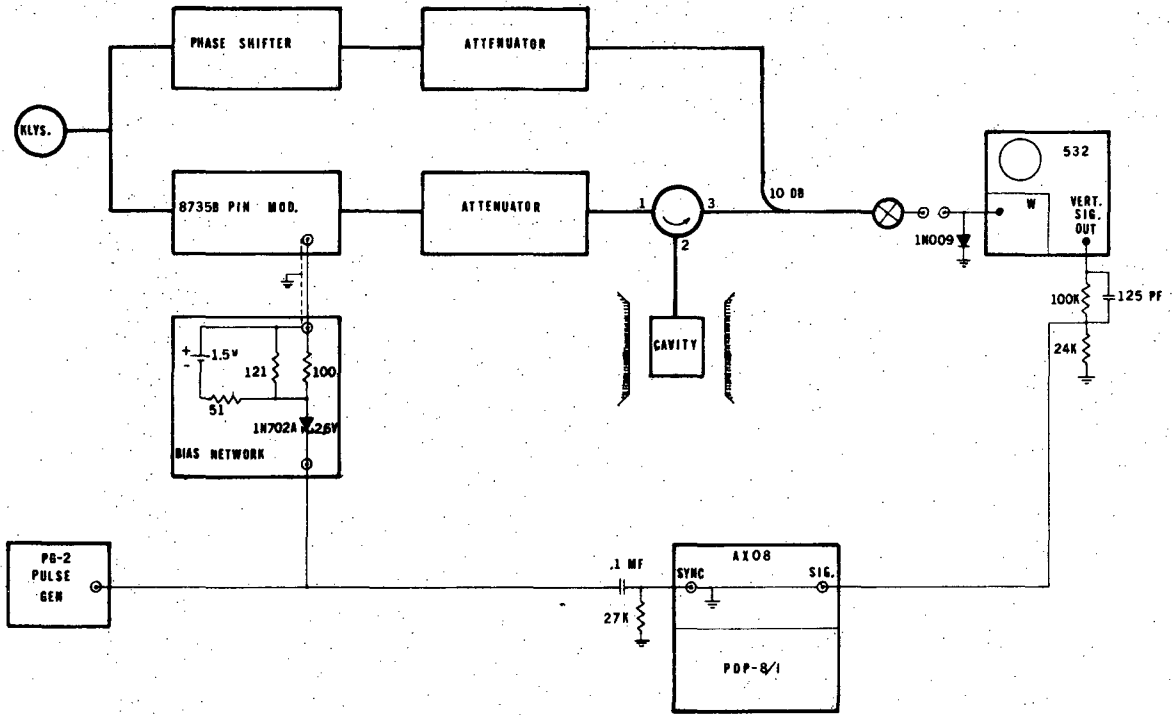
The crystals to be studied were held in a cylindrical cavity operating in the  $\text{TE}_{011}$  mode. The crystals were oriented with the cylindrical axis of the cavity contained in the plane of the crystal so that the magnetic field could be rotated in the ac plane of the crystal. The relaxation time determinations were performed with the magnetic field oriented along the

c axis which was located with the following procedure. The magnetic field was rotated until the two high field lines in the spectrum were superimposed. This occurred at the so-called magic angle of  $37^\circ$  (Jindo, 1971) where the three nickel energy levels are accidentally equidistant. The magnet was then rotated by  $37^\circ$  to obtain the c axis.

The temperature of the sample was varied by changing the speed of pumping on the liquid helium in which the sample was immersed. The temperature, which was varied between 1.2 and  $4.2^\circ\text{K}$ , was determined from the equilibrium vapor pressure of the helium.

The pulse-saturation spectrometer used in these experiments consisted of the normal homodyne detection spectrometer, which has been described previously (Pratt, 1967; Batchelder, 1969), and in addition, a PIN modulator, a pulse generator, an oscilloscope, and a LAB-8/I digital computer system (see Fig. 35). The homodyne spectrometer was modified by the introduction of the Hewlett-Packard Model 8735B PIN modulator into the cavity arm of the bridge. This unit could vary the power reaching the cavity from full power to 80 dB attenuation. In practice, the modulator and the attenuator in the cavity arm were adjusted so that the saturating power reaching the cavity was about 50 milliwatts, while the observing power was more than 40 dB below the saturating power.

The modulator was pulsed to the full transmitting state by means of an Intercontinental Instruments, Inc., Model PG-2 pulse generator. The pulse widths were adjusted to about 5 milliseconds. Pulses were repeated at a maximum rate of once every 300 msec. which was sufficient to permit the spin system to return to equilibrium. The pulses were applied to the modulator through a biasing network which is also detailed in Fig. 35.



XBL 711-96

Fig. 35. Block diagram of pulse-saturation spectrometer.

The biasing network served the double purpose of biasing the modulator to control the observing power, and to isolate the pulse generator from the modulator. The pulse generator was found to have ripple in the output in its quiescent state which could modulate the observing power and cause noise. The zener diode in the network isolates the pulse generator after the pulse has been delivered and also prevents the pulse height from accidentally becoming large enough to damage the modulator. The biasing voltage was provided by a 1.5 V dry cell which is a stable DC voltage source. The resistors were adjusted for ca. 45 dB attenuation in the modulator.

The recovery signals were observed as absorption signals using straight DC detection from the crystal diode detector. The absorption signals were on the order of millivolts and could easily be displayed on an x-y recorder or on an oscilloscope. The recovery curves were monitored with a Tektronix Model 532 oscilloscope equipped with a Type W differential amplifier plug-in. The differential amplifier was necessary to offset the detector bias voltage in order to preserve the full gain in the amplifier. The type W unit is susceptible to a thermal recovery problem if presented with a high signal level as would happen when a pulse was received. This effect was reduced by placing a clipping diode (1N009) on the input of the type W unit to prevent overdriving. The oscilloscope also served the purpose of amplifying the recovery signals for presentation to the computer system.

A synchronizing signal from the pulse generator and the recovery signal from the oscilloscope vertical signal output were presented through impedance matching networks to the LAB-8/I digital computer system.

The LAB-8/I computer system, as purchased from Digital Equipment Corp. consists of only a 4K PDP-8/I computer with teletype, and an AX08 laboratory peripheral. Our system includes, in addition, a DF32 disk (32K words), a PC08 high speed paper tape reader and punch, a KE8I extended arithmetic element, and an extra 4K of memory. The AX08 laboratory peripheral processes all analog signals and contains an analog-to-digital converter (ADC) which is multiplexed between four inputs, a crystal clock and an RC timing clock, a display control consisting of two analog outputs from a digital-to-analog converter and an intensify signal, and some trigger inputs for synchronization. There are also a number of miscellaneous digital inputs and outputs. The ADC is a 9 bit successive approximation converter and can perform a conversion in 17 microseconds. This is the ultimate limitation of how short a relaxation time may be measured with the computer system. The preamplifier of the ADC has a  $\pm 1V$  input range.

The operation of the spectrometer is relatively straight-forward. The spectrometer is first tuned and adjusted in the normal manner, except that the klystron is not locked to the cavity. The klystron frequency lock is not used in order to prevent the lock recovery after a pulse from interfering with the signal recovery. The PIN modulator is adjusted to provide the proper attenuation for the observing power. The magnetic field is then adjusted to the proper resonance, and the pulse generator is turned on. The averaging program is then started (presently this is the BASIC AVERAGER provided by DEC). After a sufficient number of scans have been accumulated, the averaging program is halted. At this time the LOGLINE overlay (see Appendix) is started to either punch the data on the



high speed punch, or to analyze the data for relaxation times. The data are normally punched either for later analysis or to save the data.

### C. Rate Equations

In a two level system relaxation can be viewed simply as a process of transferring spin population from one level to the other level. This process is readily described by a single decaying exponential. In a three level system the problem is somewhat more complicated. The population in one level may transfer to either of the two remaining levels. The signal observed in a relaxation experiment is proportional to the population difference between the two levels being observed. We must consider the form of the signal expected in a pulse saturation experiment. This is normally done by means of the rate equations.

We shall consider the rate equations for the 3 level system shown in Fig. 36. Each of the levels,  $i$ , contains an instantaneous population  $N_i^0$ , and the excess population,  $n_i$ , by

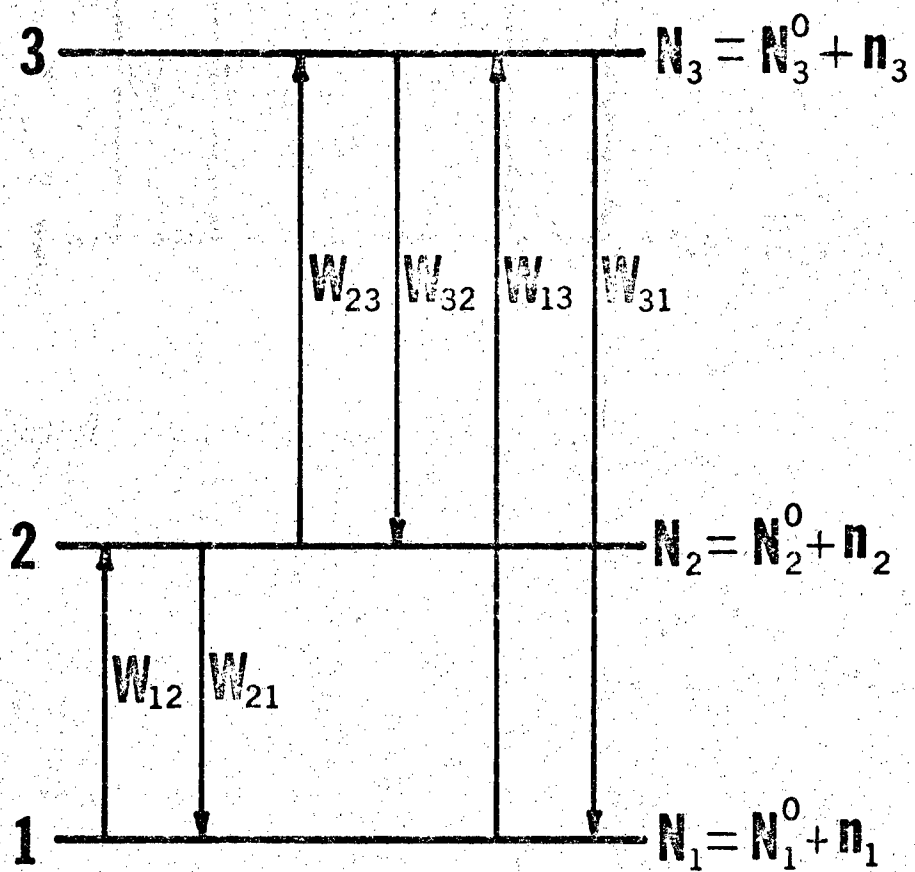
$$N_i = N_i^0 + n_i \quad (5.1)$$

The levels are connected by the spontaneous transition probabilities  $w_{ij}$  (probability  $i \rightarrow j$ ). The rate equations are then

$$\begin{aligned} \dot{N}_1 &= N_3 w_{31} + N_2 w_{21} - (w_{12} + w_{13}) N_1 \\ \dot{N}_2 &= N_3 w_{32} + N_1 w_{12} - (w_{21} + w_{23}) N_2 \end{aligned} \quad (5.2)$$

where the third equation for  $N_3$  has been omitted since it is related to the other two by

$$\dot{N}_1 + \dot{N}_2 + \dot{N}_3 = 0 \quad (5.3)$$



XBL 741-98

Fig. 36. Transitions and populations of a three level system.

However, since

$$n_3 = -n_1 - n_2 \quad (5.4)$$

and

$$\begin{aligned} N_1^0/N_2^0 &= \exp(-E_{12}/kT) \\ w_{12}/w_{21} &= \exp(E_{12}/kT) \end{aligned} \quad (5.5)$$

where  $E_{12}$  is the energy difference between levels 1 and 2, and with similar relations for the other pairs of levels we may obtain the following equations

$$\begin{aligned} \dot{n}_1 &= -(w_{12} + w_{13} + w_{31})n_1 + (w_{21} - w_{31})n_2 \\ \dot{n}_2 &= (w_{12} - w_{32})n_1 - (w_{21} + w_{23} + w_{32})n_2 \end{aligned} \quad (5.6)$$

These are simultaneous linear differential equations of the form

$$\begin{aligned} \dot{n}_1 &= a_1 n_1 + b_1 n_2 \\ \dot{n}_2 &= a_2 n_1 + b_2 n_2 \end{aligned} \quad (5.7)$$

where

$$\begin{aligned} a_1 &= -(w_{12} + w_{13} + w_{31}) \\ a_2 &= w_{12} - w_{32} \\ b_1 &= w_{21} - w_{31} \\ b_2 &= (w_{21} + w_{23} + w_{32}) \end{aligned} \quad (5.8)$$

These equations may be solved using standard techniques (Kaplan, 1958).

The solutions are of the form

$$n_1 = \alpha \exp(\lambda t) \quad n_2 = \beta \exp(\lambda t) \quad (5.9)$$

where  $\lambda$  may be obtained from the related homogeneous equations obtained from Eq. 5.9 and 5.7

$$\begin{aligned} (a_1 - \lambda)\alpha + b_1 \beta &= 0 \\ a_2 \alpha + (b_2 - \lambda)\beta &= 0 \end{aligned} \quad (5.10)$$

These equations have a solution if the determinant is zero so that we may obtain

$$\lambda = 1/2 \left( (a_1 + b_2) \pm \sqrt{(a_1 + b_2)^2 - 4(a_1 b_2 - a_2 b_1)} \right) \quad (5.11)$$

Ratios of alpha and beta may be obtained from Eq.s 5.10 and 5.11. In any case, the general solutions are

$$\begin{aligned} n_1 &= C_1 \alpha_1 e^{\lambda_1 t} + C_2 \alpha_2 e^{\lambda_2 t} \\ n_2 &= C_1 \beta_1 e^{\lambda_1 t} + C_2 \beta_2 e^{\lambda_2 t} \end{aligned} \quad (5.12)$$

where the C's are determined by the initial conditions. The solutions in which we are interested is the population difference given by

$$n_2 - n_1 = C_1 (\beta_1 - \alpha_1) e^{\lambda_1 t} + C_2 (\beta_2 - \alpha_2) e^{\lambda_2 t} \quad (5.13)$$

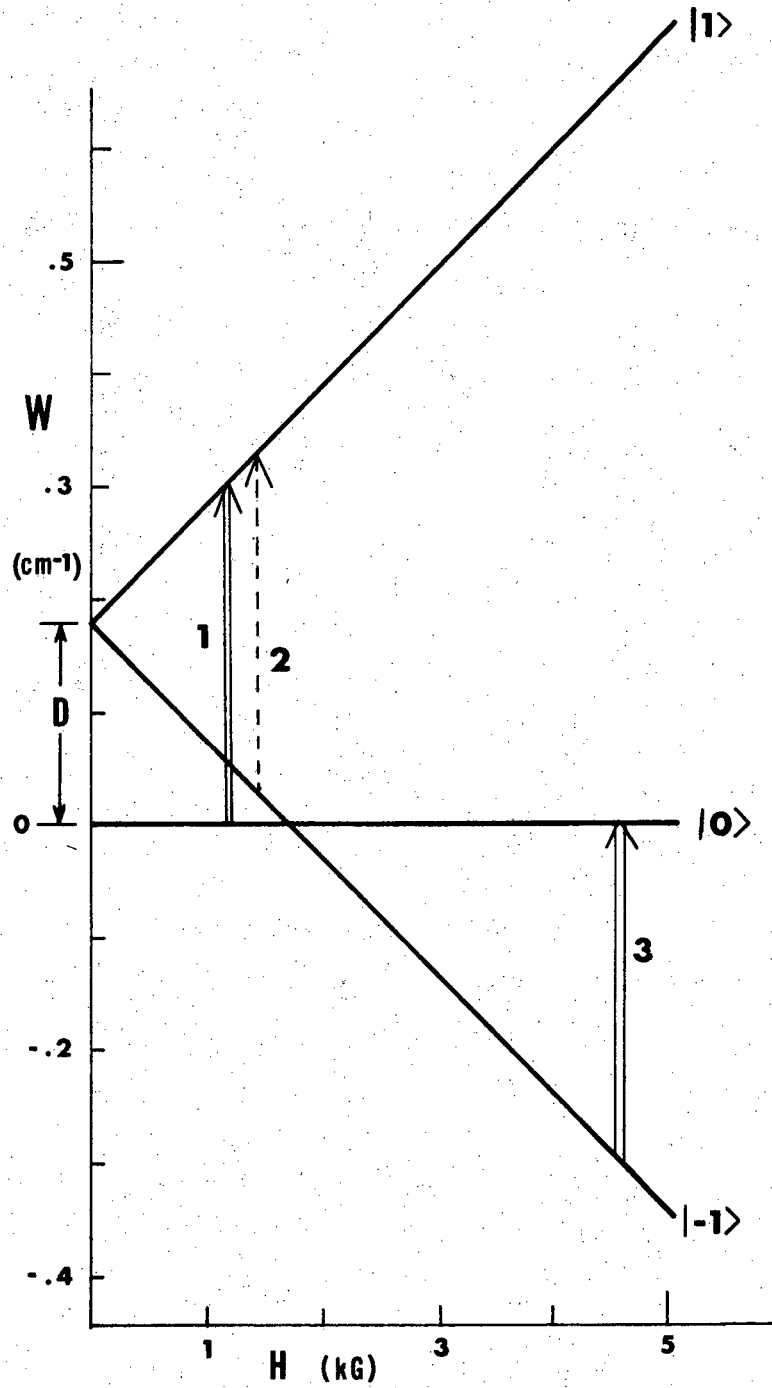
Similar solutions may be obtained for the other level pairs. We can see that the observed recovery curve will be a sum of two exponentials rather than a simple single exponential. The relaxation times will be the reciprocals of the  $\lambda$ 's, and are related in a complicated manner by Eq.s. 5.11 and 5.8 to the transition probabilities. Theoretical results will, in general, be for the transition probabilities. Hence, a complete comparison of experiment with theory requires experimental values for the w's. This will necessitate a detailed consideration of the coefficients of the exponentials as well as the  $\lambda$ 's. This will not be considered here since we have shown what we wished: the recovery curve is a sum of two exponentials. Furthermore, for a constant field, the same relaxation times should be obtained for each of the transitions.

D. Discussion and Results

With the magnetic field oriented along the c axis of the crystal, the EPR spectrum of the Ni/LMN system consists of three lines which correspond to the transitions indicated in Fig. 37. The first and third lines, if the lines are numbered from low to high field, are strong allowed transitions. The second line is a "forbidden" transition. Jindo (1971) determined the spin Hamiltonian parameters to be  $g_{\parallel} = 2.235$ ,  $g_{\perp} = 2.233$ ,  $D = +.2005 \text{ cm}^{-1}$ , and  $E = .0007 \text{ cm}^{-1}$ . The small E value was necessary to fit the data, though the ion with no lattice distortion is expected to be at a site of trigonal symmetry. These parameters have a small temperature dependence which may require minor modifications to any theoretical relaxation treatment of the system.

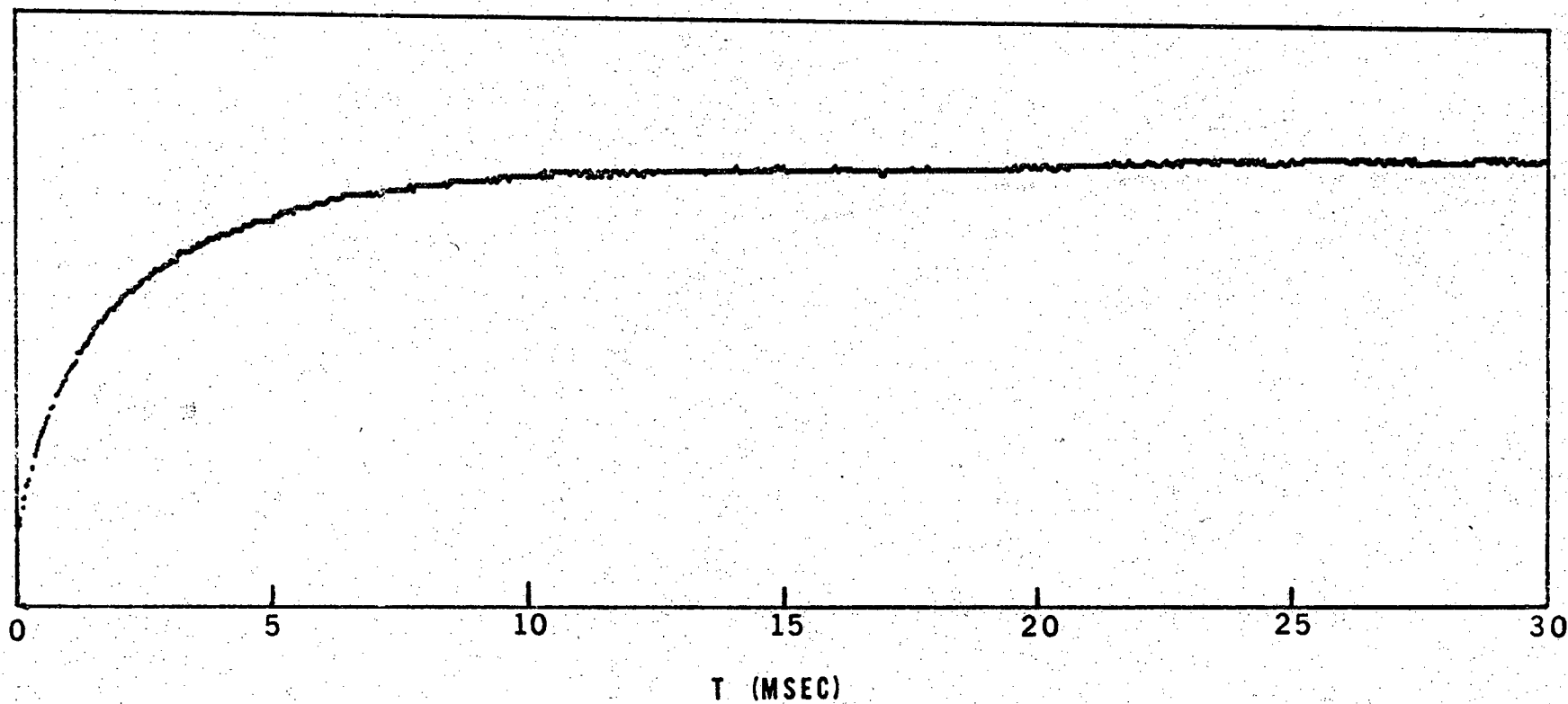
Relaxation time measurements have been made for each of the lines over a temperature range of 1.3 to 4.2°K using the pulse saturation-recovery method. An example of a typical recovery curve is shown in Fig. 38 which shows the recovery of the high field line for  $T = 1.37^{\circ}\text{K}$ . The data show an excellent signal to noise ratio and have been collected to essentially complete recovery so that the baseline of the recovery is well known. A logarithmic presentation of the data with the baseline subtracted is shown in Fig. 39. The logarithm is essentially linear at long times but shows curvature near the start of the recovery curve. Possible reasons for this behavior are discussed later. A reasonable relaxation time may be obtained from the linear portion of the curve.

The relaxation data obtained for the low and high field lines of the fairly concentrated sample are presented in Figs. 40 and 41. The data are



XBL 711-100

Fig. 37. Energy levels and transitions for  $\text{Ni}^{2+}$  in lanthanum magnesium nitrate hydrate with the magnetic field oriented along the c axis (Jindo, 1971)



-104-

Fig. 38. Exponential recovery curve for the low field line at 1.37 °K. An average of 50 experiments.

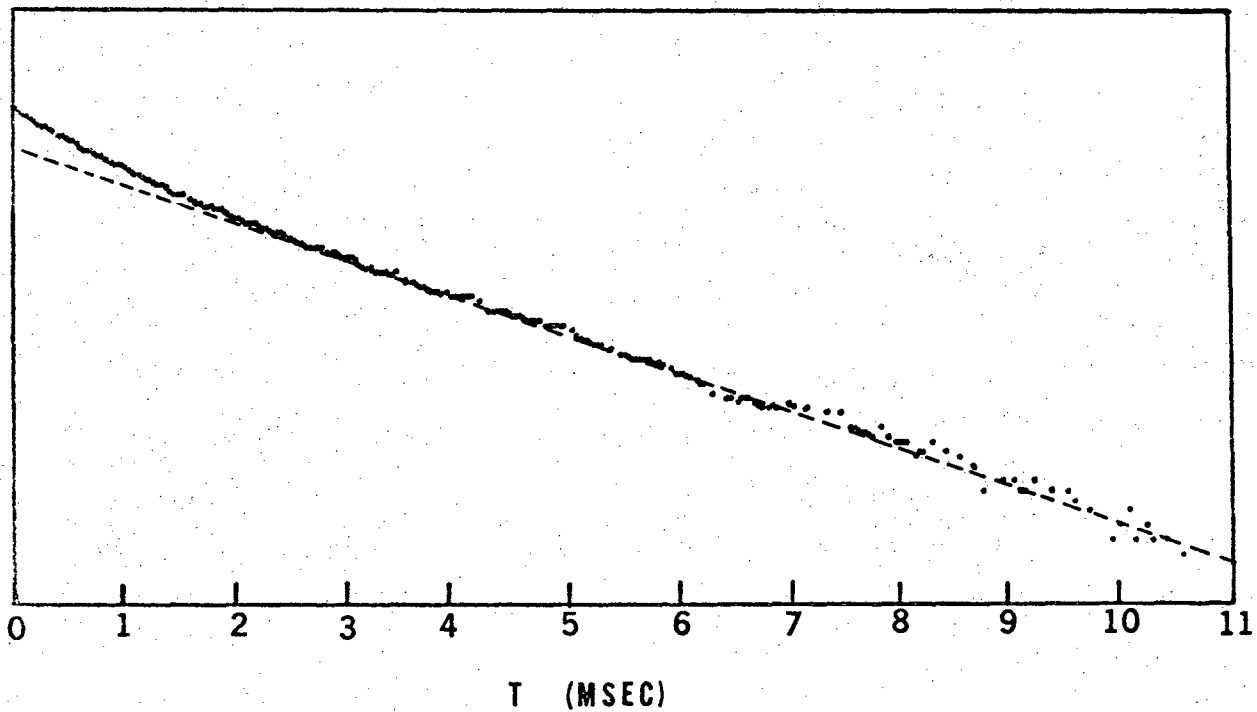
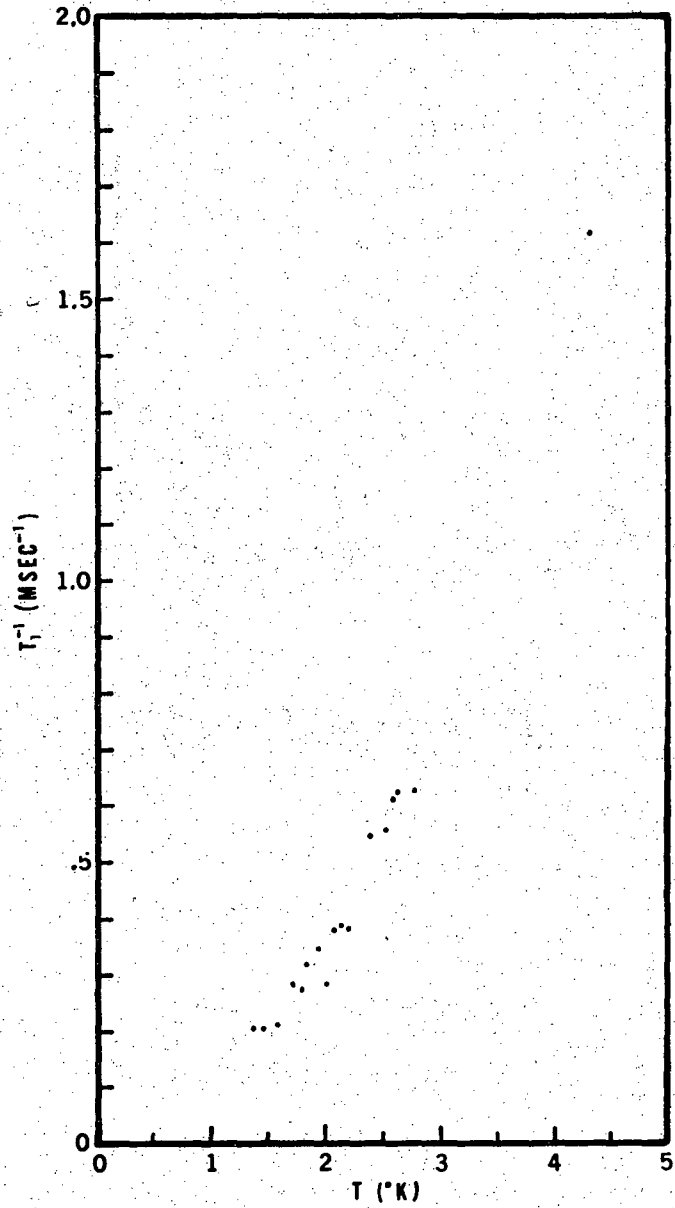


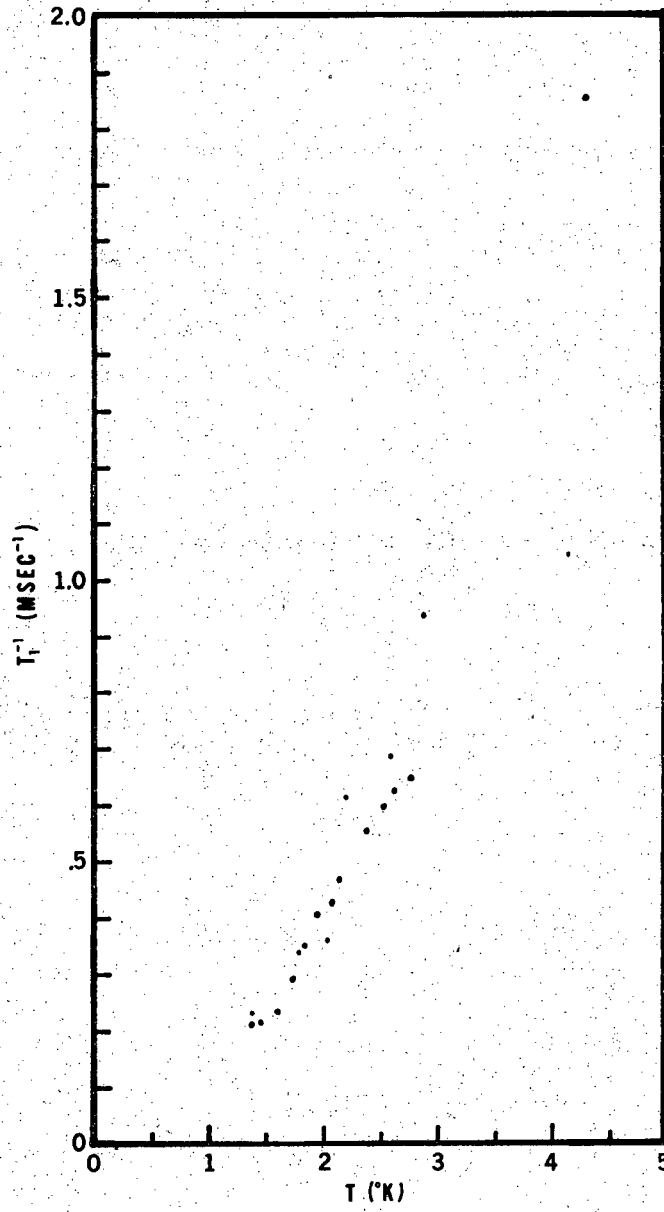
Fig. 39. Logarithm of the data in Fig. 38 with the baseline removed. Dashed line is a straight line fit to the data with a time constant (reciprocal slope) of 3.15msec. Curvature at start of data may indicate the presence of a second shorter time constant.





XBL 711-99

Fig. 40.  $T_1^{-1}$  vs. T for the low field line.



XBL 711-97

Fig. 41.  $T_1^{-1}$  vs.  $T$  for the high field line.

somewhat scattered so that a functional relationship between  $T_1^{-1}$  and the absolute temperature may not be established with confidence. The lack of data between 3 and 4°K is also somewhat unfortunate. This data was not obtained in these preliminary experiments because of the difficulty of regulating and measuring the temperature with our present apparatus. The data suggest that the inverse relaxation time is linear in the absolute temperature, but the scatter is such that a quadratic could also fit the data.

The data obtained for the dilute sample are similar to that for the concentrated sample. The data were more difficult to obtain since the signal was weaker than in the concentrated sample. The data seem to indicate a slightly shorter relaxation time in this sample, but this may in fact be experimental error.

Relaxation times were also determined for line 2, the "forbidden" line in the spectrum. The intensity of this transition was very much weaker than that of the other two transitions and the data were correspondingly more difficult to obtain. The relaxation times for this line were much longer than those for the other two lines, but this result is doubtful at best. In fact, the relaxation times varied quite widely and may be an experimental artifact.

A number of relaxation mechanisms have been utilized to explain the data in solid state measurements (Standley and Vaughan, 1969). For a non-Kramers salt, such as  $Ni^{2+}$  system, the direct process, the Raman process, and the Orbach process give rise to a linear, a seventh power, and an exponential temperature dependence, respectively, for the inverse relaxation times. The data in the Ni/LMN system could be consistent with either

a linear or a quadratic function of temperature. The linear function would be consistent with a direct process. However, if a straight line is fit to the data and extrapolated to zero temperature, the line does not pass through zero, whereas the contribution from the direct process to  $T_1^{-1}$  should go to zero.

The data would seem to be fit better with a quadratic function of the form

$$T_1^{-1} = D T^2 \quad (5.14)$$

where D is a proportionality constant. This temperature dependence is consistent with a phonon bottleneck wherein a phonon-bath interaction rather than a spin-lattice process is observed. If we attempt to least squares fit the data with Eq. 5.14, we obtain a value of  $D=.0874$  for the low field line (Fig. 40) and  $D=.0866$  for the high field line (Fig. 41). These values are essentially identical. If the observed relaxation is due to a Phonon bottleneck process, we would expect D to be directly proportional to the resonance linewidth and inversely proportional to the concentration and the thickness of the crystal (Scott and Jeffries, 1962). The possibility of a shorter relaxation time in the dilute sample supports the proposal of a phonon bottleneck. The relaxation time is not drastically shorter in the dilute sample because of compensation from the dependence on the linewidth. The linewidth for the dilute sample is much narrower than that of the concentrated sample. The relaxation time seems to be well described by a phonon bottleneck, although we cannot completely rule out the possibility of a direct process since the data are scattered.

It was mentioned earlier that the logarithm of the recovery curve exhibited curvature near the start of the recovery. This could indicate the presence of a second relaxation time in the recovery. Data was obtained for the short time constant by stripping the part of the curve due to the longer time from the data and then examining the residual recovery curve. However, the relaxation times obtained by this procedure were extremely scattered. No correlation with temperature or with the longer relaxation time was evident.

Part of the difficulty in these determinations lies in the analytical procedure. The second recovery curve is revealed by removing from the original data that portion which is due to the first recovery curve. Small errors in the determination of the first recovery curve could cause large deviation in the second curve which is much smaller than the first curve. It should be mentioned that the second curve is itself a cause of error in determining the first curve.

The short relaxation time may be due to two main sources. First, if the relaxation is phonon bottlenecked, the short relaxation could be the tail end of a  $T_1$  relaxation which is becoming rapidly bottlenecked. This relaxation might follow a direct process, but the determination is very difficult. Secondly, if the observed relaxation is the true spin-lattice process, then two relaxation times are expected as shown in Section V-C. Furthermore, if the process is phonon bottlenecked but the short relaxation is the true relaxation time, then this short relaxation process should contain both of the relaxation times predicted in Section V-C. If this is so, the analysis of the short relaxation time is quite difficult.

It is possible that other processes are responsible for the initial relaxation. The first problem is whether the spectrometer is linear in its response to the recovery signal. The signals which are observed are quite strong so that with relatively large changes in cavity Q, the spectrometer may be nonlinear. The amplifiers may be overdriven so that the short relaxation may be the end of the recovery of an overdriven system.

A second problem is that of spectral diffusion in the line. If the nickel lines are inhomogeneously broadened, then it is possible to saturate the center of the line, but then observe a recovery due to the wings of the line growing toward the center. This would give a hyperbolic recovery curve (Mims, et al., 1961). The short relaxation time could then be an incorrect analysis of the recovery curve.

It is evident that much work remains to be done in the Ni/LMN system. Detailed studies of the relaxation times should be made for each of the transitions as a function of temperature. The crystal size and the nickel concentration should be varied to confirm the hypothesis of a phonon bottleneck. The concentration study is also important for studies of exchange effects. Studies should also be made of the dependence of the relaxation times on the pulse widths and on the value of the saturating power. (Preliminary investigations indicated no dependence). Possible anisotropy in the relaxation times should be studied by making measurements as a function of angle. Indeed, measurements at the so-called magic angle of  $37^\circ$  (Jindo, 1971) could prove very interesting. At this angle the nickel transitions are superimposed, since the energy levels are accidentally equidistant. The possibility of double quantum transitions exists, especially at high power levels. A double quantum transition should

not occur at the power levels used for monitoring. However, the initial spin distributions produced by the saturating pulse might be studied. Furthermore, Slichter (Slichter, 1963; Hebel and Slichter, 1959) has shown that, in systems with equidistant energy levels which can be described by a spin temperature, only one relaxation time should be observed.

In summary, we have developed an experimental method which should be useful for spin-lattice relaxation time measurements. The acquisition and analysis process in our small computer system should be relatively convenient. However, the problems associated with the operation of a pulse spectrometer are still present, and they are the reason for the scatter in our data. Possible problems are the drift of the klystron frequency which would cause drifts in the recovery signal, and possible interference effects from the dispersion signal. Since the relaxation time could vary across the resonance lineshape, the setting of the resonance magnetic field is a possible error source. These problems should be studied and eliminated.

APPENDIX I: LORENTZ LINESHAPES AND  
LEAST SQUARES THEORY

The real and imaginary parts of the complex susceptibility,  $\chi = \chi' + i\chi''$ , which are derived from the Bloch Equations are given

$$\chi'(\omega) = 1/2 \chi_0 \omega_0 \frac{T_2^2 (\omega_0 - \omega)}{1 + T_2^2 (\omega_0 - \omega)^2 + \gamma^2 H_1^2 T_1 T_2} \quad (A-1)$$

$$\chi''(\omega) = 1/2 \chi_0 \omega_0 \frac{T_2}{1 + T_2^2 (\omega_0 - \omega)^2 + \gamma^2 H_1^2 T_1 T_2} \quad (A-2)$$

where  $H_1$  is the rf magnetic field,  $T_1$  and  $T_2$ , the spin-lattice and spin-spin relaxation times respectively,  $\chi_0$  the static magnetic susceptibility, and  $\gamma$  the magnetogyric ratio relating the resonance frequency,  $\omega_0$ , to the resonance field,  $H_0$ , by  $\omega_0 = \gamma H_0$ . In the typical magnetic resonance experiment the spectrometer is tuned to observe only the absorption,  $\chi''$  so that the dispersion,  $\chi'$ , is neglected. Furthermore, magnetic resonance experiments are performed at low powers so that  $\gamma^2 H_1^2 T_1 T_2 \ll 1$  and  $\chi''$  reduces to

$$\chi''(\omega) = 1/2 \chi_0 \omega_0 \frac{T_2}{1 + T_2^2 (\omega_0 - \omega)^2} \quad (A-3)$$

Examination of Eq. A-3 reveals that it is similar to the Lorentz line-shape function

$$f(\omega) = \frac{T_2}{\pi} \frac{1}{1 + T_2^2 (\omega - \omega_0)^2} \quad (A-4)$$

Hence, the susceptibility is usually written in the form of a Lorentz function

$$\chi''(\omega) = F \frac{T_2}{\pi} \frac{1}{1 + T_2^2 (\omega - \omega_0)^2} \quad (A-5)$$

where  $F$  is the line intensity such that

$$F = \int_{-\infty}^{\infty} \chi''(\omega) d\omega.$$



From Eq. A-4 we can see that the maximum in the function is  $T_2/\pi$  and also that  $T_2$  is the half width at half height. We may also observe that the units of  $T_2$  are seconds per radian.

Because of experimental convenience magnetic resonance experiments are performed with the magnetic field as the independent variable rather than the frequency so that the lineshape becomes

$$L(H) = \frac{F}{\pi} \frac{\delta}{\delta^2 + (H-H^0)^2} \quad (A-6)$$

where  $\delta$  is the half width at half height (in gauss), and  $H^0$  is the resonance center of the line. Furthermore, EPR spectroscopy is done with the derivative of the absorption given by

$$\begin{aligned} L'(H) &= -\frac{2}{\pi} F\delta \frac{H - H^0}{[\delta^2 + (H-H^0)^2]^2} \\ &= \frac{2}{\pi} F\delta \frac{H^0 - H}{[\delta^2 + (H^0 - H)^2]^2} \end{aligned} \quad (A-7)$$

The peak-to-peak distance,  $\Delta H$ , of this function is given by

$$\Delta H = (2/\sqrt{3}) \delta \quad (A-8)$$

and is related to  $T_2$  by Eq. 1.2.

In general an EPR spectrum consists of a number of lines with different centers, widths, and intensities, so that the spectrum is described by a sum of Lorentz lineshapes

$$g(H) = \frac{2}{\pi} \sum_k F_k \frac{(H_k^0 - H) \delta_k}{[(H_k^0 - H)^2 + \delta_k^2]^2} \quad (A-9)$$

Except in unusual cases the  $H_k^0$  are not independent of each other. A spectrum with several components is usually due to hyperfine structure so that the line centers are determined by a spin Hamiltonian. The line

centers are then given to second order by (for spin 1/2 complexes)

$$H_k^0 = H_0 - A m - A^2 ((I(I+1) - m^2)/2H_0) \quad (A-10)$$

where  $H_0$  is the spectrum center,  $A$ , the hyperfine coupling constant,  $I$ , the nuclear spin, and  $m$ , the nuclear spin quantum number. The  $k$ 'th line corresponds to a given value of  $m$ . In the general case the spectrum is described by more than one coupling constant and  $H_k^0$  is given by

$$H_k^0 = H_0 - \sum_j (A_j m_j + A_j^2 ((I_j(I_j+1) - m_j^2)/2H_0)) \quad (A-11)$$

In the case of organic radicals the second order contribution is usually neglected.

A further simplification is usually possible when the lines are due to hyperfine structure. In this case the line intensities are usually given by the ratios of whole numbers which can be computed from the number of nuclei and the nuclear spin. The line intensity is a known fraction of the total intensity of the overall spectrum. We may then rewrite the lineshape as

$$g(H) = \frac{2}{\pi} F \sum_k R_k \frac{(H_k^0 - H) \delta_k}{[(H_k^0 - H)^2 + \delta_k^2]^2} + S + DH \quad (A-12)$$

where  $R_k$  is the intensity ratio for the  $k$ 'th hyperfine component.  $S$  and  $D$  are terms which are added to account for a baseline shift and a baseline drift. In the most general case the spectrum consists of several species each of which has a lineshape characterized by Eq. A-12. The lineshape then consists of a sum of terms similar to the first term in Eq. A-12.

We are now in possession of an analytic function to describe our experimental spectra. If we have values for the spectrum intensities at

various magnetic fields, we can perform a least squares fit of the function in Eq. A-12. The theory of least squares is well known and will not be rederived here (Deming, 1938; Shoemaker and Garland, 1962). However, the object is to minimize the sum of the squares of the differences between the experimental points  $y(H)$  and the theoretical value  $g(H)$ . For this purpose we require the values of the derivatives of Eq. A-12 with respect to each of the parameters which we wish to determine. These derivatives are given by

$$\frac{\partial g(H)}{\partial F} = \frac{2}{\pi} \sum_k R_k \frac{(H_k^o - H) \delta_k}{[(H_k^o - H)^2 \delta_k^2]^2} \quad (A-13)$$

$$\frac{\partial g(H)}{\partial \delta_k} = \frac{2}{\pi} F R_k \frac{(H_k^o - H)^3 - 3 (H_k^o - H) \delta_k^2}{[(H_k^o - H)^2 + \delta_k^2]^3} \quad (A-14)$$

$$\frac{\partial g(H)}{\partial H_o} = \frac{2}{\pi} F \sum_k (1 + f(k)) \frac{\delta_k^3 - 3 (H_k^o - H)^2 \delta_k}{[\delta_k^2 + (H_k^o - H)^2]^3} \quad (A-15)$$

$$f(k) = \sum_j \frac{A_j^2}{2 H_o^2} [I_j (I_j + 1) - m_j^2]$$

$$\begin{aligned} \frac{\partial g(H)}{\partial A_i} &= - \frac{2}{\pi} F \sum_k [m_j + \frac{A_j}{H_o} (I_j (I_j + 1) - m_j^2)] \\ &\times R_k \frac{\delta_k^3 - 3 (H_k^o - H)^3 \delta_k}{[\delta_k^2 + (H_k^o - H)^2]^3} \end{aligned} \quad (A-16)$$

$$\frac{\partial g(H)}{\partial S} = 1 \quad (A-17)$$

$$\frac{\partial g(H)}{\partial D} = H$$

The value of  $k$  is determined by a particular combination of  $m_j$  values. The value of the function,  $f(k)$  is different for each  $k$  since the values of  $m_j$  change. In the case of transition metal complexes with hyperfine only from the central ion, the spin Hamiltonian is given by Eq. A-10 rather than Eq. A-11 so that the sum over  $j$  reduces to one term. Using a standard least squares treatment the derivatives are formulated into a set of normal equations in the following manner.

Let us assume that the parameters which we seek are  $x_n$ . We have an initial guess  $x_n^0$  and we wish to find a value  $\Delta x_n$  to obtain a new value for the parameters

$$x_n = x_n^0 + \Delta x_n \quad (\text{A-18})$$

We also assume that the errors are only in the  $y(H)$  with no errors in  $H$ .

Then we must solve the following set of equations

$$\begin{aligned} \sum_i \frac{\partial g_i}{\partial x_1} \frac{\partial g_i}{\partial x_1} \Delta x_1 + \sum_i \frac{\partial g_i}{\partial x_1} \frac{\partial g_i}{\partial x_2} \Delta x_2 + \dots + \sum_i \frac{\partial g_i}{\partial x_1} \frac{\partial g_i}{\partial x_n} \Delta x_n &= \sum_i \frac{\partial g_i}{\partial x_1} (y_i - g_i) \\ \sum_i \frac{\partial g_i}{\partial x_2} \frac{\partial g_i}{\partial x_1} \Delta x_1 + \sum_i \frac{\partial g_i}{\partial x_2} \frac{\partial g_i}{\partial x_2} \Delta x_2 + \dots + \sum_i \frac{\partial g_i}{\partial x_2} \frac{\partial g_i}{\partial x_n} \Delta x_n &= \sum_i \frac{\partial g_i}{\partial x_2} (y_i - g_i) \\ & \dots \\ \sum_i \frac{\partial g_i}{\partial x_n} \frac{\partial g_i}{\partial x_1} \Delta x_1 + \sum_i \frac{\partial g_i}{\partial x_n} \frac{\partial g_i}{\partial x_2} \Delta x_2 + \dots + \sum_i \frac{\partial g_i}{\partial x_n} \frac{\partial g_i}{\partial x_n} \Delta x_n &= \sum_i \frac{\partial g_i}{\partial x_n} (y_i - g_i) \end{aligned} \quad (\text{A-19})$$

The sums are taken over all the points in the spectrum. These equations are of the form

$$\underline{A} \underline{X} = \underline{B} \quad (\text{A-20})$$

where  $\underline{A}$  is an  $N \times N$  matrix where  $N$  is the number of parameters to be determined,  $\underline{X}$  and  $\underline{B}$  are vectors. These equations are solved by standard methods, for example, matrix inversion, to obtain values for the corrections  $\Delta x_n$ .

New values of the parameters are obtained from Eq. A-18. In the simplest case this is all that is necessary to obtain a least squares value for the parameters. In general we must perform an iterative procedure, using the new value for the parameter as a starting point for another solution of Eq. A-19. The iterations are then repeated until the residuals are minimized in the least squares sense. If the fitted function is linear in the parameters, then the iterative procedure will converge rapidly to a solution. Unfortunately, the Lorentz function is not linear in the parameters.

A non-linear least squares treatment is not guaranteed to converge. In fact, the correction vectors obtained from the solution of Eq. A-19 may not be correct in magnitude. In this case the solution may diverge or may oscillate widely about the true solution. This behavior is minimized by adjusting the correction vectors so that only a fraction of the magnitude is used to compute the new value of the parameter. The fraction used will depend upon the parameter and the function.

APPENDIX II: DIGITAL PROGRAMS

A. Data Acquisition System Programs

1. SUMTAP3

The SUMTAP3\* program is used to read the magnetic tapes which are produced by the data acquisition system (Model S6114) and to produce a Fortran compatible data tape for processing by FITESR (see following discussion). The program will read the data tape; select the data in a given file corresponding to either up-field or downfield sweeps, disregarding data inconsistent with smooth sweeps; smooth the y values with a second order polynomial; store the smoothed data points in predetermined channels; and sum complete sweeps to produce an averaged spectrum. The output from the program consists of a printed listing of the summed and normalized spectrum, a plot of the spectrum and its integral, and a magnetic tape of the spectral data for further processing by least squares programs.

a. Format of Input Data Tape

The data acquisition system organizes a special work mark character, the 7 digit counter measurement, and the 5 digit voltmeter measurement plus a sign into a 14 character word. A word is a measured data point. The words are organized into 80 word records and is recorded in IBM compatible NRZI format on the magnetic tape. The data belonging to a spectrum consists of a number of 80 word record blocks which make up a file. The word "file" is used with two slightly different meanings in this discussion. When applied to the input tape, the word, "file", refers to a record or number of records which is isolated from other similar records by a file mark or end-of-file gap. The data within a file may

\* Original written by Dr. Alfred Bauder (Bauder and Myers, 1968).

consist of one or more spectra. When applied to the output tape, the word, "file", refers to the data for a given spectrum. It is not separated from other such files by an end-of-file gap. (This permits the data to be read by a Fortran program without special tests for file marks.)

Both upfield and downfield sweeps may be included in a single file on the input tape. If several sweeps are included in a single file, the sweeps are averaged to form an averaged spectrum on the output tape. However, only upfield sweeps or only downfield sweeps may be averaged; upfield and downfield sweeps may not be averaged together. Two different spectra may be obtained from a mixture of upfield and downfield sweeps, one the average of the upfield sweeps, and the other the average of the downfield sweeps. The x-axis data of a given sweep must be either all increasing or all decreasing. Otherwise, the sweep may be regarded as incomplete and ignored.

The end-of-file gap on the input tape serves the purpose of indicating to the program the end of a given data set. When the file gap is encountered, the program will plot the spectrum it has found within the file and also write the spectrum on the output tape in a Fortran compatible format. If a file gap is encountered before data is found, the file is regarded as empty. Note that, therefore, empty files count as files for the purpose of numbering the files. If four sequential file marks are encountered without data, the program will assume that the tape contains no more spectra and will terminate. For this reason, all tapes should be ended with four file marks to ensure program termination.

b. Input Data Cards

The data cards are used to describe the spectra on the input tape and to indicate the processing to be performed on the spectra.

Card 1 (Format 8A10)

NAME An arbitrary name for the output tape which will contain the smoothed spectra. 10 alphanumeric characters. This name is used to identify the tape for subsequent programs.

COMMENT any arbitrary title or comment to be printed for identification

Card 2 (Format 3I5, 25X, 4A10)

NFILE1 the number of the file to be analyzed. Files must be processed in the order in which they are found on the tape. If several files are to be processed (by providing several of card 2), the files must be processed in order of increasing file number.

IK =+1 upfield sweep

=-1 downfield sweep

KK =0 do not read a new card 3. Assume the parameters are the same as provided by a previous card 3.

≠0 read new parameters from the card 3

Card 3 (Format 2I5, 2E10.0) provided only if KK≠0

KP spectra will be smoothed with  $2 * KP + 1$  points (KP must be less than 10)

NUM number of smoothed data points of the spectrum to be stored on the output tape

FMIN lower limit for sweep

FMAX upper limit for sweep; must always be greater than FMIN (FMIN and FMAX are in the units of the x axis which was recorded on the input tape)



The following cards repeat the sequence from card 2, until no further files are to be processed. A blank card at the end of the data deck (which corresponds to NFILE1=0) is used to terminate program execution.

c. Subroutines

SMOOTH2

SMOOTH2 is used to perform digital filtering (Savitzky and Golay, 1964) of the data and to select the absorption value for a given channel. It is assumed that measurements of the frequency (x axis) and the derivative absorption signal (y axis) are made at equal intervals of time. Both of the measurements are subject to noise, which is to be minimized with a smoothing function. The x axis is smoothed with a linear function  $x = r + s*t$ . The y axis is smoothed with a quadratic,  $y = a + b*t + c*t**2$ . Here, t is the relative time of the measurement.

The program uses  $2*KP+1$  points and automatically selects those points which are evenly distributed on both sides of a channel. It uses the linear function to calculate r and s and then uses these constants to determine the time difference from the center of the current channel to the nearest experimental point. The y values are smoothed simultaneously with the quadratic to determine the constants, a, b, and c. A smoothed value for y at the center of the channel is then computed.

The determination of the constants a, b and c, is simplified by the assumption of equal time intervals in the measurements. The time interval is assumed to be unity so that the relative time is an integer between -KP and +KP. The constants are then determined by a least squares procedure by solving the following normal equations: ( $k=kP$ )

$$a \sum_{-k}^k 1 + b(0) + c \sum_{-k}^k I^2 = \sum_{-k}^{+k} y_I$$

$$a(0) + b \sum_{-k}^k I^2 + c(0) = \sum_{-k}^{+k} I y_I$$

$$a \sum_{-k}^{+k} I^2 + b(0) + c \sum_{-k}^k I^4 = \sum_{-k}^{+k} I^2 y_I$$

The solution is simplified with the following summation formulae:

$$\sum_{-k}^{+k} I = \sum_{-k}^{+k} I^3 = 0$$

$$\sum_0^k I^2 = (1/6)k(k+1)(2k+1)$$

$$\sum_0^k I^4 = (1/30)k(k+1)(2k+1)(3k^2+3k-1)$$

#### IBITS (I1,I2,X)

IBITS is an ASCENTF coded subroutine which selects the bits I1 to I2, inclusive, of X and stores them right justified in IBITS. The bits are numbered from 1 to 60 from left to right. The spectral data on the input tape is read by SUMTAP3 as BCD coded information without conversion to a binary number. SUMTAP3 performs the BCD to binary conversion. The IBITS subroutine is used to locate a digit from the tape so that SUMTAP3 can perform the conversion to binary. This subroutine is coded specifically for a CDC 6600 digital computer, and may require changes if the computer or operating system is changed.

### Plotting Subroutines

The following subroutines are used to plot the spectra. They are assumed to be available in the computer library as part of the FORTRAN compiler. A brief description is included to illustrate their usage. CCGRID (5,2, 6HNOLBLS, 4). This subroutine draws a grid around the spectrum. The x axis is divided into 5 divisions each of which is subdivided into two parts by tick marks. The y axis is divided into 4 divisions. The grid is not to be labeled with a scale.

CCLTR (20., 300., 1,2) This subroutine letters the graph at x position 20. and y position 300. in a direction specified by 1 and a size specified by 2. The information to be lettered has been previously provided.

CCPLOT (SX,SY,NUM, 4HJOIN, 0,0) Plots the NUM points in (SX,SY). The first 0 specifies a symbol for the plot, and the second 0 indicates that every point in the array is to be plotted.

CCNEXT This subroutine spaces the chart paper so that another graph may be plotted. The previous graph is ended.

CCEND. This subroutine is called at the conclusion of the program to terminate the plotting.

### Special Subroutines for the CDC 6600

BUFFER IN (1,0) (W(1), W(120)) This subroutine reads a record from the input tape into the array, W.

IF(UNIT,1) 103, 110, 105, 104 This statement checks the status of the input tape and transfers to 103 if a read is still in progress; to 110 when the read operation is complete; to 105 if an end-of-file is found on the tape; to 105 if a parity error occurs during reading.

CALL RECALL(1) This statement places SUMTAP3 in an inactive status until the read operation on the input tape is complete.

LENGTHF(1) This function computes the length of the record which was just read from the input tape. The record length is usually  $80 \times 14 / 10 = 112$  words long.

IF (WARN(IME).NE.0) This statement checks the amount of time remaining to the program. If nonzero, the time limit has almost been reached and SUMTAP3 will terminate gracefully.

Note

The SUMTAP3 program was written in FORTRAN IV and ASCENTF to run on a CDC 6600 computer. If the computer is changed or if the operating system is changed, the program may require revision.

```
PROGRAM SUMTAP3 (INPUT,OUTPUT,TAPE1,TAPE2=INPUT,TAPE3=OUTPUT,  
* TAPE4,TAPE5,TAPE98,TAPE99)  
1 FORMAT(A10,2I5,E20.13)  
2 FORMAT(4E20.13)  
3 FORMAT(8A10)  
4 FORMAT(1H1,25X,44H*** ESR TAPE READING AND SUMMING PROGRAM ***//  
* 10X,7A10//20X,28HRESULTS ON TAPE4, LABELED **,A10,2H**)  
5 FORMAT(3I5,25X,4A10)  
6 FORMAT(/////5X,4HFILE,I3,13X,4A10//25X,I4,17H CHANNELS BETWEEN,  
* F13.4,4H AND,F13.4,5X,13HCHANNEL WIDTH,F12.6//)  
7 FORMAT(2I5,2E10.0)  
8 FORMAT(15X,15HSUMMED SPECTRUM,10X,10HTOTAL AREA,E20.10,5X,  
* 15H(INTEGRAL RANGE,E14.4,3H /,E14.4,1H)//)  
9 FORMAT(25X,20HNO COMPLETE SPECTRUM,5X,11HFIRST VALUE,F9.0,5X,  
* 10HLAST VALUE,F9.0)  
10 FORMAT(1H0,16H*****INPUT ERROR)  
11 FORMAT(//20X,22HRESULTS STORED AS FILE,I3,9H ON TAPE4//)  
12 FORMAT(10(10F12.6//))  
13 FORMAT(5HTAPE ,A10,5X,4HFILE,I3)  
14 FORMAT(4A10)  
15 FORMAT(//15X,26HTOTAL INTEGRATED INTENSITY,E20.10)  
16 FORMAT(15X,28HSECOND ORDER POLYNOMIAL WITH,I3,11H POINTS AS ,  
* 18HSMOOTHING FUNCTION,10X,I5,16H SPECTRA FOUND (,I4,  
$ 12H INCOMPLETE//)  
17 FORMAT(//5X,4HFILE,I3,12H NOT ON TAPE)  
18 FORMAT(1H0, 10X,32HPARITY ERROR ON TAPE1 IN RECORD , I5 ,  
1 6H FILE , I5 )  
19 FORMAT( 1H0, 16H YOU FOOL FILE , I5, 10H IS EMPTY //  
1 5X, 5H*****, 80H WARNING,-- CHAOS MAY OCCUR -- ASSUMING YOU WISHE  
2D FILE + 1, AND CONTINUING , 5H***** // )  
20 FORMAT( 1H0 , 20H CONTENTS OF BUFFER )  
21 FORMAT( 6X , 10A10 )  
DIMENSION COMMENT(7)  
DIMENSION FX(250),FY(250),W(120),SZ(2000)  
COMMON/ASPEC/ NSPEC  
COMMON/FSPEC/SX(2000),SY(2000)  
COMMON/FPAR/ISA,NUM,MM,MN,KP,FOIF,EMIN,EMAX,SW  
COMMON/CCPOOL/XMIN,XMAX,YMIN,YMAX,CCXMIN,CCXMAX,CCYMIN,CCYMAX  
COMMON/CCFACT/FACTOR  
EQUIVALENCE (SX(21),FX(1)),(SX(321),FY(1)),(SX(601),W(1))  
DATA KP,NUM,FMIN,FMAX/3,500,300.,9/90./  
C  
INITIALIZATION  
REWIND 1  
REWIND 4  
REWIND 5  
XMIN=0.  
XMAX=10000.  
IGRID=0  
NEOF=0  
NFILE=1  
NFILE2=1  
C  
INPUT SECTION  
50 READ (2,3) NAME,(COMMENT(J),J=1,7)  
WRITE (3,4) (COMMENT(J),J=1,7),NAME  
60 READ (2,5) NFILE1,IK,KK,(COMMENT(J),J=1,4)  
IF (NFILE1.LE.0) GOTO 401
```

```
SW=1.
IF (IK.LT.0) SW=-1.
IF (KK.EQ.0) GOTO 61
READ (2,7) KP,NUM,FMIN,FMAX
IF (KP.GT.9.OR.KP.LT.3) GOTO 398
IF (NUM.GT.2000) GOTO 398
IF (FMIN.GE.FMAX) GOTO 398
61 DO 62 J=1,NUM
62 SZ(J)=0.
C SET UP CHANNELS
70 FDIF=(FMAX-FMIN)/(NUM+2*KP-1)
FINT=KP*FDIF
EMIN=FMIN+FINT
EMAX=FMAX-FINT
FDIF=SW*FDIF
WRITE (3,6) NFILE1,(COMMENT(J),J=1,4),NUM,EMIN,EMAX,FDIF
71 NREC=0
NGO=0
NSPEC=0
NER=0
MN=0
M=1
FX2=0.
IF (IK.LT.0) FX2=1.E8
100 NREC=NREC+1
101 IPAR=0
C READ DATA TAPE --- SPECIAL 6600 FUNCTION
BUFFERIN (1,0) (W(1),W(120))
102 IF (UNIT,1) 103,110,105,104
103 CALL RECALL(1)
GOTO 102
C PRINT PARITY ERROR INFORMATION FOR DEBUGGING
104 WRITE( 3, 18 ) NREC, NFILE2
WRITE( 3, 20 )
WRITE( 3, 21 ) ( W(I) , I = 1, 120 )
GOTO 110
105 NEOF=NEOF+1
NFILE2=NFILE2+1
IF (NEOF.GE.2) GOTO 400
IF( NGO .EQ.1 ) GO TO 160
IF( NFILE2 .NE. NFILE1 + 1 ) GO TO 71
GO TO 300
110 NEOF=0
111 IF (NFILE2.NE.NFILE1) GOTO 101
112 NL=LENGTHF(1)-1
IF (NL.GT.112) NL=112
113 NC=NL*10
I=0
120 I=I+1
121 IF (I+13.GT.NC) GOTO 100
122 NW=(I+9)/10
J2=(I-(NW-1)*10)*6
J1=J2-5
C SEARCH FOR WORD MARK
L=IBITS(J1,J2,W(NW))
123 IF (L.NE.658) GOTO 120
```

```
124 ND=7
125 NN=10** (ND-1)
    IX=0
126 DO 127 J=1,ND
    I=I+1
    NW=(I+9)/10
    J2=(I-(NW-1)*10)*6
    J1=J2-5
C   GET A DIGIT
    L=IBITS(J1,J2,W(NW))
    IF (L.LT.338.OR.L.GT.448) GOTO 120
    IX=IX+NN*(L-338)
127 NN=NN/10
128 IF (ND.LT.6) GOTO 144
C   CHECK THAT POINT IS WITHIN SPECTRAL LIMITS
129 FX(M)=IX
    IF (NREC.EQ.1.AND.I.LT.13) FX1=FX(M)
    IF (IK.LT.0) GOTO 136
    IF (NGO-1) 130,132,135
130 IF (IX.LT.FMIN.OR.IX.GT.EMIN) GOTO 120
131 NGO=1
    GOTO 140
132 IF (IX.LT.FMAX.AND.IX.GT.FMIN) GOTO 140
    IF (FX(M1).GT.EMAX) GOTO 134
    IF (IX.GT.FX2) FX2=IX
    IF (FX(M1).GT.EMIN) GOTO 140
133 NGO=0
    GOTO 160
134 NGO=2
    GOTO 150
135 IF (IX.LE.FMIN) NGO=0
    GOTO 120
136 IF (NGO-1) 137,138,139
137 IF (IX.GT.FMAX.OR.IX.LT.EMAX) 120,131
138 IF (IX.GT.FMIN.AND.IX.LT.FMAX) GOTO 140
    IF (FX(M1).LT.EMIN) GOTO 134
    IF (IX.LT.FX2) FX2=IX
    IF (FX(M1).LT.EMAX) 140,133
139 IF (IX.GE.FMAX) NGO=0
    GOTO 120
140 I=I+1
141 NW=(I+9)/10
    J2=(I-(NW-1)*10)*6
    J1=J2-5
C   GET A DIGIT
    L=IBITS(J1,J2,W(NW))
142 LS=1
C   CHECK FOR SIGN OF NUMBER
    IF (L.EQ.458) GOTO 143
    IF (L.NE.468) GOTO 120
    LS=-1
143 ND=5
    GOTO 125
144 FY(M)=LS*IX
    M1=M
    M=M+1
```

```
145 IF (M.LE.250) GOTO 120
150 MM=M-1
      M=1
      M1=250
      MN=MN+MM
      WRITE (5) (FX(J),FY(J),J=1,MM)
151 GOTO (120,200), NGD
160 NER=NER+1
      M=1
161 MN=0
      REWIND 5
      IF (NEOF.EQ.0) 120,300
200 REWIND 5
      ISA=0
201 MM=250
      IF (MN.LT.MM) MM=MN
      READ (5) (FX(J),FY(J),J=1,MM)
      MN=MN-MM
      IF (MN.EQ.0) ISA=-1
      CALL SMOOTH2
202 IF (ISA.GT.0) GOTO 201
203 NSPEC=NSPEC+1
C     SUM SPECTRA
      DO 204 J=1,NUM
204  SZ(J)=SZ(J)+SY(J)
      REWIND 5
      IF (WARN(IME).NE.0) GOTO 300
C     OUTPUT SPECTRA AND INTEGRATE
      IF (NEOF.EQ.0) GOTO 120
300 IF (NSPEC.EQ.0) GOTO 399
      CCXMAX=1070.
      IF (NUM.GT.1000) CCXMAX=2070.
      XLTR=1140.
      IF (NUM.GT.1000) XLTR=2140.
      CALL CCGRID(5,2,6HNOLBLS,4)
      IGRID=1
      WRITE (98,13) NAME,NFILE1
      CALL CCLTR(20.,300.,1,2)
      WRITE (98,14) (COMMENT(J),J=1,4)
      CALL CCLTR(XLTR,200.,1,2)
      IF (EMAX.LE.10000.) GOTO 310
      XMIN=EMIN
      XMAX=EMAX
310 SMIN=SZ(1)
      SMAX=SMIN
      DO 311 J=1,NUM
      IF (SZ(J).GT.SMAX) SMAX=SZ(J)
      IF (SZ(J).LT.SMIN) SMIN=SZ(J)
311 CONTINUE
      AMP=SMAX-SMIN
      SHIFT=(SMAX+SMIN)/2.
312 SMIN=0.
      SMAX=0.
      SX(1)=EMIN-FDIF
      IF (IK.LT.0) SX(1)=EMAX-FDIF
      SY(1)=0.
```



```
A=0.
J1=1
DO 313 J=1,NUM
SX(J)=SX(J1)+FDIF
SZ(J)=(SZ(J)-SHIFT)/AMP
SY(J)=SY(J1)+SZ(J)
A=A+SY(J)
IF (SY(J).GT.SMAX) SMAX=SY(J)
IF (SY(J).LT.SMIN) SMIN=SY(J)
313 J1=J
KP1=2*KP+1
WRITE (3,16) KP1,NSPEC,NER
A=A*FDIF
WRITE (3,8) A,SMIN,SMAX
WRITE (3,12) (SZ(J),J=1,NUM)
YMIN=-1.5
YMAX=0.5
CALL CCPLLOT(SX,SZ,NUM,4HJOIN,0,0)
WRITE (4,1) NAME,NFILE,NUM,A
WRITE (4,2) (SX(J),SZ(J),J=1,NUM)
A=A-SY(NUM)*FDIF*(EMAX-EMIN)/2.
WRITE (3,15) A
WRITE (3,11) NFILE
YMIN=SMIN
YMAX=2.*SMAX-SMIN
CALL CCPLLOT(SX,SY,NUM,4HJOIN,0,0)
CALL CCNEXT
NFILE=NFILE+1
IF( WARN(TIME) ) 401, 60, 401
398 WRITE (3,10)
GOTO 60
399 WRITE (3,9) FX1,FX2
GOTO 60
C  TERMINATION PROCEDURE
400 IF( NEOF.LE.3 ) GO TO 403
IF (IGRID.NE.0) CALL CCEND
WRITE (3,17) NFILE1
401 STOP
403 IF( NFILE2 .EQ. NFILE1 + 1 ) GO TO 405
GO TO 71
405 WRITE( 3, 19 ) NFILE1
NFILE2 = NFILE2 - 1
GO TO 71
END
```

```
SUBROUTINE SMOOTH2
C 2. ORDER SMOOTHING AND INTERPOLATION OF Y-VALUES ACCORDING TO
C 1. ORDER SMOOTHED AND CHECKED X-VALUES
COMMON/FSPEC/SX(2000),SY(2000)
COMMON/FPAR/ISA,NUM,MM,MN,KP,FDIF,EMIN,EMAX,SW
COMMON/ASPEC/ NSPEC
DATA (J=0)
I=19-KP
IM=MM+20-KP
IF (J.GT.0) GOTO 2
C DEFINE SMOOTHING COEFFICIENTS
1 FAC=2.*KP+1.
AO=((KP+1)*KP)/3.
A3=1./((4.*KP+4.)*KP-3.)
A1=((9.*KP+9.)*KP-3.)*A3
A2=-15.*A3
A3=-A2/AO
EDIF=(EMAX-EMIN)/(MM+MN)
GAP=10.*EDIF
EDIF=SW*EDIF
FF=EMIN*FAC
IF (SW.LT.0.) FF=EMAX*FAC
DEL=FDIF*FAC
2 IF (ISA) 10,20,30
C TAKE CARE OF GAPS IN DATA
10 IM=MM+20
DO 11 N=1,20
N1=N+IM
SX(N1)=SX(IM)+N*EDIF
11 SX(N1+300)=SX(IM+300)
IF (J.NE.0) GOTO 30
20 DO 21 N=1,20
SX(N)=SX(21)-EDIF*(21-N)
21 SX(N+300)=SX(321)
IF (ISA.EQ.0) ISA=1
I=20
30 I1=I+1
T=SX(I)
DO 35 N=I1,IM
IF (ABS(SX(N)-T).LT.GAP) GOTO 34
L=1
31 IF (ABS(SX(N+L)-T).LT.(L+1)*GAP) GOTO 32
L=L+1
IF (L.LE.3) GOTO 31
32 DIF=(SX(N+L)-T)/(L+1)
DO 33 M=1,L
33 SX(N+M-1)=T+M*DIF
T=SX(N+L)
N=N+L
GOTO 35
34 T=SX(N)
35 CONTINUE
40 L=I-KP
M=I+KP
S=0.
DO 41 N=L,M
```

```
41 S=S+SX(N)
   T=S
   GOTO 101
C   SET UP FOR A CHANNEL POINT
100 IF (I.GE.IM) GOTO 110
   T=S
   I=I+1
   S=S+SX(I+KP)-SX(I-KP-1)
101 IF (SW*(S-FF)) 100,103,102
102 IF (SW*(S+T-2.*FF).LE.0.) GOTO 103
   I=I-1
   S=T
103 J=J+1
   IF (J.GT.NUM) GOTO 130
C   J INDICATES THE CHANNEL      I POINTS TO NEAR CENTER OF CHANNEL
C   COMPUTE THE CHANNEL POINT
104 L=I-KP
   M=I+KP
   Q=0.
   R=0.
   V=0.
   W=0.
   DO 105 K=L,M
   N=K-I
   Q=Q+N*SX(K)
   U=SX(K+300)
   R=R+U
   U=N*U
   V=V+U
105 W=W+N*U
   Q=(S-FF)/Q
C   QUADRATIC INTERPOLATION OF Y WITH X FROM LINEAR INTERPOLATION
106 SY(J)=R*A1+W*A2-Q*V+(Q*A0)**2*(R*A2+W*A3)
   FF=FF+DEL
   GOTO 101
110 IF (ISA.LT.0) GOTO 103
120 DO 121 N=1,20
   N1=N+MM
   SX(N)=SX(N1)
121 SX(N+300)=SX(N1+300)
   RETURN
130 J=0
   ISA=-1
   RETURN
   END
```

```
ASCENTF SUBROUTINE IBITS(I1,I2,X)
  RSSZ 1      .THIS ROUTINE SELECTS BITS I1 TO I2 (INCLU-
  BSSZ 1      .SIVE) OF X, AND STORES THEM (RIGHT ADJUSTED)
  BSSZ 1      .WITH ZERO FILL) IN IBITS.
  BSSZ 1      .BITS ARE 1 TO 60 LEFT TO RIGHT
  BSSZ 1
  RET        BSSZ 1      .DCS,6/22/66
  SA1  P1      .I1=(X1)
  SB1= X1-1
  SA2  B2      .I2=(X2)
  IX2= X2-X1
  SB4= X2-59   .N=NUMBER OF BITS=I2-I1+1=(B4)-60
  SA3  B3      .X=(X3)
  LX6= B1,X3   .LEFT SHIFT (X3), I1-1 BITS
  EQ   B0,B4 RET .DONE IF N=60
  LX6  B4,X6   .RIGHT SHIFT TO END OF WORD
  MX0  1
  SB4  B4+1
  LX0  B4,X0   .FORM 60-N BIT MASK
  BX6= -X0*X6
  EQ   B0,B0 RET .C/EST FINI
END
```

## 2. FITESR

FITESR\* performs a least squares fit of Lorentz lineshapes to experimental EPR spectra using the procedure described in Appendix I. It is suitable for spectra with a second order spin Hamiltonian and different widths for the hyperfine components (of 1 nucleus). It can calculate the relative abundance of up to 5 similar compounds present in a mixture. The spectra are assumed to be stored as derivatives of the absorption lines on a magnetic tape produced by SUMTAP3.

The program operates in the following manner. It starts from a given 0<sup>th</sup> order guess of the relevant parameters for the spectrum and iteratively calculates better parameters until the sums of the squares of the deviations between the observed and calculated spectral points remains constant, or until the iteration diverges. The parameters and their corrections in successive steps, including a baseline offset and drift, are printed out. The program prints the final parameters and plots the observed and calculated spectrum based on these parameters together with enlarged curves of the errors between these spectra.

The program may operate in one of two modes. In the first mode, the spectrum is considered to be composed of up to 12 individual Lorentz lines with different intensities, linewidths, and line centers. In the second mode, the spectrum is considered to be composed of hyperfine components of one nucleus with the line centers determined by a second order spin Hamiltonian, with the same intensities for all hyperfine components, but with different linewidths. The maximum number of parameters is 38.

---

\*Originally written by Dr. Alfred Bauder (Bauder and Myers, 1968).

INPUT DATA

Card 1. (Format 8A10)

NAME The name of the tape with the measured spectra which was given in SUMTAP3. Any 10 alphanumeric symbols (blanks count). This variable is used for file protection and causes the job to abort if it does not agree with the name found on the tape.

COMMENT Any arbitrary comment to be printed for identification

Card 2. (Format 4I5, 2E10.0, 4A10)

NFILE1 the number of the file to be analyzed (in order of increasing magnitude)

IFIT =0 individual lines according to first assignment of parameters  
>0 the number of compounds with second order Hamiltonian  
(second mode of operation)

If IFIT is 0, the first mode of operation is selected; otherwise, IFIT is the number of compounds to be fit with a second order Hamiltonian

NLINE the number of hyperfine components. If IFIT=0, then NLINE is the number of individual lines to be fit.

KFIELD =0 use arbitrary field calibration without nonlinearity correction.  
>0 use arbitrary calibration with nonlinearity correction  
<0 use the HCALIB field calibration subroutine.

This is a historically provided option. Usually KFIELD is negative and the HCALIB subroutine is used to calibrate the magnetic field.

HSTART Lower limit of the field sweep in gauss  
HSTOP Upper limit of the field sweep in gauss.

If KFIELD is negative, the HCALIB routine is used, and HSTART and HSTOP are not used. They are only used if KFIELD is zero or positive.

COMMENT Any comment to be printed and plotted to identify the job.

Card 3 - and following cards (Format 8E10.0)

X(J) the 0 th order estimates of the parameters  
if IFIT=0; first, all the line centers, second all the intensities and last all the linewidths of the NLINE individual absorption lines in the same order.  
if IFIT> 0; for each compound separately, in the following order; first, the  $H_0$  field, second, the hyperfine coupling constant, third, the integrated intensity, and last all the linewidths of the hyperfine components ordered according to ascending azimuthal quantum number.  
In both cases, the last two parameters are the baseline offset and baseline drift.

Cards are repeated from Card 2 to analyze additional spectra. A blank card at the end terminates the program execution.

#### SUBROUTINES

HCALIB (K,N,F) calibrates the N points in the array F according to the calibration specified by K (see listing)

MATINV (A,N,B,M, DETERM) solves the matrix equation  $AX=B$  for X. A is an  $N \times N$  matrix. M is the number of column vectors in B and should

be one. DETERM contains the determinant of A after the equations have been solved. The solution X is returned in B, and the inverse of A is returned in A.

NOTE

If the data for the spectrum is to be input from cards rather than from magnetic tape, the PROGRAM card must be altered so that the TAPE4 specification is changed to TAPE4=INPUT. The data cards for the spectra must be placed after card 2. The format of the data can be obtained from an examination of the program listings.



```
PROGRAM FITESR(INPUT,OUTPUT,TAPE2=INPUT,TAPE3=OUTPUT,TAPE4,  
1 TAPE98,PLOT,TAPE99=PLOT )  
DATA (LOOP=0),(PI=.636619772367581)  
DIMENSION G(38),X(38),FX(1000),FY(1000),FZ(1000),H(38,38)  
DIMENSION COMMENT(7),AR(5),GR(38),SP(33),IC(33)  
DIMENSION FC(33),C(33),D(33),DD(33),DS(33)  
DIMENSION G1(38)  
DIMENSION FW(1000)  
EQUIVALENCE (H,FW)  
COMMON/CCPOOL/XMIN,XMAX,YMIN,YMAX,CCXMIN,CCXMAX,CCYMIN,CCYMAX  
COMMON/CCFACT/FACTOR  
1 FORMAT(8A10)  
2 FORMAT(1H1,10X,7A10//21X,37H*** LEAST SQUARES FIT OF ESR-SPECTRA ,  
* 3H***//20X,28HSPECTRA ON TAPE4, LABELED **,A10,2H**//)  
3 FORMAT(4I5,2E10.0,4A10)  
4 FORMAT(///5H FILE,I3,10X,17HESR-SPECTRUM WITH,I3,  
* 28H INDIVIDUAL LORENTZIAN LINES//)  
5 FORMAT(///5H FILE,I3,10X,15HESR-SPECTRUM OF,I2,13H SUBSTANCES, ,  
* 25HWHICH ARE EACH SPLIT INTO,I3,19H CjMPONENTS DUE TO ,  
* 24HSECOND ORDER HAMILTONIAN//)  
6 FORMAT(18X,30HNUMBER OF FITTING PARAMETERS (,I2,  
* 17H) OR SUBSTANCES (,I2,2H) ,  
* 26HEXCEEDS AVAILABLE CAPACITY//)  
7 FORMAT(A10,2I5,E20.13)  
8 FORMAT(18X,4HFILE,I3,13H NOT ON TAPE ,A10//)  
9 FORMAT(10X,21HINCORRECT FILE LABEL ,A10)  
10 FORMAT(4E20.13)  
11 FORMAT(20X,I4,20H DATA POINTS ON FILE,I3,5X,I2,  
* 19H FITTING PARAMETERS//)  
12 FORMAT(8E10.0)  
13 FORMAT(5HTAPE ,A10,5X,4HFILE,I3)  
14 FORMAT(10X,33HFINAL VALUES OF LEAST SQUARES FIT,  
* 36H (STANDARD DEVIATION IN PARENTHESIS)//10X,  
* 10HTOTAL AREA,5X,8HMEASURED,E15.7,5X,10HCALCULATED,E15.7//  
$ 10X,15HBASELINE (A+BX),I2X,1HA,E15.7,2H (,E15.7,1H),9X,  
$ 1HB,E15.7,2H (,E15.7,1H//)  
15 FORMAT(10X,9HCjMPONENT,10X,11HLINE CENTER,18X,9HINTENSITY,21X,  
* 9HHALFWIDTH//)  
16 FORMAT(13X,I2,F18.4,2H (,F8.4,1H),E17.5,2H (,F12.5,1H),  
* F15.4,2H (,F8.4,1H)  
17 FORMAT(10X,25HSPECTRUM MEASURED BETWEEN, F12.3,10H GAUSS AND,  
* F12.3,6H GAUSS//25H ABSOLUTE VALUES IN GAUSS//)  
18 FORMAT(3X,3HND.,7X,14HREL. INTENSITY,8X,17HHC-FIELD (CENTER),  
* 9X,18HSPLITTING CONSTANT,5X,5HCOMP.,10X,10HLINE WIDTH,  
$ 9X,11HLINE CENTER//)  
19 FORMAT(3X,I2,F13.4,2H (,F6.4,1H),2(F15.3,2H (,F8.3,1H)),I8,  
* F15.3,2H (,F8.3,1H),F15.3/(79X,I8,F15.3,2H (,F8.3,1H),  
$ F15.3))  
20 FORMAT(10X,34H*** FATAL ERROR TERMINATES JOB ***)  
21 FORMAT(///34H RELATIVE VALUES REFERRING TO PLOT//)  
22 FORMAT(/20X,14HITERATION STEP,I2,5X,2HF=,E20.12,5X,2HX=/(10E13.4))  
23 FORMAT(/20X,14HITERATION STEP,I2,9H DIVERGED)  
24 FORMAT(///)  
25 FORMAT(20X,11HCORRECTIONS,5X,2HG=/(10E13.4))  
26 FORMAT(20X,2H**,4A10,2H**//)  
27 FORMAT(4A10)
```

```
28 FORMAT(8HERRORS *,F8.3)
29 FORMAT(20X,11HTIME LIMIT.)
30 FORMAT(1H0,18HERROR EXPANSION * ,F8.3 )
C   INITIALIZATION AND INPUT SECTION
101 M1=0
    IFIN=0
    REWIND 4
C   INPUT PARAMETERS
103 READ (2,1) NAME1,(COMMENT(J),J=1,7)
    WRITE (3,2) (COMMENT(J),J=1,7),NAME1
    LOOP=1
110 READ (2,3) NFILE1,IFIT,NLINE,KFIELD,HSTART,HSTOP,(COMMENT(J),
    *           J=1,4)
111 IF (NFILE1) 401,401,112
112 IF (IFIT) 141,120,130
120 WRITE (3,4) NFILE1,NLINE
    WRITE (3,26) (COMMENT(J),J=1,4)
    NVAR=3*NLINE+2
    GOTO 140
130 WRITE (3,5) NFILE1,IFIT,NLINE
    WRITE (3,26) (COMMENT(J),J=1,4)
    NVAR=IFIT*(NLINE+3)+2
140 IF ((NVAR.LE.38).AND.(IFIT.LE.5)) GOTO 150
141 WRITE (3,6) NVAR,IFIT
    READ (2,12) (X(J),J=1,NVAR)
    GOTO 110
C   READ SECTION OF INPUT TAPE4
150 READ (4,7) NAME,NFILE,NUM,AREA
151 IF (EOF,4) 152,153
152 WRITE (3,8) NFILE1, NAME1
    GOTO 400
C   CHECK FOR PROPER TAPE
153 IF (NAME.EQ.NAME1) GOTO 155
154 WRITE (3,9) NAME
    GOTO 400
155 READ (4,10) (FX(J),FY(J),J=1,NUM)
156 IF (NFILE.NE.NFILE1) GOTO 150
160 WRITE (3,11) NUM,NFILE,NVAR
C   INITIALIZATION
    SPIN=(NLINE-1)/2.
    SPIN2=SPIN*(SPIN+1.)
    FA=1.E300
    M2=0
    M3=0
    LOOP=2
    CALL CCGRID(5,2,6HNOLBLS,5)
C   0. ORDER SPECTRAL PARAMETERS
170 READ (2,12) (X(J),J=1,NVAR)
C   FIELD CORRECTION OR CALIBRATION
    IF (KFIELD.LT.0) GOTO 190
171 HS=(HSTART+HSTOP-8500.)/2000.
    HS=9.04-24.72*HS-0.8*HS**2
    HSTART=HSTART+HS
    HSTOP=HSTOP+HS
    SWEEP=(1.E-4)*(HSTOP-HSTART)
    IF (SWEEP.EQ.0.) GOTO 110
```

```
DISPL=HSTART/SWEEP
180 IF (KFIELD.EQ.0) GOTO 200
C CORRECTION FOR SWEEP NONLINEARITY
181 DO 182 J=1,NUM
  FK=(FX(J)-5000.)*SWEEP/100.
182 FX(J)=FX(J)-3.20*FK**2
  GOTO 200
C UTILIZE USER PROVIDED FIELD CALIBRATION IF K IS NEGATIVE
190 CALL HCALIB(KFIELD,NUM,FX)
  SWEEP=1.
  DISPL=0.
  HSTART=FX(1)
  HSTOP=FX(NUM)
C CLEARING OF ARRAYS USED FOR THE NORMAL EQUATIONS
200 F=0.
  DO 201 J=1,NVAR
    G(J)=0.
  DO 201 M=J,NVAR
201 H(J,M)=0.
C CALCULATION OF THE PARAMETERS, USED IN THE LEAST SQUARES FIT
C FC CONTAINS THE CENTER FREQUENCIES
C C CONTAINS THE INTENSITIES
C D CONTAINS THE HALFWIDTHS
202 IF (IFIT) 215,210,215
C IFIT = 0 USE INDIVIDUAL LINES
210 DO 211 J=1,NLINE
  J1=2*NLINE+J
  FC(J)=X(J)
  C(J)=X(J+NLINE)
211 D(J)=X(J1)
  GOTO 219
C IFIT .NE. 0 USE 2ND ORDER HAMILTONIAN
215 J1=0
  DO 217 I=1,IFIT
    X1=X(J1+1)
    X2=X(J1+2)
    C1=X(J1+3)/NLINE
  DO 216 J=1,NLINE
    K=(I-1)*NLINE+J
    SPIN3=J-SPIN-1.
    SP(J)=X2**2*(SPIN2-SPIN3**2)/2.
    FC(K)=X1-X2*SPIN3-SP(J)/(X1+DISPL)
    C(K)=C1
216 D(K)=X(J+J1+3)
217 J1=J1+NLINE+3
219 A=X(J1+1)
  B=X(J1+2)
C START OF LEAST SQUARES FIT ITERATIONS
220 DO 271 N=1,NUM
221 FZ(N)=A+B*FX(N)
C CLEARING THE ARRAY FOR THE DERIVATIVES
DO 222 J=1,NVAR
222 GR(J)=0.
  GR(NVAR-1)=1.
  GR(NVAR)=FX(N)
  J1=0
```

```
230 DO 262 I=1,IFIT
240 DO 261 J=1,NLINE
C   CALCULATION OF INTERMEDIATE VALUES
    K=(I-1)*NLINE+J
    S=FC(K)-FX(N)
    T=S*D(K)
    R=S*S+D(K)**2
    P=R*R
    R=P*R
    P=PI*T/P
    Q=PI*C(K)*(D(K)**3-3.*T*S)/R
    R=PI*C(K)*(S**3-3.*T*D(K))/R
C   CALCULATION OF THE FUNCTION
241 FZ(N)=FZ(N)+P*C(K)
C   CALCULATION OF THE DERIVATIVES
242 IF (IFIT) 260,250,260
250 J1=2*NLINE+J
    GR(J)=Q
    GR(J+NLINE)=P
    GR(J1)=R
    GOTO 261
260 SPIN3=J-SPIN-1.
    W=X(J1+1)+DISPL
    U=SP(J)/W**2+1.
    V=2*SP(J)/W/X(J1+2)+SPIN3
    GR(J1+1)=GR(J1+1)+Q*U
    GR(J1+2)=GR(J1+2)-Q*V
    GR(J1+3)=GR(J1+3)+P/NLINE
    GR(J+J1+3)=R
261 CONTINUE
    J1=J1+NLINE+3
262 CONTINUE
C   SUM OF RESIDUALS SQUARED
270 FD=FZ(N)-FY(N)
    F=F+FD**2
C   CALCULATION OF THE NORMAL EQUATION
    DO 271 J=1,NVAR
    G(J)=G(J)+FD*GR(J)
    DO 271 M=J,NVAR
    H(J,M)=H(J,M)+GR(J)*GR(M)
271 H(M,J)=H(J,M)
272 WRITE (3,22) M1,F,(X(J),J=1,NVAR)
C   SOLVE H*X=G ( X IS ACTUALLY SOLVED INTO G )
280 CALL MATINV(H,NVAR,G,1,DET)
    WRITE (3,25) (G(J),J=1,NVAR)
C   TERMINATION CRITERIA
    IF (WARN(TIME)) 289,281,289
281 IF (M1.GE.19) GOTO 292
    IF (FA-F.LT.F*1.E-3) GOTO 290
C   CALCULATION OF THE NEXT ORDER PARAMETERS
    M2=M1
282 DO 285 J=1,NVAR
    IF (J.GE.NVAR-1) GOTO 284
C   CHECKING THE IMPROVEMENTS FOR THE PARAMETERS
C   ADJUST CORRECTION VECTORS TO HELP PREVENT DIVERGENCE
    IF (G(J)**2.LT.F*H(J,J)/NUM/10.) GOTO 284
```

```
GA=ABS(G(J))
GB=ABS(X(J))/5.
IF (M3.NE.1) GOTO 283
GC=ABS(G1(J))
FAC=1.
IF (GA.GT.GC) FAC=2.
IF (G(J)**2.GT.F*H(J,J)/(NUM-NVAR)) FAC=FAC*2.
IF (SIGN(GA,G1(J)).NE.G(J)) FAC=FAC*3.
G(J)=G(J)/FAC
GA=ABS(G(J))
283 IF (GA.GT.GB) G(J)=SIGN(GB,G(J))
C CALCULATE NEXT SET OF PARAMETERS
284 X(J)=X(J)-G(J)
G1(J)=G(J)
285 CONTINUE
IF (M2.NE.M1) M3=1
286 M1=M1+1
FA=F
GOTO 200
289 IFIN=1
WRITE (3,29)
GOTO 292
290 IF (FA-F) 291,292,292
C PERMIT FIT TO DIVERGE ONLY THREE TIMES
291 WRITE (3,23) M1
IF (F-FA.LT.F/20.) GOTO 292
IF (M1-M2.LT.2) GOTO 282
IF (M2.EQ.0) GOTO 360
C CALCULATION OF THE STANDARD DEVIATIONS
292 DO 293 J=1,NVAR
293 G(J)=SQRT(F*H(J,J)/(NUM-NVAR))
C OUTPUT AND PLOTTING SECTION
300 XMIN=0.
IF (KFIELD.LT.0) XMIN=FX(1)
XMAX=10000.
IF (KFIELD.LT.0) XMAX=FX(NUM)
WRITE (3,24)
WRITE (98,13) NAME,NFILE
CALL CCLTR(20.,300.,1,2)
WRITE (98,27) (COMMENT(J),J=1,4)
CALL CCLTR(1140.,200.,1,2)
C SEARCH FOR THE LIMITS OF THE PLOT
YMIN = FZ(1)
YMAX = FZ(1)
YL=0.
DO 301 J=1,NUM
IF (FZ(J).LT.YMIN) YMIN=FZ(J)
IF (FY(J).LT.YMIN) YMIN=FY(J)
IF (FZ(J).GT.YMAX) YMAX=FZ(J)
IF (FY(J).GT.YMAX) YMAX=FY(J)
FW(J)=FZ(J)-FY(J)
ZY=ABS(FW(J))
IF (ZY.GT.YL) YL=ZY
301 CONTINUE
Y1=(YMAX-YMIN)/YL/8.
WRITE (98,28) Y1
```

```
CALL CCLTR(70.,30.,0,2)
YMIN=(5.*YMIN-YMAX)/4.
CALL CCPLT(FX,FZ,NUM,4HJOIN,0,0)
CALL CCPLT(FX,FY,NUM,6HNOJOIN,23,3)
YMIN=-YL
YMAX=9.*YL
CALL CCPLT(FX,FW,NUM,4HJOIN,0,0)
CALL CCNEXT
C CHECKING OF THE INTEGRATED INTENSITIES
310 ARE=0.
DO 312 I=1,IFIT
AR(I)=0.
DO 311 J=1,NLINE
K=(I-1)*NLINE+J
311 AR(I)=AR(I)+C(K)
312 ARE=ARE+AR(I)
313 Y=FX(NUM)-FX(1)
ARA=ARE+A*Y**2/2.+B*Y**3/6.
320 WRITE (3,14) AREA,ARA,A,G(NVAR-1),B,G(NVAR)
C OUTPUT OF THE RESULTS
321 IF (IFIT) 350,340,350
340 WRITE (3,21)
WRITE (3,15)
DO 341 J=1,NLINE
CT=G(J+NLINE)
DT=G(J+2*NLINE)
341 WRITE (3,16) J,FC(J),G(J),C(J),CT,D(J),DT
GOTO 360
350 WRITE (3,17) HSTART,HSTOP
WRITE (3,18)
J1=0
DO 352 I=1,IFIT
DO 351 J=1,NLINE
K=(I-1)*NLINE+J
IC(K)=J
DD(K)=D(K)*SWEEP
SP(K)=G(J+J1+3)
DS(K)=G(J+J1+3)*SWEEP
351 C(K)=FC(K)*SWEEP+HSTART
K=(I-1)*NLINE+1
K1=K+NLINE-1
FH=HSTART+X(J1+1)*SWEEP
FG=X(J1+2)*SWEEP
FS=G(J1+1)*SWEEP
FT=G(J1+2)*SWEEP
AR(I)=AR(I)/ARE
GR(I)=G(J1+3)/ARE
IF (KFIELD.LT.0) GOTO 352
WRITE (3,19) I,AR(I),GR(I),FH,FS,FG,FT,(IC(J),DD(J),DS(J),C(J),
* J=K,K1)
352 J1=J1+NLINE+3
IF (KFIELD.LT.0) GOTO 353
WRITE (3,21)
WRITE (3,18)
353 J1=0
DO 354 I=1,IFIT
```

```
K=(I-1)*NLINE+1
K1=K+NLINE-1
WRITE (3,19) I,AR(I),GR(I),X(J1+1),G(J1+1),X(J1+2),G(J1+2),(IC(J),
*      U(J),SP(J),FC(J),J=K,K1)
354 J1=J1+NLINE+3
360 M1=0
      WRITE( 3, 30 ) Y1
      WRITE (3,24)
      IF (IFIN) 401,110,401
C     PROGRAM TERMINATION
400 WRITE (3,20)
401 IF (LOOP.EQ.2) CALL CCEND
      STOP
      END
```

```
      SUBROUTINE HCALIB ( K, N, F )
      DIMENSION F(1000)
C     SAMPLE CALIBRATION ROUTINE
C     CALIBRATE THE VALUES IN F      N POINTS
C     OR CONVERT FROM ONE UNIT TO ANOTHER UNIT
C     FOR EXAMPLE IF F CONTAINS NMR FREQUENCIES
C     DO 10 J = 1, N
C 10   F(J) = F(J) / 425775
C     FOR FIELDIAL CALIBRATION WITH COEFFICIENTS FROM PROGRAM GAUSS
C     DO 10 J=1,N
C 10   F(J) = A+B*F(J)+C*F(J)**2
C     IF DATA REQUIRE SEVERAL DIFFERENT CALIBRATIONS
C     K MAY BE USED TO SELECT CALIBRATION
C     IK=-K
C     GO TO ( 1,2,3, ...ETC....)IK
C     DO 10 J=1, N
10   F(J) = 2834.7580+( 1.0366706E-01 -2.2958270E-07*F(J) ) *F(J)
      RETURN
      END
```



```

C      FORTRAN IV SUBROUTINE MATINV(A,N,B,M,DETERM)
C      MATRIX INVERSION WITH ACCOMPANYING SOLUTION OF LINEAR EQUATIONS
C      DIMENSION IPIVOT(38),A(38,38),B(38,1),INDEX(38,2),PIVOT(38)
C      EQUIVALENCE (IROW,JROW), (ICOLU,JCOLU), (AMAX, T, SWAP)
C      INITIALIZATION
C      10 DETERM=1.0
C      15 DO 20 J=1,N
C      20 IPIVOT(J)=0
C      30 DO 550 I=1,N
C      SEARCH FOR PIVOT ELEMENT
C      SEARCH FOR PIVOT ELEMENT
C      40 AMAX=0.0
C      45 DO 105 J=1,N
C      50 IF (IPIVOT(J)-1) 60, 105, 60
C      60 DO 100 K=1,N
C      70 IF (IPIVOT(K)-1) 80, 100, 740
C      80 IF (ABS(AMAX)-ABS(A(J,K))) 85, 100, 100
C      85 IROW=J
C      90 ICOLU=K
C      95 AMAX=A(J,K)
C      100 CONTINUE
C      105 CONTINUE
C      IF(AMAX) 110,800,110
C      110 IPIVOT(ICOLU)=IPIVOT(ICOLU)+1
C      INTERCHANGE ROWS TO PUT PIVOT ELEMENT ON DIAGONAL
C      130 IF (IROW-ICOLU) 140, 260, 140
C      140 DETERM=-DETERM
C      150 DO 200 L=1,N
C      160 SWAP=A(IROW,L)
C      170 A(IROW,L)=A(ICOLU,L)
C      200 A(ICOLU,L)=SWAP
C      205 IF(M) 260, 260, 210
C      210 DO 250 L=1, M
C      220 SWAP=B(IROW,L)
C      230 B(IROW,L)=B(ICOLU,L)
C      250 B(ICOLU,L)=SWAP
C      260 INDEX(I,1)=IROW
C      270 INDEX(I,2)=ICOLU
C      310 PIVOT(I)=A(ICOLU,ICOLU)
C      320 DETERM=DETERM*PIVOT(I)
C      DIVIDE PIVOT ROW BY PIVOT ELEMENT
C      330 A(ICOLU,ICOLU)=1.0
C      340 DO 350 L=1,N
C      350 A(ICOLU,L)=A(ICOLU,L)/PIVOT(I)
F4020003
F4020004
ANF40201
F4020002
F4020007
F4020008
F4020009
F4020010
F4020011
F4020012
F4020013
F4020014
F4020015
F4020016
F4020017
F4020015
F4020016
F4020017
F4020015
F4020016
F4020017
F4020018
F4020019
F4020020
F4020021
F4020022
F4020024
F4020025
F4020026
F4020027
F4020028
F402REV.
F4020029
F4020030
F4020031
F4020032
F4020033
F4020034
F4020035
F4020036
F4020037
F4020038
F4020039
F4020040
F4020041
F4020042
F4020043
F4020044
F4020044
F4020045
F4020046
F4020047
F4020048
F4020049
F4020050
F4020051
F4020052
F4020053
```

355 IF(M) 380, 380, 360	F4020054
360 DO 370 L=1,M	F4020055
370 B(ICOLUM,L)=B(ICOLUM,L)/PIVOT(I)	F4020056
C	F4020057
C     REDUCE NON-PIVOT ROWS	F4020058
C	F4020059
380 DO 550 L1=1,N	F4020060
390 IF(L1-ICOLUM) 400, 550, 400	F4020061
400 T=A(L1,ICOLUM)	F4020062
420 A(L1,ICOLUM)=0.0	F4020063
430 DO 450 L=1,N	F4020064
450 A(L1,L)=A(L1,L)-A(ICOLUM,L)*T	F4020065
455 IF(M) 550, 550, 460	F4020066
460 DO 500 L=1,M	F4020067
500 B(L1,L)=B(L1,L)-B(ICOLUM,L)*T	F4020068
550 CONTINUE	F4020069
C	F4020070
C     INTERCHANGE COLUMNS	F4020071
C	F4020072
600 DO 710 I=1,N	F4020073
610 L=N+1-I	F4020074
620 IF (INDEX(L,1)-INDEX(L,2)) 630, 710, 630	F4020075
630 JROW=INDEX(L,1)	F4020076
640 JCOLUM=INDEX(L,2)	F4020077
650 DO 705 K=1,N	F4020078
660 SWAP=A(K,JROW)	F4020079
670 A(K,JROW)=A(K,JCOLUM)	F4020080
700 A(K,JCOLUM)=SWAP	F4020081
705 CONTINUE	F4020082
710 CONTINUE	F4020083
740 RETURN	F4020084
800 DETERM = 0.	F402REV.
RETURN	F402REV.
END	

### 3. GAUSS

When the digital data acquisition system is used with the Varian spectrometer system, a NMR tracking system is not normally employed. In this case the recorder x-axis drive voltage from the Fieldial is applied to a Vidar voltage-to-frequency converter and this frequency is measured as the magnetic field coordinate. In order for the least squares fitting programs to work in units of gauss, a calibration of the Vidar frequencies in terms of magnetic field must be performed. The GAUSS program relates the Vidar frequencies to the magnetic field.

A series of measurements of the magnetic field (using proton NMR) is made over the entire range of the sweep. This produces a set of paired measurements of the magnetic field (NMR frequency) and of the Vidar frequency. A quadratic equation

$$Y = A + B * X + C * X**2$$

is fit to these points to produce the coefficients A, B, C. Then, given a Vidar frequency (X), the magnetic field (Y) may be computed. These coefficients are used to write the subroutine HCALIB which is used by FITESR. The input to the program is the measurements X(I), the Vidar frequency; and Z(I), the proton frequency corresponding to Y(I) the magnetic field in gauss. The proton NMR frequency is converted to gauss by the program. The output consists of the coefficients A, B, and C and a comparison of the experimental field with the theoretical field for a given Vidar value.

INPUT DATA

Card 1 (Format I5, 7A10)

N            number of pairs of Points used in the calibration (minimum of  
             three)

TITLE        any identification information

Card 2 (Format 8E10.0)

X(I)        Vidar reading in terms of tens of cycles (decacycles)

Z(1)        Proton NMR frequency in kilocycles

X(2)        etc. until X(N), Z(N)

Z(2)

There are as many of Card 2 as needed to contain N points, 4 points  
to a card.

If several calibrations are to be performed at once, continued  
with data from Card 1, etc. A blank card at the end of the data will  
terminate processing.

The GAUSS program requires the subroutine MATINV which is described  
in the discussion of FITESR.

```
PROGRAM GAUSS(INPUT,OUTPUT)
C PROGRAM FOR LEAST SQUARES FIT TO  $A + B*X + C*(X**2) = Y$ 
C VERSION TO SEPT. 1, 1969. JAMES J. CHANG.
  DIMENSION X(25), Y(25), Z(25), DIF(25), PRED(25)
  DIMENSION A(20, 10), B(20), SIGMA(10), TITLE(7)
C INPUT SECTION
1 READ 100, N, ( TITLE(I), I= 1,7 )
  IF(N) 80,80, 3
3 CONTINUE
  READ 101, ( X(I), Z(I), I= 1,N )
C X(I) IS VIDAR FREQUENCY IN TENS OF CYCLES
C Z(I) IS PROTON NMR FREQUENCY IN KC.
  PRINT 102, ( TITLE(I), I= 1,7 )
  PRINT 103
  PRINT 120
C SECTION TO CLEAR STORAGE
  XSUM = 0.0
  XSUMSQ = 0.0
  XSUMC = 0.0
  XSUM4 = 0.0
  YSUM = 0.0
  XYSUM = 0.0
  X2YSUM = 0.0
C SECTION TO COMPUTE MATRIX ELEMENTS
DO 20 I = 1, N
C CONVERSION TO MAGNETIC FIELD
10 Y(I) = Z(I) * 0.234875
  XSUM = XSUM + X(I)
  XSUMSQ = XSUMSQ + X(I) * X(I)
  XSUMC = XSUMC + X(I) * X(I) * X(I)
  XSUM4 = XSUM4 + ( X(I) * X(I) * X(I) * X(I) )
  YSUM = YSUM + Y(I)
  XYSUM = XYSUM + X(I) * Y(I)
  X2YSUM = X2YSUM + X(I) * X(I) * Y(I)
20 CONTINUE
C SET UP MATRIX OF NORMAL EQUATIONS
  A(1,1) = N
  A(1,2) = XSUM
  A(1,3) = XSUMSQ
  A(2,2) = XSUMSQ
  A(2,3) = XSUMC
  A(3,3) = XSUM4
  A(2,1) = XSUM
  A(3,1) = XSUMSQ
  A(3,2) = XSUMC
  B(1) = YSUM
  B(2) = XYSUM
  B(3) = X2YSUM
  PRINT 109
  DO 40 I = 1,3
40 PRINT 110, ( A(I,J), J= 1,3 ), B(I)
  CALL MATINV( A,3,B,1,DETERM)
  PRINT 152, DETERM
C SECTION TO COMPUTE PREDICTED VALUES AND DIFFERENCES
  F = 0.0
  DO 50 I = 1, N
```

```
PRED(I) = B(1) + B(2) * X(I) + B(3) * ( X(I) * X(I) )
DIF(I) = Y(I) - PRED(I)
F = F + DIF(I) * DIF(I)
50 CONTINUE
AN = N
S = SQRT( F/(AN-3.0) )
PRINT 121
PRINT 122, ( X(I), Z(I), Y(I), PRED(I), DIF(I), I= 1,N )
C SECTION TO COMPUTE STANDARD DEVIATIONS OF PARAMETERS
DO 55 I = 1,3
SIGMA(I) = S * SQRT( A(I,I) )
55 CONTINUE
PRINT 125, F, S
PRINT 130
PRINT 150
PRINT 151, ( B(I) , SIGMA(I) , I= 1, 3 )
PRINT 155, B(1), B(2), B(3)
GO TO 1
80 CALL EXIT
100 FORMAT (I5, 7A10)
101 FORMAT( 8E10.5 )
102 FORMAT( 1H1, 20X, 7A10 )
103 FORMAT(1H0,5X,*VIDAR FIELD CALIBRATION,SEPT 1,1969 VERSION* //)
109 FORMAT( 1H0, 20H NORMAL EQUATIONS )
110 FORMAT( 10X, 3E16.7, 15X , E16.7)
120 FORMAT(1H0, 45H INPUT POINTS, CONVERSION FACTOR = 0.234875 //)
121 FORMAT(20X, 1HX,19X,1HZ,19X,1HY, 16X,4HPRED,18X, 3HDIF )
122 FORMAT( 10X, 5( F16.3 , 4X ) )
125 FORMAT( 1H0, 10H RESIDUALS , F16.7, 5X, 6HSIGMA , E16.7 )
130 FORMAT( 1H0, 20X, 30H FIT TO Y = A + B*X + C*(X**2) //)
150 FORMAT (1H0, 20H COEFFICIENTS ARE )
151 FORMAT( 1H0, 5X, 2HA=, E16.7, 2H ( ,E13.7,1H),/ 6X,2HB=,E16.7,
1 2H ( ,E13.7, 1H),/ 6X,2HC=,E16.7,2H ( ,E13.7,1H),// )
152 FORMAT( 20X, 15H DETERMINANT , F16.7//)
155 FORMAT( 1H0, 6X, 6HF(J)= , F10.4, 4H + ( , E14.7, 1H+,
1 E14.7, 15H *F(J) ) * F(J) )
END
```

B. Simulation Programs

1. IMITATE

The IMITATE program is used to simulate isotropic EPR spectra for both transition metals and organic radicals. The line positions are determined by a g value and the coupling constants according to Eq. A-11. The lineshapes are produced by Eq. A-12 which is expanded to account for more than one species. The program is at present capable of simulating a spectrum containing as many as four separate spectra each of which is characterized by g values and A values. The program is well suited for simulating spectra of a system containing several isotopic species.

In operation, the program first computes the resonance fields for each of the lines in the spectrum. Because of the storage limitations the program is limited to a maximum of 1600 lines. This may be changed by changing the DIMENSION statements. The intensity ratios of the lines are computed by SUBROUTINE RATIO. Again because of dimension limitation a given coupling constant should not produce more than 25 lines.

INPUT DATA

Card 1 (Format 2I5, 30X, 4A10)

NSPECY The number of species to be simulated. Maximum value of 4.

If NSPECY=0, the job is terminated.

NUM The number of points to be computed in the spectrum

COMMENT(J) Any comment information

Card 2 (Format 10I5)

NCOUP(J) The number of coupling constants for each species. For one species there is NCOUP (1); for two, there are NCOUP (1) and NCOUP (2). NCOUP (1)=1 for one coupling constant; =2 for two constants, etc.

Card 3. (Format 5(I5, F10.5))

NEQ(J1,J) The number of equivalent nuclei corresponding to a particular coupling constant (which is given later), for the Jth species. All of the NEQ(J1,J) for the same species are on the same card.

S(J1,J) The nuclear spin for the NEQ nuclei. For two protons NEQ=2;S=0.5.

There are as many of card 3 as there are species. Note that if there are more than 5 sets of equivalent nuclei for a given species, the data must be on a second card 3(maximum of 10 sets possible).

Card 4. (Format 8F10.5)

HSTART The starting field for the simulation

HSTOP The ending field for the simulation. The spectra are computed from HSTART to HSTOP

ALPHA Baseline offset

BETA Baseline drift. Normally ALPHA and BETA are zero.

Card 5. (Format 8F10.5)

FINT(J) The intensity of the Jth species. This is an arbitrary number but the relative values of FINT should correspond to the relative intensities of the different species.

HZERO(J) The resonance center for the Jth species. This should be computed from the g value and the microwave frequency.

A(J1,J) The coupling constants corresponding to the NEQ(J1,J) of card 3. for the Jth species. More than 6 constants are continued on the next card.

Card 6. (Format 8F10.5)

FLAG =0 read the widths of all of the lines

≠0 all the lines have the same width



Card 7. (Format 8F10.5)

W(K) The linewidth. If FLAG=0, the widths for all the lines must be provided on as many of card 7 as required. For the purpose of identifying a given line, each line is identified by a K value in addition to its identification by the  $m_I$  values. The value of K is determined by the  $m_I$  values and by the order in which the spins were presented on card 3. K=1 occurs when all the  $m_I$  have their lowest values. When the first  $m_I$  (corresponding to the first S on card 3) has the second from lowest value, with all other  $m_I$  at their lowest value, then K=2. If the second  $m_I$  is at its second from lowest value, with all other  $m_I$  at their lowest values, then  $K=2S_1+2$  where  $S_1$  is the maximum value of the first S on card 3. If FLAG≠0, only one width is provided (requires only 1 card).

There are as many of cards 5, 6, and 7 as there are species. Note that the cards 5, 6, 7 must come together. For two species the order is card 5, card 6, card 7, card 5, card 6, card 7.

If more than one spectrum is to be simulated, the data are continued from card 1. A blank card at the end of the data will terminate processing. The following is a sample data set which could be used to simulate hexaquocopper (II).

Col.5	10	20	30		
1	500			SAMPLE COPPER SPECTRUM	
1					
1	1.5				
2750.0		3250.0	0.0		0.0
100.		3000.0	-34.4		
0.0					
60.0		58.0	56.0		56.0
(blank card)					

```
PROGRAM IMITATE(INPUT,OUTPUT,TAPE98,PLOT,TAPE99=PLOT)
C PROGRAM FOR SIMULATING MANY SPECIES EPR SPECTRA
COMMON/SPINS/NCOUP(10),NEQ(10,4),S(10,4),SMI(10,4),SM(10),NLINE(4)
COMMON/FSPEC/NUM,AREA,FX(2000),FZ(2000),NSPECY
COMMON/STORE1/A(10,4),FINT(4),W(1600),R(1600),H(1600),JS
COMMON/CCPOOL/XMIN,XMAX,YMIN,YMAX,CCXMIN,CCXMAX,CCYMIN,CCYMAX
COMMON/CCFACT/FACTOR
DIMENSION COMMENT(4),HZFRD(4)
DATA(TWOPI = .636619772367581)
5 CONTINUE
C SECTION FOR INPUT OF SPECTRUM PARAMETERS
READ 401, NSPECY, NUM, (COMMENT(J), J = 1,4)
C TERMINATION TEST
IF( NSPECY ) 99, 99, 10
10 CONTINUE
READ 402, ( NCOUP(J), J = 1, NSPECY )
DO 20 J = 1, NSPECY
C READ NO. OF NUCLEI AND SPIN
JX = NCOUP(J)
READ 404, (NEQ(J1,J),S(J1,J),J1=1,JX)
NLINE(J) = 1
DO 20 J1 = 1, JX
NLINE(J) = (2*NEQ(J1,J)*S(J1,J) + 1) * NLINE(J)
20 CONTINUE
DO 15 J = 1, NSPECY
KP = KP + NLINE(J)
IF ( KP .GT. 1600 ) GO TO 4
GO TO 15
4 PRINT 421, KP
GO TO 5
15 CONTINUE
READ 405, HSTART, HSTOP, ALPHA, BETA
KP = 0
DO 25 J = 1, NSPECY
KP = KP + 1
JX = NCOUP(J)
READ 405, FINT(J),HZERO(J),(A(J1,J),J1 = 1,JX)
J2 = NLINE(J)
READ 405, FLAG
C FLAG = 0 IMPLIES READ WIDTHS FOR ALL LINES
C FLAG .NE.0 ALL LINES HAVE SAME WIDTH
IF( FLAG ) 21, 24, 21
21 READ 405, W(KP)
DO 22 J1 = 1, J2
KP=KP + 1
W(KP) = W(KP-1)
22 CONTINUE
GO TO 25
24 CONTINUE
KP1 = KP + J2
READ 405, ( W(J1), J1= KP, KP1 )
KP = KP1
25 CONTINUE
PRINT 410, NSPECY, NUM
PRINT 411, ALPHA, BETA, HSTART, HSTOP
PRINT 420, ( COMMENT(J), J = 1, 4 )
```

```
      AR = 0.0
      DO 30 J = 1, NSPECY
      AR = FINT(J) + AR
30    CONTINUE
      CALL RATIO
      DO 60 J = 1, NSPECY
      JX = NCOUP ( J )
      KP = 1 + NLINE(J) * ( J-1 )
      FACT = 1.0 / R(KP)
      RINT = FINT(J) / AR
      PRINT 412
      PRINT 413, J, FINT(J), RINT, HZERO(J), (A(J1, J), NEQ(J1, J),
1    S(J1, J) , J1= 1, JX )
C$$$  START OF LARGE NESTED LOOP FOR COUNTING THROUGH M SUB I AND
C    ARRIVING AT A PROPER K VALUE
C$$$  LOOP INITIALIZATION
      PRINT 415
      K = 0
      LOOP = JX
100   SM(LOOP) = -SMI(LOOP, J )
110   IF( LOOP .EQ. 1 ) GO TO 120
      LOOP = LOOP - 1
      GO TO 100
C$$  START OF LOOP WORK
120   CONTINUE
C
C    START LINE COUNT
      K = K + 1
      FIRST = 0.0
      SECOND = 0.0
C    COMPUTE THE RESONANCE FIELDS
      DO 40 K1 = 1, JX
      FIRST = FIRST + SM(K1) * A(K1, J)
      SPIN = SMI(K1, J) * ( SMI(K1, J) + 1.0 ) - SM(K1) * SM(K1)
      SECOND = SECOND + ( A(K1, J) * A(K1, J) / (2.0 * HZERO(J) ) ) * SPIN
40    CONTINUE
      KP = K + NLINE(J) * ( J- 1 )
      H(KP) = HZERO(J) - FIRST - SECOND
      REL = R(KP) * FACT
      PRINT 416, K, W(KP), H(KP), REL, (SM(I), I=1, JX )
C$$$  ENDING OF LARGE NESTED LOOP
C    INNER LOOP CONTROL
130   SM(LOOP) = SM(LOOP) + 1.0
      IF ( SM(LOOP) .LE. SMI(LOOP, J) ) GO TO 120
C    MOVING LOOP CONTROL
140   LOOP = LOOP + 1
C    MAIN LOOP TERMINATION TEST
      IF( LOOP .GT. JX ) GO TO 150
      SM(LOOP) = SM(LOOP) + 1.0
      IF ( SM(LOOP) .GT. SMI(LOOP, J) ) GO TO 140
      LOOP = LOOP - 1
      GO TO 100
150   CONTINUE
C***  LOOP IS ENDED
60    CONTINUE
C
```

```
C SECTION TO GENERATE FIELDS
  ANUM = NUM
  FDIF = ( HSTOP - HSTART ) / ANUM
  FX(1) = HSTART
  DO 61 N = 2, NUM
    AN = N
    FX(N) = HSTART + AN * FDIF
61 CONTINUE
C SECTION FOR COMPUTING THE LINESHAPE
  DO 80 N = 1, NUM
    FZ(N) = 0.0
    DO 75 J = 1, NSPECY
      JN = NLINE ( J )
      TSHAPE = 0.0
      DO 70 K = 1, JN
        KP = K + JN * ( J - 1 )
        FIELD = H(KP) - FX(N)
        FIELD2 = FIELD * FIELD
        TAU2 = W(KP) * W(KP)
        DENOM1 = FIELD2 + TAU2
        DENOM2 = DENOM1 * DENOM1
        SHAPE = FIELD * W(KP) / DENOM2
        TSHAPE = R(KP) * SHAPE + TSHAPE
70 CONTINUE
      FZ(N) = TWOPI * FINT(J) * TSHAPE + FZ(N)
75 CONTINUE
      FZ(N) = FZ(N) + ALPHA + BETA * FX(N)
80 CONTINUE
C SET THE PLOT SIZE
  CCXMAX = 1070.
  IF( NUM .GT. 1000 ) CCXMAX = 2070.
  CALL CCGRID(5,2,6HNOLBLS,5)
  XLTR = 1140.
  IF( NUM .GT. 1000 ) XLTR = 2140.
82 CONTINUE
  WRITE (98,201)(COMMENT(J),J=1,4)
  CALL CCLTR( XLTR , 200. , 1, 2 )
C SEARCH FOR THE LIMITS OF THE PLOT
  XMIN = FX(1)
  XMAX = FX(NUM)
  YMIN = FZ(1)
  YMAX = FZ(1)
  DO 85 N = 1, NUM
    IF( FZ(N) .LT. YMIN ) YMIN = FZ(N)
    IF( FZ(N) .GT. YMAX ) YMAX = FZ(N)
85 CONTINUE
  CALL CCPLLOT(FX,FZ,NUM,4HJOIN,0,0)
  CALL CCNEXT
  GO TO 5
99 CALL CCEND
  CALL EXIT
201 FORMAT(4A10)
401 FORMAT( 2I5, 30X, 4A10 )
402 FORMAT ( 10I5 )
404 FORMAT( 5 ( I5, F10.5 ) )
405 FORMAT( 8F10.5 )
```

```
410  FORMAT( 1H1, 34H SIMULATION OF EPR SPECTRUM WITH      , I5,  
      1  9H SPECIES  ,5X,I5, 8H POINTS  )  
411  FORMAT( X, *ALPHA * ,E16.5,* BETA * , E16.5, 5X, * HSTART * ,  
      1  F12.3, 2X, * HSTOP * , F12.3 )  
412  FORMAT( 1H0, 3HNO., 5X,10HINTENSITY ,10X, 10H RELATIVE ,  
      1  7X, 3HHO ,15X, 20H COUPLING CONSTANT  
      2  2X, 5H NtQ  , 5X, 4H SI  )  
413  FORMAT(X,I2,5X,F10.3, 10X,F7.3, 5X,F10.3,15X,F10.3,10X,I5,5X,  
      1  F5.1/ ( 65X,F10.3, 10X,I5, 5X, F5.1 ) )  
415  FORMAT(1H0, 10H COMPONENT  ,1X, 12H LINEWIDTH  ,1X,  
      1  14H LINE CENTER  )  
416  FORMAT(X,I5,F10.3,5X, F10.3,F8.1,10( 2X,F4.1 ) )  
420  FORMAT( 1H0, 30X, 4A10, // )  
421  FORMAT( 1H0, I7, 32H EXCEEDS NO. OF POSSIBLE LINES  )  
      END
```

```

SUBROUTINE RATIO
SUBROUTINE RATIO CALCULATES THE INTENSITY RATIO OF THE HYPERFINE
COMPONENTS
COMMON/SPINS/NCOUPL(10),NEQ(10,4),S(10,4),SMI(10,4),SM(10),NLINE(4)
COMMON/FSPEC/NUM,AREA,FX(2000),FZ(2000),NSPECY
COMMON/STORE1/A(10,4),FINT(4),W(1600),R(1600),H(1600),JS
DIMENSION ID(25,25)
DIMENSION F(400)
EQUIVALENCE ( FX, ID )
EQUIVALENCE ( F, FZ )
DO 4 JS = 1, NSPECY
LIN=1
NEQ2 = NCOUP( JS )
KP = 1 + NLINE(JS) * ( JS-1 )
R(KP) = 1.0
DO 4 I = 1, NEQ2
J1 = 2 * S( I, JS )
J2 = NEQ( I, JS )
N1=J1*J2+1
IF ( N1 .GT. 25 ) GO TO 5
SMI( I, JS) = S(I, JS) * J2
FAC=1.
FC=1./(J1+1)
ID(1)=1
DO 1 J=2,25
1 ID(J)=0
DO 2 J=1,J2
J3=J+1
FAC=FAC*FC
DO 2 K=1,25
J4=K-J1
IF (J4.LE.0) J4=1
ID(K,J3)=0
DO 2 L=J4,K
2 ID(K,J3)=ID(K,J3)+ID(L,J)
L=1
DO 3 J=1,N1
DO 3 K=1,LIN
KP = K + NLINE(JS) * ( JS-1 )
F(L) = R(KP) * ID(J,J3) * FAC
3 L=L+1
LIV=L-1
DO 4 J=1,LIN
KP = J + NLINE( JS ) * ( JS-1 )
4 R(KP) = F(J)
RETURN
5 LIN=1
PRINT 10, N1, NEQ( I,JS), S( I,JS)
RETURN
10 FORMAT(20X,24H*** NUMBER OF COMPONENTS,I3,4H FOR,I3,
* 28H EQUIVALENT NUCLEI WITH SPIN,F4.1,18H EXCEEDS LIMIT ***)
END
```

## 2. VAESR\*

VAESR is used to simulate polycrystalline or glass spectra for transition metal complexes with spin 1/2 and an axial spin Hamiltonian. The method used is due to Vanngard and Aasa (1962). The input essentially consists of the microwave frequency, and the spin Hamiltonian parameters. The main output is a computer drawn plot of the spectrum.

### Method

The lineshape used is given by

$$I(H) = g_{\perp}^2 \frac{1}{8(2I+1)} \int_0^1 S'(H-H^0) [(g_{\parallel}/g)^2 + 1] dz$$

where  $z = \cos \theta$ ,  $\theta$  is the angle between the molecular axis and the applied magnetic fields,  $S'$  a shape function. For a Lorentz lineshape, the shape function is given by

$$S'(x) = \frac{2}{\pi} \frac{1}{\alpha^3} x [1 + (x/\alpha)^2]^{-2}, \quad \alpha = (\sqrt{3}/2)\Delta H$$

where  $\Delta H$  is the peak-to-peak derivative width. The resonance field is given by

$$H^0 = H_0 - KM_I/g\beta - (1/4H_0) (g\beta)^{-2} A_{\perp}^2 (A_{\parallel}^2 + K^2) K^{-2} [I(I+1) - m_I^2]$$

$$- (1/2 H_0) (g\beta)^{-2} (A_{\parallel}^2 - A_{\perp}^2) K^{-2} g_{\parallel}^2 g_{\perp}^2 g^{-4} z^2 (1-z^2) m_I^2$$

$$g^2 = g_{\perp}^2 + (g_{\parallel}^2 - g_{\perp}^2) z^2 \quad K^2 g^2 = A_{\parallel}^2 g_{\parallel}^2 z^2 + A_{\perp}^2 g_{\perp}^2 (1-z^2)$$

$$H_0 = h\nu/g\beta$$

A variable linewidth is permitted for each hyperfine component, and the lineshape is summed over the hyperfine components. The integral is evaluated using Simpson's rule.

\*  
The original version of this program was supplied by W. Burton Lewis. The program has been considerably altered.

INPUT DATA

Card 1 (Format I5, 6A10)

MCI the number of hyperfine components (maximum of 8)

LABEL any title information for the plot

Card 2 (Format 8F10.0)

XM(I) the  $m_I$  values for the hyperfine components (in order)

Card 3 (Format I5, 3F10.0)

N The number of points over which the Simpson's Rule integration is to be performed; must be odd.

DZ The size of the interval for the integration. May range from 0 to 1.0 ( $DZ = \cos\theta$ ). For  $N=201$ ,  $DZ = .005$ .

HT The lowest point in the magnetic field for the calculation and plotting of the spectrum.

HFNAL The highest point in the magnetic field.

Card 4 (Format 8F10.0)

A  $A_{||}$  in gauss

B  $A_{\perp}$  in gauss

C leave blank (not used)

GPL  $g_{||}$

GPR  $g_{\perp}$

XI I, the nuclear spin (eg. for  $I=3/2$ ,  $XI=1.5$ )

SH  $h\nu/\beta$  (for  $\nu=9.15$  GHz,  $SH=6537.565$ )

CMP The value by which the magnetic field is to be stepped for calculations. The intensity of the spectrum is calculated at each point,  $n$ , where the value of the field at the  $n$ th point is  $HT+n*CMP$ .



Card 5 (Format 8F10.0)

DH(I)      The linewidths for each of the hyperfine components

Card 6 (Format 8F10.0)

ZERO      Vertical distance in inches from the bottom of the plot to the  
            baseline. May be from 0 to 10 inches. This defines the  
            baseline for the plot.

SIZE      Length of the largest peak in inches from the baseline (ZERO).

Note: If the peak is negative going, then SIZE is negative.

Cards are repeated from card 1 to simulate additional spectra. A  
blank card at the end of the data is used to terminate the program.

```
PROGRAM VAESR( INPUT,OUTPUT,TAPE98,PLOT, TAPE99=PLOT )
C
C ESR SPECTRUM FITTING PROGRAM
C
COMMON/CCPOOL/XMIN,XMAX,YMIN,YMAX,CCXMIN,CCXMAX,CCYMIN,CCYMAX
COMMON/CCFACT/FACTOR
DIMENSION HZ(201), ZS(201), T3(201), G(201), XKM(201,8)
DIMENSION XMS(8), XM(8), DH(8), D11(8), D12(8), H(201,8)
DIMENSION HAT(1002), HAV(1002), HAV2(1002), LABEL(7)
C
PRINT 117
PRINT 118
118 FORMAT(* VERSION AS OF 8/8/70 J.J.C. * )
C SET COORDINATES FOR CALCOMP
CCXMIN = 70.0
CCXMAX = 1570.0
C
C DATA SECTION INPUT
50 READ 115, MCI, ( LABEL(I), I = 1, 7 )
52 READ 101, ( XM(I), I = 1, MCI )
1 READ 100, N, DZ, HT, HFNAL, IPT
READ 101, A, B, C, GPL, GPR, XI, SH, CMP
READ 101, ( DH(I), I = 1, MCI )
READ 101, ZERO, SIZE
PRINT 119, ( LABEL(I), I = 1, 7 )
PRINT 111, N, DZ, HT, HFNAL
PRINT 106, XI, SH, GPL, GPR, A, B
PRINT 112, ( XM(I), I = 1, MCI )
PRINT 116, ( DH(I), I = 1, MCI )
CALL CCGRID(5,6HNOLRLS,4)
REWIND 98
WRITE(98,120) ( LABEL(I), I = 1,7 )
CALL CCLTR ( 70. , 65. , 0, 2 )
100 FORMAT( I5, 8F10.0 , 11 )
101 FORMAT ( 8F10.0 )
102 FORMAT(1H1,2(46H FIELD I(H) NORMALIZED I ))
103 FORMAT( 1X, 6E16.7 )
104 FJRMAT ( 1H1 )
106 FORMAT(1H0, 10X, 4H I= ,F5.2, 5X, 10H HNU/BETA , F11.5, 4X,
1 5H GPL= ,F10.5,5X, 5H GPR= , F10.5 /
2 50X, 5H APL= , F10.5, 5X, 5H APR= , F10.5 // )
111 FORMAT(1H0, 3H N=,I5,4H DZ=,F10.5,4H HT=,F10.3,7H HFNAL=,F10.3)
112 FORMAT( 10H M.CAP I= 8F10.2 )
115 FORMAT( I5, 7A10 )
116 FORMAT( 10H DELH I = 8F10.2 )
117 FORMAT( 1H1, 20X,32H EPR GLASS SIMULATION PROGRAM )
119 FORMAT(1H0 , 16H IDENTIFICATION ,3X, 7A10 )
120 FORMAT( 1H , 7A10 )
131 FORMAT( 20X, I5, 4X, F10.3, 16X, F10.3 )
130 FORMAT( 1H0, 10X, 16HRESONANCE FIELDS , 4X, 8HPARALLEL, 12X,
1 14HPERPENDICULAR / 29X, F10.3, 16X, F10.3 // )
C
C THIS SECTION CALCULATES COEFFICIENTS
HA=HT
2 D= A*A *GPL * GPL
D1= B*B*GPR * GPR
```

```
D2= D*D1
D3= (D-D1) * (D-D1)
D4= GPL* GPL
D5= GPR*GPR
D6= D*D4
D7= D1*D5
D8= D4-D5
D9= D3*D4*D5
D10= XI*( XI + 1.0)
DO 15 I = 1, MCI
11 XMS(I) = XM(I) * XM(I)
D11(I) = 0.8660254 * DH(I)
15 D12(I) = ( ( D11(I) ) ** (-3)) * 0.63661977
D13 = D5 / ( 8.0 * ( 2.0 * XI + 1.0 ) )
C
PRINT 251
PRINT 252, D, D1, D2, D3, D4, D5, D6, D7, D8, D9, D10, D13
251 FORMAT( 1H0 , 10H D TO D13 )
252 FFORMAT( 1H0 , 7E16.7 )
C
C FIELD CALCULATION SECTION
C CALCULATES RESONANCE FIELD FOR EACH HYPERFINE COMPONENT AS
C FUNCTION OF ANGLE
C
DI= 0.0
DO 3 I= 1, N
Z= DI*DZ
ZS(I) = Z*Z
C DO SOME SPEED OPTIMIZING FOR LOOP
BIG= ZS(I)
SINSQ = 1.0 - BIG
GS = D5 + D8 * BIG
G(I) = SQRT ( GS )
XK = ( D6 * BIG + D7 * SINSQ ) / GS
HZ(I) = SH / G(I)
T = 1.0 / ( GS * XK * 2.0 * HZ(I) )
T1 = T * ( 0.5 * ( D2 + D1 * XK ) )
T2 = T1 * D10
T = T * D9 * ( 1.0 / ( GS * GS ) ) * BIG * SINSQ
TEM = SQRT ( XK ) / G( I )
T3(I) = ( D4 / GS ) + 1.0
DO 4 J = 1 , MCI
XKM ( I, J ) = TEM * XM ( J )
H(I, J) = HZ(I) - XKM(I, J) - ( T2 - T1*XMS(J) ) - ( T* XMS(J) )
4 CONTINUE
DI = I
3 CONTINUE
PRINT 130, HZ(N) , HZ(1)
PRINT 131, ( J, H( N, J ) , H(1, J) , J = 1, MCI )
C
C INTEGRATION SECTION
C SIMPSON S RULE INTEGRATION
C INTEGRATE OVER N ANGLES AT EVERY POINT
C AND SUM OVER HYPERFINE COMPONENTS
C
M = N-1
```

```
      CON = 6.0
      BIG = 0.0
20  DO 21 L= 1,1002
      ABC = L
      SMKS = 0.0
      SMJS = 0.0
      DO 23 J= 1,MCI
      X = HA-H( 1,J)
C   USE FSIZE FOR TEMPORARY FOR SPEED
      FSIZE = D11 ( J )
      Y = ( ( X/FSIZE) **2 ) + 1.0
      Y = 1.0/ (Y*Y)
      TEMP = D12 ( J )
      SMINT = T3(1) * TEMP * X * Y
      TEM = 4.0
      DO 24 I= 2,M
      X = HA - H(I,J)
      Y = ( ( X/FSIZE) **2 ) + 1.0
      Y = 1.0/ (Y*Y)
      SUM = T3 ( I ) * TEMP * X * Y
      SMINT = SMINT + SUM*TEM
      TEM = CON - TEM
24  CONTINUE
      X = HA - H(N,J)
      Y = ( ( X/FSIZE) **2 ) + 1.0
      Y = 1.0/ (Y*Y)
      SUM = T3 ( N ) * TEMP * X * Y
      SMINT = ( SMINT + SUM ) * DZ/3.0
      SMJS = SMJS + SMINT
C
C
23  CONTINUE
      SMKS = SMKS + SMJS
22  CONTINUE
C
C
      HAV(L) = SMKS* D13
C   START TO FIND MAXIMUM FOR SCALING
      TEMP = ABS ( HAV ( L ) )
      IF( TEMP - BIG ) 30, 30, 32
32  BIG = TEMP
30  CONTINUE
      HAT(L) = HA
      HA = HT + CMP*ABC
      IF( HA-HFNAL ) 21, 21, 9
21  CONTINUE
9   M = ABC
C SECTION TO SCALE SPECTRUM FOR PLOTTING
      XMIN= HT
      XMAX= HFNAL
      YMIN= -1000.
      YMAX = 1000. * ( 1.0 - ZERO / 10. ) * (10. / ZERO )
      IF( SIZE ) 40 , 40 , 41
40  FSIZE = ( SIZE / ZERO ) * YMIN
      GO TO 42
41  FSIZE = ( SIZE / ( 10.0 - ZERO ) ) * YMAX
```

```
42  SIZE = - ( FSIZE / BIG )
      DO 35 I = 1, M
35   HAV2(I) = HAV(I) * SIZE
      CALL CCPLT(HAT, HAV2, M, 4HJOIN,0,0 )
C   PRINTING OF SPECTRUM IS SUPPRESSED
C   REMOVE C S TO RESTORE PRINTING
C   PRINT 102
C   PRINT 103,      ( HAT(I) , HAV(I), HAV2(I), I= 1, M )
C TEST FOR MORE PLOTS
      READ 115, MCI, ( LABEL(I), I = 1, 7 )
      IF(MCI) 57, 57, 51
51   CALL CCNEXT
      PRINT 104
      GO TO 52
C
57  CALL CCEND
      CALL EXIT
      END
```

C. T<sub>1</sub> Analysis Program - LOGLINE

The LOGLINE program was written to operate in connection with the BASIC AVERAGER program supplied by the Digital Equipment Corp. with the LAB-8/I computer system. It is used to analyze the exponential recovery curves obtained in pulse-saturation-recovery experiments. It can, however, analyze any exponential recovery curve. The LOGLINE program can punch the experimental data acquired by the BASIC AVERAGER on the high speed punch; read in previously punched data for analysis; display the data on a storage display scope; or analyze the recovery curve for the time constant. The program operates under the control from the teletype; the analysis is performed interactively, on-line, with the operator using the teletype to control the analysis, and the display oscilloscope to observe the results.

LOADING

The following program tapes must be loaded in order using the BINDARY LOADER

1. Lab-8 Basic Control Tape DEC-LB-T21A-PB
2. Lab-8 Basic Averager DEC-LB-U21A-PB
3. LOGLINE program tape
4. Floating Point Pkg. #3 DEC-08-YQ3A-PB without EAE or  
DIGITAL-8-25-F-BIN with EAE

At the end of the loading operation the Control tape and the Basic Averager are in Field 0. The main part of the LOGLINE program and the floating point package are in Field 1. Note that the operation of these programs requires a PDP-8/I equipped with 8K of memory, a high

speed paper tape reader and punch, a DF32 disk, and an AX08 laboratory peripheral.

#### OPERATION

The programs are first loaded with the binary loader. The program is started at address 07603<sub>8</sub>. The basic averager is used to acquire a recovery curve (The operation of the Basic Averager is discussed in the DEC manual, DEC-LB-T20A-B). The inputs to the AX08 should be adjusted so that the recovery curve is all negative; that is, the recovery curve grows from minus infinity to zero. The reason for this is that the data is converted to an exponential decay curve for the purpose of the logarithmic analysis simply by making all the data positive.

After the data has been acquired the LOGLINE program is entered from the basic averager by typing CTRL/P. LOGLINE types "R" to request the sample rate. The sample rate should be typed in some appropriate unit such as milliseconds. The sample rate is the time between data points and defines the time scale for the experiment. After the sample rate is typed the user may either punch the data or proceed to analyze the data. If the data is to be punched, CTRL/N is typed. LOGLINE will ask FIRST and LAST and the starting and ending channel to be punched should be provided. Note that the high speed punch should now be turned on. The user now types CTRL/P to punch the data. After the data is punched, the punch is turned off and the user may proceed to analyze the data.

The first step in the data analysis is to type the ALT MODE key. This causes the Basic Averager to be stored on the disk, thus freeing FIELD 0 for data manipulations. LOGLINE will reply with the message CORE SWAPPED after the operation is completed. At this time the baseline

should be subtracted from the data. Type CTRL/N to redefine FIRST and LAST to the channels near the end of the recovery, for example, FIRST=960 and LAST=990. Now type CTRL/B to compute the baseline from the average of the data from FIRST to LAST. LOGLINE will reply with the value of the baseline. Now type CTRL/A to subtract the baseline. New values of FIRST and LAST are requested for the baseline subtraction. (Note: all operations on the data are performed with FIRST and LAST as limits).

At this time the data may be examined on the display scope by typing CTRL/D to display the data from FIRST to LAST. The logarithm of the data is displayed by CTRL/F. The display may be expanded or contracted by typing as many X's or C's as are required.

The data are now analyzed for the time constants. CTRL/N is typed and the limits are redefined for the next command. CTRL/V is typed to command LOGLINE to fit the logarithmic data from FIRST to LAST with a straight line. At the end of this operation LOGLINE types the constants of the straight line and types the relaxation time. (A is the intercept and B is the slope of the straight line). The theoretical curve can be compared with the experimental curve by typing CTRL/L to display the theoretical logarithm. If the fit is bad, the limits should be changed with CTRL/N and the fit performed again with CTRL/V. CTRL/N may be used at any time to change limits of fitting or of displaying data.

If there are additional time constants present in the data, the theoretical logarithm should now be stripped from the data by typing CTRL/S. The analysis can then proceed with a CTRL/N, CTRL/V combination as before. These operations are repeated to extract all the time constants. The progress of the fit is checked at all times with the display commands.



At the end of the processing the BASIC AVERAGER is reentered by typing CTRL/Q. At this point LOGLINE reads the basic averager into field 0 from the disk and then jumps to the basic averager. Note that if a mistake has been made in analyzing the above data, the data can be restored by typing CTRL/Q to return to the averager and then CTRL/P to return to LOGLINE with the original data. The analysis may then be repeated from the beginning.

To analyze data which has been previously punched, the LOGLINE program is first entered from the averager with CTRL/P. The data tape is placed in the high speed reader and CTRL/R is typed. LOGLINE will read the data tape. The analysis may now proceed as if LOGLINE had just been entered from with averager with data.

LOGLINE COMMANDS

CTRL/A strip baseline from data between FIRST and LAST

CTRL/B compute baseline from between FIRST and LAST

CTRL/D display data from FIRST to LAST

CTRL/E examine the data in the channel indicated by FIRST LOGLINE will type the contents of the (FIRST) channel. The user now has 3 options:  
space: after typing a space the user can type a new value for the channel.  
line feed: typing the line feed causes FIRST to be changed to FIRST+1 and this channel is typed  
return: typing a carriage return terminates the CTRL/E command.

CTRL/F display the logarithm of the data from FIRST to LAST

CTRL/H halt current operation. Only operates during a CTRL/N or during a CTRL/P operation. Note that a CTRL/N occurs during a CTRL/A and a CTRL/S operation as part of their function. This command permits some mistakes during operation to be corrected.

CTRL/L display theoretical logarithm from FIRST to LAST. In the special case of a CTRL/T command, this command is used to terminate the CTRL/T command.

CTRL/N define new values of FIRST and LAST. The CTRL/N operation may be halted by CTRL/H. The values of FIRST and LAST after CTRL/H are uncertain.

CTRL/P punch data from FIRST to LAST on high speed punch. Must be used before the ALT MODE command.

CTRL/Q quit. return from LOGLINE to the basic averager.

CTRL/R read a previously punched data tape. Must be used before ALT MODE.

CTRL/S strip the theoretical logarithm from the data from FIRST to LAST.

CTRL/T title. All information typed is echoed and ignored until CTRL/L is typed. This command is useful to provide descriptive information on the output during processing.

CTRL/V Fit a straight line to the logarithm of the data from FIRST to LAST.

ALT MODE swap the basic averager from field 0 to the disk; make the data positive and convert it from integer format to floating point.

X expand the display by factor of two

C contract the display by factor of two

CTRL/K These commands are not presently defined. They are provided for  
CTRL/W future expansion of the program.  
CTRL/U

```

/   LOGLINE
/
/   NOV. 28, 1970   JAMES J CHANG
/
/   PROGRAM OVERLAY TO BASIC AVERAGER
/   DEC-LB-U21A-PB
/
/   USES A WEIGHTED LOGARITHMIC LEAST SQUARES
/   TO ANALYZE EXPONENTIAL CURVES
/   OVERLAYS THE CTRL/P COMMAND TO CALL
/   THIS ROUTINE
/   PROGRAM RUNS IN FIELD 1
/   ASSUMES 1000 CHAN. AVERAGE
/
/   PATCH FIELD 0 TO ALTER CTRL/P COMMAND
/

```

```

FIELD 0
*7560
7560 7300   CLA CLL
7561 6002   IOF   /MAKE SURE INTERRUPT OFF
7562 6026   PLS   /INITIALIZE
7563 6046   TLS
7564 6211   CDF 10
7565 6212   CIF 10 /GET TO FIELD 1
7566 5767   JMP I .+1
7567 0200   0200

```

```

/
/   FIELD 1 SECTION OF PROGRAM
/   PAGE ZERO CONSTANTS AND POINTERS
/

```

```

FIELD 1
*5
0005 7400   7400   /FPP INPUT
0006 7200   7200   /FPP OUTPUT
*10
0010 0000   POINT, 0   /AUTO INDEX
0011 0000   POINT1, 0
0012 0000   0
0013 0000   POINT4, 0
0014 0000   0
0015 0000   0
0016 0000   SWITCH, 0   /I/O INDICATOR =1 FOR PUNCH
/
*20
0020 0000   SHFR, 0   /HIGH DATA PT. STOR. FOR SHIFTS
0021 0000   0   /LOW
0022 0000   TEMP, 0
0023 0000   ARITH1, 0
0024 0000   ARITH2, 0
0025 0000   ARITH4, 0
0026 0000   DISC, 0   /INDICATOR =1 IF FIELD 0 ON DISK
0027 0000   FIRST, 0
0030 0000   LAST, 0
0031 0166   SCL, 166   /POINTER TO SCALE LOCATION
0032 2212   BLK, 2212 /START OF DATA-1
0033 0240   K240, 240 /SPACE
0034 7766   KM12, -12 /-10
0035 0000   PT1, 0   /POINTER
0036 0000   COUNT, 0
0037 6030   KMD1K, -1750 /-1000

```

0062	0000	ONE,	*62 FLTG 1.0
0063	3777		
0064	7774		
0065	0001	TWO,	FLTG 2.0
0066	3777		
0067	7774		
0070	0007	HUND,	FLTG 100.0
0071	3077		
0072	7776		
0073	0000	A,	FLTG 0.0
0074	0000		
0075	0000		
0076	0000	B,	FLTG 0.0
0077	0000		
0100	0000		
0101	0000	SIGMA,	FLTG 0.0
0102	0000		
0103	0000		
0104	0000	N,	FLTG 0.0
0105	0000		
0106	0000		
0107	0000	SIGA,	FLTG 0.0
0110	0000		
0111	0000		
0112	0000	SIGB,	FLTG 0.0
0113	0000		
0114	0000		
0115	0000	BASE,	FLTG 0.0
0116	0000		
0117	0000		
0120	0000	R,	FLTG 0.0
0121	0000		
0122	0000		
0123	0000	X,	FLTG 0.0
0124	0000		
0125	0000		
0126	0000	Y,	FLTG 0.0
0127	0000		
0130	0000		
			OCTAL
0131	0400	OUT,	OUTPUT /TYPE OR PUNCH
0132	0420	CLF,	CRLF
0133	0450	NSIN,	NOUT
0134	0616	SHIFT,	SHFTS
0135	0600	GET,	GETP /GET DOUBLE PREC. DATA
0136	0500	MES,	MESSAGE /PRINT MESSAGE
0137	0243	WHATP,	WHAT /ECHO ?
0140	0213	LISTNP,	LISTEN
0141	0754	BRP,	BRAN /BRANCH ON AC MATCH
0142	0177	SPEC,	177 /DATA-1
0143	1013	INITP,	INIT
0144	1000	ENDT,	ENDTST
0145	0552	DACP,	DAC /GET DATA FROM F0 TO FAC
0146	1125	THP,	TH /COMPUTE Y=A+B*X
0147	1324	DEVP,	DEV /COMPUTE PARAMETER STD. DEV.
0150	1407	LSP,	LSQOUT /OUTPUT LST. SQ. PARAMETERS
0151	0670	IFIXP,	IFIX /FIX FAC
0152	0720	NEWCP,	NEWC /GET NEW FIRST AND LAST

0153	0565	STORE,	FACD	/PUT FAC INTO F0
0154	0656	FLOATP,	FLOAT	/FLOAT AC INTO FAC
/				
0155	1200	CLEARP,	CLEAR	/CLEAR LST SQ.
0156	1216	SUMSP,	SUMS	
0157	1247	CONSP,	CONS	
0160	0253	KEYP,	KEY	
0161	0344	DTSTP,	DTST	
0162	1516	LINP,	LINEL	
0163	0324	RDRP,	RDR	
0164	2123	STP,	STD	
0165	2144	CNV RTP,	CNV RT	
0166	2163	NUMTSP,	NUMTST	
0167	1741	HLTP,	HALT	/OPERATION STOP TEST
0170	0352	WLOGP,	WLOG	/COMPUTE WEIGHT, RETURN LOG

/

/ PROGRAM CONTROL AND INITIALIZATION

/

		*200		
0200	7300	CLA CLL		/INITIALIZE
0201	6046	ILS		
0202	6026	PLS		
0203	4532	JMS I CLF		
0204	4536	JMS I MES		/GET TIME RATE
0205	2240	TEXT "R		
0206	0000	"		
0207	4405	JMS I 5		
0210	4407	JMS I 7		
0211	6120	FPUT R		
0212	0000	FEXT		
0213	7300	LISTEN, CLA CLL		
0214	3016	DCA SWITCH		/INSURE TTY OUTPUT
0215	4253	JMS KEY		/GET COMMAND
0216	4541	JMS I BRP		/SEARCH EXECUTION LIST
0217	1136	TABLE		
0220	5700	JMP I D+00		/CTRL V
0221	5701	JMP I D+01		/CTRL S
0222	5702	JMP I D+02		/CTRL B
0223	5703	JMP I D+03		/CTRL A
0224	5251	JMP N2		/CTRL N
0225	5704	JMP I D+04		/CTRL D
0226	5705	JMP I D+05		/CTRL L
0227	5706	JMP I D+06		/CTRL F
0230	5707	JMP I D+07		/ALT. MODE
0231	5710	JMP I D+10		/CTRL P
0232	5265	JMP C1+2		/X
0233	5263	JMP C1		/C
0234	5711	JMP I D+11		/CTRL E
0235	5712	JMP I D+12		/CTRL Q
0236	5713	JMP I D+13		/CTRL R
0237	5714	JMP I D+14		/CTRL T
0240	5715	JMP I D+15		/CTRL K FOR EXPANSION
0241	5716	JMP I D+16		/CTRL W
0242	5717	JMP I D+17		/CTRL U
/				
0243	7300	WHAT,	CLA CLL	/ECHO ?
0244	1250	TAD WHAT+5		
0245	4531	JMS I OUT		
0246	4532	JMS I CLF		

```
0247 5213      JMP LISTEN
0250 0277      /
0251 4552 N2,   JMS I NEWCP   /GET NEW FIRST AND LAST
0252 5213      JMP LISTEN
0253 0000 KEY,   0           /LISTEN TO KEYBOARD
0254 7300      CLA CLL
0255 6031      KSF         /WAIT
0256 5255      JMP .-1
0257 6036      KRB
0260 4531      JMS I OUT    /ECHO
0261 1022      TAD TEMP
0262 5653      JMP I KEY
0263 7240 C1,   CLA CMA     /CONTRACT
0264 7410      SKP
0265 7201      CLA IAC     /EXPAND
0266 1671      TAD I .+3
0267 3671      DCA I .+2
0270 5213      JMP LISTEN
0271 2275      VSW
/
/ DISPATCH TABLE
/
*300
0300 0320 D,   LINE   /FIT TO LOG
0301 1347      STRIP  /STRIP LOG FROM DATA
0302 1052      BASL   /COMPUTE BASELINE
0303 1105      BSUB   /SUBTRACT BASELINE
0304 2235      DATDIS /DISPLAY DATA
0305 2222      THDIS  /DISPLAY TH. LOG
0306 2207      LOGDIS /DISPLAY LOG OF DATA
0307 2000      SWAP   /SWAP FIELD 0 ONTO DISK
0310 1600      PNCH   /PUNCH OUT DATA
0311 1551      EXAM   /LOOK AT DATA(FIRST)
0312 2042      RESTOR /RESTORE FIELD 0
0313 1650      INPT   /CTRL R READ DATA
0314 0336      TTL    /CTRL T GET HEADER(TITLE) INFO
0315 0243      WHAT   /CTRL K FOR FUTURE EXPANSION
0316 0243      WHAT   /CTRL W
0317 0243      WHAT   /USER PROG. NOT YET DEFINED
/
0320 4561 LINE, JMS I DTSTP  /TEST FOR DATA
0321 4562      JMS I LINP  /FIT THE LINE
0322 4550      JMS I LSP   /PRINT CONSTANTS
0323 5540      JMP I LISTNP
/
/ ROUTINE TO READ PREVIOUSLY PUNCHED DATA
/ USES HIGH SPEED READER
/ LOC. 15=CHAR TEMPORARY CHARACTER BUFFER
/
0324 0000 RDR,   0
0325 7300      CLA CLL
0326 6014      RFC
0327 6011      RSF
0330 5327      JMP .-1
0331 6012      RRB
0332 3015      DCA 15
0333 1015      TAD 15
```

```
0334 5724      JMP I RDR
/
/ CTRL T
/ ACCEPT AND ECHO ALL INCOMING INFORMATION
/ THIS IS FOR TITLING PURPOSES
/ ALL INFORMATION TYPED IS IGNORED , BUT IS TYPED
/ UNTIL A CTRL L IS RECEIVED.
/ THIS PERMITS DOCUMENTATION OF THE PROGRESS
/ OF EXPERIMENT ANALYSIS.
/
0335 7564      -214 /CTRL L
0336 4560 TTL,   JMS I KEYP   /GET INFO
0337 1335      TAD TTL-1   /CHECK FOR STOP SIGNAL
0340 7640      SZA CLA
0341 5336      JMP TTL           /NO
0342 4532      JMS I CLF   /YES
0343 5540      JMP I LISTNP
/
/ SUBROUTINE TO CHECK IF DATA IS PRESENT
/ DISC=0 IF DATA NOT PRESENT
/ =1 IF DATA PRESENT
/ RETURN IF DATA PRESENT; ? IF NOT
/
0344 0000 DTST,  0 /CHECK FOR DATA
0345 7300      CLA CLL
0346 1026      TAD DISC
0347 7650      SNA CLA
0350 5537      JMP I WHATP
0351 5744      JMP I DTST
/
/ SUBROUTINE TO GET POINT; COMPUTE LEAST SQUARES WEIGHT
/ AND RETURN WITH LOG IN FAC
/ WEIGHT Y:2 IS STORED IN SIGA TEMPORARILY
/
0352 0000 WLOG,  0
0353 4545      JMS I DACP   /GET A POINT
0354 4407      JMS I 7
0355 6022      FPUT TEMP
0356 0001      SQUARE /COMPUTE WEIGHT Y:2
0357 6107      FPUT SIGA /SIGA IS WEIGHT DURING SUM COMP.
0360 5022      FGET TEMP
0361 0007      LOG
0362 0000      FEXT
0363 5752      JMP I WLOG
/
/ OUTPUT SECTION
*400
0400 0000 OUTPUT, 0 /SWITCH=0 TYPE
0401 3022      DCA TEMP / .NE.0 PUNCH
0402 1016      TAD SWITCH
0403 7640      SZA CLA
0404 5212      JMP PUNCH
0405 1022      TAD TEMP
0406 6041      TSF
0407 5206      JMP --1
0410 6046      TLS
0411 5216      JMP PUNCH+4
0412 1022 PUNCH, TAD TEMP
0413 6021      PSF
0414 5213      JMP --1
```

0415	6026		PLS	
0416	7200		CLA	
0417	5600		JMP I OUTPUT	
/				
0420	0000	CRLF,	0	
0421	1226		TAD K215	
0422	4200		JMS OUTPUT	
0423	1227		TAD K212	
0424	4200		JMS OUTPUT	
0425	5620		JMP I CRLF	
0426	0215	K215,	215	
0427	0212	K212,	212	
/				
/ RADIX DEFLATION TO GET DIGIT				
/ # IN ARITH4; DEFLATION NO. IN AC				
/ DIGIT RETURNED IN AC				
/				
0430	0000	GDIGIT,	0	
0431	3023		DCA ARITH1	
0432	3022		DCA TEMP	/HOLDS FINAL DIGIT
0433	1025		TAD ARITH4	
0434	3025	GLOOP,	DCA ARITH4	
0435	1025		TAD ARITH4	
0436	1023		TAD ARITH1	/SUBTRACT DEFLATION
0437	2022		ISZ TEMP	/COUNT SUBTRACTIONS
0440	7500		SMA	
0441	5234		JMP GLOOP	
0442	7200		CLA	
0443	1247		TAD K257	/DIGIT IS TEMP-1
0444	1022		TAD TEMP	
0445	4531		JMS I OUT	
0446	5630		JMP I GDIGIT	
0447	0257	K257,	257	
/				
0450	0000	NOUT,	0	/CHECK SIGN
0451	3025		DCA ARITH4	/FOR CONVERSION
0452	1025		TAD ARITH4	
0453	7710		SPA CLA	/POS?
0454	1276		TAD K15	/NO
0455	1033		TAD K240	/PRINT MINUS OR BLANK
0456	4531		JMS I OUT	
0457	1025		TAD ARITH4	
0460	7510		SPA	
0461	7041		CIA	/MAKE POS.
0462	3025		DCA ARITH4	/SAVE NO. FOR CONVERSION
0463	1037		TAD KMD1K	
0464	4230		JMS GDIGIT	
0465	1277		TAD KMD100	
0466	4230		JMS GDIGIT	
0467	1034		TAD KM12	
0470	4230		JMS GDIGIT	
0471	7240		CLA CMA	/-1
0472	4230		JMS GDIGIT	
0473	1033		TAD K240	/SPACE AFTER NO.
0474	4531		JMS I OUT	
0475	5650		JMP I NOUT	
/				
/				
0476	0015	K15,	015	
0477	7634	KMD100,	-144	



```

/
/ MODIFIED VERSION OF
/ DIGITAL 8-18-U
/ MESSAGE TYPE-OUT
/ CALL WITH A JMS MESSAGE
/ WITH DATA FOLLOWING
/ RETURN FOLLOWING END OF MESSAGE
/ CODE(00)
/ USES NOUT FOR TEMPORARY STORAGE
/ CANNOT BE PRINTING NO. AT SAME TIME
/ PRINTING MESSAGE
/

```

```

0500 0000 MESSAGE, 0
0501 7240 CLA CMA /SET C(AC)=-1
0502 1300 TAD MESSAGE /ADD LOCATION
0503 3010 DCA 10 /AUTO-INDEX REGISTER
0504 1410 TAD I 10 /FETCH FIRST WORD
0505 3250 DCA NOUT /SAVE IT
0506 1250 TAD NOUT
0507 7012 RTR
0510 7012 RTR /ROTATE 6 BITS RIGHT
0511 7012 RTR
0512 4316 JMS TYPECH /TYPE IT
0513 1250 TAD NOUT /GET DATA AGAIN
0514 4316 JMS TYPECH /TYPE RIGHT HALF
0515 5304 JMP MESSAGE+4 /CONTINUE
0516 0000 TYPECH, 0 /TYPE CHARACTER IN C(AC)6-11
0517 0344 AND MASK77
0520 7450 SNA /IS IT END OF MESSAGE?
0521 5410 JMP I 10 /YES: EXIT
0522 1345 TAD M40 /SUBTRACT 40
0523 7500 SMA /<40?
0524 5327 JMP .+3 /NO
0525 1346 TAD C340 /YES: ADD 300
0526 5342 JMP MTP /TO CODES <40
0527 1347 TAD M3 /SUBTRACT 3
0530 7440 SZA /IS IT ZERO?
0531 5334 JMP .+3 /NO
0532 1227 TAD K212 /YES: CODE 43 IS
0533 5342 JMP MTP /LINE-FEED (212)
0534 1350 TAD M2 /SUBTRACT 2
0535 7440 SZA /IS IT ZERO?
0536 5341 JMP .+3 /NO
0537 1226 TAD K215 /YES: CODE 45 IS
0540 5342 JMP MTP /CARRIAGE-RETURN (215)
0541 1351 TAD C245 /ADD 200 TO OTHERS >40
0542 4200 MTP, JMS OUTPUT /TYPE MESSAGE
0543 5716 JMP I TYPECH

/CONSTANTS
0544 0077 MASK77, 77
0545 7740 M40, -40
0546 0340 C340, 340
0547 7775 M3, -3
0550 7776 M2, -2
0551 0245 C245, 245

/
/ GET FIELD 0 DATA INTO FAC
/
0552 0000 DAC, 0
0553 7200 CLA

```

```
0554 6201      CDF 0
0555 1412      TAD I 12      /12 IS PRESET POINTER
0556 3044      DCA 44
0557 1412      TAD I 12
0560 3045      DCA 45
0561 1412      TAD I 12
0562 3046      DCA 46
0563 6211      CDF 10
0564 5752      JMP I DAC      /* IS IN FAC
```

/  
/ PUT FAC INTO FIELD 0 DATA BLOCK  
/

```
0565 0000      FACD, 0
0566 7200      CLA
0567 6201      CDF 0
0570 1044      TAD 44
0571 3414      DCA I 14      /14 IS PRESET POINTER
0572 1045      TAD 45
0573 3414      DCA I 14
0574 1046      TAD 46
0575 3414      DCA I 14
0576 6211      CDF 10
0577 5765      JMP I FACD
```

/

/

/ PAGE 3

/

\*600  
/ SUBSECTION TO GET A DOUBLE PREC. DATA PT.  
/ ASSUMES POINT1 PRESET TO ARRAY  
/ LEAVES POINT1 SET TO NEXT POINT  
/

```
0600 0000      GETP, 0
0601 7200      CLA
0602 6201      CDF 0 /POINTS IN FIELD 0
0603 1411      TAD I POINT1 /REVERSE LO AND HIGH ORDER
0604 3021      DCA SHFR+1
0605 1411      TAD I POINT1
0606 3020      DCA SHFR
0607 6211      CDF 10
0610 7344      CLA CLL CMA RAL      /MINUS TWO
0611 1013      TAD POINT4      /GET SCALE FACTOR
0612 7041      CMA IAC      /SET FOR RIGHT SHIFT
0613 4534      JMS I SHIFT      /SCALE POINT
0614 1021      TAD SHFR+1      /RETURN WITH POINT
0615 5600      JMP I GETP      /IN AC
```

/

/SHIFTING SUBROUTINE SEE DEC LISTINGS  
/ OF BASIC AVERAGER  
/DOUB. PREC. SHIFT OF HIGH AND LOW  
/CALL TAD KXXX NEG. FOR RIGHT SHIFT

/ SHFT  
/ RETURN  
/ SHFR, SHFR+1 FOR SHIFT WORDS  
/

```
0616 0000      SHFTS, 0
0617 7100      CLL
0620 7450      SNA      /DONE IF COUNT=0
0621 5616      JMP I SHFTS
0622 7500      SMA      /RIGHT OR LEFT
```

```
0623 7061 CML CMA IAC /LEFT
0624 3255 DCA SHCNT
0625 7430 SZL /RIGHT?
0626 5243 JMP SHLEFT /NO
0627 1020 SHRIT, TAD SHFR
0630 7510 SPA /SET L=1 IF NEG
0631 7020 CML
0632 7010 RAR
0633 3020 DCA SHFR
0634 1021 TAD SHFR+1
0635 7010 RAR
0636 3021 DCA SHFR+1
0637 7100 CLL
0640 2255 ISZ SHCNT
0641 5227 JMP SHRIT
0642 5616 JMP I SHFTS
0643 1021 SHLEFT, TAD SHFR+1
0644 7104 CLL RAL
0645 3021 DCA SHFR+1
0646 1020 TAD SHFR
0647 7004 RAL
0650 3020 DCA SHFR
0651 7100 CLL
0652 2255 ISZ SHCNT
0653 5243 JMP SHLEFT
0654 5616 JMP I SHFTS
0655 0000 SHCNT, 0 /TEMP TO HOLD SHIFT COUNT
/
/
/ FLOAT THE # IN THE AC INTO FAC
/
0656 0000 FLOAT, 0 / 0<#<2047
0657 3045 DCA 45
0660 3046 DCA 46
0661 1267 TAD C13
0662 3044 DCA 44
0663 4407 JMS I 7
0664 7000 FNOR
0665 0000 FEXT
0666 5656 JMP I FLOAT
0667 0013 C13, 0013
/
/
/ FIX NO. IN FAC
0670 0000 IFIX, 0
0671 7200 CLA
0672 1044 TAD 44 /GET EXP
0673 7540 SZA SMA /CHECK FOR <1
0674 5277 JMP *+3
0675 7200 CLA /YES: MAKE ZERO
0676 5316 JMP IFIX2+1
0677 1317 TAD M13 /NO
0700 7450 SNA
0701 5670 JMP I IFIX
0702 7500 SMA /CHECK IF TOO LARGE
0703 5670 JMP I IFIX /YES: IGNORE IT
0704 3044 DCA 44
0705 7100 IFIX1, CLL
0706 1045 TAD 45 /GET MANTISSA
0707 7510 SPA /CHECK FOR <0
```

```
0710 7020 CML /YES
0711 7010 RAR
0712 3045 DCA 45
0713 2044 ISZ 44
0714 5305 JMP IFIX1
0715 1045 IFIX2, TAD 45 /ANSWER IN AC
0716 5670 JMP I IFIX
0717 7765 M13, -13 /-11
/
/ SUBROUTINE TO GET NEW VALUES FOR
/ FIRST AND LAST
/
0720 0000 NEWC, 0
0721 7300 CLA CLL
0722 4532 JMS I CLF /SPACE
0723 4536 JMS I MES /ASK FOR FIRST
0724 0611 TEXT "FI
0725 2223 RS
0726 2440 T
0727 4000 "
0730 1027 TAD FIRST
0731 4533 JMS I NSIN /PRINT OLD FIRST
0732 4405 JMS I 5 /GET NEW FIRST
0733 1057 TAD 57 /CHECK TERMINATOR FOR PANIC STOP
0734 4567 JMS I HLTP
0735 4551 JMS I IFIXP
0736 3027 DCA FIRST
0737 4536 JMS I MES /ASK FOR LAST
0740 1401 TEXT "LA
0741 2324 ST
0742 4040
0743 4000 "
0744 1030 TAD LAST
0745 4533 JMS I NSIN
0746 4405 JMS I 5 /GET NEW LAST
0747 1057 TAD 57 /CHECK TERMINATOR FOR PANIC STOP
0750 4567 JMS I HLTP
0751 4551 JMS I IFIXP
0752 3030 DCA LAST
0753 5720 JMP I NEWC
/
/ SUBROUTINE TO BRANCH ON MATCH OF AC WITH TABLE
/ CALL BRAN
/ TABLE
/ ... JMP ENTRY
/ TABLE ENDS WITH NEG ENTRY
/
0754 0000 BRAN, 0
0755 3023 DCA ARITH1 /SAVE CODE
0756 1754 TAD I BRAN /GET FIRST TABLE ENTRY
0757 3024 DCA ARITH2 /SAVE TABLE ADDRESS
0760 1424 BRLOOP, TAD I ARITH2 /GET ENTRY
0761 7500 SMA /CHECK FOR NEG.
0762 7041 CMA IAC
0763 2354 ISZ BRAN /INDEX RETURN ADDRESS
0764 1023 TAD ARITH1 /CHECK FOR MATCH
0765 7650 SNA CLA
0766 5754 JMP I BRAN /YES
0767 1424 TAD I ARITH2 /NO-TEST FOR END
0770 2024 ISZ ARITH2 /INDEX ENTRY POINTER
```

```
0771 7700 SMA CLA
0772 5360 JMP BRLOOP /NOT LAST-CONTINUE
0773 2354 ISZ BRAN /FELL THROUGH TABLE
0774 5754 JMP I BRAN /RETURN TO DEFAULT
/
/
PAUSE
/
/ PAGE 4
+1000
/
/ ROUTINE TO CHECK FOR END OF PROCESSING
/ A SECTION FROM FIRST TO LAST
/
1000 0000 ENDTST, 0
1001 7200 CLA
1002 4407 JMS I 7 /ALSO INCREMENT X FOR NEXT POSITION
1003 5123 FGET X
1004 1120 FADD R
1005 6123 FPUT X
1006 0000 FEXT
1007 2036 ISZ COUNT /RETURN TO CALL+2 IF DONE
1010 5600 JMP I ENDTST / CALL+1 TO CONTINUE
1011 2200 ISZ ENDTST
1012 5600 JMP I ENDTST
/
/ ROUTINE TO INITIALIZE PROCESSING OF SECTION
/ SET N, COUNT, FIRST X, POINTER 12, 14 TO DATA
/ N=LAST-FIRST+1
/
1013 0000 INIT, 0
1014 7300 CLA CLL
1015 1027 TAD FIRST /COMPUTE -N FOR COUNT
1016 7041 CIA
1017 1030 TAD LAST
1020 7001 IAC
1021 3022 DCA TEMP
1022 1022 TAD TEMP
1023 7041 CIA
1024 3036 DCA COUNT /SET COUNTER
1025 1022 TAD TEMP
1026 4554 JMS I FLOATP
1027 4407 JMS I 7
1030 6104 FPUT N /SET UP N
1031 0000 FEXT
1032 7300 CLA CLL
1033 1027 TAD FIRST /SET FIRST X
1034 4554 JMS I FLOATP
1035 4407 JMS I 7
1036 3120 FMPY R
1037 6123 FPUT X
1040 0000 FEXT
1041 7300 CLA CLL
1042 1027 TAD FIRST /SET UP POINTERS
1043 7004 RAL /REQUIRE 3 LOC. PER POINT
1044 1027 TAD FIRST
1045 1142 TAD SPEC /LOC-1 OF DATA
1046 3012 DCA 12 /12= DATA TO FAC POINTER
1047 1012 TAD 12
1050 3014 DCA 14 /14=FAC TO DATA POINTER
```

```
1051 5613      JMP I INIT
/
/ SUBROUTINE TO COMPUTE BASELINE BETWEEN
/ FIRST AND LAST
/
1052 4543  BASL,  JMS I INITP  /INITIALIZE
1053 3115      DCA BASE    /CLEAR BASE
1054 3116      DCA BASE+1
1055 3117      DCA BASE+2
1056 4545  B1,    JMS I DACP   /GET A POINT
1057 4407      JMS I 7
1060 1115      FADD BASE
1061 6115      FPUT BASE
1062 0000      FEXT
1063 4544      JMS I ENDT  /CHECK FOR DONE
1064 5256      JMP B1
1065 4407      JMS I 7
1066 5115      FGET BASE
1067 4104      FDIV N /COMPUTE AVERAGE
1070 6115      FPUT BASE
1071 0000      FEXT
1072 4532      JMS I CLF
1073 4536      JMS I MES    /PRINT BASELINE
1074 0201      TEXT "BA
1075 2305      SE
1076 1411      LI
1077 1605      NE
1100 4075      =
1101 4040      "
1102 0000      "
1103 4406      JMS I 6
1104 5540      JMP I LISTNP
/
/ SUBSECTION TO SUBTRACT BASELINE BETWEEN
/ FIRST AND LAST
/
1105 4561  BSUB,  JMS I DTSTP  /MAKE SURE DATA PRESENT
1106 4552      JMS I NEWCP  /GET FIRST AND LAST
1107 4543      JMS I INITP  /INITIALIZE
1110 4545      JMS I DACP   /GET POINT
1111 4407      JMS I 7
1112 2115      FSUB BASE
1113 0000      FEXT
1114 4553      JMS I STORE  /STORE CORRECTED POINT
1115 4544      JMS I ENDT
1116 5310      JMP --6
1117 4536      JMS I MES
1120 5502      TEXT "--B
1121 0123      AS
1122 0545      EX
1123 4300      #''
1124 5540      JMP I LISTNP
/
/ SUBSECTION TO COMPUTE THEORETICAL Y=A+B*X
/ X IS ALREADY SET
/
1125 0000      TH,    0
1126 7300      CLA CLL
1127 4407      JMS I 7
1130 5076      FGET B
```

1131 3123 FMPY X  
1132 1073 FADD A  
1133 6126 FPUT Y  
1134 0000 FEXT  
1135 5725 JMP I TH

/  
/ TABLE OF COMMAND CODES FOR BRAN ROUTINE  
/ DISPATCH JUMPS IN PAGE 1  
/

1136	0226	TABLE,	226	/CTRL V	FIT LOG
1137	0223		223	/CTRL S	STRIP LOG
1140	0202		202	/CTRL B	COMPUTE BASELINE
1141	0201		201	/CTRL A	STRIP BASELINE
1142	0216		216	/CTRL N	GET NEW FIRST AND LAST
1143	0204		204	/CTRL D	DISPLAY DATA
1144	0214		214	/CTRL L	DISPLAY TH. LOG
1145	0206		206	/CTRL F	DISPLAY LOG DATA
1146	0375		375	/ALT. MODE	SWAP CORE
1147	0220		220	/CTRL P	PUNCH DATA
1150	0330		330	/X	EXPAND DISPLAY
1151	0303		303	/C	CONTRACT DISPLAY
1152	0205		205	/CTRL E	EXAMINE DATA(FIRST)
1153	0221		221	/CTRL Q	QUIT RETURN TO AVERAGER
1154	0222		222	/CTRL R	READ DATA
1155	0224		224	/CTRL T	TITLE INFO
1156	0213		213	/CTRL K	EXPANSION COMMANDS
1157	0227		227	/CTRL W	
1160	7553		-225	/CTRL U	USER ROUTINE

/  
/ TABLE FOR CONTROL OF CTRL E OPERATIONS  
/

1161	0240	CTAB,	240	/SPACE	CHANGE
1162	0212		212	/LF	OPEN NEXT
1163	7563		-215	/CR	CLOSE AND EXIT

/  
/ TABLE FOR CONTROL OF TAPE READING OPERATIONS  
/ IDENTIFIES INPUT CHARACTERS FOR PROCESSING  
/

1164	0000	NTAB,	0	/BLANK	TAPE
1165	0255		255	/-	
1166	0253		253	/+	
1167	7540		-240	/SPACE	

/  
EXP=6  
LOG=7  
SQROOT=2  
SQUARE=0001  
/

/ SUBROUTINES FOR PROCESSING LEAST SQUARES  
/

			*1200		
1200	0000	CLEAR,	0	/CLEAR	SUMS
1201	7300		CLA	CLL	
1202	3044		DCA	44	/CLEAR FLOAT AC
1203	3045		DCA	45	
1204	3046		DCA	46	
1205	4407		JMS	I	7
1206	6101		FPUT	SIGMA	
1207	6302		FPUT	SUMX2	
1210	6310		FPUT	SUMXY	

```
1211 6305      FPUT SUMX
1212 6313      FPUT SUMY
1213 6316      FPUT SUMY2
1214 0000      FEXT
1215 5600      JMP I CLEAR
1216 0000      SUMS, 0 /COMPUTE SUMS
1217 4407      JMS I 7
1220 5123      FGET X / SUMX=SUMX+X
1221 3107      FMPY SIGA /SUMX=SUM W*X
1222 1305      FADD SUMX
1223 6305      FPUT SUMX
1224 5123      FGET X / SUMX2=SUMX2+X*X
1225 0001      SQUARE
1226 3107      FMPY SIGA /SUMX2=SUM W*X*2
1227 1302      FADD SUMX2
1230 6302      FPUT SUMX2
1231 5123      FGET X / SUMXY=SUMXY+X*Y
1232 3126      FMPY Y
1233 3107      FMPY SIGA /SUMXY=SUM W*X*Y
1234 1310      FADD SUMXY
1235 6310      FPUT SUMXY
1236 5126      FGET Y / SUMY=SUMY+Y
1237 3107      FMPY SIGA /SUMY= SUM W*Y
1240 1313      FADD SUMY
1241 6313      FPUT SUMY
1242 5107      FGET SIGA /SUMY2=SUM W=SUM SIGA=SUMY2+Y*Y
1243 1316      FADD SUMY2
1244 6316      FPUT SUMY2
1245 0000      FEXT
1246 5616      JMP I SUMS
1247 0000      CONS, 0 /COMPUTE LST SQUARES CONSTANTS
1250 4407      JMS I 7
1251 5305      FGET SUMX / DELTA=N*SUMX2-SUMX**2
1252 0001      SQUARE
1253 6321      FPUT DELTA
1254 5302      FGET SUMX2
1255 3316      FMPY SUMY2 /SUMY2=N WITH WEIGHT
1256 2321      FSUB DELTA
1257 6321      FPUT DELTA
1260 5310      FGET SUMXY / A=(SUMX2*SUMY-SUMX*SUMXY)/DELTA
1261 3305      FMPY SUMX
1262 6073      FPUT A
1263 5313      FGET SUMY
1264 3302      FMPY SUMX2
1265 2073      FSUB A
1266 4321      FDIV DELTA
1267 6073      FPUT A
1270 5313      FGET SUMY / B=(N*SUMXY-SUMX*SUMY)/DELTA
1271 3305      FMPY SUMX
1272 6076      FPUT B
1273 5310      FGET SUMXY
1274 3316      FMPY SUMY2
1275 2076      FSUB B
1276 4321      FDIV DELTA
1277 6076      FPUT B
1300 0000      FEXT / FINALLY DONE
1301 5647      JMP I CONS
1302 0000      SUMX2, FLTG 0.0
1303 0000
1304 0000
```



1305 0000 SUMX, FLTG 0.0  
1306 0000  
1307 0000  
1310 0000 SUMXY, FLTG 0.0  
1311 0000  
1312 0000  
1313 0000 SUMY, FLTG 0.0  
1314 0000  
1315 0000  
1316 0000 SUMY2, FLTG 0.0  
1317 0000  
1320 0000  
1321 0000 DELTA, FLTG 0.0  
1322 0000  
1323 0000

/  
/ COMPUTE STANDARD DEVIATIONS  
/ SIGA, SIGB, SIGMA ACTUALLY ARE VARIANCES  
/ SIGA USED TEMPORARILY TO HOLD WEIGHTS  
/ DURING FORMATION OF LEAST SQUARES SUMS  
/

1324 0000 DEV, 0  
1325 7300 CLA CLL  
1326 4407 JMS I 7  
1327 5104 FGET N  
1330 2065 FSUB TWO  
1331 6022 FPUT TEMP  
1332 5101 FGET SIGMA  
1333 4022 FDIV TEMP  
1334 6101 FPUT SIGMA  
1335 5101 FGET SIGMA  
1336 4321 FDIV DELTA  
1337 6022 FPUT TEMP /TEMP=SIGMA/DELTA  
1340 3302 FMPY SUMX2  
1341 6107 FPUT SIGA /SIGA=TEMP\*SUMX2  
1342 5022 FGET TEMP  
1343 3104 FMPY N  
1344 6112 FPUT SIGB /SIGB=TEMP\*N  
1345 0000 FEXT  
1346 5724 JMP I DEV

/  
/ SUBROUTINE TO STRIP EXPONENTIAL FROM DATA  
/ CTRL S  
/

1347 4561 STRIP, JMS I DTSTP  
1350 4552 JMS I NEWCP /GET FIRST AND LAST  
1351 4543 JMS I INITP /INITIALIZE  
1352 4546 JMS I THP /COMPUTE Y=A+B\*X  
1353 4407 JMS I 7  
1354 5126 FGET Y  
1355 0006 EXP  
1356 6126 FPUT Y  
1357 0000 FEXT  
1360 4545 JMS I DACP /GET A POINT  
1361 4407 JMS I 7  
1362 2126 FSUB Y  
1363 0000 FEXT  
1364 4553 JMS I STORE /STORE CORRECTED POINT  
1365 4544 JMS I ENDT /TEST FOR END  
1366 5355 JMP STRIP+6 /KEEP GOING

```
1367 4536 JMS I MES
1370 0530 TEXT "EX
1371 2040 P
1372 2325 SU
1373 0224 BT
1374 2245 RZ
1375 4300 #"
1376 5540 JMP I LISTNP
/
OCTAL
*1400
/ PAGE 5
/
1400 0000 0 /ENTRY TO PRINT "DEV."
1401 4536 JMS I MES
1402 4040 TEXT "
1403 0405 DE
1404 2656 V.
1405 4000 "
1406 5600 JMP I 1400
/
1407 0000 LSQOUT, 0 /PRINT LST. SQUARES PARAMETERS
1410 7200 CLA
1411 4532 JMS I CLF
1412 3055 DCA 55 /REMOVE CRLF
1413 4536 JMS I MES
1414 0175 TEXT "A="
1415 4000 "
1416 4407 JMS I 7
1417 5073 FGET A
1420 0000 FEXT
1421 4406 JMS I 6
1422 4200 JMS 1400
1423 4407 JMS I 7
1424 5107 FGET SIGA
1425 0002 SQROOT
1426 0000 FEXT
1427 4406 JMS I 6
1430 4532 JMS I CLF
1431 4536 JMS I MES
1432 0275 TEXT "B="
1433 4000 "
1434 4407 JMS I 7
1435 5076 FGET B
1436 0000 FEXT
1437 4406 JMS I 6
1440 4200 JMS 1400
1441 4407 JMS I 7
1442 5112 FGET SIGB
1443 0002 SQROOT
1444 0000 FEXT
1445 4406 JMS I 6
1446 4532 JMS I CLF
1447 4536 JMS I MES
1450 2417 TEXT "TO
1451 2401 TA
1452 1440 L
1453 2601 VA
1454 2211 RI
1455 0116 AN
```

```
1456 0305 CE
1457 4075 =
1460 4000 "
1461 4407 JMS I 7
1462 5101 FGET SIGMA
1463 0000 FEXT
1464 4406 JMS I 6
1465 4532 JMS I CLF
1466 4532 JMS I CLF
1467 4536 JMS I MES
1470 2461 TEXT "T1
1471 4075 =
1472 4000 "
1473 4407 JMS I 7
1474 5062 FGET ONE
1475 4076 FDIV B
1476 0000 FEXT
1477 4406 JMS I 6
1500 7240 CLA CMA
1501 3055 DCA 55 /RESTORE CRLF
1502 4200 JMS 1400
1503 4407 JMS I 7 /GET DEV. FOR T1
1504 5076 FGET B
1505 0001 SQUARE
1506 6022 FPUT TEMP
1507 5112 FGET SIGB
1510 0002 SQROOT /SIG(T1)=SIGB/B*2
1511 4022 FDIV TEMP
1512 0000 FEXT
1513 4406 JMS I 6
1514 4532 JMS I CLF
1515 5607 JMP I LSQOUT
/
/
/ LEAST SQUARES SUBROUTINE
/ ORGANIZES FIT
/ DOES FIT TO LOGARITHM
/
1516 0000 LINEL, 0 /ENTRY FOR LOG LST. SQUARES
1517 4543 JMS I INITP /INITIALIZE POINTERS
1520 4555 JMS I CLEARP /CLEAR SUMS
1521 4570 JMS I WLOGP /GET LOG AND WEIGHT
1522 4407 JMS I 7
1523 6126 FPUT Y
1524 0000 FEXT
1525 4556 JMS I SUMSP /COMPUTE LST. SQ. SUMS
1526 4544 JMS I ENDT /MOVE AND CHECK FOR DONE
1527 5321 JMP LINEL+3 /CONTINUE
1530 4557 JMS I CONSP /COMPUTE CONSTANTS
1531 4543 JMS I INITP /RESTART TO GET SIGMA
1532 4546 LST, JMS I THP /COMPUTE THEORY
1533 4570 JMS I WLOGP /GET LOG AND WEIGHT
1534 4407 JMS I 7
1535 2126 FSUB Y
1536 0001 SQUARE
1537 3107 FMPY SIGA /MULTIPLY BY WEIGHT
1540 1101 FADD SIGMA
1541 6101 FPUT SIGMA
1542 0000 FEXT
1543 4544 JMS I ENDT
```

```
1544 5332      JMP LST
1545 4547      JMS I DEVP      /COMPUTE DEVIATIONS
1546 5716      JMP I LINEL
/
/ SUBSECTION TO HANDLE CTRL E  EXAMINE LOCATION
/ PRINTS FIRST AND DATA(FIRST)
/ RESPONDING WITH SPACE GIVES OPTION OF CHANGING
/ THE DATA POINT;CR TO CLOSE;LINE FEED TO
/ OPEN NEXT POINT
/
1547 2027 LFN,    ISZ FIRST      /MOVE TO NEXT POINT
1550 4532      JMS I CLF
1551 7300 EXAM,    CLA CLL
1552 1027      TAD FIRST
1553 4533      JMS I NSIN      /PRINT FIRST
1554 4543      JMS I INITP     /SET POINTER
1555 4545      JMS I DACP     /GET NO.
1556 3055      DCA 55 /CLEAR CRLF
1557 4406      JMS I 6       /PRINT NO.
1560 7240      CLA CMA
1561 3055      DCA 55 /RESTORE CRLF
1562 4560      JMS I KEYP     /ASK FOR COMMAND
1563 4541      JMS I BRP     /IDENTIFY COMMAND
1564 1161      CTAB
1565 5371      JMP K /CHANGE DATA
1566 5347      JMP LFN      /OPEN NEXT
1567 4532      JMS I CLF
1570 5540      JMP I LISTNP    /FELL THROUGH TABLE
1571 4561 K,     JMS I DTSTP    /CHECK FOR DATA PRESENT
1572 4543      JMS I INITP
1573 4405      JMS I 5       /INPUT NO.
1574 4553      JMS I STORE    /STORE IT
1575 1057      TAD 57 /GET TERMINATOR
1576 5363      JMP K-6      /IDENTIFY COMMAND
```

\*1600

/ PAGE 6  
/SUBSECTION TO PUNCH DATA

```
1600 7300 PNCH,  CLA CLL
1601 4532      JMS I CLF
1602 1026      TAD DISC      /CHECK FOR AVERAGER
1603 7640      SZA CLA
1604 5537      JMP I WHATP     /AVERAGER NOT THERE
1605 1032      TAD BLK      /SET POINTER TO AVER. BLOCK
1606 3011      DCA POINT1
1607 1030      TAD LAST
1610 4533      JMS I NSIN    /PRINT UPPER LIMIT
1611 1030      TAD LAST
1612 7040      CMA
1613 3036      DCA COUNT
1614 6201      CDF 0
1615 1431      TAD I SCL     /GET SCALE
1616 3013      DCA POINT4
1617 1411      TAD I POINT1
1620 6211      CDF 10
1621 4533      JMS I NSIN    /PRINT NO. OF SWEEPS
1622 4532      JMS I CLF
1623 2016      ISZ SWITCH    /SET FOR PUNCH
1624 1034 LOOP, TAD KM12     /SET POSITION COUNTER
```

```

1625 3024      DCA ARITH2
1626 4567      JMS I HLTP      /CHECK FOR PANIC STOP
1627 2036      ISZ COUNT
1630 7410      SKP
1631 5240      JMP SCRAM      /DONE
1632 4535      JMS I GET      /GET A POINT
1633 4533      JMS I NSIN     /OUTPUT THE POINT
1634 2024      ISZ ARITH2     /CHECK POSITION
1635 5226      JMP LOOP+2     /GET MORE
1636 4532      JMS I CLF     /START A NEW LINE
1637 5224      JMP LOOP      /CONTINUE TILL DONE
1640 4532      SCRAM, JMS I CLF
1641 3016      DCA SWITCH    /RESET FOR TTY
1642 5540      JMP I LISTNP

/
      *1650
/ THIS SECTION READS DATA IN ON THE HIGH SPEED READER
/ Y VALUES ONLY EXPECTED
/ DATA IS PLACED INTO THE BUFFER AREA
/ MAINTAINED BY THE BASIC AVERAGER IN FIELD 0
/ CORE MUST STILL BE SWAPPED TO GET AT THE DATA
/ CHAR=15; SIGN=ARITH4; NUM=17 TEMP USED HERE
/
/ CTRL R
/
1650 7300      INPT,  CLA CLL      /INITIALIZE
1651 3027      DCA FIRST
1652 3030      DCA LAST
1653 1032      TAD BLK      /GET THE BUFFER AREA
1654 7001      IAC
1655 3010      DCA POINT    /USED BY STD
1656 3017      DCA 17 /CLEAR NUMBER BUILDER
1657 3025      DCA ARITH4   /CLEAR SIGN

/
1660 4563      START, JMS I RDRP   /SEARCH FOR START OF TAPE
1661 4541      JMS I BRP     /IDENTIFY INPUT CHARACTER
1662 1164      NTAB
1663 5260      JMP START
1664 5270      JMP MINUS    /# IS NEG.
1665 5273      JMP PLUS     /# IS POS.
1666 5273      JMP PLUS
1667 5260      JMP START    /NOT IN TABLE
1670 7240      MINUS, CLA CMA      /SET - SIGN
1671 3025      DCA ARITH4
1672 5275      JMP DAT
1673 7300      PLUS,  CLA CLL
1674 3025      DCA ARITH4
1675 4563      DAT,  JMS I RDRP   /PROCESS MAIN TAPE
1676 4566      JMS I NUMTSP  /TEST FOR NUMBERS
1677 5302      JMP .+3
1700 4565      JMS I CNVRTP  /PERFORM BCD TO BIN
1701 5275      JMP DAT      /GET REST OF #
1702 4564      JMS I STP     /STORE # IN BUFFER
1703 2030      ISZ LAST     /COUNT IT
1704 4563      FIN,  JMS I RDRP   /SEARCH FOR END OF TAPE
1705 4566      JMS I NUMTSP
1706 7610      SKP CLA
1707 5300      JMP DAT+3
1710 1015      TAD 15      /GET THE CHARACTER
1711 4541      JMS I BRP     /IDENTIFY

```

```
1712 1164      NTAB
1713 5320      JMP .+5        /BLANK; FINISHED
1714 5270      JMP MINUS
1715 5273      JMP PLUS
1716 5273      JMP PLUS
1717 5304      JMP FIN        /FELL THROUGH TABLE
1720 7300      CLA CLL
1721 4532      JMS I CLF
1722 4536      JMS I MES
1723 1401      TEXT "LA
1724 2324      ST
1725 4020      P
1726 1711      OI
1727 1624      NT
1730 4000      "
1731 7240      CLA CMA
1732 1030      TAD LAST
1733 3030      DCA LAST
1734 1030      TAD LAST
1735 4533      JMS I NSIN
1736 4532      JMS I CLF
1737 5540      JMP I LISTNP  /RETURN
/
/ SUBROUTINE TO DO EMERGENCY HALT IF CTRL/H TYPED
/ PRESENTLY CALLED FROM NEWC AND PNCH ONLY
/ RETURNS TO CALL IF NORMAL
/
1740 7570      -210  /CTRL/H
1741 0000      HALT,  0
1742 7440      SZA    /USE AC FOR CHAR IF NONZERO
1743 5347      JMP .+4
1744 6031      KSF    /CHECK FOR TTY
1745 5741      JMP I HALT  /NO; RETURN
1746 6036      KRB    /YES ;GET COMMAND
1747 4541      JMS I BRP
1750 1740      HALT-1 /CHECK FOR CTRL/H
1751 5540      JMP I LISTNP /YES; STOP
1752 7300      CLA CLL  /NO; IGNORE CHARACTER
1753 5741      JMP I HALT
/
*2000
/SUBSECTION TO DO THE DISK OPERATIONS
/ROUTINE TO SWAP AVERAGER OUT TO DISK
/AND CONVERT DATA TO FLOATING POINT
/
2000 7300      SWAP,  CLA CLL
2001 1026      TAD DISC  /CHECK IF ALREADY THERE
2002 7640      SZA CLA
2003 5537      JMP I WHATP /ITS ALREADY THERE
2004 4261      JMS WRITE /NO-WRITE IT OUT
2005 7201      CLA IAC
2006 3026      DCA DISC  /SET INDICATOR
/
/REARRANGE FIELD 0 DATA TO FL. PT. NO.
/ DATA ASSUMED NEGATIVE AND IS MADE POS.
/
2007 1032      TAD BLK    /SET POINTERS
2010 7001      IAC
2011 3011      DCA POINT1
2012 1037      TAD KMD1K
```

```
2013 3036          DCA COUNT
2014 1142          TAD SPEC
2015 3014          DCA 14
2016 6201          CDF 0 /SET SCALE FOR GET
2017 1431          TAD I SCL
2020 3013          DCA POINT4
2021 6211          CDF 10
2022 4535          F1, JMS I GET
2023 7041          CIA
2024 4554          JMS I FLOATP
2025 4553          JMS I STORE
2026 2036          ISZ COUNT
2027 5222          JMP F1
2030 4536          JMS I MES
2031 0317          TEXT "CO
2032 2205          RE
2033 4023          S
2034 2701          WA
2035 2020          PP
2036 0504          ED
2037 0000          "
2040 4532          JMS I CLF
2041 5540          JMP I LISTNP
/
/ THIS SECTION RESTORES THE BASIC AVERAGER
/ AND RETURNS TO IT THROUGH A CTRL Q
/
2042 7300          RESTOR, CLA CLL
2043 1026          TAD DISC          /IS IT ALREADY PRESENT
2044 7650          SNA CLA
2045 5250          JMP RET
2046 4270          JMS READ          /NO-GET IT
2047 3026          DCA DISC          /CLEAR INDICATOR
2050 6032          RET, KCC          /CLEAR FLAGS
2051 6042          TCF
2052 6022          PCF
2053 6601          6601          /=DCMA
2054 6201          CDF 0
2055 6202          CIF 0
2056 5657          JMP I .+1
2057 6506          6506          /BASIC AVER. CTRL/Q
/
/ DISC HANDLING SUBSECTION
/
2060 6605          6605          /DMAW=WRITE
2061 0000          WRITE, 0
2062 7300          CLA CLL
2063 1260          TAD WRITE-1          /SET WRITE INSTR
2064 3312          DCA INSTR
2065 4276          JMS DISK
2066 5661          JMP I WRITE
/
2067 6603          6603          /=DMAR=READ
2070 0000          READ, 0
2071 7300          CLA CLL
2072 1267          TAD READ-1
2073 3312          DCA INSTR          /SET READ INSTR
2074 4276          JMS DISK
2075 5670          JMP I READ
2076 0000          DISK, 0
```

```
2077 1142 TAD SPEC /MOVE LOC. 200-6377
2100 6201 CDF 0
2101 3720 DCA I CA
2102 6211 CDF 10
2103 1322 TAD WCV
2104 6201 CDF 0
2105 3721 DCA I WC
2106 6211 CDF 10
2107 1317 TAD TRACK /USE LAST TWO DISK TRACKS
2110 6615 6615 /=DEAL LOAD DISK EA AND EMA
2111 7200 CLA /DISK ADDRESS IS 0
2112 0000 INSTR, 0 /READ OR WHITE
2113 6622 6622 /DFSC WAIT FOR COMPLETION
2114 5313 JMP .-1
2115 6601 6601 /DCMA
2116 5676 JMP I DISK
2117 0700 TRACK, 0700
2120 7751 CA, 7751
2121 7750 WC, 7750
2122 1600 WCV, 1600
/
/ PROCESSING SUBROUTINES FOR CTRL R COMMAND
/
/ SUBROUTINE TO STORE THE SINGLE PREC. NO. READ
/ AS A DOUBLE PREC. NO. IN THE BUFFER AREA
/ IN FIELD 0
/ USES POINT AS A POINTER; SHOULD BE SET BEFORE CALL
/ IS SET TO NEXT POINT AFTER CALL
/
2123 0000 STD, 0
2124 7300 CLA CLL
2125 1025 TAD ARITH4 /TEST SIGN
2126 7700 SMA CLA
2127 5333 JMP .+4 /POS.
2130 1017 TAD 17 /GET NUMBER
2131 7041 CIA
2132 7410 SKP
2133 1017 TAD 17
2134 6201 CDF 0
2135 3410 DCA I POINT /STORE NO.
2136 1025 TAD ARITH4 /SAVE HIGH ORDER
2137 3410 DCA I POINT
2140 6211 CDF 10
2141 3017 DCA 17 /CLEAR NO.
2142 3025 DCA ARITH4 /CLEAR SIGN
2143 5723 JMP I STD
/
/ ROUTINE TO PERFORM BCD TO BINARY CONVERSION
/ BY MULTIPLE CALLS
/ ASCII NO.S EXPECTED
/
2144 0000 CNVRT, 0
2145 7300 CLA CLL
2146 1017 TAD 17 /MULTIPLY PREVIOUS PART BY 10
2147 7006 RTL
2150 3022 DCA TEMP
2151 1017 TAD 17
2152 7004 RAL
2153 1022 TAD TEMP
2154 1022 TAD TEMP
```



```
2155 3022          DCA TEMP
2156 1015          TAD 15          /GET THE INPUT DIGIT
2157 1376          TAD KM260         /REMOVE ASCII BIAS
2160 1022          TAD TEMP          /FORM NO.
2161 3017          DCA 17 /SAVE IT
2162 5744          JMP I CNVRT        /FOR NEXT CALL; OR DONE
/
/ SUBROUTINE TO TEST WHETHER THE INPUT
/ CHARACTER IS A NUMBER
/
2163 0000 NUMTST, 0          /RETURN TO
2164 7300          CLA CLL          / CALL+1 IF NO
2165 1015          TAD 15 /          CALL +2 IF YES
2166 1376          TAD KM260
2167 7510          SPA
2170 5763          JMP I NUMTST      /NO; <260
2171 1034          TAD KM12
2172 7700          SMA CLA
2173 5763          JMP I NUMTST      /NO; >271
2174 2363          ISZ NUMTST
2175 5763          JMP I NUMTST      /YES
2176 7520          KM260, -260
/
          *2200
/ DISPLAY ROUTINES
/ SUBROUTINE TO SET UP DISPLAY
/
2200 0000          XINIT, 0
2201 7300          CLA CLL
2202 4543          JMS I INITP
2203 1027          TAD FIRST        /USE FIRST FOR X ORIGIN
2204 1276          TAD XS
2205 3277          DCA XDIS         /SET START X
2206 5600          JMP I XINIT
/
/ DISPLAY LOG OF DATA
/ CTRL F
/
2207 4200          LOGDIS, JMS XINIT
2210 4545          JMS I DACP        /GET POINT
2211 4407          JMS I 7
2212 0007          LOG
2213 3070          FMPY HUND        /MULT. LOG BY 100 FOR VISUAL EFFECT
2214 6126          FPUT Y
2215 0000          FEXT
2216 4246          JMS DISP
2217 4544          JMS I ENDT        /CHECK FOR DONE
2220 5210          JMP LOGDIS+1
2221 5540          JMP I LISTNP
/
/ DISPLAY THEORETICAL LOG CTRL L
/
2222 4200          THDIS, JMS XINIT
2223 4546          JMS I THP
2224 4407          JMS I 7          /MULT. LOG BY 100
2225 5126          FGET Y /TO EXPAND FOR SCOPE DISPLAY
2226 3070          FMPY HUND
2227 6126          FPUT Y
2230 0000          FEXT
2231 4246          JMS DISP
```

```

2232 4544      JMS I ENDT
2233 5223      JMP THDIS+1
2234 5540      JMP I LISTNP
/
/ DISPLAY DATA  CTRL D
/
2235 4200 DATDIS, JMS XINIT
2236 4545      JMS I DACP      /GET DATA
2237 4407      JMS I 7
2240 6126      FPUT Y
2241 0000      FEXT
2242 4246      JMS DISP
2243 4544      JMS I ENDT
2244 5236      JMP DATDIS+1
2245 5540      JMP I LISTNP
/
/ DISPLAY SUBROUTINE
/ INCREMENTS XDIS BY XDEL AT END
/ AND DISPLAYS SHIFTED VERSION OF Y
/
2246 0000 DISP,  0
2247 7300      CLA CLL      /SET X COORDINATE
2250 1277      TAD XDIS
2251 6303      6303      /DXC DXL
2252 1300      TAD XDEL
2253 3277      DCA XDIS
2254 4407      JMS I 7
2255 5126      FGET Y /GET Y FOR DISPLAY
2256 0000      FEXT
2257 4551      JMS I IFIXP
2260 3021      DCA SHFR+1
2261 1021      TAD SHFR+1      /SET THE SIGN
2262 7710      SPA CLA
2263 7040      CMA
2264 3020      DCA SHFR
2265 1275      TAD VSW
2266 4534      JMS I SHIFT      /PERFORM SHIFT
2267 1301      TAD VSH      /BIAS SCOPE DISPLAY
2270 7041      CIA
2271 1021      TAD SHFR+1      /GET Y
2272 6317      6317      /DYC DYL DIS
2273 7300      CLA CLL
2274 5646      JMP I DISP
/
2275 0000 VSW,  0      /SHIFTING FACTOR
2276 0000 XS,   0
2277 0000 XDIS, 0
2300 0001 XDEL, 0001
2301 0000 VSH,  0      /Y BIAS FOR SCOPE
/
/

```

REFERENCES

- A. Abragam, The Principles of Nuclear Magnetism (Oxford University Press, London, 1961).
- A. Abragam and B. Bleaney, Electron Paramagnetic Resonance of Transition Ions (Oxford University Press, London, 1970).
- S. A. Al'tshuler and K. A. Valiev, Zh. Eksp. Teor. Fiz. 35, 947(1958); Sov. Phys. JETP 10, 661(1959).
- S. A. Al'tshuler and B. M. Kozyrev, Electron Paramagnetic Resonance (Academic Press, New York, 1964).
- P. N. Argyres and P. L. Kelley, Phys. Rev. 134, A98(1964).
- N. M. Atherton and G. R. Luckhurst, Mol. Phys. 13, 145(1967).
- P. W. Atkins, Mol. Phys. 12, 133(1967).
- P. W. Atkins and Daniel Kivelson, J. Chem. Phys. 44, 169(1966).
- V. I. Avvakumov, Zh. Eksp. Teor. Fiz. 37, 1017(1959); Sov. Phys. JETP 10, 723(1960).
- V. I. Avvakumov, N. S. Garif'yanov, B. M. Kozyrev, and P. G. Tishkov, Zh. Eksp. Teor. Fiz. 37, 1564(1959); Sov. Phys. JETP 10, 1110(1960).
- William Thomas Batchelder, The Electron Paramagnetic Resonance Spectra of  $\alpha\text{-NiSO}_4 \cdot 6\text{H}_2\text{O}$  at Liquid Helium Temperature (Ph. D. Thesis), UCRL-19157, May 1970.
- Alfred Bauder and Rollie J. Myers, J. Mol. Spectrosc. 27, 110(1968).
- George B. Benedek, Robert Englman, and John A. Armstrong, J. Chem. Phys. 39, 3349(1963).
- I. B. Bersuker, Sov. Phys. JETP 17, 836(1963).
- I. B. Bersuker and B. G. Vekhter, Sov. Phys. Sol. State 7, 986(1965).
- S. M. Blinder, J. Chem. Phys. 33, 748(1960).
- F. Bloch, Phys. Rev. 70, 460(1946).
- F. Bloch, Phys. Rev. 102, 104(1956).
- F. Bloch, Phys. Rev. 105, 1206(1957).
- N. Bloembergen, Phys. Rev. 104, 324(1956).
- N. Bloembergen, E. M. Purcell, and R. V. Pound, Phys. Rev. 73, 679(1948).

- K. D. Bowers and W. B. Mims, Phys. Rev. 115, 285(1959).
- D. P. Breen, D. C. Krupka, and F. I. B. Williams, Phys. Rev. 179, 241(1969).
- J. Burgess and M. C. R. Symons, Quart. Rev. 22, 276(1968).
- R. Calvo and R. Orbach, Phys. Rev. 164, 284(1967).
- A. Carrington and G. R. Luckhurst, Mol. Phys. 8, 125(1964).
- Alan Carrington and Andrew D. McClachlan, Introduction to Magnetic Resonance(Harper & Row, New York, 1967).
- P. F. Cox and L. O. Morgan, J. Am Chem. Soc. 81, 6409(1959).
- C. F. Davis, Jr., M. W. P. Strandberg, and R. L. Kyhl, Phys. Rev. 111, 1268(1958).
- W. Edwards Deming, Statistical Adjustment of Data(John Wiley & Sons, Inc., New York, 1938). Reprinted by Dover Publications, Inc., New York, 1964.
- J. M. Deutch and Irwin Oppenheim, Adv. in Magnetic Resonance 3, 43(1968).
- Lawrence S. Frankel, J. Phys. Chem. 72, 736(1968).
- George K. Fraenkel, J. Phys. Chem. 71, 139(1967).
- Jack H. Freed, J. Chem. Phys. 49, 376(1968).
- Jack H. Freed and George K. Fraenkel, J. Chem. Phys. 39, 326(1963).
- Shizuo Fujiwara and Hisaharu Hayashi, J. Chem. Phys. 43, 23(1965).
- Robert L. Fulton, J. Chem. Phys. 41, 2876(1964).
- N. S. Garif'ianov and B. M. Kozyrev, Doklady Akad. Nauk S. S. S. R. 98, 929(1954).
- N. S. Garif'yanov, B. M. Kozyrev, R. Kh. Timerov, and N. F. Usacheva, Zh. Eksp. Teor. Fiz. 41, 1076(1961); Sov. Phys. JETP 14, 768(1962a).
- N. S. Garif'yanov, B. M. Kozyrev, R. Kh. Timerov, and N. F. Usacheva, Zh. Eksp. Teor. Fiz. 42, 1145(1962); Sov. Phys. JETP 15, 791(1962b).
- N. S. Garif'yanov and N. F. Usacheva, Russ. J. Phys. Chem. 38, 752(1964).
- H. R. Gersmann and J. D. Swalen, J. Chem. Phys. 36, 3221(1962).
- L. van Gerven, J. Talpe, and A. van Itterbeck, Physica 33, 207(1967).

- J. C. Gill, Proc. Phys. Soc.(Lond.) 85, 119(1965).
- C. J. Gorter, Paramagnetic Relaxation(Elsevier Publishing Co., Amsterdam, 1947).
- Robert G. Hayes, Electron Spin Resonance Line Widths of Transition Metal Ions and Complexes in Solution(Ph. D. Thesis), UCRL-9873, Sept. 1961.
- L. C. Hebel and C. P. Slichter, Phys. Rev. 113, 1504(1959).
- Paul S. Hubbard, Phys. Rev. 131, 1155(1963).
- A. Hudson and G. R. Luckhurst, Chem. Revs. 69, 191(1969).
- James A. Ibers and J. D. Swalen, Phys. Rev. 127, 1914(1962).
- H. A. Jahn, Proc. Roy. Soc.(Lond.) 164, 117(1938).
- H. A. Jahn and E. Teller, Proc. Roy. Soc.(Lond.) 161, 220(1937).
- Akira Jindo, Single Crystal Studies of Hydrated Transition Metal Ions by Electron Paramagnetic Resonance(Ph. D. Thesis), UCRL-20386, 1971.
- Theron S. Johnston and Harry G. Hecht, J. Mol. Spectrosc. 17, 98(1965).
- J. B. Jones and M. F. Lewis, Solid State Commun. 5, 595(1967).
- Wilfred Kaplan, Ordinary Differential Equations(Addison-Wesley Publishing Company, Inc., Reading, Mass., 1958).
- Daniel Kivelson, J. Chem. Phys. 27, 1087(1957).
- Daniel Kivelson, J. Chem. Phys. 33, 1094(1960).
- Daniel Kivelson, J. Chem. Phys. 41, 1904(1964).
- Daniel Kivelson, J. Chem. Phys. 45, 751(1)(1966a).
- Daniel Kivelson, J. Chem. Phys. 45, 1324(1966b).
- Daniel Kivelson and George Collins, ESR Line Widths in Liquids, in Paramagnetic Resonance, Vol. II, W. Low, Ed.(Academic Press, New York, 1963), p. 496.
- Daniel Kivelson and Robert Neiman, J. Chem. Phys. 35, 149(1961).
- Fritz Kurt Kneubuhl, J. Chem. Phys. 33, 1074(1960).
- B. M. Kozyrev, Disc. Faraday Soc. 19, 135(1955).

- B. M. Kozyrev, *Izv. Akad. Nauk S.S.S.R. ser. Fiz.* 21, 828(1957)(Eng. Trans).
- Ryogo Kubo and Katushi Tomita, *J. Phys. Soc. Japan* 9, 888(1954).
- Ronald Lee, James Neely, and Rochelle (Cooper) Dreyfuss, private communication(1968).
- W. Burton Lewis, Mohammed Alei, Jr., and L. O. Morgan, *J. Chem. Phys.* 44, 2409(1966).
- W. Burton Lewis and L. O. Morgan, *Paramagnetic Relaxation in Solutions, in Transition Metal Chemistry, Vol. 4*, R. Carlin, Ed.(Marcel Dekker, Inc., New York, 1968).
- M. F. Lewis and A. M. Stoneham, *Phys. Rev.* 164, 271(1967).
- A. H. Maki and B. R. McGarvey, *J. Chem. Phys.* 29, 31(1958a).
- A. H. Maki and B. R. McGarvey, *J. Chem. Phys.* 29, 35(1958b).
- Douglas C. McCain, *The Measurement of Electron Spin Relaxation Times of Ions in Aqueous Solution*(Ph. D. Thesis), UCRL-17064, Aug. 1966.
- Douglas C. McCain and Rollie J. Myers, *J. Phys. Chem.* 71, 192(1967).
- A. D. McClachlan, *Proc. Roy. Soc.(Lond.)* 280, 271(1964).
- R. E. D. McClung and Daniel Kivelson, *J. Chem. Phys.* 49, 3380(1968).
- Harden M. McConnell, *J. Chem. Phys.* 25, 709(1956).
- B. R. McGarvey, *J. Phys. Chem.* 60, 71(1956).
- B. R. McGarvey, *J. Phys. Chem.* 61, 1232(1957).
- Charles W. Merideth, *Temperature Dependence of Transverse Relaxation Times of Oxygen-17 in Aqueous Solutions Containing Cupric and Chromous Ions*(Ph. D. Thesis), UCRL-11704, Jan. 1965.
- W. B. Mims, K. Nassau, and J. D. McGee, *Phys. Rev.* 123, 2059(1961).
- L. O. Morgan and A. W. Nolle, *J. Chem. Phys.* 31, 365(1959).
- Robert Neiman and Daniel Kivelson, *J. Chem. Phys.* 35, 156(1961).
- Mary C. M. O'Brien, *Proc. Roy. Soc.(Lond.)* A281, 323(1964).
- David Wixon Pratt, *Magnetic Resonance Spectra of  $VCl_4$  and other Paramagnetic Species*(Ph. D. Thesis), UCRL-17406, April 1967.

- U. Opik and M. H. L. Pryce, Proc. Roy. Soc. (Lond.) A238, 425(1957).
- G. E. Pake and R. H. Sands, Phys. Rev. 98, 266(A)(1955).
- A. G. Redfield, IBM J. Res. Dev. 1, 19(1957).
- A. G. Redfield, The Theory of Relaxation Processes, in Adv. in Magnetic Resonance, Vol. 1, John S. Waugh, Ed. (Academic Press, New York, 1962), p. 1.
- J. Reuben and D. Fiat, Inorg. Chem. 6, 579(1967).
- J. Reuben and D. Fiat, J. Am Chem. Soc. 91, 4652(1969a).
- J. Reuben and D. Fiat, Inorg. Chem. 8, 1821(1969b).
- R. N. Rogers and G. E. Pake, J. Chem. Phys. 33, 1107(1960).
- Robert T. Ross, J. Chem. Phys. 42, 3919(1965).
- D. Sames, Zeit. fur Physik 188, 108(1965).
- D. Sames, Zeit. fur Physik 198, 71(1967).
- R. H. Sands, Phys. Rev. 99, 1222(1955).
- Abraham Savitzky and Marcel J. E. Golay, Anal. Chem. 36, 1627(1964).
- Jan W. Schreurs and Daniel Kivelson, J. Chem. Phys. 36, 117(1962).
- P. L. Scott and C. D. Jeffries, Phys. Rev. 127, 32(1962).
- Joel Selbin, Chem. Rev. 65, 153(1965).
- Joel Selbin and L. H. Holmes, Jr., J. Inorg. Nucl. Chem. 24, 1111(1962).
- David P. Shoemaker and Carl W. Garland, Experiments in Physical Chemistry (McGraw-Hill Book Company, Inc., New York, 1962).
- Hans Sillescu and Daniel Kivelson, J. Chem. Phys. 48, 3493(1968).
- E. Simanek and R. Orbach, Phys. Rev. 145, 191(1966).
- Charles P. Slichter, Principles of Magnetic Resonance (Harper & Row, New York, 1963).
- F. J. Smith, J. K. Smith, and S. P. McGlynn, Rev. Sci. Instrum. 33, 1367(1962).
- Zoltan G. Soos, J. Chem. Phys. 49, 2493(1968).

- John B. Spencer, Electron Spin Resonance Studies of Transition Metal Ion Complexes(Ph. D. Thesis), UCRL-16175, Aug. 1965.
- K. J. Standley and R. A. Vaughan, Electron Spin Relaxation Phenomena in Solids(Plenum Press, New York, 1969).
- K. W. H. Stevens, Rept. Prog. Physics XXX part 1, 129(1967).
- A. M. Stoneham, Proc. Phys. Soc.(Lond.) 85, 107(1965).
- J. D. Swalen and H. M. Gladney, IEM J. Res. Dev. 8, 515(1964).
- T. J. Swift and Robert E. Connick, J. Chem. Phys. 37, 307(1962).
- E. E. Vainshtein and I. I. Antipova-Karataeva, Russ. J. Inorg. Chem. 4, 355(1959).
- K. A. Valiev and M. M. Zaripov, Zh. Eksp. Teor. Fiz. 41, 756(1961); Sov. Phys. JETP 14, 545(1962).
- K. A. Valiev and M. M. Zaripov, Opt. Spektrosk. 20, 108(1966); Optics & Spect. 20, 56(1966).
- R. M. Valishev, Sov. Phys. Sol. St. 7, 733(1965).
- Tore Vanngard and Roland Aasa, ESR Line Shapes of Polycrystalline Samples of  $S=1/2$  Transition Element Ions, in Paramagnetic Resonance Vol. II, W. Low, Ed.(Academic Press, New York, 1963), p. 509.
- J. H. van Vleck, J. Chem. Phys. 7, 72(1939).
- G. P. Vishnevskaya and B. M. Kozyrev, Zh. Strukt. Khimii 6, 667(1965); J. Struct. Chem. 6, 637(1965).
- Walter M. Walsh, Jr., Jean Jeener, and N. Bloembergen, Phys. Rev. 139A, 1338(1965).
- R. K. Wangsness and F. Bloch, Phys. Rev. 89, 728(1953).
- F. I. B. Williams, D. C. Krupka, and D. P. Breen, Phys. Rev. 179, 255(1969).
- Raymond Wilson and Daniel Kivelson, J. Chem. Phys. 44, 154(1966a).
- Raymond Wilson and Daniel Kivelson, J. Chem. Phys. 44, 4440(1966b).
- Raymond Wilson and Daniel Kivelson, J. Chem. Phys. 44, 4445(1966c).
- Amnon Yariv and W. H. Louisell, Phys. Rev. 125, 558(1962).



Allan Zalkin, J. D. Forrester, and David H. Templeton, J. Chem. Phys. 39,  
2881(1963).

M. M. Zaripov, Optics & Spect. 18, 136(1965).

#### ACKNOWLEDGMENTS

Many people have helped to make my stay in Berkeley a most enjoyable experience. I would like to thank my research director, Professor Rollie J. Myers, for his patience and guidance during my many years of graduate school. His expertise in getting experimental set-ups to work has been very beneficial; it has been educational to watch him work. The members of my research group have been most helpful. The conversations which I have had with Doug McCain, Dave Pratt, and Aki Jindo have been very stimulating and in many cases guided my thoughts along lines which I may not otherwise have followed. I would also like to acknowledge Fredi Bauder who wrote the initial versions of the data acquisition system programs; also Raymond Pao, Tom Hynes, and Joyce Tevebaugh; and, of course, Eloise.

I would like to thank the many friends which I have made in Berkeley for their comradeship and encouragement, especially my roommates. My association with the 5th floor, particularly with the members of the Jolly group, has enriched my life. The many "quickies" were enjoyable and a welcome break from sometimes tedious research.

This work was performed under the auspices of the United States Atomic Energy Commission through the Inorganic Materials Research Division of the Lawrence Radiation Laboratory.

LEGAL NOTICE

*This report was prepared as an account of work sponsored by the United States Government. Neither the United States nor the United States Atomic Energy Commission, nor any of their employees, nor any of their contractors, subcontractors, or their employees, makes any warranty, express or implied, or assumes any legal liability or responsibility for the accuracy, completeness or usefulness of any information, apparatus, product or process disclosed, or represents that its use would not infringe privately owned rights.*

TECHNICAL INFORMATION DIVISION  
LAWRENCE RADIATION LABORATORY  
UNIVERSITY OF CALIFORNIA  
BERKELEY, CALIFORNIA 94720